The University Of Sheffield.

An Analysis of Electric Field Strength for Planning Indoor Wireless Networks at Various Frequencies

By:

Yasir Hemed Alharbi

A thesis submitted in partial fulfilment of the requirements for the degree of Doctor of Philosophy

The University of Sheffield
Faculty of Engineering
Departments of Electronic and Electrical Engineering

May 2016

Acknowledgments

First of all, I would like to thank God for giving me the encouragements, patience and power all the way through my life.

I would like to thank Prof Richard Langley for help, guidance and encouragements throughout my research. Special thanks go to thank Dr. Jonathan Rigelsford for his continuous assistance, enthusiasm and his valuable ideas to complete my research. I am also grateful to Dr Ahmad Alamoudi for his encouragements, suggestions and for supporting me throughout my study.

Also I would like to thank the University of Taibah in Saudi Arabia for its financial support.

I would like to thank my friends and colleagues at University of Sheffield for their support and their fruitful discussions.

I would like to express my gratitude to my parents, wife and children for their encouragements, emotional support and love all the time.

Abstract

Understanding the characteristics of radio wave propagation is a very important task for ensuring the required signal coverage for indoor wireless communication systems. The received signal strengths are highly affected when blocked by obstacles such as human occupants, doors, walls, windows, etc. This thesis investigated the E-field distributions inside a Victorian terraced house. Many scenarios are presented to investigate some important elements that have a significant effect on E-field distributions, such as opening and closing doors, the movement and number of human occupants and the location of the transmitter. These are considered for indoor signal propagation at various frequencies, specifically 5.8 GHz, 2.4 GHz, 868 MHz and 433 MHz. The distribution of the E- field strength within the building has been obtained using the FEKO simulation suite. The methods used in the simulation are geometrical optics and the uniform theory of diffraction. The results demonstrate that when the transmitter is located near to a wall, then the field distributions within the Victorian house are attenuated due to more reflections and multipath effects. Also, the results show that the door's status and human occupancy effect on the electric field coverage at 5.8 GHz and 2.4 GHz is more significant than at 868 MHz and 433 MHz. The practical results demonstrate that the radio signals can penetrate through several adjacent walls within the same floor, however they became very weak when they go through different floors. This indicates that the deployment and positioning of smart meters in domestic properties has to be carefully considered. Our results clearly prove that extensive E-field measurements should be performed prior to the deployment of wireless communication system within the building.

Table of Contents

List of Tables

List of Figures

Chapter 1– Introduction

1.1 Background

In the last decade there has been widespread deployment of indoor wireless communication which has resulted in an increased demand for various wireless services supporting data, voice, and video which require better quality of service (QoS). For example, between 2014 and 2018, global Wi-Fi hotspot numbers will grow to more than 340 million, equivalent to one Wi-Fi hotspot for every 20 people in world [1]. Wireless communication system users usually experience significant performance and reliability issues. The deployment of these free space systems is considered more complicated than wired network deployment due to the use of radio frequency (RF) links. Each location has its own RF characteristics and thus unexpected signal propagation issues have to be mitigated. In general, in order to deploy a wireless communication system, five key issues need to be addressed: coverage, capacity, security, mobility and QoS [2]. Improving the performance of wireless systems is becoming a very crucial element especially inside buildings. The signal coverage is one of the key elements that has received attention by researchers to improve the performance of wireless systems inside and outside the buildings [3]. Many parameters can affect RF signal propagation inside the buildings. Among them are the building structure, the type of materials used in construction and the incident angle of a wave into the wall, windows or any other obstacles [4]. Other parameters can have also a great effect on the signal propagation such as doors open or closed and the presence of occupants inside the building. These parameters cause reflection, diffraction, scattering, absorption and multipath on the received signals [5]. Many research studies have focused on improving the performance of the wireless communication systems inside a building in the context of signal coverage. There is growing interest in developing techniques to predict and control radio propagation within buildings. Understanding and modeling the radio wave propagation characteristics is a very important factor for ensuring QoS and reliable RF links for indoor wireless

communication systems [6]. This motivated many researchers to develop more accurate models of the propagated signals for wireless communication systems inside the buildings [7] [8] [9] [10].

1.2 Motivation

Indoor wireless systems provide a low-cost wireless connectivity in homes and offices and have become very popular recently [6]. High date rate devices are deployed in nearly every home to provide Internet access to unlimited users [1]. Efficient evaluation of radio wave propagation inside the building is a key element in the deployment of indoor wireless communication systems [11]. Effective design, evaluation and installation of a wireless communication system in an indoor environment require an accurate characterization of the propagation signals [12]. Predicting the propagation of the radio waves is a very challenging and complicated task as it is affected by many factors in the environment and the multipath propagation makes the prediction even more complicated [13]. This is very clear in the indoor environment where signals are received via more than one path, especially when there is no direct line of sight between the transmitter and the receiver as the signal is highly affected by reflection, diffraction and scattering [14]. Many methods have been used to characterize the signal propagation inside buildings. For example, the Finite- Difference Time-Domain (FDTD) method has been used to model the propagation in a multi-floor building at 1.0 GHz [6]. Artificial Neural Networks (ANN) have been used to predict the body shadowing and furniture effects in indoor radio wave propagation [15]. Site-specific ray-tracing methods such as Geometric optics (GO) and Uniform Theory of Diffraction (UTD) have been used to model the propagation inside the buildings [10]. Also, the method of moments (MoM) is used when the building is small or just for when one or two rooms are modeled [16]. These methods were used to investigate many factors that have a significant impact on the propagation such as human occupants, doors, walls, windows, etc [17].

The vast majority of existing studies as discussed in the literature review in chapter 2 have investigated the signal propagation using the above-mentioned methods and at different

frequencies. It is clear that there is a great deal of interest to study the signal propagation which motivated us to investigate the signal propagation using a simulation tool called FEKO across many different frequencies (433 MHz, 868 MHz, 2.4 GHz and 5.8 GHz) within a Victorian house. FEKO is an acronym derived from the German phrase "FEldberechnung bei Körpern mit beliebiger Oberfläche"[18]. This translated to English as Field computations involving bodies of arbitrary shape. More details about FEKO are presented in section 3.3. The parameters that were investigated are related to the environment inside the building which are doors open or closed and the presence of occupants inside the building. The reasons for choosing to study the effect of the doors and people on the propagated signals are that these factors are not stationary in the building whereas the wall and the furniture are considered to be very stationary [19] [14].

1.3 Thesis Objectives

In this thesis, the primary aim is to model the propagation of radio signals within a Victorian house using the FEKO simulation suite. The Geometrical Optics (GO) method with Uniform Theory of Diffraction (UTD) that is available in the FEKO is used to model and evaluate the E-Field distribution inside the house. The GO is used for large structures, which suits our model. Furthermore this method often requires much less computation time and memory than other methods such as in [20] where the author showed the results using FDTD require a huge time and large memory compared to GO especially when the targeted area is large.

The E-field distribution was investigated at the following frequencies: 433 MHz, 868 MHz, 2.4 GHz and 5.8 GHz. These are unlicensed band close to existing mobile system and the propagation effects can be considered representative not differ significantly. These frequencies are used in indoor wireless communication for the following applications: at 433 MHz – just above the Trans-European Trunk Radio (TETRA) at 400 MHz which is close to the free band at 433 MHz, and used for the emergency services radio communications. At 868 MHz – just below the 900 MHz cellular band the ISM medical transmission band used for data telemetry, mobile communication (GSM) at 890-960

MHz; at 2.4 GHz - sensor networks (Zigbee), medical ISM band and Wi-Fi, respectively; at 5.8 GHz – Wi-Fi predominantly.

The overall goal of this study is to model the E-Field distribution within a Victorian house across the different frequencies for many different scenarios which can be used to determine the signal coverage and capacity at each frequency which means the QoS may be assessed. A small terraced house was chosen as a case study to investigate how the various wireless systems performed and to keep the simulations within reasonable computer memory and power demands. One aspect was to study where a smart meter might be placed within the house and still be able to communicate with a base node at the consumer meters. Due to the low transmitter power, the position of the device and other factors such as open and closed doors, human occupancy etc. have a significant effect on the E-field even in a small terraced house. The E-field distribution was simulated in a horizontal plane on the ground floor and in a vertical plane between floors. In order to achieve this major goal, five measurable objectives, listed below, have been identified:

1- Model the statistical significance of human occupancy and the effects of opening and closing doors on the electric field distribution across the above-mentioned frequencies within the Victorian house.
2- The parameters stated in 1 were investigated in the horizontal plane with respect to a transmitter in the ground floor and the position of the antenna was at the corner of the kitchen.
3- As in (2) but with the antenna positioned opposite the door of the kitchen.
4- As in (3) but when the receivers are at vertical plane with respect to transmitter in the multi floors (basement, ground floor and first floor).
5- The amplitude probability and the cumulative probability distributions of the E-field distribution have been used to analyses the results and a comprehensive comparison between all the scenarios were obtained.

1.4 Areas of Novelty and Originality

In this thesis, the propagation of radio signals within a Victorian house was modeled using the FEKO simulation suite at different frequencies. The GO method with UTD was used to evaluate the E-Field distribution inside the house for all studied frequencies. Three significant variable factors that affect the radio signal propagation were investigated. These factors are the human occupancy, door status and the position of the transmitter. A comprehensive comparison between the studied frequencies was provided. To conclude this chapter, the areas of original work within this research are listed below:

1. New results that showed the changes in the electric field strength of wave propagation within the ground floor of a Victorian house at 5.8 GHz, 2.4 GHz, 868 MHz and 433 MHz.
2. New results that showed the effect of changing the position of the transmitter on the electric field strength of wave propagation within the ground floor of a Victorian house at 5.8 GHz, 2.4 GHz, 868 MHz and 433 MHz.
3. New results that showed the distribution of the E-field strength within the basement, ground floor and first floor in the Victorian house at 5.8 GHz, 2.4 GHz, 868 MHz and 433 MHz.
4. The results confirm that at low frequencies the effect of doors and human in propagation study can be neglected while at high frequencies should be taken into account.
5. The results clearly demonstrate that location of transmitter is vital at both high and low frequencies in the propagation study.
6. The results indicate that if the number of people increased a more attention in propagation study required as the effect may become significant.

1.5 Thesis Outline

This section provides an overview of the content of the thesis. In chapter 2, a literature review of the relevant research was provided. This includes the indoor and outdoor radio

wave propagations at different frequencies with the effect of many parameters. This chapter emphasises the necessity of the research done in this thesis.

Chapter 3 investigates the wave propagation within the ground floor of a Victorian house where the antenna was placed in the middle of the open door. The investigations were carried out at different frequencies with the effect of human occupancy and open and closed doors. Chapter 4 investigates the wave propagation on the three floors (basement, ground floor and first floor) and the antenna was placed at the middle of the open door. Chapter 5 provides similar investigations scenarios except the antenna was placed in the corner of the kitchen. Chapter 6 provides a case study of measurements to assess the suitability of using Zigbee within domestic properties for smart metering applications. Finally, in chapter 7 a summary of the work covered in this thesis is presented and the main conclusions are provided. This chapter also outlines some potential areas for future work based on the results provided in the thesis.

Chapter 2 – Literature Review

2.1 Propagation Models

This chapter describes prior work which has been done in the field of radio wave propagation modelling in three different environments. Before starting the literature review some analysing methods that used to model the wave propagation are presented. The main methods used are Finite-difference time-domain (FDTD) and geometric optics GO. The main types of deterministic models are: Ray-optical models and Finite-difference time-domain (FDTD) models. Moreover, Ray-optical modes can be further divided into two subtypes: the ray launching model and the ray tracing model.

2.1.1 FDTD Model

The FDTD method is a time domain solution of the Maxwell's equations described in differential form and due to its simplicity is widely used in circuit analysis. Maxwell's equations provide an accurate description of the propagation of electromagnetic wave, however, their form of partial differential equations make them too difficult to solve. In 1966, Kane Yee proposed a set of finite-difference equations (through central-difference approximations of the space and time partial derivatives) to replace Maxwell's partial differential equations [21]. Maxwell's equations in an isotropic medium are [22]:

$$\nabla \times E = -\frac{\partial B}{\partial t} \qquad 2.1$$

$$\nabla \times H = -\frac{\partial D}{\partial t} + J \qquad 2.2$$

$$\beta = \mu H \qquad 2.3$$

$$\mathrm{D} = \epsilon \mathrm{E} \qquad 2.4$$

Where E is the electric field intensity(V/m), H is the magnetic field intensity(A/m), β is the magnetic flux density(W/m^2), D is the electric flux density (D/m^2) and J, ε and μ are assumed to be given functions of space and time. The finite-difference equations were further investigated by Allen Taflove into the FDTD method [13]. Allen in his model takes all the propagation phenomena into account, which results in a high modelling accuracy.

As a result, numerical solutions it divides the investigated space into finite grid elements upon which a time and space approximation of the electrical and magnetic field strength is performed. The Yee algorithm [23] is used to replace a set of partial differential equations with a set of finite difference equations as shown in Figure 2.1 [24]. The E-field components are orthogonal to H-field components and are also interleaved in time. The interleaving means if the H-field is calculated at discrete time instance t then the E-field is calculated at t+0.5, followed by the calculation of H field at t+1 and E-field at t+1.5 and so on until the required transient or steady state E-field behaviour is obtained. At each time step, the E-field components are updated using the equations. This technique requires the computer storage and running time must be proportional to the electrical size of the volume being modelled as well as the mesh grid cell size. The size of the mesh grid can be set to any fraction of a wavelength. The mesh grid cell size should satisfy the Courant-Friedrichs-Levy (CFL) stability condition [25]:

$$\Delta t \leq \frac{1}{c}\frac{\sqrt{\epsilon\mu}}{\sqrt{\left(\frac{1}{\Delta x}\right)^2+\left(\frac{1}{\Delta y}\right)^2+\left(\frac{1}{\Delta z}\right)^2}} \qquad 2.5$$

Where $\Delta x, \Delta y \; and \; \Delta z \; are$ the cell grid size in the X, Y and Z directions, ϵ is the permittivity, μ is the permability and c is the speed of light. When the cell grid is uniform in all directions, the equation can be reduced to equation:

$$\Delta t \leq \frac{\Delta}{c\sqrt{\varepsilon}} \qquad 2.6$$

The biggest dimensions of the cell should normally be > $\frac{\lambda_{min}}{20}$. One of the weakness of the FDTD method is that it needs a full discretization of the electric and magnetic fields throughout the entire volume domain [26]. The disadvantages of FDTD are that the upper points on time step and space steps results in huge memory requirements and the

simulation consumes a significant time. Therefore, FDTD is usually used for modelling the radio wave propagation in small environments [20].

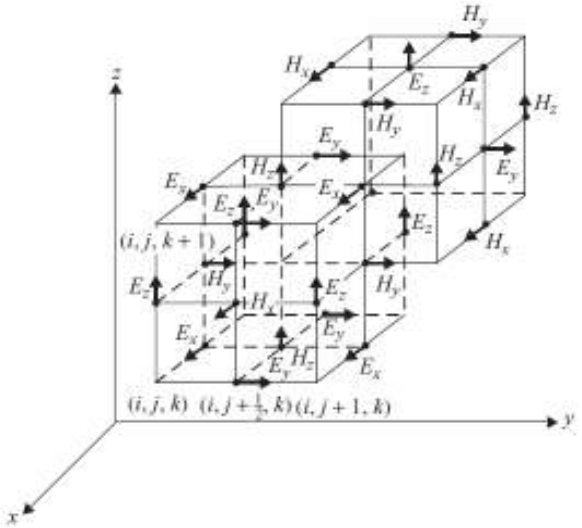

Figure 2.1: Basic Element of FDTD Yee Grid [21].

2.1.2 Geometry Models

Radio wave propagation can be modelled using geometry rays, which interact with the environment during the passing through different media. The rays may be reflected, diffracted, scattered, or pass through obstructions before reaching their final destination. The signal strength of a ray is decreased along the propagation path, and the total received signal strength is obtained from all the rays arriving at the destination point and their phase shifts. Geometry models determine the multi-path components (MPCs) between the transmitter and receiver based on path searching algorithms, and are also referred to as ray-based (or ray optical) models. The received signal strength modelled by geometry models are expressed as follows:

$$P_r = P_t - \sum_{i=1}^{N} \omega\left(\tau_i, L(f, d_i)\right) + G_t + G_r \qquad 2.7$$

$$L(f, d_i) = F(f, d_i) + \sum_{i=1}^{R} \emptyset(M_i, t_i) \qquad 2.8$$

Where P_r is the received signal power in dBm, P_t is the transmit power level in dBm, G_t And G_r are the antenna gains in dBi of the transmitter and the receiver, respectively, N is the number of MPCs arriving at the receiver, τ_i is the delay of the ith MPC, ω sums up the power carried by the MPCs, $L(f, d_i)$ is the path loss of the ith MPC, d_i is the distance that the *ith* MPC propagates along its path, f is the carrier frequency, $F(f, d_i)$ is the path loss as a function of d_i and f, $\emptyset(M_i, t_i)$ and is the interaction loss as a function of M_i and t_i, which denote the material type and the type of interaction (e.g., reflection or diffraction) of the ith MPC, respectively. Geometry model can be divided into ray launching model and ray tracing model.

The ray launching model [27] is based on the Geometrical Optics (GO) which simulates the propagation of a radio wave according to physical phenomenon, such as reflections, refractions and diffractions. The ray launching model launches a number of rays from the transmitter end as shown in Figure 2.2. A small angle separates these rays, so each of them has a different transmit direction. After the rays have been launched they interact with the objects in the propagation environment according to the physical phenomenon, the propagation of a ray vanishes either when its power falls below a specified threshold or when the number of interactions with objects reaches a predefined number or the received power at the receiver. Ray launching is usually called the 'brute force' method since it launches many rays with very similar angles [28].

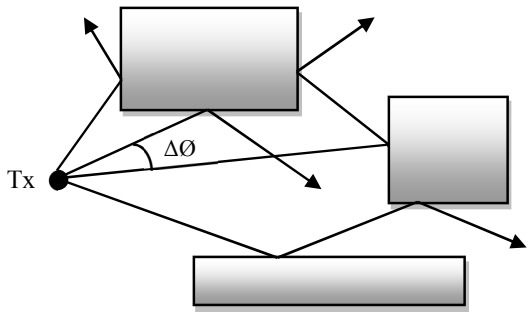

Figure 2.2: Ray Launching.

The ray tracing model traces rays backwards which is different from the ray launching model which traces rays forwards. The ray tracing is an image-based model that assumes all objects in the concerned environments are potential reflectors as shown in Figure 2.3. In implementation, the ray tracing model uses the images of the transmitter relative to all the reflectors. However, ray tracing takes into account only the paths which really exist between the transmitter and the receiver. The drawback of this method is that its computational time grows exponentially with the order of calculated reflections. Both in the ray launching and ray tracing models, the strengths of reflected rays and refracted rays are computed according to the geometrical optics. The ray tracing models are suitable for point to point field strength computation, but not suitable for coverage prediction due to the computational complexity. The diffracted rays are computed according to e.g. the UTD theory [21].

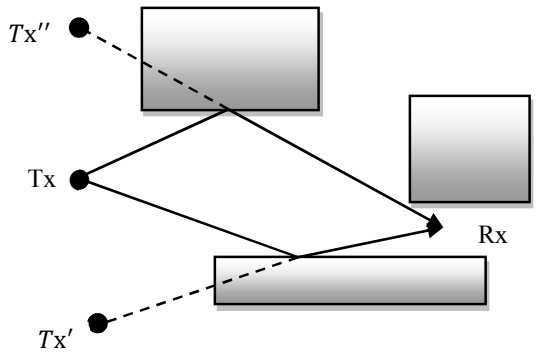

Figure 2.3: Ray Tracing.

Geometrical optics fails to estimate a certain optical phenomena called diffraction. However, an extension of geometrical optics, which makes account for these phenomena is described below and it is called the geometrical theory of diffraction (GTD).

$$E^{GTD} = E^{go} + E^{d} \qquad 2.9$$

Diffraction occurs at the edge of an object when the radius of curvature of the edge is significantly smaller than the radio wavelength which results in the radio wave bypassing the obstruction causing many secondary rays in new directions [21]. GTD was first proposed to estimate the electromagnetic near field of diffraction and determine diffraction coefficients. The GTD analyses diffracted rays. The presence of these rays can be represented using Fermat's principle, with the one dimensional constraint bounded to the edge. This issue appears in Keller's cone [29], where an infinite number of rays on this cone can pass into the shadow region, where the GO rays cannot penetrate. Keller's GTD predicts wrong results at and near the incident and reflected shadow boundaries. Therefore, the GTD was later extended and developed into UTD to solve this problem. The UTD is introduced to remedy the singularity issue in GTD by modifying the diffracted field as described in [29].

The reason behind introducing the most common methods that are used for simulating the radio wave propagation to discuss the limitations of each method which enables us to find the most suitable method for our modelling. Based on this discussion the GO – ray launching – with UTD method was selected for our model. Also introducing these methods is for the benefit of the reader as most of the discussed studied in the literature review are based on one of them.

After introducing the common methods used for simulating the radio wave propagation, the research that was carried out in the area of RF propagation in three different environments is discussed.

2.2 Outdoor Propagation

Firstly, we started reviewing the previous works in the area of outdoor propagation environments. The outdoor propagation is mainly considered in three types of areas: urban, suburban, and rural areas. In order to characterize the outdoor RF propagation, the terrain profile of the area has to be taken into account. The terrain profile is highly dependent on the type of the area and may vary from a simple, curved earth to a highly mountainous region. There are other factors which affect the outdoor propagation such as trees, buildings, moving cars, and other obstacles also should be taken into account. The

received signal is usually combination of the direct path, reflections from the ground and buildings and diffraction from the corners and roofs of buildings [17].

In recent years, the path loss propagation models have received significant attention by researchers. The path loss is a strength reduction in the signal when it propagates from the transmitter to the receiver. The general classification of modeling the path loss includes deterministic, statistical and empirical. The deterministic uses Maxwell's equations while the statistical models use probability analysis by finding the probability density function. The empirical models use equations derived from extensive measurements efforts. These empirical models provide accurate results but need complex computational techniques [30].

Reflection, diffraction and scattering are the three basic propagation mechanism that have an impact on the propagation in wireless communication systems. The multipath is due to the joint impact of reflection, diffraction, and scattering together. The received signals may attenuated extremely due to the destructive combination of the multipath composite [5].

The deterministic model is hardly used as the data for the outdoor environment is usually not available and the computational effort is very high whereas the empirical models are widely used for path loss outdoor propagation due to their simplicity [31]. The Okumura model was simplified by Masaharu Hata in 1980 [21]. It is valid for frequencies in the range from 150 MHz to 1920 MHz and the distance of 1 km to 100 km and the base station's antenna height from 30 m to 100 m. The Hata model is an empirical formulation produced by Okumura and is valid for frequencies from 150 MHz to 1500 MHz. The Hata model was extended and enhanced by COST 231Hata [32]. It is valid for frequencies from 1500 MHz to 2000 MHz.

The Bertoni-Walfisch model is suitable for signal propagation through buildings in urban areas [33]. The model assumed all the heights of buildings are the same and the distance between them is equal. The propagation is calculated by the process of multiple diffraction past these rows of buildings. In [33] the authors carried out a comparison study between studied Hata, Cost-231 and Bertoni-Walfish at 900 MHz. Their results showed that the average mean error for 8 different base stations is 16.6 dB, 14.8 dB and 9.6 dB for Hata,

Cost-231 and Bertoni-Walfish, respectively. This result indicated that the Bertoni-Walfish model provide better performance than the other two models. In [34], the authors also carried out a comparison study between Okumura model, Hata model and Lee model in urban area using Matlab simulation at 900 MHz. The results in [34] concluded that the performance of Okumura model is better than other models. In [35], the received signal strength for three types of path loss model are calculated using Matlab simulation in urban, suburban and rural areas. These models are Hata model, COST231 Walfisch-Ikegami and Lee model. The results showed that the highest received signal strength in urban area was by using COST231 Walfisch-Ikegami and in suburban and rural areas was by using Hata model. Therefore, the suitable model for urban area is COST231 Walfisch-Ikegami and the suitable model for suburban and rural areas is Hata model.

The Stanford University Interim (SUI) model was developed by Stanford University and is an extension of the Hata model with correction parameters for frequencies above 1900 MHz. The SUI model is proposed as a solution for planning the WiMAX network at the 3.5 GHz band. The SUI model can be used for the base station antenna height from 10 m to 80 m, the receiving antenna height between 2 m and 10 m and the cell radius between 0.1 km and 8 km [36]. Another study in [30] compared the performance of the following models: Hata model, SUI model Okumura model, COST231 and ECC-33 model ,which is developed by Electronic Communication Committee(ECC), in urban, suburban and rural areas at 900 MHz and 1800 MHz. The results showed that the ECC-33 and SUI model provide the best path loss model in urban area. In suburban area, ECC-33, SUI and COST-231 are the best. Also, in rural area, Hata and log distance models give the better results. The results indicated that the Okumara model provided better results in urban and suburban areas. In [37] the authors compared the three different path loss models which are the SUI model, COST-231 model and ECC-33 model at 3.5 GHz for fixed wireless access (FWA) system in urban, suburban and rural areas. The authors concluded that the ECC-33 model is recommended for urban area whereas in suburban and rural areas. The ECC-33 and COST-231 have the lowest errors in suburban area while the SUI in urban area has the lowest error. Another study for comparing four path loss models at 3.5 GHz in urban and suburban was investigated in [38]. The models obtained in this study are SUI

model, COST-231, Hata model, Macro model and Model 999. The measurements were carried out in two separate locations, line of sight (LOS) and non-line of sight (NLOS). By comparing the measurements for the four models, in the case of NLOS the best path loss model was SUI model whereas in the case of LOS the SUI provided high error prediction. The Macro model and Model 999 have a better performance in the case of LOS than the other two models [38].

2.3 Outdoor to Indoor Propagation

Secondly, we move on to review the outdoor to indoor propagation modelling. Outdoor to indoor propagation occurs when the transmitter is located outside the building and receiver placed inside the building. One example of outdoor to indoor application is the smart metering, the meter located inside the building and the repeaters or data collector located on street lamps or rooftops [39]. Also in mobile system the base station positioned outside the building and the user may be positioned inside the building. The modeling of outdoor to indoor propagation is more complicated than the outdoor propagation [40]. This is due to the fact that the outdoor to indoor propagation is dependent on the building structure, the different types of construction materials, the size and the number of windows, floor height, internal layout, the location of the receiver inside the building and the nature of perimeter buildings [41].

In order to predict the performance of field strength between the transmitter outside the building and the receiver inside the building, the building penetration loss (BPL) was used. BPL is defined as the difference between the received signals strength in building and the received signals strength outside the building measured in dB [42] [43].

Many researchers have studied the relation between the different frequencies and the penetration loss [44-48]. In [44], the authors studied the penetration loss at 441 MHz, 900 MHz and 1400 MHz. They found that the average penetration loss was decreased when the transmission frequencies were increased. When the frequency changed from 441 MHz to 900 MHz, the average penetration loss decreased by 1.5 dB and decreased by 4.3 dB when the frequency changed from 441 MHz to 1400 MHz. Also in [45], the researchers studied the penetration loss at 900 MHz, 1800 MHz and 2300 MHz. The results showed

that the penetration loss was decreased when the frequency was increased. At 900 MHz, 1800 MHz and 2300 MHz the penetration loss was 14.2 dB, 13.4 dB and 12.8 dB, respectively. Also, the results illustrated that the penetration loss at 900 MHz, 1800 MHz and 2300 MHz were -1.4 dB per floor and for higher than six floors the loss decreased to -0.4 per floor. In [47], the propagation of the signals into three different types of buildings at 1.9 GHz and 3.5 GHz was measured. The authors found that the penetration loss at 3.5 GHz is higher than at 1.9 GHz by 5 dB. Also, the attenuation of external wall for modern buildings is higher than for old building by 10 dB. In case of shop building, the attenuation at 3.5 GHz is higher than at 1.9 GHz by 3 dB. The old building has the least attenuation among the buildings due to the difference in materials types and the thicknesses.

Many researchers have studied the effect of the height of the building on penetration loss [41] [49-55]. In [49] [41] [52] [53] [55], the studies concluded that the penetration loss is decreased when the height of building is increased at frequencies from 400 MHz to 2300 MHz. In [49] the penetration loss was -1.2 dB per floor at 880 MHz and was -2.4 dB per floor at 1922 MHz and the floor higher than the fifth floor tend to be level off. Also in [54], at 1800 MHz the penetration loss was 34 dB at floor below the ground whereas was -17 dB at the highest floor which a floor gain was 7 dB per floor. It can be seen that from the same study, the penetration loss at 950 MHz is lower than 1800 MHz by 2 to 4 dB on lower floor whereas on the higher floor it was equal or higher than at 1800 MHz. On the contrary, some research has reported that at 1700 MHz [50] [51] the penetration loss neither decreases nor increases as a function of increasing floor level. This is due to the fact that when the number of levels in the building increased, the reflecting, the scattering and multipath loss increases. In [56], the penetration loss from mobile stations to the mobile nodes inside different types of buildings and rooms at 900 MHz, 1800 MHz and 2100 MHz are obtained. The results showed that the average attenuation is decreased with higher floors by 0.8 dB and for floors above the sixth it decreases by 0.4 dB per floor. Also, the difference in penetration loss between 900 MHz and 1800 MHz was 0.8 dB and between 900 MHz and 2300 MHz was 1.4 dB.

The characterization of the outdoor-to-indoor propagation at 169 MHz (used for smart metering applications) has been described in [57]. The measurements were carried out for

two different buildings, central urban areas and suburban residential areas of many European cities. Windows with metallic bars were present in the ground floors only. Different reception modes for the smart meter (namely, "open air," "double pot," and "metal grid") were considered. A Gaussian distribution can be approximately assumed for BPL, with mean value and standard deviation found equal to about 7.5 and 4.5 dB, respectively. The authors in [57] found that outdoor-to-indoor signal penetration slightly benefits from the presence of windows. Also their results showed that underground placement and (partly) metallic housing represent a rather serious effect, with a mean installation loss (IL) equal to 7.75 and 13.5 dB in case of "metal grid" reception mode and meter placement in the building basement, respectively. Finally, they suggested that a cost-effective deployment of wireless smart metering systems in the 169-MHz band could be based on a large reuse of the existing infrastructure of cellular wireless systems.

It has been noticed that another important factors affecting the penetration and the overall path loss are the number and size of windows that exist at the illuminated building. These windows can provide a relatively low loss propagation path as shown in [40, 41, 52, 53, 55, 58].

2.4 Indoor Propagation

Finally, having reviewed the outdoor and the outdoor to indoor propagations, our main area of interest which is the indoor propagations is reviewed in detail. There is exponential growth in the deployment of wireless communication systems within buildings, such as Wi-Fi, Bluetooth, Femto cells and wireless sensor networks. The deployment of these systems requires a characterisation of indoor radio channel. Understanding of such radio environments leads to the optimization of the communication network design, which results in best possible signal coverage and quality for multi-user applications. The ray-tracing approach for indoor channel characterisation has been a hot topic of research [1-8] in recent years.

Improving the performance of wireless systems is becoming a very important element especially inside buildings. For a wireless friendly building, improving the signal coverage is one of the main elements studied in the literature [3, 8, 9, 16, 59-61]. There

are many parameters that can affect RF signal's propagation inside the buildings such as the structure of building, the type of materials and the incident angle of wave into the wall, windows or any other obstacles [4]. Obstacles such as human occupants, doors, walls and windows cause multipath and shadowing effects, which reduce the received signal strength. As new materials are used to develop more energy efficient buildings they raise new challenges for deploying the wireless communication systems inside the buildings [62].

A large diversity of values of conductivity and permittivity for different types of building construction are used for frequencies of 900 MHz to 2.44 GHz in [9, 16, 59]. The effects of various building dielectric parameters and structures of internal wall on the performance of wideband channels have been investigated in [8, 61, 63]. In [8], the effects of permittivity, dielectric loss tangent and thickness of the internal wall on the indoor signal propagation characteristics was investigated using the FDTD method. The results showed that the path loss due to the obstruction increases linearly with any of the three internal wall parameters increasing. The results also showed the root mean square (RMS) delay spread is sensitive to the dielectric loss tangent and the thickness of the internal wall. In [61], the authors investigated the effect of wall materials and different wall thicknesses on the propagated signals at 433 MHz, 868 MHz, 2.4 GHz and 5.0 GHz. The wall materials used are wood, concrete and plaster board with wall thickness of 0.2 m, 0.25 m, 0.3 m and 0.4 m. The results illustrated that effects of the wooden wall are sensitive to the operating frequency not to the thickness of wall due to low conductivity of the wood. However, the effects of concrete and plasterboard are sensitive to both the frequency and the thickness of wall and the concrete wall attenuated the signals more than the rest. In our models the same parameters are investigated in a different environment which is a Victorian house using different simulation tools. In [60], the effect of the different types of wall on the propagated signals inside the building at 900 MHz and 2.4 GHz had been investigated by using the brute-force ray tracing method. The materials used are cement, wood and iron with refractive index 1.8, 4 and 14, respectively. It has been found that the received power inside the building using iron material wall was attenuated by 5 dB compared to wooden material. The effect of metal door status (open or closed) on indoor

radio channel at 900 MHz, 2.4 GHz and 5.2 GHz by using FDTD method has been studied in [64]. The results depicted that the variation of the received signal strength between open and closed metal door at 900 MHz, 2.4 GHz and 5.2 GHz are 20 dB, 24 dB and 26 dB, respectively. Also, it has been found that the decrease in the received signal strength was higher on the receiver near to the metal door whereas the effect of the door at the receivers which were located far away from the door was small. The authors in [14] studied the effect of the doors when they are open or closed on the E-field propagation for cases, line of sight (LOS) and non-line of sight (NLOS) using finite element method (FEM) at 2.4GHz. Their results showed that the door status has a more significant effect on the signal strength in the case of the LOS scenario than for the NLOS scenario. Based on the guiding effects of hallways authors in [65] presented a new model for UHF (850-950 MHz) propagation in large buildings. By comparing the power levels in hallways and rooms in an office building, the importance of the guiding mechanism was very clear. The results also showed that the power levels in hallways were higher in most cases, even when the hallway was further from the transmitter than the rooms.

The effect of the human body on wireless signals in an indoor environment has been investigated by many researchers [19, 66-72]. In [66], it was shown that the attenuation behind a wall becomes lower than the attenuation behind human and the reflection waves in front of people are very high. Also, the influence of human movement on wireless sensor networks in indoor radio propagation has been studied in [19, 67, 68]. It was concluded that the electric field is significantly affected by the number of people and their mobility in the rooms. The signal level was decreased in case of slow speed movement but the trends at slow and medium speeds have the same effect as the number of people was increased [67].

In [69] the effect of 4 people movement on indoor propagation at 2.45 GHz using ray tracing and UTD method were investigated. When there was no people, the average received power level was -51.7 dBm, but when the pedestrians were moving around, the average received power level was -52.6 dBm. Although the difference in received power was small, severe fading when the pedestrians were moving was present and the received power fluctuated between -80 dBm and -40 dBm. In [70] the authors used the same

environment as in [69] to investigate the excess loss values caused by human body for LOS at 2.45 GHz, 5.7 GHz and 62 GHz using. It has been found that the excess loss for human body increased when the frequency is increased. The excess losses for human body are 12.3 dB, 16 dB, 26.5 dB at 2.45 GHz, 5.7 GHz and 62 GHz, respectively. Another investigation was carried out in [71] to measure the effect of the number of human bodies on the received signals in rectangular office for LOS at 5.2 GHz. Four different scenarios were investigated: empty room, one human obstructed the LOS, tow human simultaneously obstructed the LOS and three human obstructed the LOS. The results showed that the human body movement in the room caused significant variations on the received power. The attenuation of body shadowing effect in these scenarios was up to 10 dB. The effect of people movement on channel capacity for LOS at 5.2 GHz in unfurnished room was investigated in [72]. By using cumulative distribution function (CDF) for the measurements, the results showed that the received power decreased when the number of people was increased.

The effect of multiple floors on the signal propagation inside the building has been investigated in [73] [6] by using FDTD method at 1.0 GHz. The floor is made of concrete with relative permittivity of 4.0. It has been found that the received power was attenuated linearly by 10 to 15 dB per floor. Also the author in [6] investigated the signal reflections and scattering from furniture and fittings at 1.0 GHz. By comparing the FDTD simulated path loss on the same floor with and without clutter, it has been found that the averaged path loss with clutter was higher than without clutter by up to 15 dB. In [74] the authors extended the investigation in [6] by studying the interference of propagated signals between two adjacent buildings with the same number of floors (six floors).The results illustrated that the scattering from nearby buildings can cause co-channel interference to access points on distant floors and that significant energy levels can arise due to the propagation paths between buildings especially floors with approximately similar height. The indoor coverage at 1700 MHz and 900 MHz in a modern multistory office was studied in [75]. The results showed that the attenuation caused by a floor at 1700 MHz is higher than at 900 MHz by 11 dB and if the number of floors is increased, the attenuation increased by 6 dB per floor. In [76] the effects of surrounding buildings on the multi floor

signal propagations using FDTD method at 4.5 GHz was investigated. In order to study this effect, two buildings were modeled: the first building was surrounded by two multistory buildings whereas the second building is isolated on all surfaces. The results showed that the received signal in adjacent floors is increased by 9.7 dB due to the reflections from nearby buildings.

In [77] [78] the indoor propagation path loss at 900 MHz, 2.5 GHz and 60 GHz has been measured. The results showed that the signals at 60 GHz may cover a single room whereas the signals at 900 MHz and 2.5 GHz could cover several rooms. This makes 60 GHz suitable for small rooms with small obstacles between transmitter and receiver.

The researchers in [79] investigated the electromagnetic wave propagation in industrial environments at 433 MHz, 868 MHz and 2.4 GHz. The common materials used in industrial environments are steel, iron and metals which are different from a residential environment such as wood, brick and glass. The simulation results showed that the signals coverage at low frequencies was higher than at high frequencies. The received signal level at 2.4 GHz is lower than at 868 MHz and 433 MHz by 30 dB.

This chapter reviewed the propagation models for the outdoor, the outdoor to indoor and the indoor environments. It is obvious that there is a significant work was done for outdoor propagation modelling. The statistical models that developed with measurements allow to make estimation in complex environment which is a very difficult to compute. However, the indoor propagation models are much newer and they can be done computationally. Although outdoor and outdoor to indoor modelling are important in the built environment only indoor propagation is considered in this thesis. The effects of some parameters (such as doors, walls, properties of materials and human) at different frequencies in indoor environments have been described above. As mentioned in the literature, the effects of doors and human occupancy on the E-field coverage were investigated at single or two frequencies. However, these studies did not consider most of the frequencies that could be used for wireless devices inside the buildings. Therefore, this thesis investigates the effect of door's status and human occupancy - which are unstationary - on the E-field coverage at 5.8 GHz, 2.4 GHz, 868 MHz and 433 MHz which are used for wireless devices inside the buildings.

Chapter 3 – Analysis of E-Field Distributions on Horizontal Plane for Configuration A in Single Floor within House

This chapter investigates the distribution of the E-fields in configuration A in a horizontal plane. Configuration A defined as follows, the dipole antenna transmitter is placed in the middle of the kitchen opposite the door to the front living room at ground floor level in a Victorian house at four frequencies.

3.1 Introduction

In order to perform effective network planning inside the Victorian house, the electric field distributions should be carefully studied. In this chapter, the door status and the occupants which are the two main factors that affect the electric field (E-field) strength of a vertically polarized dipole antenna transmitter have been investigated. The transmitter power in the simulation was 50 mW, and the investigations were carried out at a selected range of frequencies 5.8 GHz, 2.4 GHz, 868 MHz and 433 MHz which represents the used wireless devices in the houses. The distribution of Electric Field strength within the building has been calculated using the FEKO simulation suite [18]. Several scenarios have been considered to investigate the effect of human occupancy and the effect of opening doors on the electric field distribution of the ground floor, comprising a kitchen and front room. In this chapter, the transmitter was located in the middle of the kitchen 1.2 m above the ground, 1.3 m from middle wall and 2.1 m from external wall facing exactly the centre of the kitchen door to the living area as shown in Figure 3.5. The received fields are in a horizontal plane with respect to the transmitter on the ground floor. The methodology that used is described in the next section. In section 3.3 Simulation of the E-Field Distributions on the Horizontal Plane with the transmitter antenna is on the middle of the door in the kitchen at 5.8 GHz is presented while in section 3.4 2.4 GHz is investigated, 868 MHz in section 3.5 and 433 MHz in section 3.6 . A further discussion of the results and other parameters are summarized in section 3.7, section 3.8 and section 3.9. Section 3.10 concludes this chapter.

3.2 Methodology

In the following sections the methodology that was used in our investigations is described.

3.2.1 Simulation Software (FEKO)

FEKO is a software Suite designed to analyses a wide range of electromagnetic problems. Applications include EMC analysis, antenna design, microstrip antennas and circuits, dielectric media, scattering analysis, cable modelling and many more. FEKO has graphical user interfaces called CADFEKO as shown in Figure 3.1 and POSTFEKO as shown in Figure 3.2 which make use of the ribbon user interface. CADFEKO allow users to create the geometrical and the numerical analysis techniques and also the calculation needed by the user. POSTFEKO allow users to read and display results obtained from the FEKO solver.

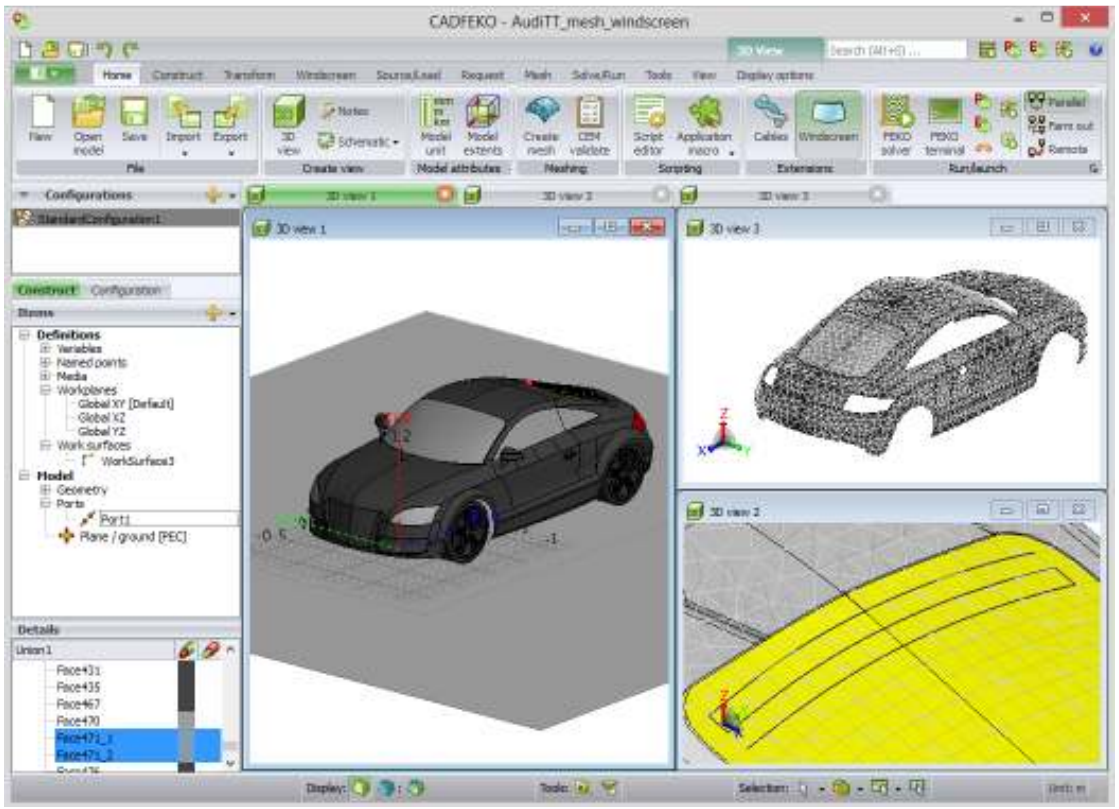

Figure 3.1: CADFEKO Interface [18]

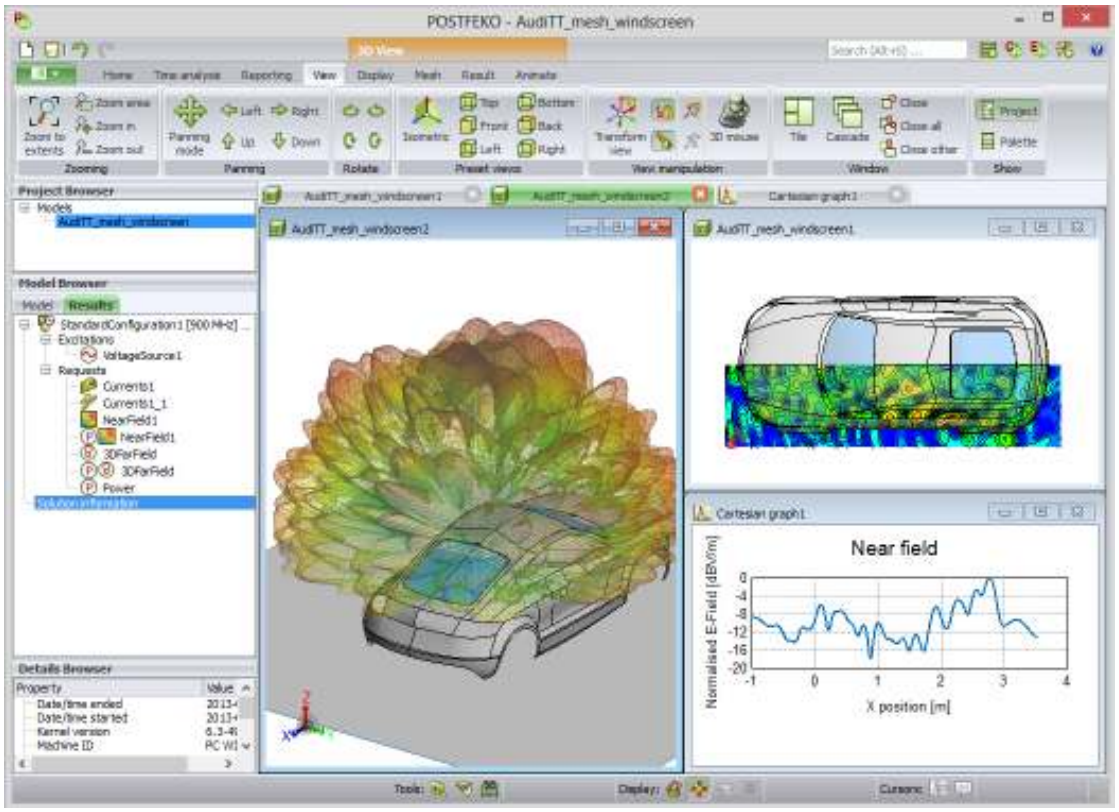

Figure 3.2: POSTFEKO Interface [18].

The numerical analysis techniques in FEKO used in the simulation were GO and UTD. GO is suitable for solving a large model and inhomogeneous structures [18]. Thin Dielectric Sheet (TDS) is used to model the walls and rooms of the building. In such cases, the walls are modeled with one surface and the real thickness defined in a layered structure. In TDS, the thickness in 3D cannot be modeled while FEKO computes the equivalent real thickness of the wall and rooms. Determining the direction of the thickness sheet in TDS properties in FEKO suite can be done by changing the geometry of the model using the element normal function in FEKO by choosing the required colour. The green color means that the normal points towards the observer while the brown colour means the other way around. After creating the walls and the room with their properties, the geometry should be joined using union function FEKO and the required frequency for the modeling should be selected. The solver sitting function in FEKO enables us to select the method of simulation technique and their properties. The types of material for each wall

can selected from the face properties. FEKO solver runs the model and the results are displayed in POSTFEKO. The POSTFEKO display has two main purposes: the first purpose is to validate the geometry and the second purpose is to analyses the results. Validation of the geometry modelling enables the users to confirm the accuracy of their models before starting their simulation. Once the model has been run, POSTFEKO can be used to display and review the results. Different tools are available to assist in visualizing the data in a constructive manner [18]. The data results can be extracted from the POSTFEKO and can be analyzed in other programs such as Matlab or Excel.

3.2.2 Experiment setup and House specifications

The simulations were implemented in a typical Victorian terrace house of three levels as shown in Figure 3.3 and Figure 3.4. The simulated house includes a basement, ground floor and first floor. The first floor has two bedrooms and the ground floor includes the front room and kitchen. The kitchen is 3.5 m wide and 3.2 m long, while the front room is 3.5 m wide and 3.8 m long. The materials and dimensions of house are listed in Table 3.1.

Figure 3.3: Victorian terrace house used in this work.

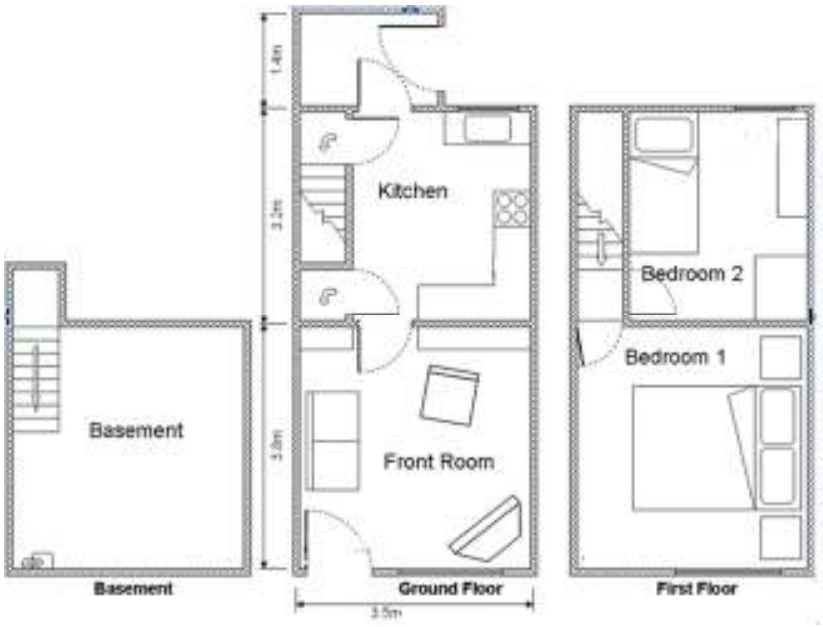

Figure 3.4: Floor plane inside Victorian house.

Table 3.1: Materials and dimension of house construction.

No	Object	Material	Dimension
1	**External wall**	Brick	20 cm
2	**Internal wall**	Brick	10 cm
3	**Floor**	Wood	10 cm
4	**Ceiling**	Wood	10 cm
6	**Door**	Wood	5 cm

Simulations were performed using a dipole antenna to generate the E-fields and was positioned in the kitchen 1.2 m above the ground, 1.3 m from middle wall and 2.1 m from external wall. The properties of materials used in the simulation for the house at the investigated four frequencies are shown in Table 3.2.

Table 3.2: Dielectric properties showing the Permittivity (ε) and Loss tangent (tan δ) of typical building materials at different frequencies.

	5.8 GHz		2.4 GHz		868 MHz		433 MHz	
Materials	**E**	**tan δ**	**ε**	**tan δ**	**ε**	**tan δ**	**ε**	**tan δ**
Brick	4.29	0.809	3.8	0.55	3.73	0.38	3.73	0.38
Wood	2.1	0.29	2.1	0.23	2.24	0.198	2.24	0.198
Glass	6.47	0.29	6.39	0.129	6.35	0.04	6.35	0.04
Plasterboard	2.14	0.005	2.41	0.09	2.26	0.005	2.26	0.005

Different occupancy scenarios were analyzed in the following section.

3.2.3 Simulation Scenarios

Ten different scenarios were designed (A to J) to investigate the statistical significance of human occupancy and the effects of opening doors and the presence of humans on the electric field distribution in the rooms. These scenarios are defined in Table 3.3. Figure 3.5 illustrates the layout of the ground floor of the house and shows the locations of the occupants, the door and the transmitting antenna.

These scenarios were designed based on the fact that the house consists of two bedrooms, a kitchen and front room. The estimated number of people who may live in this kind of house is expected to be four. People are expected to be anywhere in the house; however, we assume that people spend most of their time in the kitchen or the front room. Usually the sofa's location in front room is placed near to the door and the TV is located in the corner side of the front room, for these reasons the effect of orientation of human on electric field distribution within house is taken into account as seen in location 5 in Figure 3.5. In these scenarios, the effect due to furniture and other equipment existing inside the house was neglected. The geometry of the human used in the scenarios was as follows: height = 170 cm, the width = 35 cm and the thickness = 15 cm.

Table 3.3: Scenarios used for statistical analysis.

	Occupied	Door Open	Location	Rotation
A	No	Yes	-	-
B	No	No	-	-
C	Yes (x1)	Yes	1	-
D	Yes (x1)	No	1	-
E	Yes (x1)	Yes	3	-
F	Yes (x1)	No	3	-
G	Yes (x1)	Yes	5	90°
H	Yes (x1)	No	5	90°
I	Yes (x4)	Yes	1,2,3 and 4	-
J	Yes (x4)	No	1,2,3 and 4	-

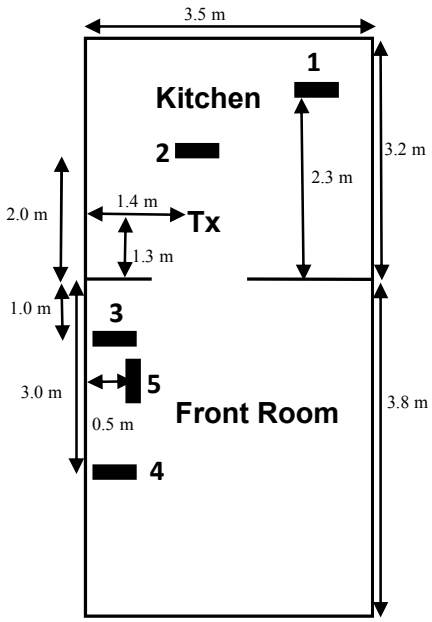

Figure 3.5: Relative positions of occupants for configuration A.

3.3 Simulation of the E-field distributions on horizontal plane for configuration A at 5.8 GHz

The FEKO simulation suite was used to calculate the distribution of Electric Field strength within the building on the ground floor. Angular resolutions for the transmitting rays of $\theta = 0.08^{\circ}$ and $\emptyset = 0.03^{\circ}$ have been carefully selected for this simulation based on a trial and error mechanism. The angular resolutions have been chosen after many trials of until the required accuracy values are obtained. TDS is used to model the walls and rooms of the building.

Simulations were performed using a 5.8 GHz half wavelength dipole antenna to generate the E-fields. The dipole antenna has a length of 23.26 mm and a wire segment radius of 0.5 mm. It was positioned as described in section 3.2.2 as shown in Figure 3.5.

Analysis was performed for different occupancy scenarios as described in the section 3.2.3. The dielectric properties of the human body at 5.8 GHz have been chosen as described in [80], where the whole body relative permittivity is $\varepsilon_r = 48.2$ and conductivity$\sigma = 6\, S/m$.

The results of the E-field amplitude distributions for the ground floor of the Victorian house are presented. Results were sampled in a plane 1.2 m above the ground, at the same height as the source antenna. 840 samples of the E-field amplitude were obtained from the simulations in both the kitchen and front room. The amplitude probability and the cumulative probability distributions of the E-field distribution have been used for analysis purposes. The methods used to analysis the results are:

Method A – E-field Distribution Calculations.

Method B – E-field Distribution Difference Calculations.

Method C – E-field Amplitude and Cumulative Probability Distribution.

3.3.1 Method A results

The E-field amplitude distribution within Victorian house in the kitchen and the front room for the ten scenarios at 5.8 GHz are shown in Figure 3.6. In the case of open door and no occupants exist in the ground floor, high E-field levels are observed in the kitchen and the area near to the door in the front room ranged between 0 dBV/m to 3 dBV/m which represented by the colour 'orange' as shown in Figure 3.6 (a). This is due to the transmitter was located in the middle of the kitchen facing exactly the middle of door in the kitchen which caused high signals propagated through the door to the front room. The results also show that the closed door has a significant effect on the E-field distributions within the front room. The propagated signals coming through the closed door is attenuated by approximately 21 dBV/m compared to the propagated signals when the door was open as shown again in Figure 3.6 (a) and Figure 3.6 (b), respectively. When there was one human in the kitchen, the signals behind the human are attenuated by approximately 3 dBV/m. While the presence of one occupant in the front room caused attenuation to the E-field by 6 dBV/m. When the number of occupants was increased to four, the E-field levels behind the occupants in the kitchen are attenuated by 9 dBV/m. It is clear from the figures that when the doors are open and there is no human the E-field strength is highest whereas in the other scenarios the E-field decreases and this explains disappearance of the color orange in the figures.

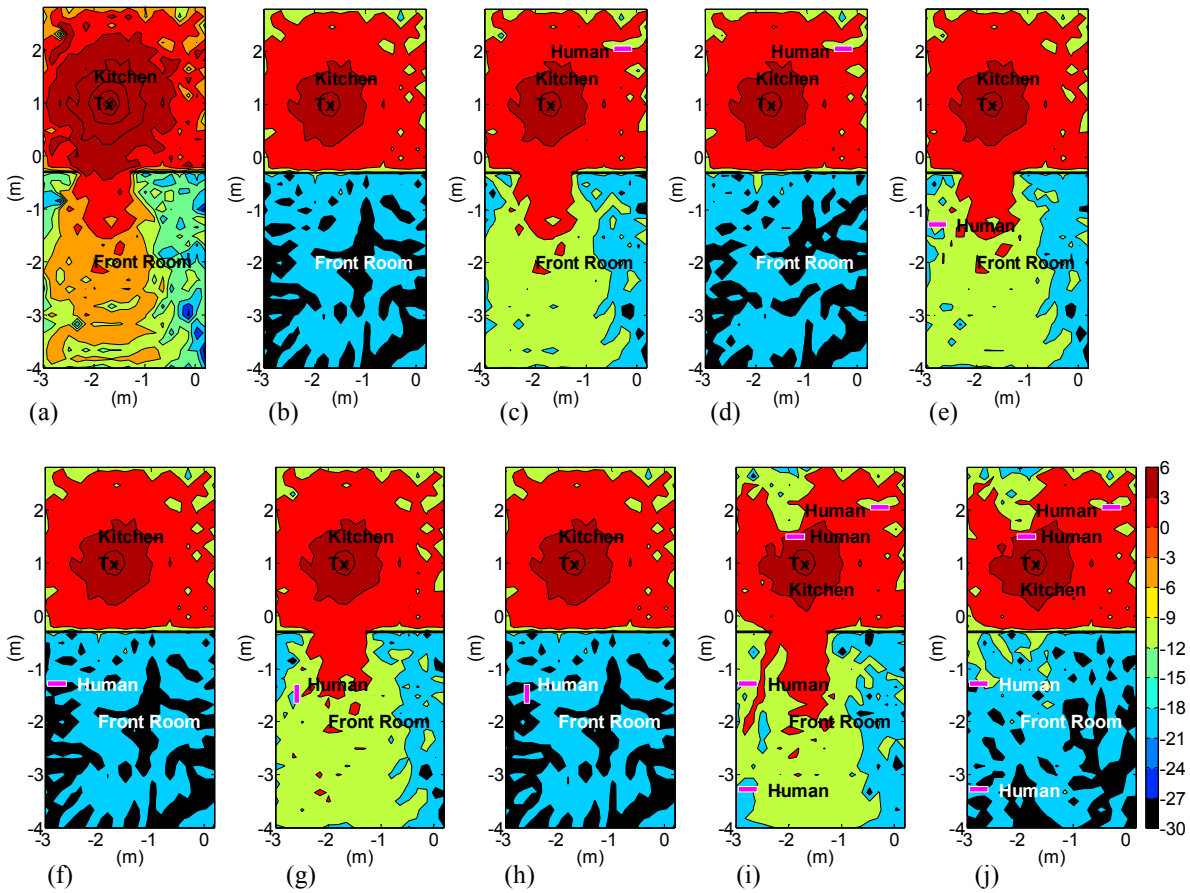

Figure 3.6: Simulated E-field (dBV/m) distributed on the Ground Floor for configuration A at 5.8GHz:

(a) Scenario A (b) Scenario B (c) Scenario C (d) Scenario D (e) Scenario E (f) Scenario F (g) Scenario G (h) Scenario H (i) Scenario I (j) Scenario J.

3.3.2 Method B results

E-field distribution difference plots are used to give a general overview of the spot regions of high or low field levels within the Victorian house. E-field distribution difference plots for a given frequencyΔE (f), was generated using Equation 3.1.

$$\Delta \mathbf{E}\,(\mathbf{f}) = \mathbf{E}(\mathbf{f})_{\mathbf{n}} - \mathbf{E}(\mathbf{f})_{\mathbf{ref}} \qquad (3.1)$$

Whereby $E(f)_{ref}$ is the E-field distribution of the reference scenario (typically A), and $E(f)_n$ is the E-field distribution of the scenario of interest. These results can be used to

visualize and quantify the differences in E-field strength between the ten scenarios described in Section 3.2.3.

Figure 3.7 shows the simulated results for the E-field difference plot between scenarios A (unoccupied, open door) and other scenarios at 5.8 GHz. The E-field strength is shown in dBV/m and the positive values (shown as yellow to red) in figure represent areas with a higher E-field when compared to the reference scenario (A). The negative values (shown as green and blues) in figure represent a weaker E-field when compared to the reference scenario.

When a human occupant was at position 1 and/or 2 within the kitchen, the attenuation various between 3 to 9 dB as shown in Figure 3.7 (b) to Figure 3.7 (i). Figure 5.4 (h) show that the E-field strength is increased at the small area located between the middle wall and the occupant within the front room also varying from 3 dB to 9 dB. This is due to the presence of the occupants in the front room and the middle wall which caused multipath effect. The results of all scenarios clearly demonstrate that the doors status (open or closed) has a significant effect on the E-field coverage in the front room. It can be seen that the orientation of the occupant in the front room has a very limited effect on the signal propagation within the front room as shown in Figure 3.7 (d) and Figure 3.7 (f). When the number of occupants increased from one to four, the E-field distributions in some areas in the front room are increased up to 9 dB.

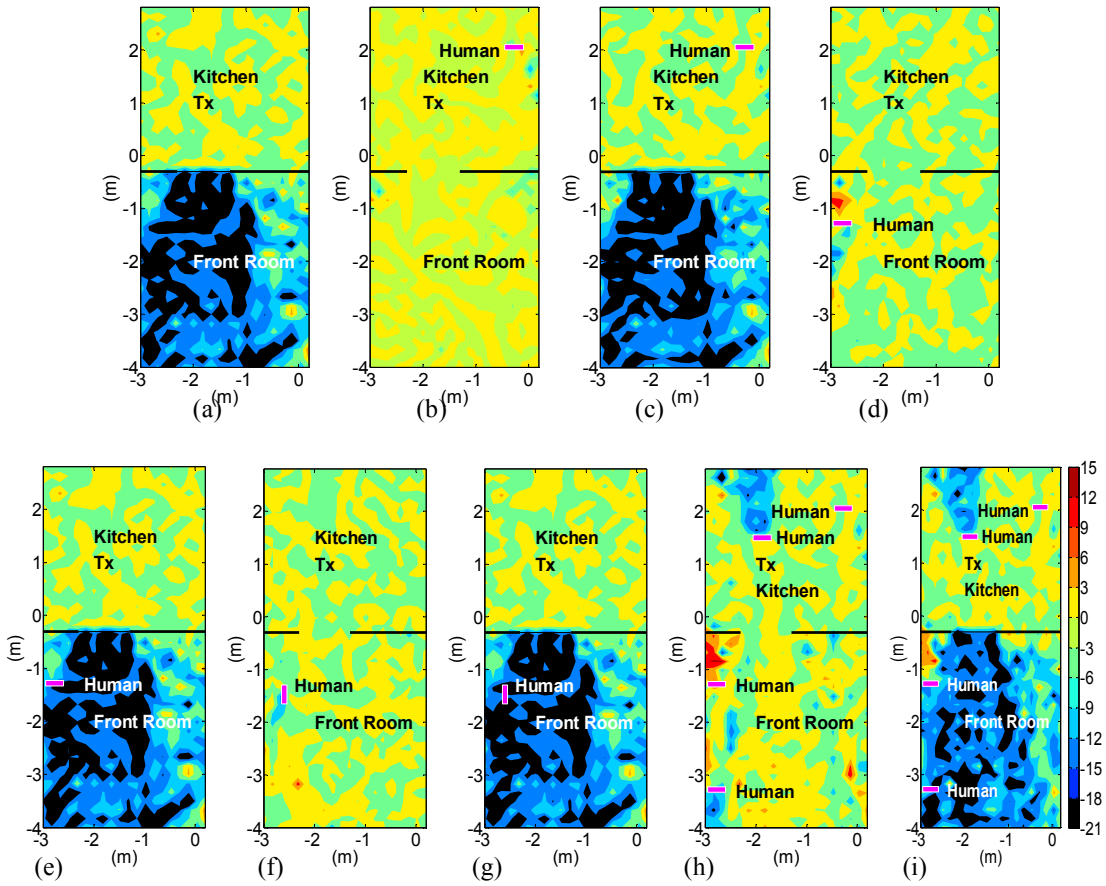

Figure 3.7: Simulated E-field (dB) difference between scenarios for configuration A at 5.8 GHz: (a) Scenario A & B (b) Scenario A & C (c) Scenario A & D (d) Scenario A & E (e) Scenario A & F (f) Scenario A & G (g) Scenario A & H (h) Scenario A & I (i) Scenario A & J.

3.3.3 Method C results

For method C, the amplitude and cumulative probability distributions are used to provide a comparison between different scenarios of the E-field values within the Victorian house at 5.8 GHz. Figure 3.8 (a) and Figure 3.8 (b) show the results of E-field amplitude and cumulative probability distributions from scenario A to scenario J, respectively within the kitchen and front room. The x-axis represents the distribution of the E-field levels while y-axis represents its probability percentage. The results demonstrate that there is no noticeable difference in the E-field distribution in the kitchen for all scenarios. However,

the E-field distributions in the front room have significant variations between the scenarios. It was clear that the closed door has reduced the average value of the E-field by 12 dBV/m attenuation due to the change of the door status from open to closed door. The presence of one occupant in the kitchen or in the front room has a very little effect on the E-field distribution. However, when the number of occupants was increased to four within the ground floor, the E-field distributions are attenuated by 3 dBV/m. It can be seen that from Figure 3.8 (a) the lowest amplitude of the E-field in the kitchen is in case of open door with two occupants in kitchen and two occupants in the front room scenario with an amplitude probability distribution of 16 % at 3 dBV/m. This is due to the presence of four occupants in the ground floor which cause some signals are absorbed and some are reflected.

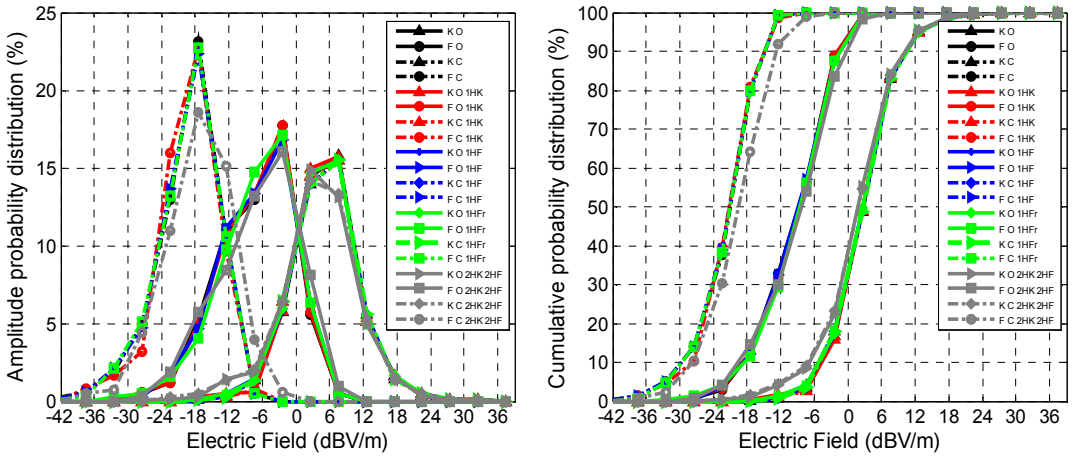

Figure 3.8: E-field amplitude and cumulative probability distribution for configuration A at 5.8 GHz for all scenarios from A to J.

(Key: K = kitchen, F = front room, O = open door, C = closed door, 2HK = two occupants in the kitchen, 2HF= two occupants in the front room, 1HF=one occupant in front room and 1HFr=one occupant rotated in front room).

3.4 Simulation of the E-Field Distributions on Horizontal Plane for configuration A at 2.4 GHz

A dipole antenna resonated at 2.4 GHz frequency was used in the simulation to generate the E-field. The maximum angular resolutions used in the GO calculations were $\theta = 0.15^{\circ}$ and$\emptyset = 0.08^{\circ}$. The dielectric properties of the human body at 2.4 GHz have been chosen as described in [80], where the whole body relative permittivity is $\varepsilon_r = 52.7$ and conductivity $\sigma = 1.95\ S/m$. The length of the dipole antenna is 57.46 mm. The wire segment radius of the dipole antenna is 2 mm.

E-field amplitude distributions were calculated for the ground floor of the Victorian house. Results were sampled in a plane at the same height as the source antenna (1.2 m above the ground). Amplitude probability and the cumulative probability distributions of the E-field distributions have been used for the analysis purposes as described in [81] and [82]. Results obtained from scenario A to scenario J are presented in this section. The same three methods (A, B and C) are used in this section.

3.4.1 Method A Results

The E-field distributions results are presented for the ten scenarios as shown from Figure 3.9 (a) to Figure 3.9 (j). In case of open door and no occupants exist in the ground floor, it can be seen that high E-field levels are obtained in the kitchen and the area near to the door in the front room ranged between 0 dBV/m and 6 dBV/m. However, low E-field levels are obtained in most area in the front room ranged between -21 dBV/m and -9 dBV/m. This is due to the high distance between the transmitter and the receiver which is more than 3 m and also the middle wall has attenuated the propagated signals by 12 dBV/m. Comparing Figure 3.9 (a) and Figure 3.9 (b), the closed door has attenuated the E-field levels in the front room by 12 dBV/m. The presence of one occupant in the kitchen or in the front room has decreased the E-field levels behind it by 3 dBV/m. However, when the number of occupants was increased to four (two occupants exist in the kitchen and two occupants in the front room), low E-field levels are obtained in the large area

behind the nearest occupant in the kitchen ranged between -12 dBV/m and 0 dBV/m. While in the front room, high E-field levels are obtained at the middle of the front room whereas low E-field levels are obtained near to the exterior wall in the front room. The presence of the occupant in the kitchen near to the transmitter caused strong reflection from the occupant passing through to the front room as shown in Figure 3.9 (i).

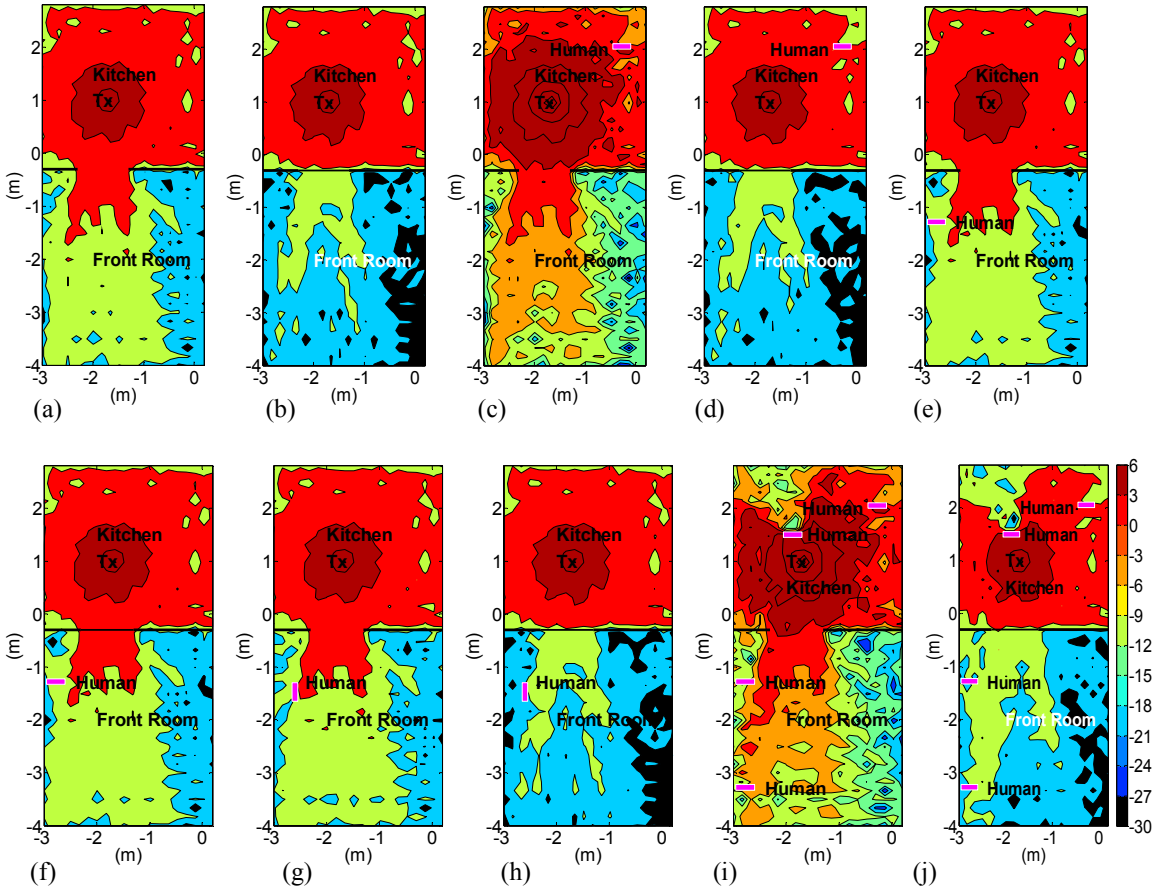

Figure 3.9: Simulated E-field (dBV/m) distributed on the Ground Floor for configuration A at 2.4GHz:

(a) Scenario A (b) Scenario B (c) Scenario C (d) Scenario D (e) Scenario E (f) Scenario F (g) Scenario G (h) Scenario H (i) Scenario I (j) Scenario J.

3.4.2 Method B Results

Figure 3.10 illustrates the E-field level differences between scenario A and the other nine scenarios at 2.4 GHz. It can be seen that the E-field levels in the whole front room is been attenuated by 15 dB due to the closed door between the kitchen and the front room as shown in Figure 3.10 (a). While the presence of one occupant in the kitchen or front room has a gradual effect on the E-field distribution in the ground floor. The E-field strength within ground floor is decreased in range between 3 to 6 dB due to the presence of one occupant in the kitchen or the front room. As the number of the occupants was increased to four and the door was closed, the E-field distributions within the ground floor is attenuated significantly ranged between -6 dB to -18 dB. The occupant in the kitchen which was located 0.5 m away from transmitter decreases the E-field distribution by 18 dB.

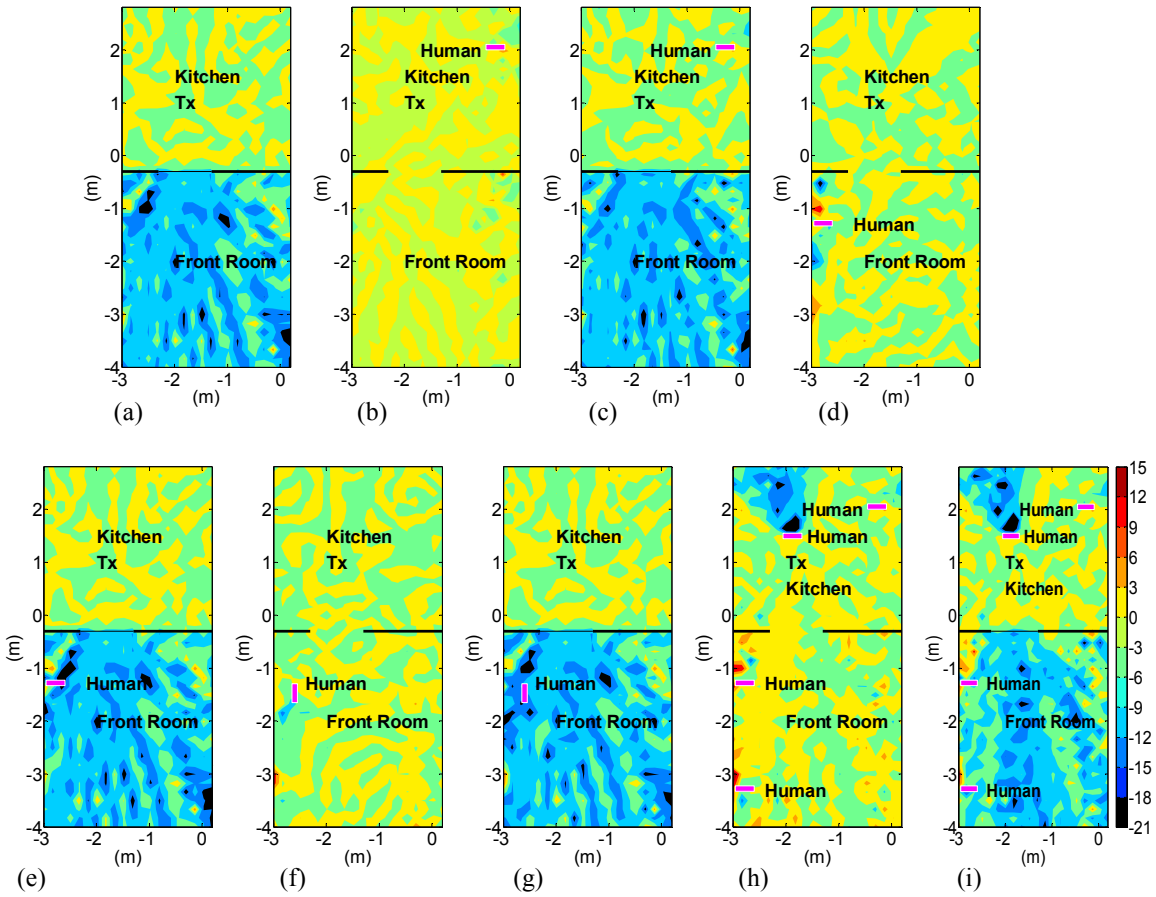

Figure 3.10: Simulated E-field (dB) difference between scenarios for configuration A at 2.4GHz: (a) Scenario A & B (b) Scenario A & C (c) Scenario A & D (d) Scenario A & E (e) Scenario A & F (f) Scenario A & G (g) Scenario A & H (h) Scenario A & I (i) Scenario A & J.

3.4.3 Method C Results

The amplitude and cumulative probability distributions are used to analysis the E-field values for the ten scenarios within the Victorian house at 2.4 GHz as shown in Figure 3.11. The results show that there are very little variations in the E-field distribution values between these scenarios in the kitchen. However, the E-field distributions in the front room have significant variations between scenarios. The results of the cumulative probability distribution show that the average value of the signal in case of the open door in the front room is -9 dBV/m whereas the average value in case of closed door in the

front room is -18 dBV/m, a 9 dBV/m. This attenuation is due to the change of the door status from open to closed door. The presence of one occupant in the kitchen or in the front room has a very little effect on the E-field distribution. However, when the number of occupants was increased to four within the ground floor, the E-field distributions is attenuated by 3 dBV/m. Figure 3.11 shows that the lowest amplitude of the E-field in the kitchen was in case of open door with two occupants in kitchen and two occupants in the front room scenario with an amplitude probability distribution of 14 % at 9 dBV/m. This is due to the presence of four occupants in the ground floor as explained before.

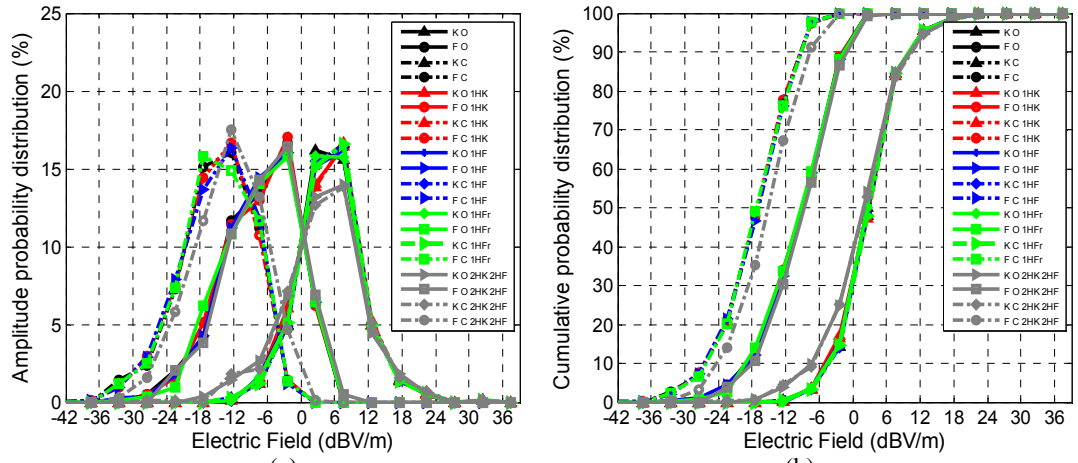

(a) (b)

Figure 3.11: E-field amplitude and cumulative probability distribution for configuration A at 2.4 GHz for all scenarios from A to J.

3.5 Simulation of the E-field distributions on Horizontal Plane for configuration A at 868 MHz

Simulations were carried out using 868 MHz dipole antenna to generate the E-fields. The antenna was located at the same place as described in section 3.4. The locations of transmitter and receivers also located in FEKO simulations at the same place described in section 3.4. In order to select the values of the angular resolutions, many trials were carried out and the final values that selected for this simulation of GO calculations are $\theta = 0.2^{\circ}$ and$\emptyset = 0.2^{\circ}$. The dielectric properties of the human body at 868 MHz were selected based on the characteristics presented in [10]. In this case, the body relative permittivity is $\varepsilon_r =$

55.1 and conductivity$\sigma = 0.9\ S/m$. The dipole antenna has been configured for the 868 MHz with length of 158.88 mm. For these configurations the wire segment radius of the dipole antenna is 2 mm. The same ten scenarios (A to J) described in the previous section are also investigated in this section.

The same parameters that used in the previous section are used in following simulation scenarios. The samples are selected for a plane of 1.2 m above the ground. Around 840 samples of E-field amplitude in both the kitchen and front room were simulated. The amplitude probability and the cumulative probability distributions are used to analysis the E-field distributions. This section presents the results obtained from the scenarios described in section 3.2.3. The same three methods (A, B and C) are also used for analysis.

3.5.1 Method A Results

The E-field amplitude distribution results are calculated for the ten scenarios at 868 MHz as shown in Figure 3.12. High E-field levels were obtained in the kitchen and some area in the front room ranged between -6 dBV/m to 6 dBV/m for the case of open door and no occupant exist in the ground floor. The results illustrates that when the door was closed the E-field strength is reduced by approximately 3 dBV/m. This is due to the low frequency used in the transmitter results in high coverage as shown in Figure 3.12 (b). When one human was in the kitchen or the front room, the signal behind the human is attenuated by approximately 6 dBV/m. While the propagated signals which are far from the occupant in the kitchen or the front room has not been affected. Figure 3.12 (i) shows that a large area behind the nearest occupant to the transmitter in the kitchen have been attenuated by 6 dBV/m when the number of occupants was increased to four.

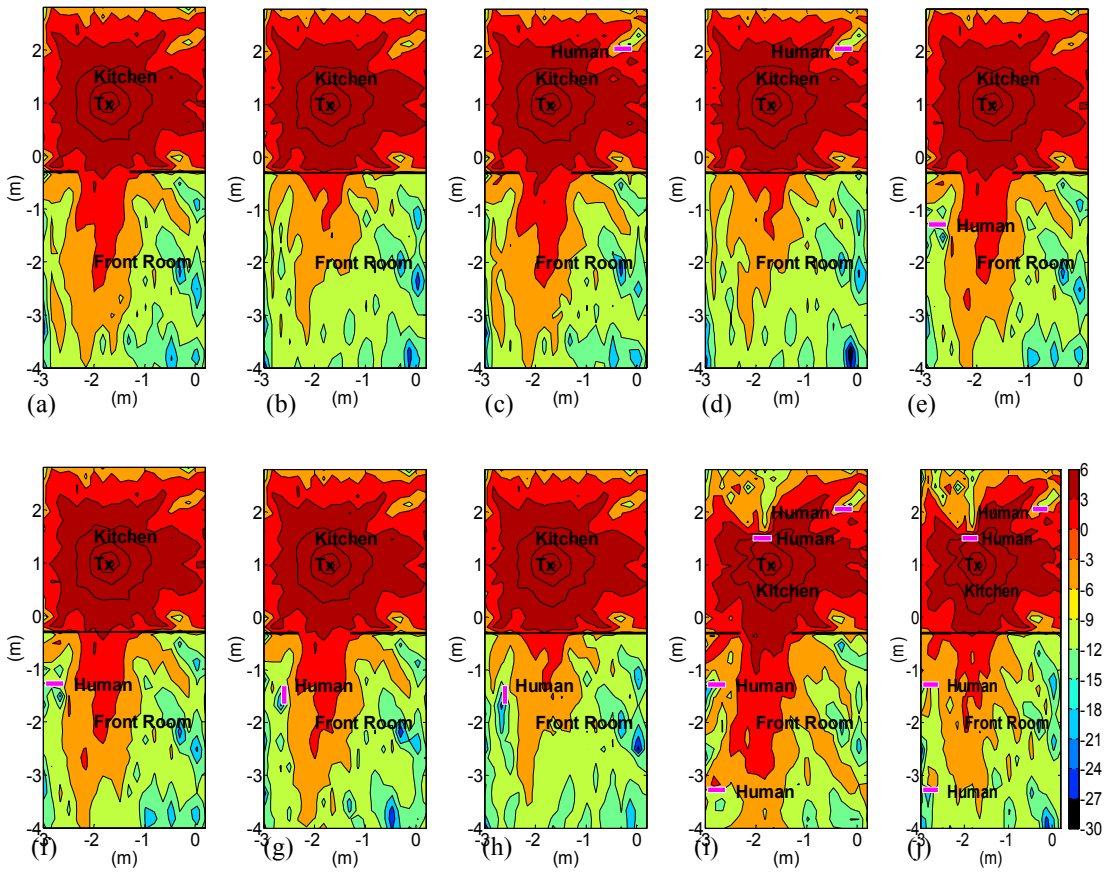

Figure 3.12: Simulated E-field (dBV/m) distributed on the Ground Floor for configuration A at 868 MHz:

(a) Scenario A (b) Scenario B (c) Scenario C (d) Scenario D (e) Scenario E (f) Scenario F (g) Scenario G (h) Scenario H (i) Scenario I (j) Scenario J.

3.5.2 Method B Results

Figure 3.13 shows the simulated results for the E-field difference between scenarios A (unoccupied, open door) and other scenarios at 868 MHz. It can be seen that the door between kitchen and front room attenuated the signals by 6 dB. However, there is a net increase in the E-field strength at some locations within the front room of 6 dB due to the multipath signals. The presence of one occupant in the kitchen or the front room has attenuated the signals by 6 dB. As the number of the occupants was increased to four and the door was open, the E-field distributions in most areas in the kitchen have been

attenuated by 3 to 9 dB. However, the area near to the occupants and the wall in the front room the E-field distributions have been decreased by 6 dB.

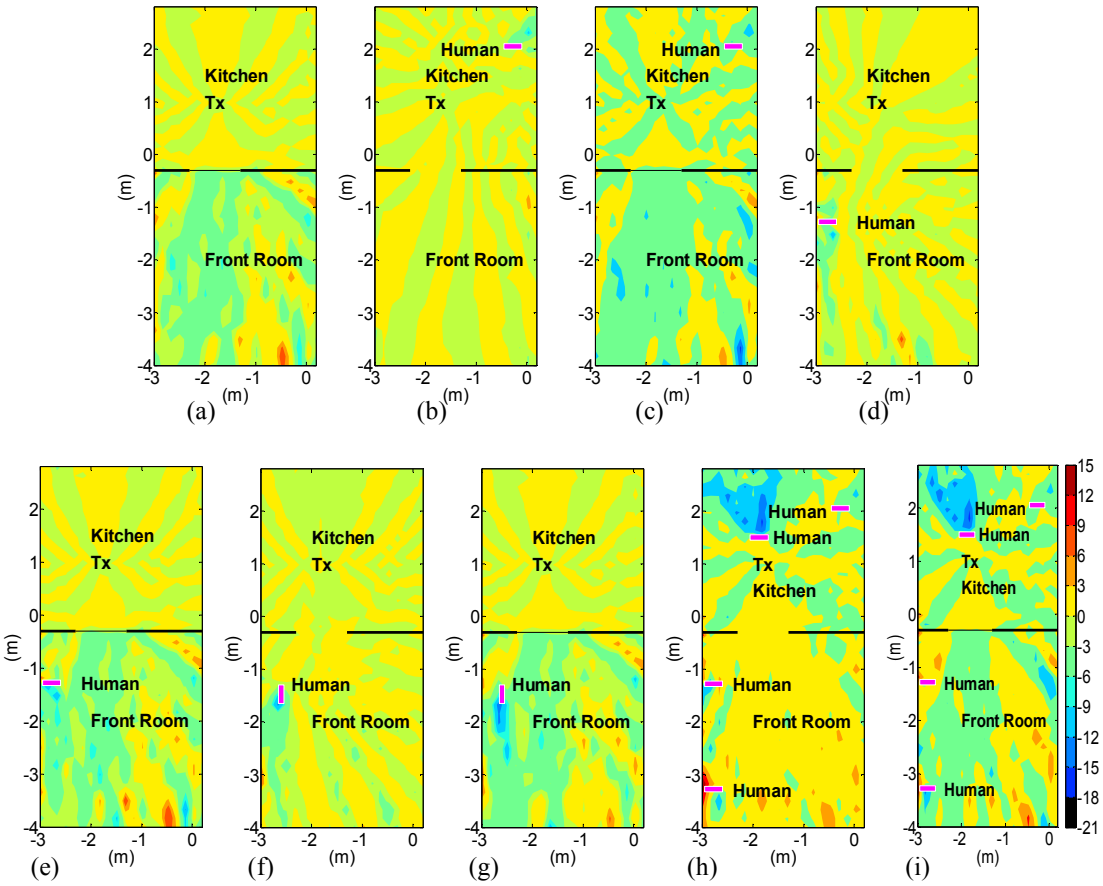

Figure 3.13: Simulated E-field (dB) difference between scenarios for configuration A at 868 MHz:

(a) Scenario A & B (b) Scenario A & C (c) Scenario A & D (d) Scenario A & E (e) Scenario A & F (f) Scenario A & G (g) Scenario A & H (h) Scenario A & I (i) Scenario A & J.

3.5.3 Method C Results

The amplitude and cumulative probability distributions are used to analysis the E-field values for the ten scenarios within Victorian house at 868 MHz as shown in Figure 3.14 . The results show that there are very little variations in the E-field distribution values between the scenarios in the kitchen.

Figure 3.14 (a) illustrates that the lowest amplitude of the E-field in the kitchen was in case of open door with two occupants in kitchen and two occupants in the front room scenario with an amplitude probability distribution of 14 % at 9 dBV/m. This is due to the presence of four occupants in the ground floor which cause some signals are absorbed and some reflected. It can be seen from cumulative probability distribution that the average values of the signals for all scenarios in the front room are within 3 dBV/m and ranged between -9 dBV/m and -6 dBV/m.

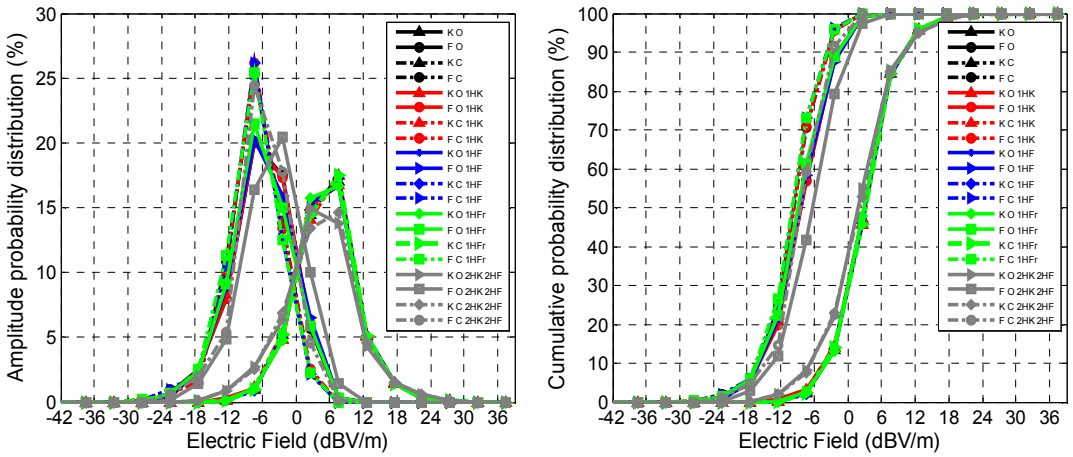

(a) (b)

Figure 3.14: E-field amplitude and cumulative probability distribution for middle antenna at 868 MHz for all scenarios from A to J.

3.6 Simulation of the E-Field Distributions on Horizontal Plane for configuration A at 433 MHz

The E-field was generated using 433 MHz dipole antenna in the following simulations. The parameters that used in these simulations are the same as described in section 3.5. The values of the angular resolutions in these simulations are $\theta = 0.2^{\circ}$ and$\emptyset = 0.2^{\circ}$. Also, in these simulations TDS is used. The dielectric properties of human body at 433 MHz were selected based on the characteristics described in [10]. In this case, the body relative permittivity is $\varepsilon_r = 56.7$ and conductivity$\sigma = 0.94\, S/m$. The length of the dipole is

325.41 mm. For this design the wire segment radius of the dipole antenna is 2 mm. Based on the design described above, ten different scenarios were designed named as (A to J). As described in the previous section, the results focus on the E-field amplitude distributions for the ground floor of the Victorian house. The numbers of samples that were analysed in these results are also 480. Again, the E-field was analysed using the amplitude probability and the cumulative probability distributions. This section presents the results obtained from the scenarios described in section 3.2.3.

3.6.1 Method A Results

The E-field amplitude distribution within Victorian house in the kitchen and the front room for the described ten scenarios at 433 MHz are shown in Figure 3.15. In case of open door and no occupant exist in the ground floor, high E-field levels are obtained in the kitchen and most areas in the front room ranged between -9 dBV/m and 6 dBV/m. The low E-field distributions are observed in some small areas near to the exterior wall in the front room with value of -18 dBV/m. The results show that when the door is closed the E-field distributions in the front room are reduced by approximately 3 dBV/m as shown in Figure 3.15 (b). When one human was in the kitchen or in the front room, the signal behind the human is attenuated approximately by 3 dBV/m whereas the signals in other areas in the kitchen and the whole front room have not been affected by the existence of human in the kitchen. Figure 3.15 (i) shows that the E-field levels are deceased between 3 to 6 dBV/m in some areas in the kitchen when the number of people was increased to four.

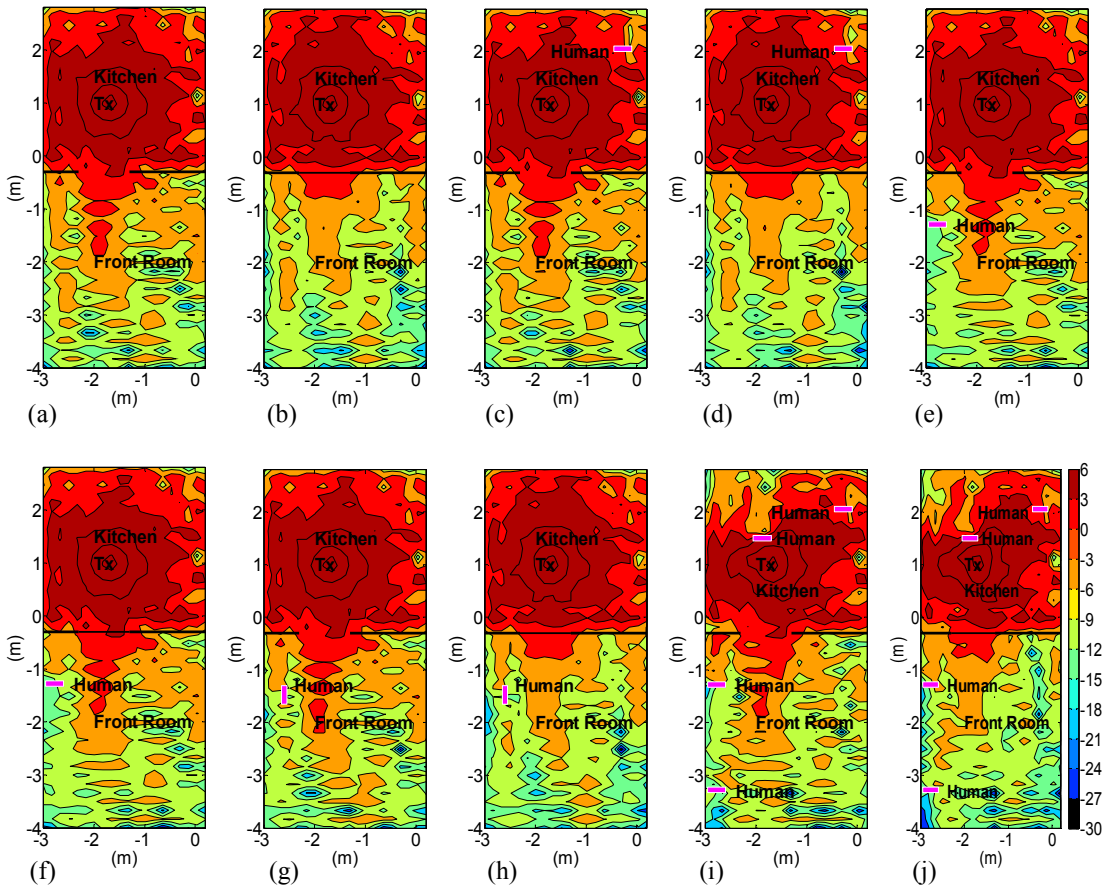

Figure 3.15: Simulated E-field (dBV/m) distributed on the Ground Floor for middle antenna at 433 MHz:

(a) Scenario A (b) Scenario B (c) Scenario C (d) Scenario D (e) Scenario E (f) Scenario F (g) Scenario G (h) Scenario H (i) Scenario I (j) Scenario J.

3.6.2 Method B Results

Similar investigations to those in the previous section were carried out in this section at 433 MHz. The differences in the E-field distribution are plotted to show the E-field strength variations between the investigated scenarios. Figure 3.16 illustrates the E-field level differences between scenario A and other nine scenarios at 433 MHz. It can be seen that the door between kitchen and front room attenuates the signals in most area in the front room by 3 dB. While the presence of the occupants in the kitchen and front room has a different effect on the E-field distribution in the ground floor. The E-field strength

in some small area behind the occupant in the kitchen is decreased by 3 dB. However, the E-field in large area behind occupant in the front room is attenuated by 6 dB. This is due to the low frequency used in the transmitter which produces a high signal coverage. As the number of the occupants increased to four in the ground floor, the E-field distributions in the ground floor is attenuated between 3 to 9 dB. The human in the Kitchen which located 0.5 m away from transmitter has a significant effect on the E-field distribution on the kitchen which attenuated approximately by 9 dB as shown in Figure 3.16 (h).

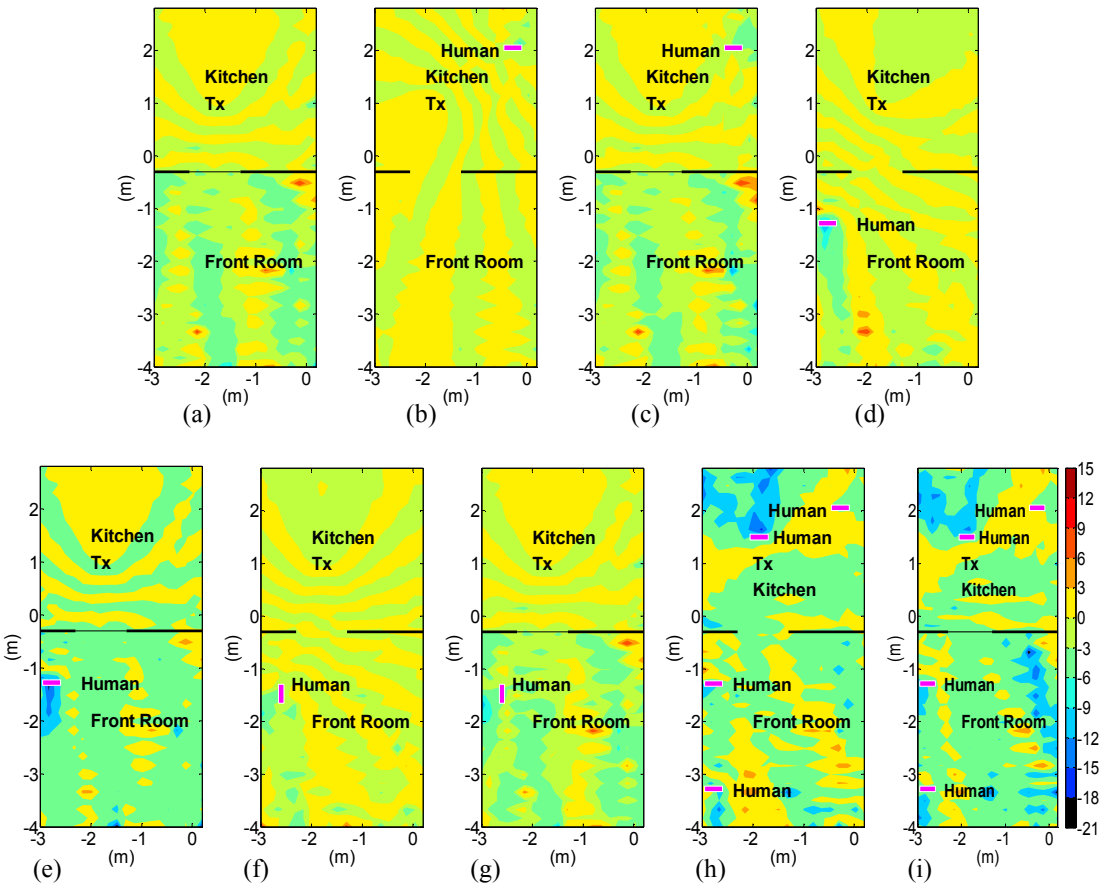

Figure 3.16: Simulated E-field (dB) difference between scenarios for middle antenna at 433 MHz:

(a) Scenario A & B (b) Scenario A & C (c) Scenario A & D (d) Scenario A & e (e) Scenario A & F (f) Scenario A & G (g) Scenario A & H (h) Scenario A & I (i) Scenario A & J.

3.6.3 Method C Results

The amplitude and cumulative probability distributions are used to analysis the E-field values for the ten scenarios within Victorian house at 433 MHz as shown in Figure 3.17. The results show that there are very little variations in the E-field distribution values between the scenarios for both the kitchen and the front room. Figure 3.17 (a) illustrates that the lowest amplitude of the E-field in the kitchen is in case of open door with two occupants in kitchen and two occupants in the front room scenario with an amplitude probability distribution of 15 % at 8 dBV/m. This is due to the presence of four occupants in the ground floor which cause some signals are absorbed and some reflected.

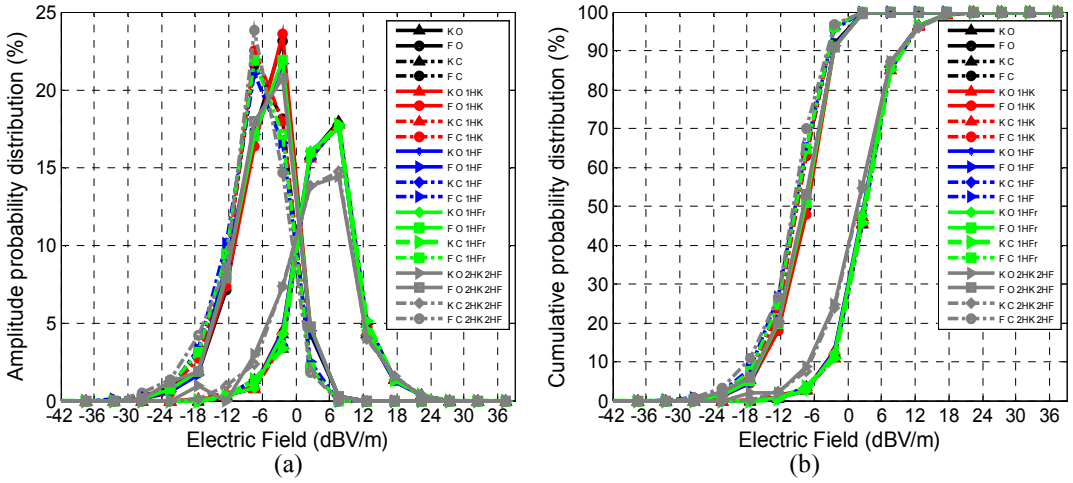

Figure 3.17: E-field amplitude and cumulative probability distribution for middle antenna at 433 MHz for all scenarios from A to J.

3.7 Summary Analysis

This section compares the results of the E-field distributions for the frequencies of 5.8 GHz, 2.4 GHz, 868 MHz and 433 MHz. The transmitter for all the frequencies was placed in the same location in the kitchen as follows: 1.2 m above the ground, 1.3 m from middle wall and 2.1 m from external wall. The scale of the E-field levels that is used at the receiver ranges from -30 dBV/m to 6 dBV/m for all frequencies. The effect of the door status and presence of occupants within ground floor on the E-field distributions across the four frequencies and comparison between them are discussed in the following section.

3.7.1 Analysis of E-field without Occupants

The E-field amplitude distributions results are presented for open door and no occupants scenario within ground floor in the Victorian house for all four frequencies as shown in Figure 3.18. Based on these results, the high E-field coverage at the low frequencies (i.e. 868 MHz and 433 MHz) is higher than at the high frequencies (i.e. 5.8 GHz and 2.4 GHz). The internal wall attenuates the signals coverage at high frequencies more than at the low frequencies. It can also be seen that the E-field levels at high frequencies with the internal wall are -15 dBV/m whereas at low frequencies are 6 dBV/m. The results demonstrate that the highest coverage signals within the front room across the four frequencies is at 433 MHz and is ranged between 3 dBV/m and -15 dBV/m whereas the lowest coverage signals within the front room was at 2.4 GHz and is ranged between 0 dBV/m and -24 dBV/m.

The effect of closing the door on the E-field amplitude coverage at the four frequencies is shown in Figure 3.19. It is observed that closing the door attenuated the propagated signal with different levels among the four frequencies. The door status (opening or closing) has a significant effect on the E-field distributions within the front room at the high frequencies. The propagated signals are attenuated by approximately 12 dBV/m when passed through the closed door at high frequencies whereas at low frequencies they are attenuated only by 3 dBV/m. The results demonstrate that the internal wall has attenuated the E-field distributions more than the door for all the four frequencies. This is due that

the internal wall made of brick and the door made of wood and the loss tangent of brick is higher than the loss tangent of wood.

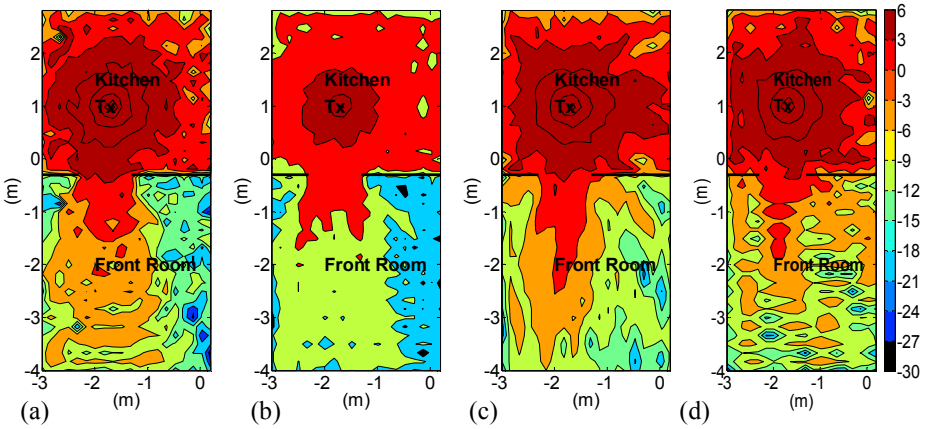

Figure 3.18: Simulated E-field (dBV/m) results for open door and middle antenna at different frequencies:

(a) 5.8 GHz (b) 2.4 GHz (c) 868 MHz (d) 433MHz.

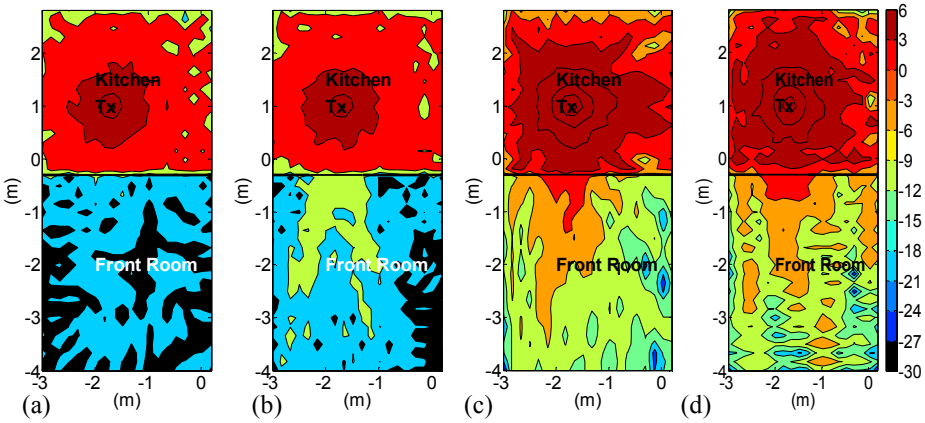

Figure 3.19: Simulated E-field (dBV/m) results for closed door and middle antenna at different frequencies:

(a) 5.8 GHz (b) 2.4 GHz (c) 868 MHz (d) 433MHz.

The amplitude and cumulative probability distributions are used to provide simplified comparison between the different four investigated frequencies of the E-field values for open door scenario within the Victorian house. Figure 3.20 (b) illustrates that the E-field distribution in the kitchen for open scenario is similar for all four frequencies. This similarity is due to the presence of the transmitter source in the kitchen and there are no

obstructions between the transmitted source and receiver probes. It can be seen from cumulative probability distribution that there is no variation in the E-field distribution in the front room for open scenario at 5.8 GHz and 2.4 GHz. Comparing the high frequencies and low frequencies in the front room for open scenario, the results demonstrate that from 0 % to 50 % of cumulative probability distribution for the low frequencies are higher than the high frequencies by 3 dBV/m. Figure 3.20 (a) shows the highest E-field amplitude probability distribution values are at 433 MHz and reached 23% at -3 dBV/m. The E-field amplitude and the E-field cumulative probabilities distributions of closed door scenario are obtained for the four frequencies within ground floor. It can be seen that from Figure 3.21 (b) the variations in the E-field amplitude probability distributions between the four frequencies in the kitchen are minimal for the case of closed door scenario. However, for the case of closed door scenario in the front room there are some noticeable variations in the E-field distribution between the different four frequencies. At low frequencies, the E-field distributions values in the front room for the case of closed door scenario are similar. The average E-field cumulative probability distributions in front room for closed door scenario at low frequencies have similar values which is approximately -9 dBV/m. The results also show that the average E-field cumulative probability distributions values in front room at 5.8 GHz and 2.4 GHz frequencies are -21 dBV/m and -17 dBV/m, respectively. The peak value of the E-field amplitude probability distribution at 868 MHz and reached 26% at -7 dBV/m while the peak for 2.4 GHz is 17 % at -12 dBV/m as observed in Figure 3.21 (a).

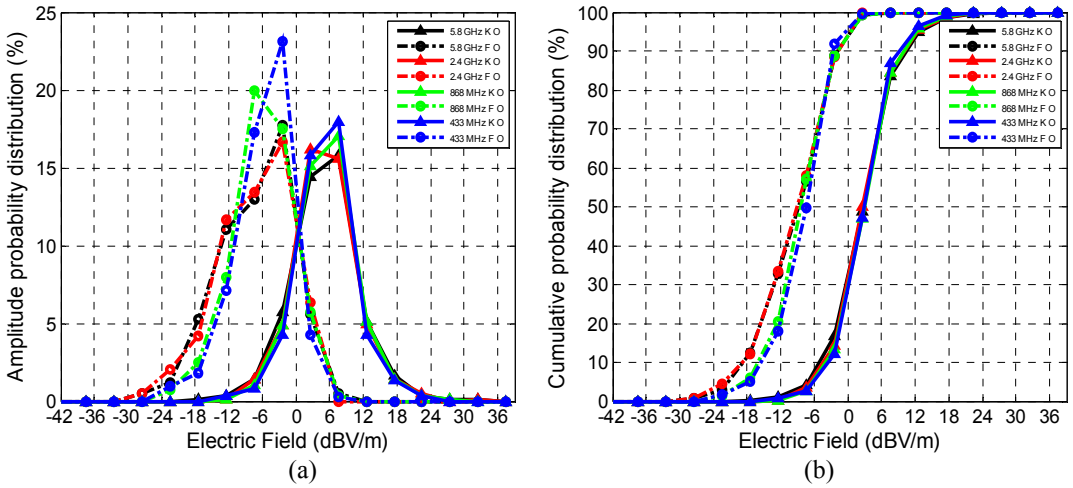

(a) (b)

Figure 3.20: E-field amplitude and cumulative probability distribution at 5.8 GHz, 2.4 GHz, 868 MHz and 433 MHz for open door and middle Antenna scenario.

(Key: K = kitchen, F = front room, O = open door).

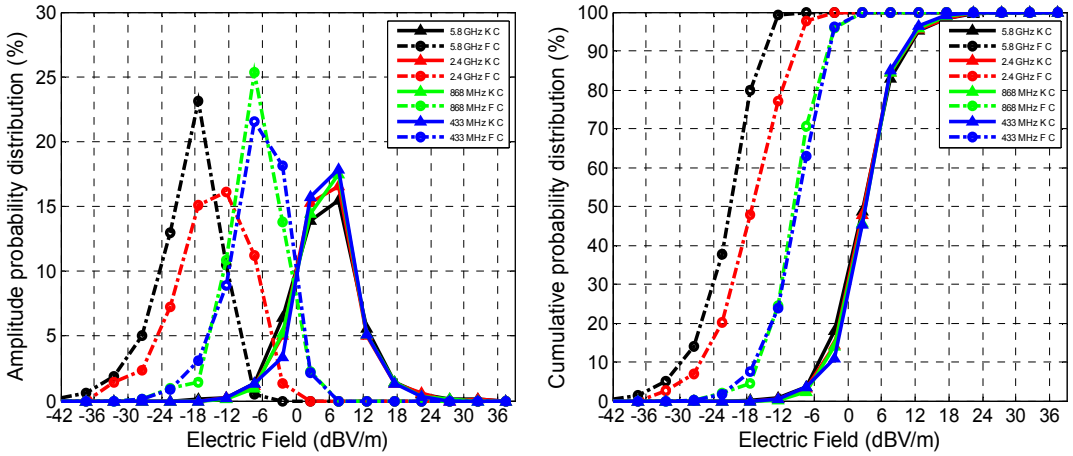

(a) (b)

Figure 3.21: E-field amplitude and cumulative probability distribution at 5.8 GHz, 2.4 GHz, 868 MHz and 433 MHz for closed door and middle antenna scenario.

(Key: K = kitchen, F = front room, C = closed door).

The E-field levels within Victorian house are used to obtain the difference between the open door and the closed door scenarios at 5.8 GHz, 2.4 GHz, 868 MHz, 433 MHz as shown in Figure 3.22. It can be observed that the door status has a significant effect on the E-field coverage in the front room. These effects are more obvious at high frequencies

than are at low frequencies. At 868 MHz and 433 MHz, the difference in E-field coverage between the open and the closed door scenarios in the front room are decreased by 6 dBV/m. However, at 2.4 GHz, the difference in E-field coverage between these scenarios in the front room are attenuated by 18 dBV/m. Comparing the effect of door status on the E-field distributions between the four frequencies, the largest effects are observed at 5.8 GHz. The E-field values at 5.8 GHz in the most of area in the front room have a very low E-field values which attenuated by -21 dBV/m. This is due to that the loss in the propagated signals at high frequencies source is higher than in the propagated signals at low frequencies.

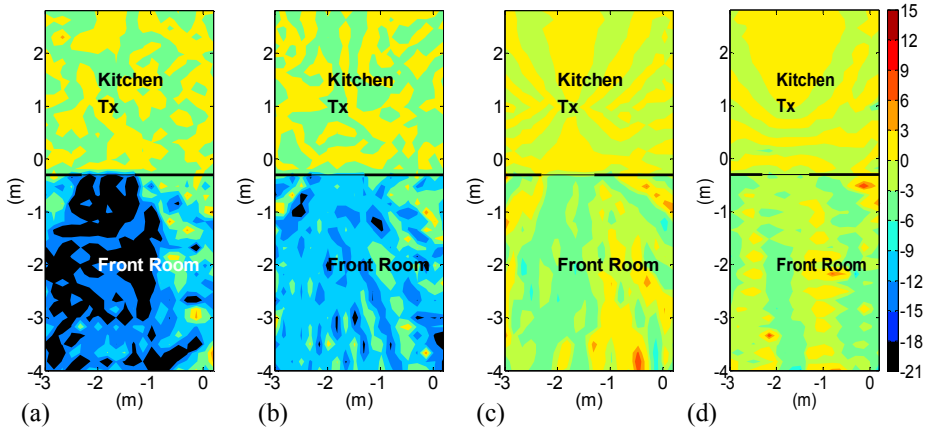

Figure 3.22: Simulated E-field (dBV/m) difference between open and closed door scenarios at different frequencies:
(a) 5.8 GHz (b) 2.4 GHz (c) 868 MHz (d) 433MHz.

3.7.2 Analysis of E-field with Occupants

The E-field amplitude distributions within Victorian house in the kitchen and in the front room for scenario (I) which includes two occupants in the kitchen and two occupants in the front room with the door is open at all four frequencies as illustrated in Figure 3.23. Comparing the results of the effect of presence of human in the kitchen across all the frequencies show that the E-field levels values behind occupant are about -12 dBV/m, -3 dBV/m, -9 dBV/m and -3 dBV/m at 5.8 GHz, 2.4 GHz, 868 MHz and 433 MHz, respectively. It can also be seen that when the number of the occupants was increased in

the kitchen, the coverage of signals in the kitchen behind the occupants are attenuated. Comparing the effect of the occupants on the E-field coverage in the front room across the four frequencies shows that the most significant effects are the high frequencies. Also, the low E-field distributions in the front room was occurred near to the exterior wall and behind the occupant at 5.8 GHz ranged between -15 dBV/m and -24 dBV/m.

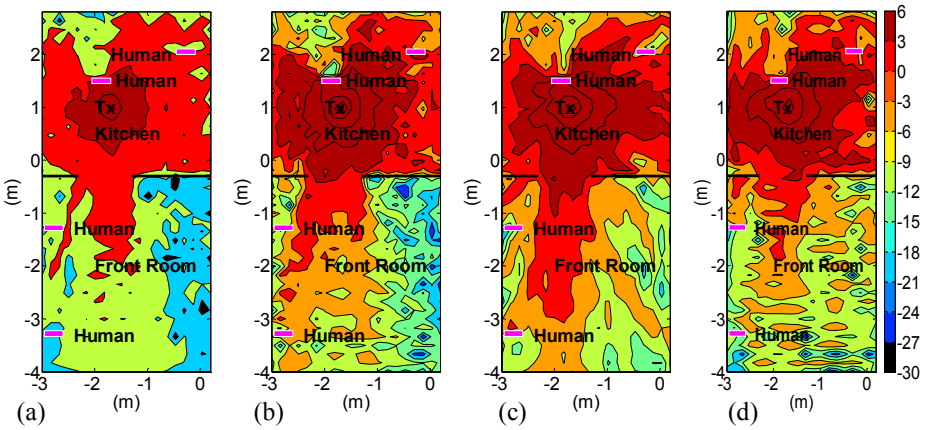

Figure 3.23: Simulated E-field (dBV/m) results for open door &4human at different frequencies: (a) 5.8 GHz (b) 2.4 GHz (c) 868 MHz (d) 433MHz.

A comparison between the results of the amplitude and cumulative probability distributions of the E- field for the scenario (I) at the difference four frequencies was carried out as shown in Figure 3.24. When comparing the E-field values in the kitchen for the all frequencies, it can be seen that there is no variations of the E-field values in the kitchen between the four frequencies which is due to presence of the transmitted source in the kitchen. In contrast, there are variations in the E-field levels between the four frequencies in the front room. At 433 MHz, the difference in the E-field cumulative probability distribution in the front room is between 0 % and 50 % with value of 33 dBV/m. However, at 2.4 GHz the level difference is about 24 dBV/m. It can be seen that there is a small variations within the region between 30 % to 100 % of the E-field cumulative probability distribution in the front room which is approximately 3dBV/m. Figure 3.24 (a) shows that the highest amplitude of the E-field values in the front room was at 433 MHz with amplitude probability distribution of 21 % at -8 dBV/m.

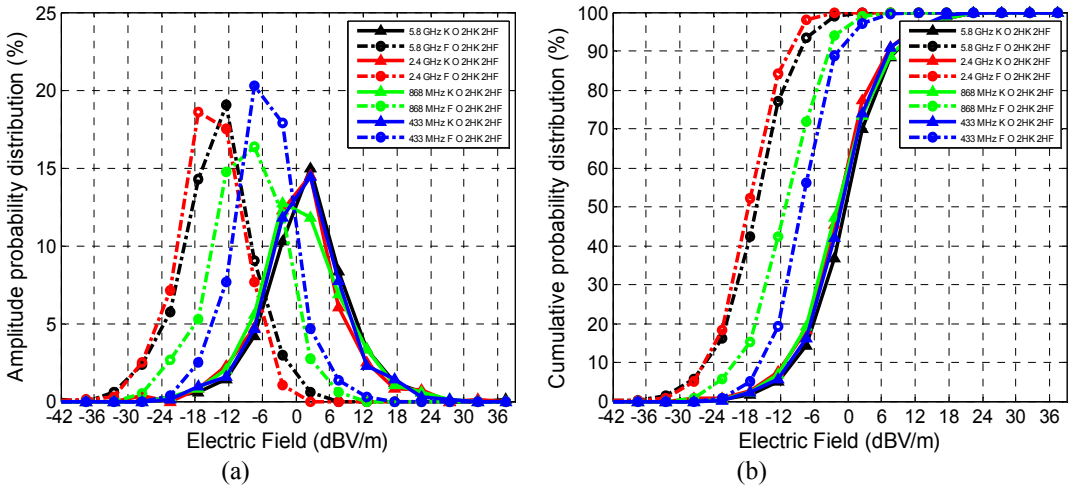

(a) (b)

Figure 3.24: E-field amplitude and cumulative probability distribution at 5.8 GHz, 2.4 GHz, 868 MHz and 433 MHz for open door with two human in kitchen and two human in front room scenario.

(Key: K = kitchen, F = front room, O = open door, 2HK = two occupants in the kitchen, 2HF= two occupants in the front room).

Figure 3.25 illustrates the simulated results for the E-field difference between the open door scenario and scenario (I) at 5.8 GHz, 2.4 GHz, 868 MHz and 433 MHz. It can be seen that the E-field coverage within kitchen are decreased when the number of the occupants in the kitchen are increased. The nearest occupant from the source transmitter in the kitchen has a biggest effect on the E-field distribution in the kitchen at 2.4 GHz which attenuated by -18 dBV/m. At 5.8 GHz and 2.4 GHz there is a net increase in the E-field strength at some locations near to the occupants within the front room between 9 dBV/m to 12 dBV/m. This is due to the constructive and the destructive reflections on the signals caused by the obstacles such as the wall, doors and human. However, these obstacles affect the field coverage levels in the most of the area within the kitchen and the front room at 433 MHz which attenuated the signal by -6 dBV/m to -15 dBV/m as shown in Figure 3.25 (d).

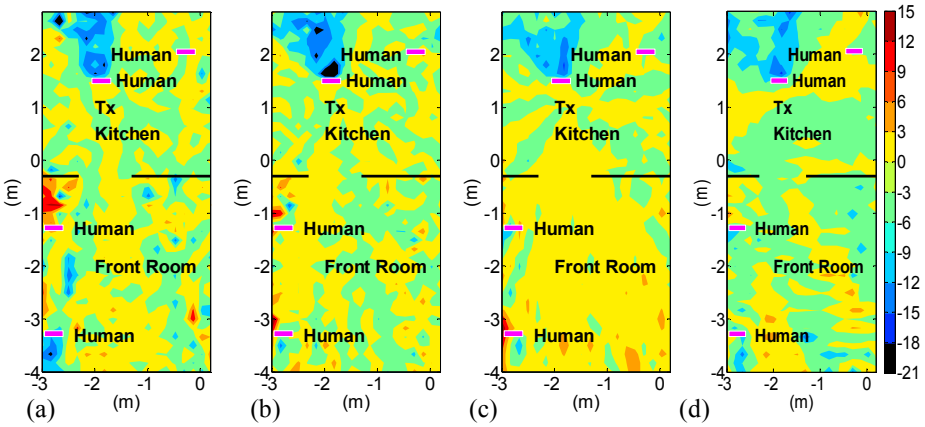

Figure 3.25: Simulated E-field (dBV/m) difference between open door and open door with two human in kitchen and two human in front room scenario at different frequencies: (a) 5.8 GHz. (b) 2.4 GHz. (c) 868 MHz. (d) 433MHz.

3.7.3 The Average E-field Analysis for All Frequencies

The average E-fields obtained for all ten scenarios in the front room and kitchen at 5.8 GHz, 2.4 GHz, 868 MHz and 433 MHz are summarized in Table 3.4. The results show that the average E-field values at 868 MHz and 433 MHz in the front room are little affected by the presences of human or door status. The impact of the closed doors on the average E-field values in the front room is becoming more apparent in the 5.8 GHz and 2.4 GHz results. By comparing scenarios A and B in the four different frequencies in the front room, the variations in the average E-field values at 5.8 GHz and 2.4 GHz are approximately 12.2 dBV/m and 7.6 dBV/m, respectively. However, the variations in the average E-field values caused by closed door in the front room at 868 MHz and 433 MHz are less than 2 dBV/m. Also it can be seen that the presence of occupants within ground floor have no effect on the average E-field values in the front room for all the four frequencies as observed in scenario A, C, E, G and I. The average E-field values in the front room at the low frequencies are higher than at the high frequencies.

The average E-field values in the kitchen are higher than the average E-field values in the front room. This is due that the transmitter source was placed in the kitchen. When comparing the average E-field values for all scenarios between the different four

frequencies, it can be observed that the average E-field values for all scenarios between the different four frequencies are similar. The door status has no effect on the average E-field value within the kitchen for all four frequencies. It can be seen that there is no effect on the average E-field values in the kitchen due to the presence of one occupant in the front room or in the kitchen for all four frequencies. When the number of the occupants within ground floor was increased to four, the average E-field values are reduced to 2dBV/m for all four frequencies as shown in scenarios I and J in Table 3.4.

Table 3.4: The average electric fields for all scenarios within Front Room and Kitchen.

Scenario	Average Electric Field in Front Room (dBV/m)				Average Electric Field in Kitchen (dBV/m)			
	5.8GHz	2.4 GHz	868 MHz	433 MHz	5.8GHz	2.4 GHz	868 MHz	433 MHz
A	-7.1	-7.5	-6.1	-5.7	5.1	5.3	5.3	5.2
B	-19.3	-15.1	-7.5	-7.1	5.1	5.3	5.4	5.4
C	-7.1	-7.5	-6.0	-5.6	5.1	5.2	5.2	5.2
D	-19.2	-15.1	-7.4	-7.0	5.1	5.2	5.3	5.4
E	-7.1	-7.4	-6.2	-5.9	5.1	5.3	5.4	5.1
F	-19.2	-15.1	-7.6	-7.4	5.1	5.3	5.4	5.4
G	-7.1	-7.4	-6.3	-5.8	5.1	5.3	5.3	5.2
H	-19.2	-15.0	-7.7	-7.3	5.1	5.3	5.4	5.4
I	-6.9	-6.9	-4.2	-6.1	4.1	3.9	4.2	3.7
J	-17.4	-13.1	-5.9	-7.9	4.0	3.9	4.3	4.0

3.8 Other Parameters that Effect the E-Field Distributions

This section investigates some other parameters that may affect the signal propagation within the building. The effect of other material properties such as the permittivity and the loss tangent on the signal propagation has been investigated. The permittivity and the loss tangent of the brick material were changed from our measured values ($\varepsilon = 5\ and\ \tan\delta = 0.04$) and compared with the standard brick material values in FEKO

library ($\varepsilon = 3.8\ and\ \tan\delta = 0.55$)which were used throughout our main investigation. Four scenarios were designed to investigate the effect of changing the permittivity and loss tangent at 2.4 GHz. In the first scenario, the permittivity of brick was changed from 3.8 to 5 and the loss tangent was fixed at 0.55. In the second scenario, the loss tangent was changed from 0.55 to 0.04 and the permittivity was fixed at 3.8. Then the permittivity and loss tangent were set to 5 and 0.04, respectively in third scenario. In the fourth scenario, the internal walls in the building were changed from brick to plasterboard material with permittivity of 2.41 and loss tangent of 0.09 as shown in Table 3.2.

The amplitude and cumulative probability distributions were used to provide a comparison between the E-field values within the Victorian house at 2.4 GHz in the four scenarios. Figure 3.26 (a) and Figure 3.26 (b) show the results of E-field amplitude and cumulative probability distributions for the previous scenarios within the kitchen and front room. The results demonstrate that there is no noticeable difference in the E-field distribution in the kitchen for all scenarios. However, the E-field distributions in the front room have significant variations between the scenarios. It is clear from scenario 2 that changing the loss tangent from 0.55 to 0.04 increased the average value of the E-field by 3 dBV/m. Scenario 1 results show that changing the permittivity of material has very little effect on the E-field distribution as shown in Figure 3.26 (b). Scenario 3 results show that the loss tangent has a dominant effect on the E-field values where the average value of the E-field is increased by 3 dBV/m which is similar to the results in scenario 2. When the internal wall material was changed from brick to plasterboard, the E-field distributions are attenuated by 3 dBV/m. Figure 3.26 (a) shows that the highest amplitude of the E-field in the front room is when the material with the permittivity of 3.8 and loss tangent of 0.04 are used and the amplitude probability distribution is 18 % at -3 dBV/m. This is due to the decrease in the loss tangent.

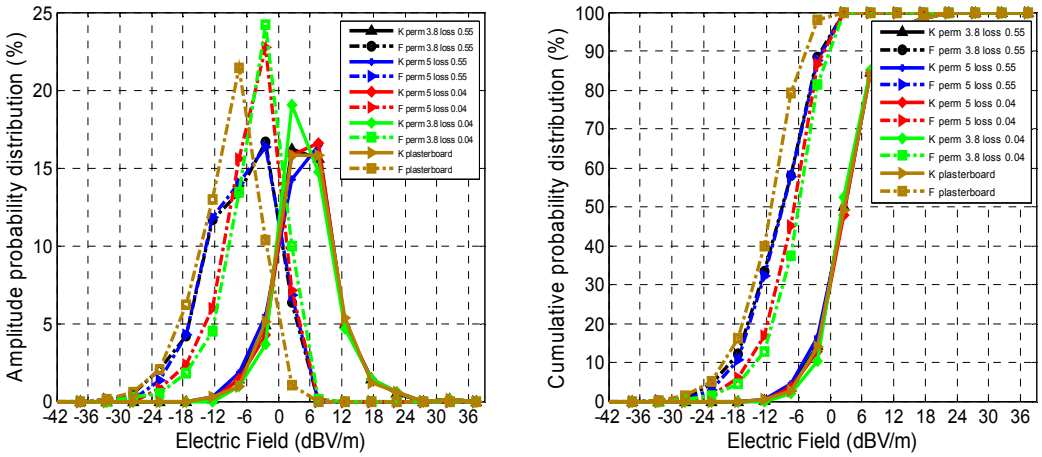

(a) (b)

Figure 3.26: E-field amplitude and cumulative probability distribution for material properties at 2.4 GHz.

The effect of internal wall thickness and the furniture such as sofa, TV and TV table placed in the front room on the E-field distribution in the kitchen and front room has been studied and compared with the results of scenario A in section 3.2.3 (no furniture and thickness of 10 cm). The sofa was placed near to the door in the front room and the TV and TV table were placed in the corner in the front room. The sofa is made of polyester ($\varepsilon = 1.6\ and\ \tan\delta = 0.02$) [83] with size of 1.2 m x 2 m. TV is made of glass ($\varepsilon = 6.39\ and\ \tan\delta = 0.129$) with size of 42 inch and TV table is made of wood ($\varepsilon = 2.18\ and\ \tan\delta = 0.23$) with size of 1m x 0.5 m. The parameters of the TV and table were taken from FEKO library. In order to carry out these investigations three scenarios were designed as follows: scenario 1 some furniture was placed in the front room, scenario 2 the thickness of internal wall was set to15 cm and in the third scenario the wall thickness was set to 20 cm. The amplitude and cumulative distributions function are used to analysis the E-field values for these scenarios within Victorian house at 2.4 GHz as shown in Figure 3.27. The word "original" in the legend of the figures refers to scenario A. By comparing the results of the three scenarios, it can be seen that there are very little variations in the E-field distribution values between the scenarios in both the kitchen and the front room as shown in Figure 3.27 (b). Figure 3.27 (a) illustrates that amplitude of the

E-field in the front room is the same for all the scenarios with an amplitude probability distribution of 17 % at -3 dBV/m.

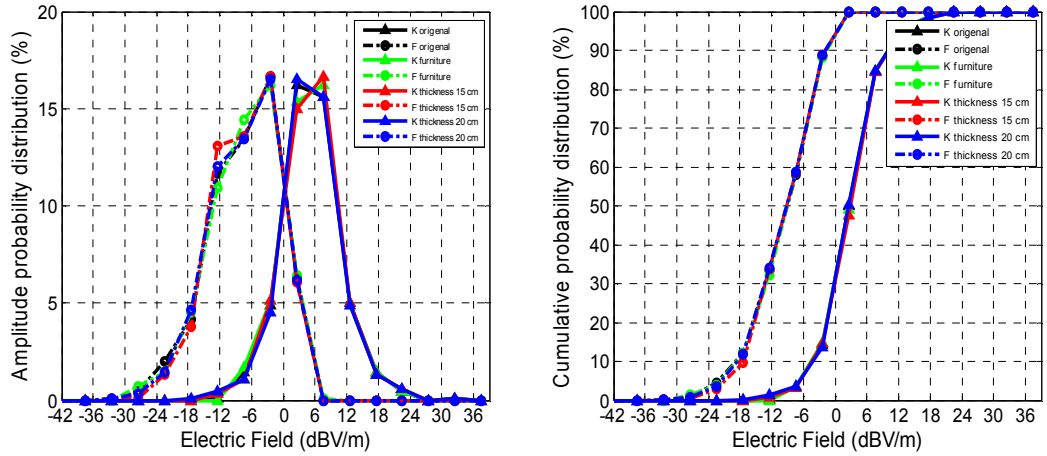

(a) (b)

Figure 3.27: E-field amplitude and cumulative probability distribution for wall thickness and the furniture at 2.4 GHz.

In order to investigate the effect of human occupants on E-field distributions, scenario I in Table 3.3 (where two humans are present in the kitchen and two humans present in the front room) was chosen as a reference. Four scenarios were designed with different dimensions of human and compared with the results of scenario I (height = 170 cm, width=35 cm and thickness=15 cm). For scenario 1 the height was changed to 190 cm, scenario 2 the width was changed to 55 cm and in scenario 3 the thickness was changed to 20 cm and in each scenario the rest of the dimensions are kept similar to scenario I. Scenario 4 the human geometry was as follows: the height =190 cm, width = 55 cm and thickness = 20 cm. The amplitude and cumulative probability distributions are used to analysis the E-field values for these scenarios within the Victorian house at 2.4 GHz as shown in Figure 3.28. The results show that there are very little variations in the E-field distribution values between these scenarios in the kitchen. However, the E-field distributions in the front room have significant variations between scenarios. The results of the cumulative probability distribution show that the average value of the signal in case

of scenario I in the front room is -7 dBV/m whereas the average value when the width is changed to 55 cm (scenario two) in the front room is -14 dBV/m, which results in 7 dB attenuation. The thickness of human has a very little effect on the E-field distribution. However, when the height, width and thickness of human were changed as in scenario 4, the E-field distributions is attenuated by 3 dB. Figure 3.28 (a) shows that the lowest amplitude of the E-field in the kitchen was in case of scenario I with an amplitude probability distribution of 14 % at 3 dBV/m compared with the four scenario.

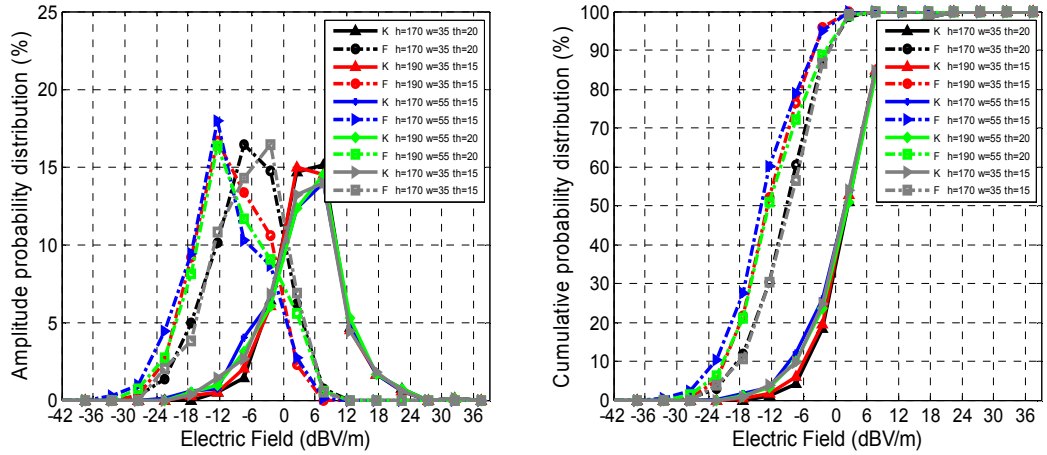

(a) (b)

Figure 3.28: E-field amplitude and cumulative probability distribution for difference dimensional of human at 2.4 GHz.

3.9 The Effect of the Transmitted Power on the E-Field Distributions.

In this section the effect of the closed doors on the E-field levels at different transmitted power values is studied at 2.4 GHz. The transmitter powers considered are 2 mW, 50 mW and 100 mW. These represent typical power values for lower Zigbee, maximum Zigbee and Wi-Fi router, respectively. Table 3.5 showed the scenarios used in this analysis. In this investigation, method B was used for the statistical analysis. Figure 3.29 (a) to Figure 3.29 (c) show the results for the E-field levels difference between scenarios A (2 mW, open door) and scenarios B (2 mW, closed door), scenarios A (50 mW, open door)

and scenarios B (50 mW, closed door) and scenarios A (100 mW, open door) and scenarios B (100 mW, closed door), respectively. The results demonstrate that the effect of door (closed and open) between kitchen and front room attenuates the signals in most area of the front room by 15 dB in all scenarios. The amplitude and cumulative probability distributions are calculated for the E-field simulated values for the difference between scenarios at the three different power values in the ground floor as shown in Figure 3.30. The results show that there are no variations in the E-field distribution values between the scenarios for the different transmitted power in the ground floor. These results confirm that the effect of the door on the E-field levels remains the same regardless of the transmitted power values. Also these results proved that the validation of our main interest which is investigating the parameters effect on the E-field is independent of the power values.

Table 3.5: Scenarios used for statistical analysis.

Scenarios	**Door Open**	**Transmitted Power (mW)**	**Frequency (GHz)**
A	Yes	2	2.4
B	No	2	2.4
A	Yes	50	2.4
B	No	50	2.4
A	Yes	100	2.4
B	No	100	2.4

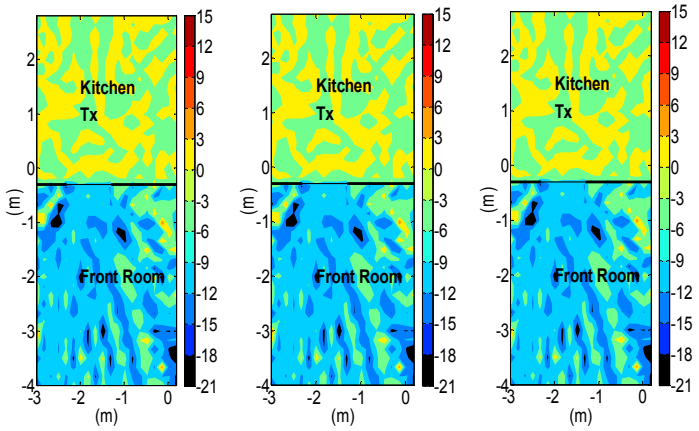

Figure 3.29: Simulated E-field (dB) difference between scenarios A & B for different transmitted power at 2.4 GHz:
(a) 2 mW (b) 50 mW (c) 100 mW.

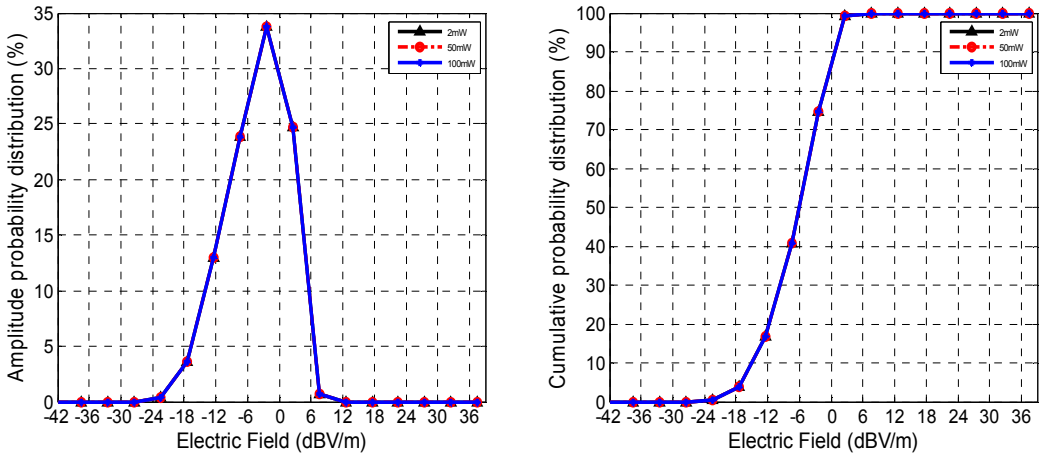

Figure 3.30: E-field amplitude and cumulative probability distribution for different transmitted power at 2.4 GHz.

3.10 Conclusions

This chapter investigated the changes in the E-field strength within the ground floor of a Victorian house at 5.8 GHz, 2.4 GHz, 868 MHz and 433 MHz. The transmitter was located in the middle of the kitchen facing exactly the middle of the kitchen door. Ten different Scenarios were compared for opening and closing doors and changing the building's occupancy level. The effects of different obstacles inside the rooms were compared and the one which has the most significant effect on the received E-field strength was highlighted. By comparing the four frequencies in case of open door and no occupants exist in the house, it can be seen that the E-field coverage levels within front room at the low frequencies are higher than that at the high frequencies. The closing door has a significant effect on the E-field coverage levels within the front room at the four frequencies whereas has less effect on the E-field coverage levels within the kitchen. The propagated signals passed through the closed door at high frequencies were attenuated by nearly 12 dB whereas at low frequencies were attenuated only by 3 dB. At 2.4 GHz, results have shown that human occupants in the kitchen can locally change the E-Field by approximately 12 dBV/m whereas human occupants in the kitchen at 5.8 GHz, 868 MHz and 433 MHz can have an effect from 3 dBV/m to 9 dBV/m. The human occupants in front room at 433 MHz have most significant effect on the electric field level in the front room. However, the presence of human in the front room has less effect on the signal propagation levels than presence of human in the kitchen.

The results showed that the door status or the presence of human within ground floor has less effect on the average of E-field values for all scenarios within the front room at lower frequencies. However, the effects of the door statues and human on the average of the E-field values for all scenarios within front room at higher frequencies were obvious. The simulation results illustrated that the lower frequencies provide a better coverage and higher average E-field levels than the higher frequencies.

The effect of the permittivity and the loss tangent on the received E-field strength was investigated and compared to the results in scenario A. The results showed that the loss tangent has the highest effect on the E-field distribution in the front room. The results also demonstrated that the thickness of internal wall and the furniture have a little effect on the

E-field coverage levels. The investigation of human geometry showed that the width of the human has a higher effect than the height and thickness on the E-field distributions. To summarise, there were large variations in the E-field distribution levels in the front room compared to the E-field distribution levels in the kitchen. This is due to the presence of the transmitter source in the kitchen. Finally, the results showed that the door status can cause a significant attenuation to the signal at all four frequencies.

Chapter 4 – Analysis of E-Field Distribution on Vertical Plane for Configuration A in Multi Floors within House

This chapter investigates the distribution of the E-field at the vertical plane cut within the basement, ground floor and first floor in a Victorian house. The dipole antenna transmitter was placed in the same location as described in chapter 3.

4.1 Introduction

Users could be anywhere in the house resulting in the need to characterise the signal coverage in a vertical plane through the multiple floors. The dipole antenna transmitter in this chapter was located in the kitchen opposite the door as in configuration A. The distribution of the E-field in the vertical plane within the basement, ground floor and first floor in a Victorian house have been investigated. Again, frequencies of 5.8 GHz, 2.4 GHz, 868 MHz, 433 MHz have been considered. Also, FEKO has been used to calculate the E-field distribution. The scenarios that were used in the previous chapter also have been used here to investigate the effect of opening and closing doors and changing the occupants positions in the E-field distributions on all three floors. The methodology is described in the next section. In section 4.3 Simulation of the E-Field Distributions in the Vertical Plane at 5.8 GHz is presented, in section 4.4 at 2.4 GHz, section 4.5 at 868 MHz and section 4.6 at 433 MHz. A further discussion of previous sections is summarized in section 4.7. Section 4.8 concludes this chapter.

4.2 Simulation Scenarios

The experiments setup are exactly the same as described in chapter 3. Twelve different scenarios were designed (A to L) presented in Table 4.1 to investigate the effects of doors status and the presence of humans on the E-field distribution in the entire three floors in the Victorian house.

Figure 4.1 illustrates the layout of the basement, ground floor and first floor of the house and shows the locations of the occupants, the door and the transmitting antenna. These scenarios designed based on the fact that the house consists of two bedrooms, kitchen and front room. In this chapter, four scenarios from the twelve different scenarios are analysed. In order to analyse the effect of opening and closing the doors, scenario A and scenario B are investigated. The estimated numbers of people who live in this kind of house are expected to be four. People are expected to be anywhere in the house; however, we assume that people spend most of their time in the kitchen or the front room or occupants could be in different rooms. For these reasons scenario J which represent two occupants in the kitchen and two occupants in the front room with closed doors scenario and scenario L which represent one occupant in the kitchen, one occupant in the front room, one occupant in bedroom 1 and one occupant in the bedroom 2 with closed doors scenario are considered for studying. In these scenarios, the effect due to furniture and other equipment existing inside the house is neglected. The results of the other eight different scenarios are presented in the appendix.

Table 4.1: Scenarios used for statistical analysis.

	Occupied	**Door Open**	**Location**
A	No	Yes	-
B	No	No	-
C	Yes (x1)	Yes	2
D	Yes (x1)	No	2
E	Yes (x2)	Yes	2 and 5
F	Yes (x2)	No	2 and 5
G	Yes (x2)	Yes	7 and 8
H	Yes (x2)	No	7 and 8
I	Yes (x4)	Yes	1,3,4 and 6
J	Yes (x4)	No	1,3,4 and 6
K	Yes (x4)	Yes	2,5,7 and 8
L	Yes (x4)	No	2,5,7 and 8

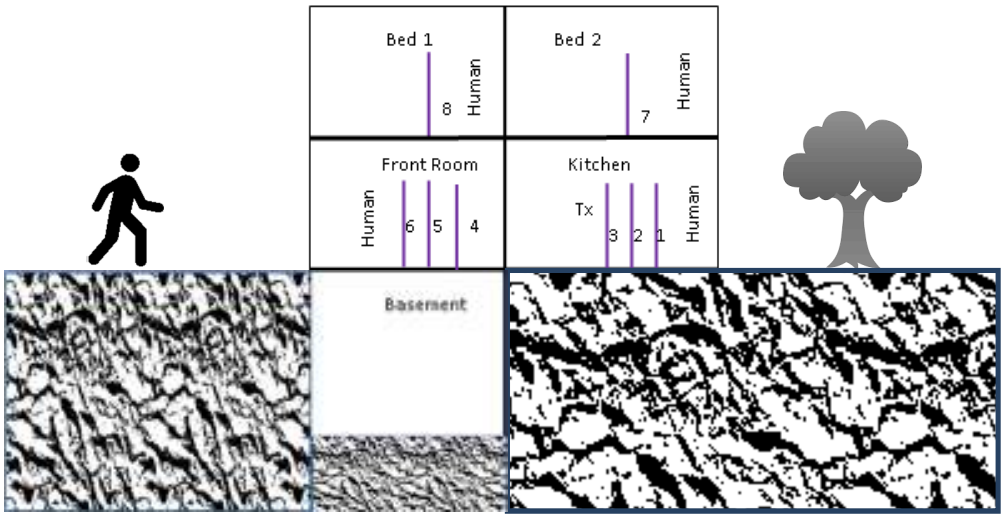

Figure 4.1: Layout of vertical cut of Victorian house.

4.3 Simulation of the E-Field Distributions on Vertical Plane for configuration A at 5.8 GHz

The simulation setup and parameters are exactly the same as described in section 3.3. Analysis is performed for different occupancy scenarios as described in the section 4.2. The results presented consider the E-field amplitude distribution obtained for the basement, the ground floor and the first floor of the Victorian house. Results were sampled in a vertical cut plane in all floors and the x-axis was in the same position of the source antenna. 840 samples of the E-field amplitude were obtained from the simulations in each floor (ground floor and first floor), while 400 samples of the E-field amplitude were obtained in the basement due to each floor has two rooms and the basement has one room. The amplitude probability and the cumulative probability distributions of the E-field distribution have been used for analysis purposes. The methods used to analysis the results are method A, B and C as stated in section 3.3.

4.3.1 Method A results

For method A, the E-field amplitude distribution in vertical cut within the Victorian house in the first floor, ground floor and basement for the scenarios A, B, J and L at 5.8 GHz are shown in Figure 4.2. In the case of open door and no occupants exist in the Victorian house, high E-field levels are observed in the ground floor in both the kitchen and the front room ranged between 6 dBV/m to -12 dBV/m while a low E-field levels are observed in the first floor and the basement as shown in Figure 4.2 (a). This is due to the transmitter was located in the middle of the kitchen facing exactly the middle of door in the kitchen which caused high signals propagated through the door to the front room and no obstacles exist between the transmitter and the receiver in the ground floor. The results also show that the closed door has a significant effect on the E-field distributions within the ground floor. The low E-field levels are obtained within the front room in the ground floor ranged between -18 dBV/m to -33 dBV/m. Due to closed doors within Victorian house, very low E-field levels obtained in the ground of the basement and the roof in the first floor ranged between -33 dBV/m to -36 dBV/m as shown in Figure 4.2 (b). When there are occupants in the kitchen, the E-field levels signals behind the human are -12 dBV/m. While the presence of occupants in the front room, the E-field levels behind the occupants are ranged between -24 dBV/m and – 33 dBV/m. Figure 4.2 (d) shows that the presence of occupants in the first floor have a little effect on the E-field distributions in the first floor.

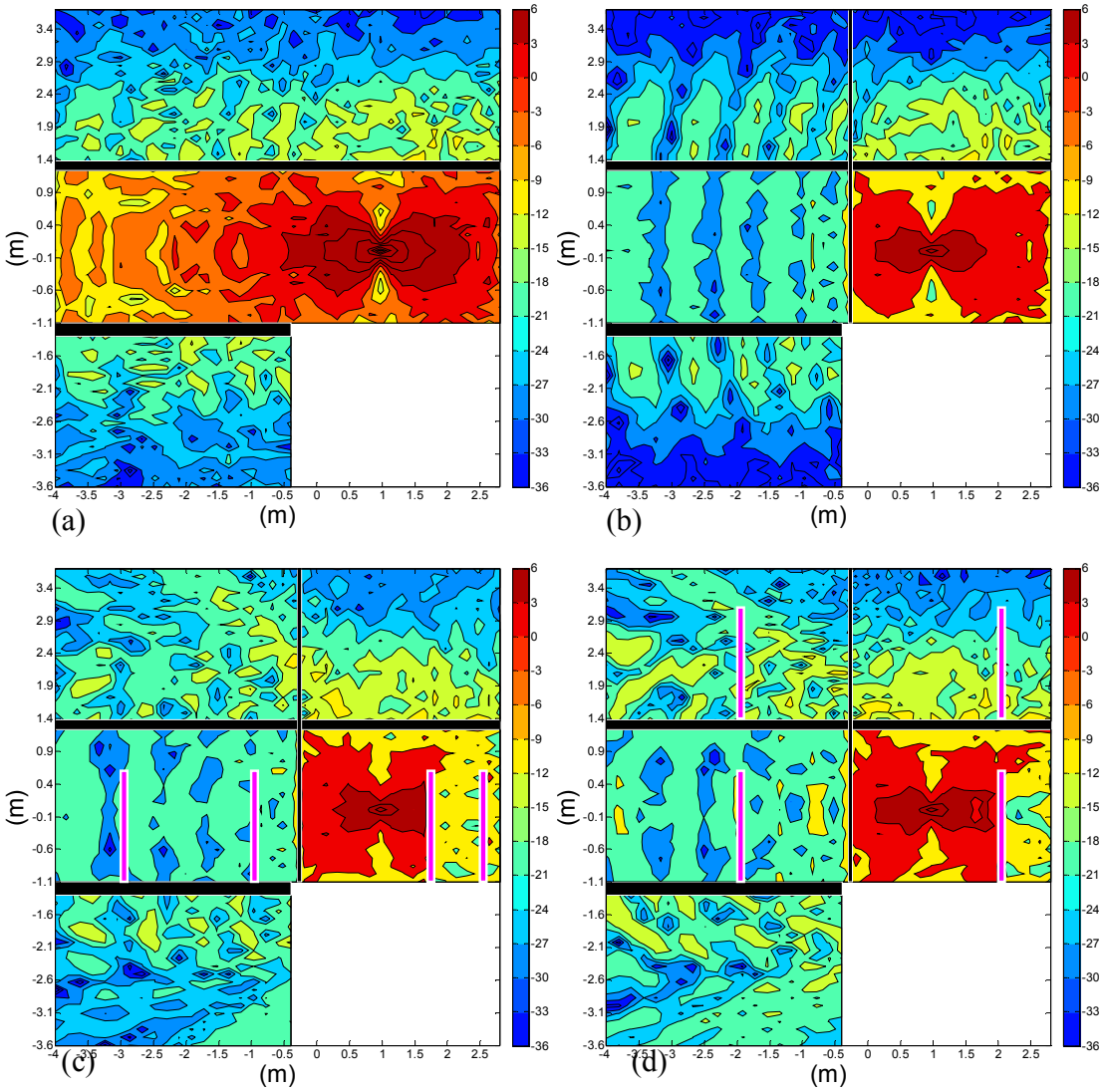

Figure 4.2: Simulated E-field (dBV/m) distributed on Vertical Cut of Victorian House at 5.8 GHz:

(a) Scenario A (b) Scenario B (c) Scenario J (d) Scenario L.

4.3.2 Method B results

For method B, either high or low field E-field distribution levels within the Victorian house are used to obtain the difference between scenarios A (unoccupied, open door) and other scenarios at 5.8 GHz as shown in Figure 4.3. Scenario (A) was used as a reference for the analysis. The positive values (shown as yellow to red) represent areas with higher

E-field distributions when compared to scenario (A). While the negative values (shown as blue and black) represent areas with lower E-field distributions.

Figure 4.3 (a) shows that the E-field distributions in the front room in the ground floor have the biggest effect when the doors status is changed. The propagated signals coming through the closed door in the front room in the ground floor is attenuated by approximately 21 dB compared to the propagated signals when the door is open. Also the E-field levels in some areas in the basement and the first floor is attenuated by -12 dB due to the changing the doors status.

The presence of occupants within Victorian house has a different effect on the E-field distributions. When all four occupants are presented in the ground floor (two in the kitchen and two in the front room), the E-field levels behind the occupants in the kitchen are attenuated ranged between -12 dB and -18 dB. Due to the reflection from the occupants and the walls, the E-field levels in some areas in the bed1 and the basement are increased by 12 dB as shown in Figure 4.3(b). In case of four occupants are distributed within the house (one in kitchen, one in the front room, one in the bed1 and one in the bed2), it can be seen that more areas in the bed1 and basemen are improved in the E-field distributions compared to when the occupants are present in the ground floor. The E-field strength is increased at the area located between the ground of the basement and one metre above the ground of the basement varying from 3 dB to 12 dB. This is due to the distribution of the occupants within the house and the middle and exterior wall which caused multipath effect. The results of all scenarios clearly demonstrate that the doors status (open or closed) have a significant effect on the E-field coverage in the Victorian house. It can be seen that the presence of the occupants in the first floor have a limited effect on the E-field distributions within the house.

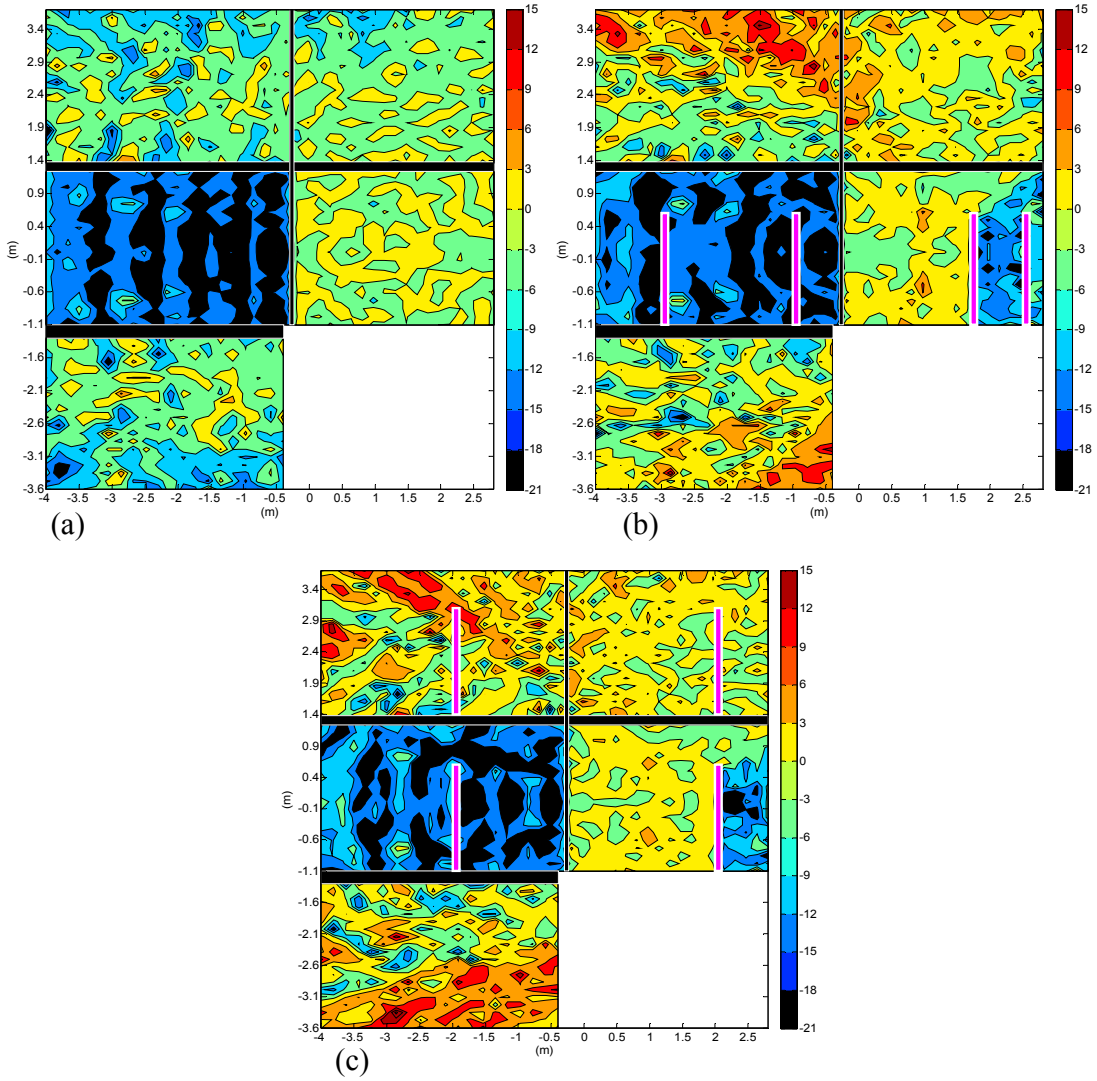

Figure 4.3: Simulated E-field (dB) on vertical cut difference plot between scenarios A (unoccupied, open door) and other scenarios at 5.8 GHz:
(a) Scenario A & B (b) Scenario A & J (c) Scenario A & L.

4.3.3 Method C results

For method C, the amplitude and cumulative probability distributions are used to provide a comparison between different scenarios of the E-field values in the basement, ground floor and first floor within the Victorian house at 5.8 GHz. Figure 4.4 (a) to Figure 4.4 (f) show the results of E-field amplitude and cumulative probability distributions from

scenario A to scenario L, respectively within the basement, ground floor and first floor. The x-axis represents the distribution of the E-field levels while y-axis represents its probability percentage. In ground floor, it can be seen from the cumulative probability distribution that the closed door has reduced the average value of the E-field by 10 dBV/m. Also the results demonstrate that from 50% to 80% of the cumulative probability distribution in the ground floor have reduced the E-field by 3 dBV/m which is due to presence of occupants within the house. It can be seen that from Figure 4.4 (a) the lowest amplitude of the E-field distribution in the basement is in case of closed door scenario with an amplitude probability distribution of 9% at -24 dBV/m. Also from the cumulative probability distribution in the basement the lowest average value of the E-field was in case of closed doors with presence of four occupants within the house at -20 dBV/m. It can be seen that from Figure 4.4 (f) the lowest average value of the E-field in the first floor was in case of closed door scenario by -24 dBV/m. This is due to the door status are changed from open to closed doors which cause some signals are absorbed and some are reflected.

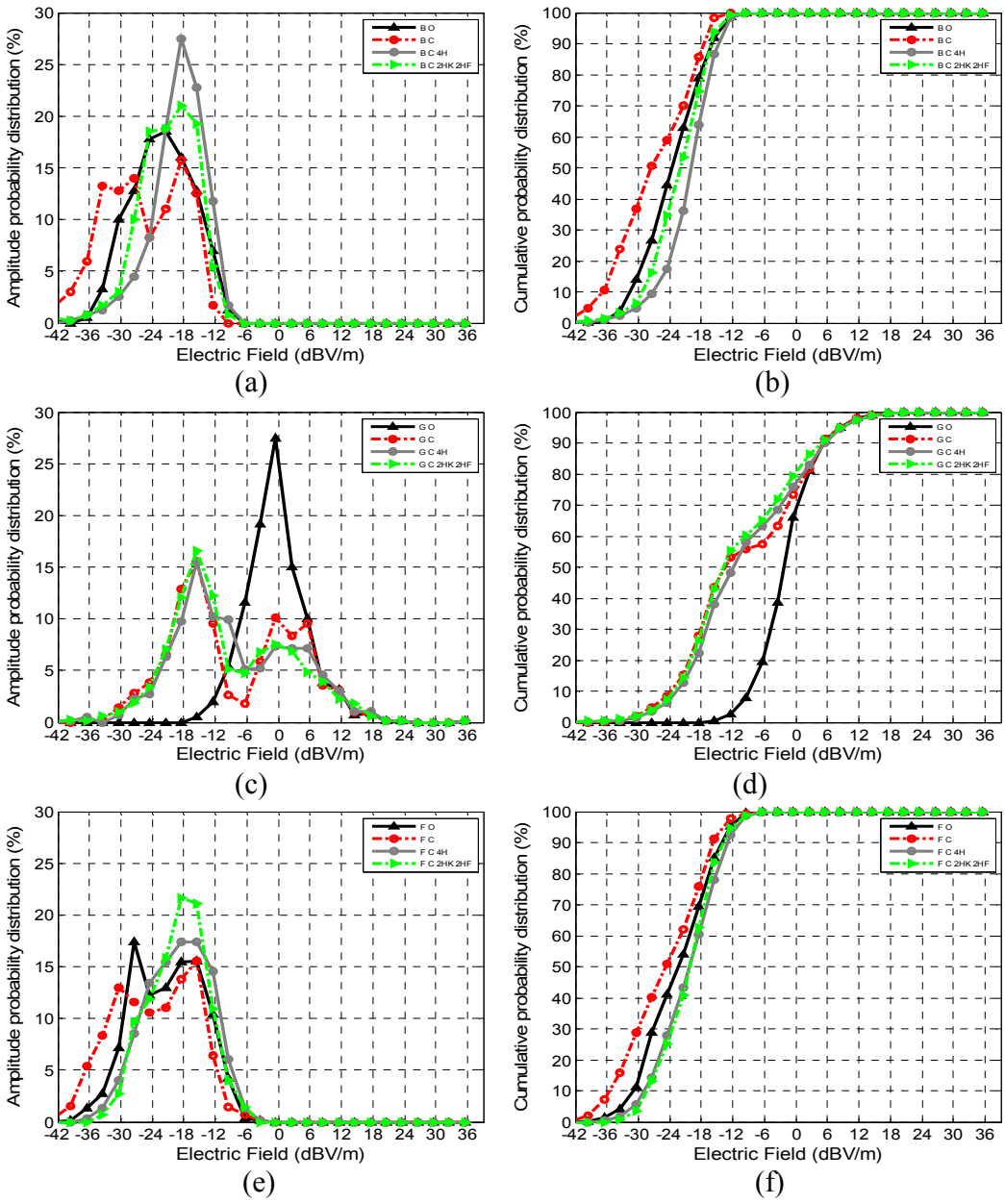

Figure 4.4: Vertical cut analysis at 5.8GHz:

(a) Basement amplitude distribution (b) Basement cumulative distribution (c) Ground Floor amplitude distribution (d) Ground Floor cumulative distribution (e) First Floor amplitude distribution (f) First Floor cumulative distribution.

(Key: B = Basement, G = Ground Floor, F=First Floor, O = open door, C = closed door, 2HK = two occupants in the kitchen and 2HF= two occupants in the front room, 1HB1=one occupant in Bedroom 1, 1HB2=one occupant in Bedroom 2).

4.4 Simulation of the E-Field Distributions on Vertical Plane at 2.4GHz

The simulation setup and parameters are exactly the same as described in the section 3.4. Analysis is performed for different occupancy levels scenarios as described in the section 4.2.

E-field amplitude distribution are obtained for the ground floor of the Victorian house. Results are sampled in a vertical cut plane in all floors and the x-axis was in the same position of the source antenna. 840 samples of the E-field amplitude were obtained from the simulations in each floor (ground floor and first floor), while 400 samples of the E-field amplitude are obtained in the basement due to each floor has two rooms and the basement has one room. Amplitude probability and the cumulative probability distributions of the E-field distribution are used for analysis purposes as described in [81] and [82]. Results obtained from scenarios A, B, J and L are used in this chapter. The same three methods (A, B and C) are used in this section.

4.4.1 Method A Results

For method A, the E-field distributions results are presented for the scenarios A, B, J and L as shown in Figure 4.5. In case of open door and no occupants exist in the Victorian house, it can be seen that high E-field levels are obtained in the ground floor and the area near to the ground floor in the first floor and the basement ranged between 6 dBV/m and -12 dBV/m. This is due to there is no obstacles between the transmitter source and the receiver in the ground floor. However, low E-field levels are obtained in most area in the first floor and the basement ranged between -18 dBV/m and -33 dBV/m. Figure 4.5 (b) shows that the E-field distribution within the Victorian house have a great effect when the doors are closed. When the doors are closed, the E-field distributions in the front room in the ground floor are ranged between -9 dBV/m and -24 dBV/m. When there are occupants in the kitchen, the E-field levels signals behind the human are attenuated by -12 dBV/m. While the presence of occupants in the front room, the E-field levels behind the occupants

are ranged between -18 dBV/m and -24 dBV/m. Figure 4.5 (d) shows that the presence of occupants in the first floor have a little effect on the E-field distributions in the first floor. Also, it can be seen that when the occupants are present in the house, the E-field distributions in the basemen are ranged between -9 dBV/m and -24 dBV/m.

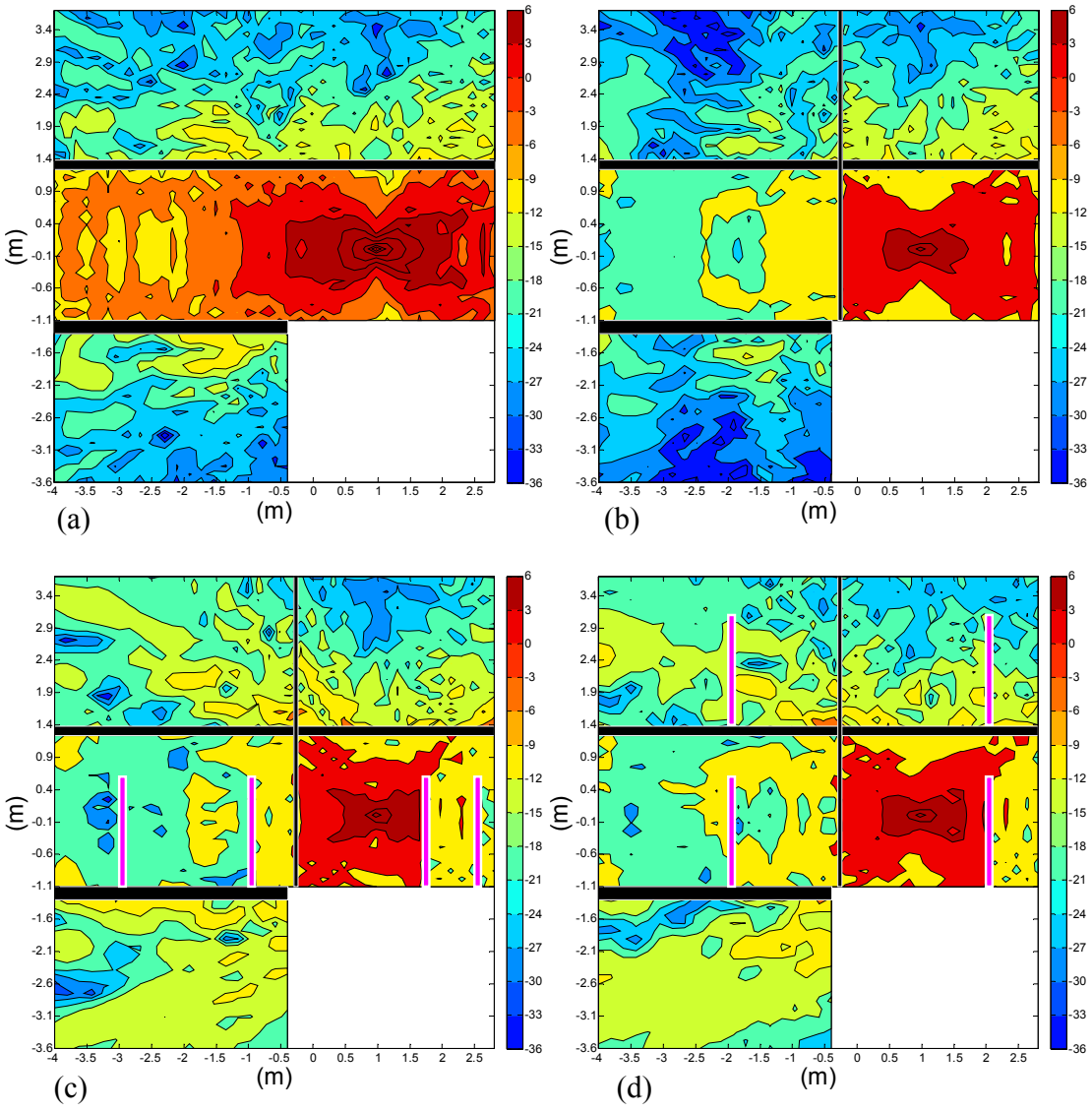

Figure 4.5: Simulated E-field (dBV/m) distributed on vertical cut of Victorian house at 2.4GHz: (a) Scenario A (b) Scenario B (c) Scenario J (d) Scenario L.

4.4.2 Method B Results

For method B, similar investigations to those in the previous section were carried out in this section at 2.4 GHz. Figure 4.6 illustrates the E-field level differences between scenario A and other scenarios at 2.4 GHz. It can be seen that the E-field levels in most area in the front room have been attenuated by 15 dB due to the closed door between the kitchen and the front room as shown in Figure 4.6 (a). Also the E-field levels in some areas in the basement and the first floor have attenuated by -12 dB due to the doors status changed. When all four occupants are present in the ground floor (two in the kitchen and two in the front room) and the doors are closed, the E-field levels behind the occupants in the kitchen are attenuated ranged between -9 dB and -18 dB. Due to the reflection from the occupants and the walls, the E-field levels in most areas in the bed 1 and the basement are improved ranged between 3 dB and 12 dB as shown in Figure 4.6 (b). In case of four occupants are distributed within the house (one in kitchen, one in the front room, one in the bed1 and one in the bed2), it can be seen that most areas in the bed1 and basemen are improved in the E-field distribution compared to when the occupants are present in the ground floor as shown in Figure 4.6 (c). The occupant in the bed2 has decreased the E-field distribution by 9 dB. The E-field distribution in most area in the basement are improved varying from 3 dB to 12 dB. This is due to the distribution of the occupants within the house and the middle and exterior wall which caused multipath effect. The results of all scenarios clearly demonstrate that the doors status (open or closed) have a significant effect on the E-field coverage in the Victorian house. It can be seen that the presence of the occupants within the house have a great effect on the E-field distribution in the basement.

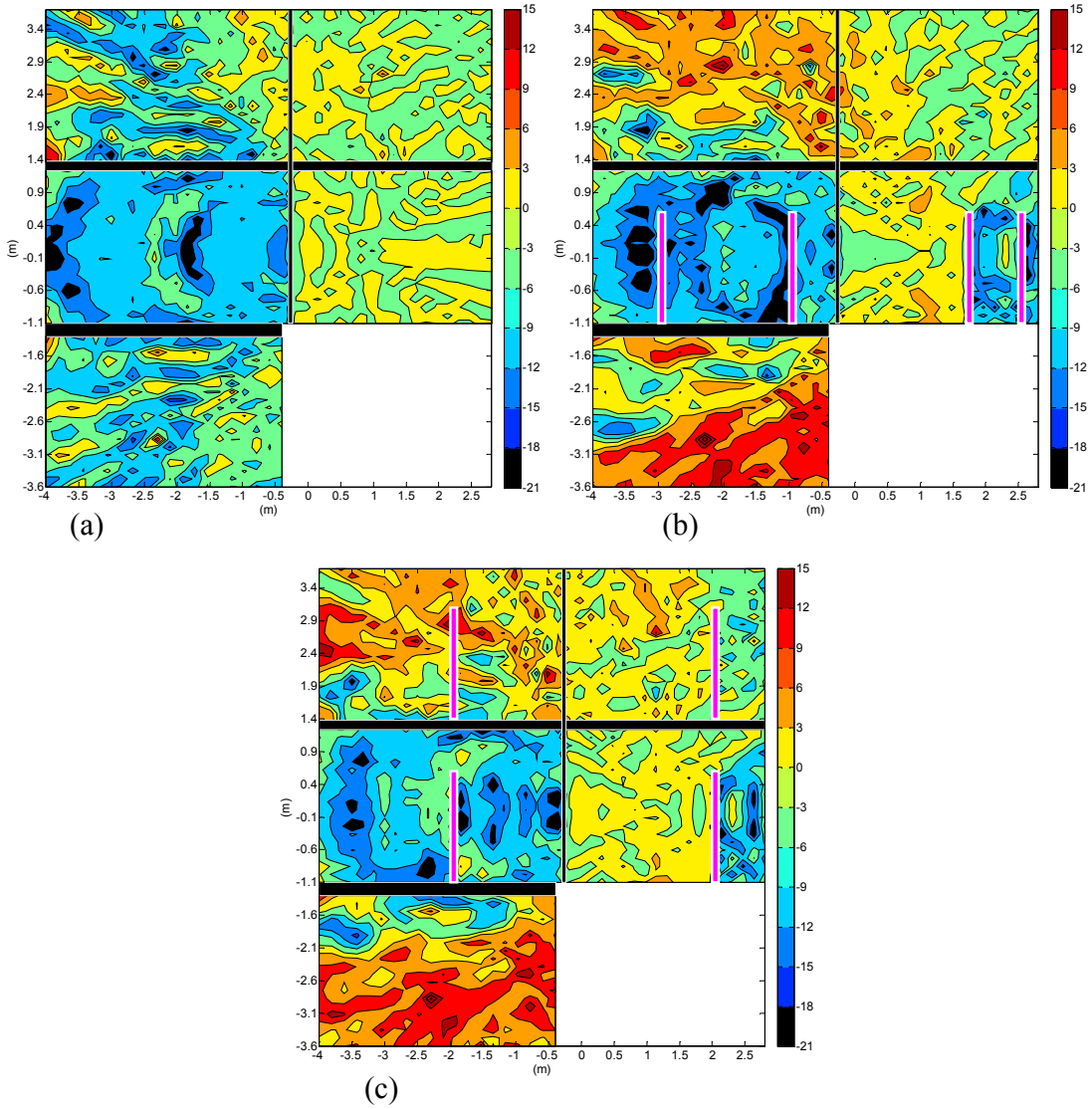

Figure 4.6: Simulated E-field (dB) on vertical cut difference plot between scenarios A (unoccupied, open door) and other scenarios at 2.4GHz:
(a) Scenario A & B (b) Scenario A & J (c) Scenario A & L.

4.4.3 Method C Results

For method C, the amplitude and cumulative probability distributions are used to analysis the E-field values for the four scenarios in the basement, ground floor and first floor within the Victorian house at 2.4 GHz as shown in Figure 4.7. The results of the cumulative probability distribution figure show that the average value of the signal in case of the open

door in the ground floor is -3 dBV/m whereas the average value in case of closed door in the ground floor is -9 dBV/m. This attenuation is due to the change of the door status from open to closed door. When occupants are present within the house, the results show that there are a little variations in the E-field distribution values in the ground floor. Figure 4.7 (c) show that the highest amplitude of the E-field within the ground floor is in case of open door scenario with an amplitude probability distribution of 24% at -3 dBV/m. It can be seen that from Figure 4.7 (b) the E-field distribution values in the basement in case of presence of occupants within the house are improved by 9 dBV/m compared in case of open door and no occupants within the house. However, when the doors is closed, the E-field distributions in the basement was attenuated by 3 dBV/m. Figure 4.7 (f) demonstrates that the presence of occupants within the house improved the E-field distribution values in the first floor. The average E-field cumulative probability distributions in the first floor for closed doors with presence of occupants within the house are -18 dBV/m. However, the average E-field cumulative probability distributions values in the first floor for closed doors scenario are -22 dBV/m. The peak value of the E-field amplitude probability distribution in the first floor in case of presence of occupants within the house is 25% at -15 dBV/m while the peak in the basement in case of presence of occupants within the house is 38% at -12 dBV/m as observed in Figure 4.7 (e) and Figure 4.7 (a), respectively.

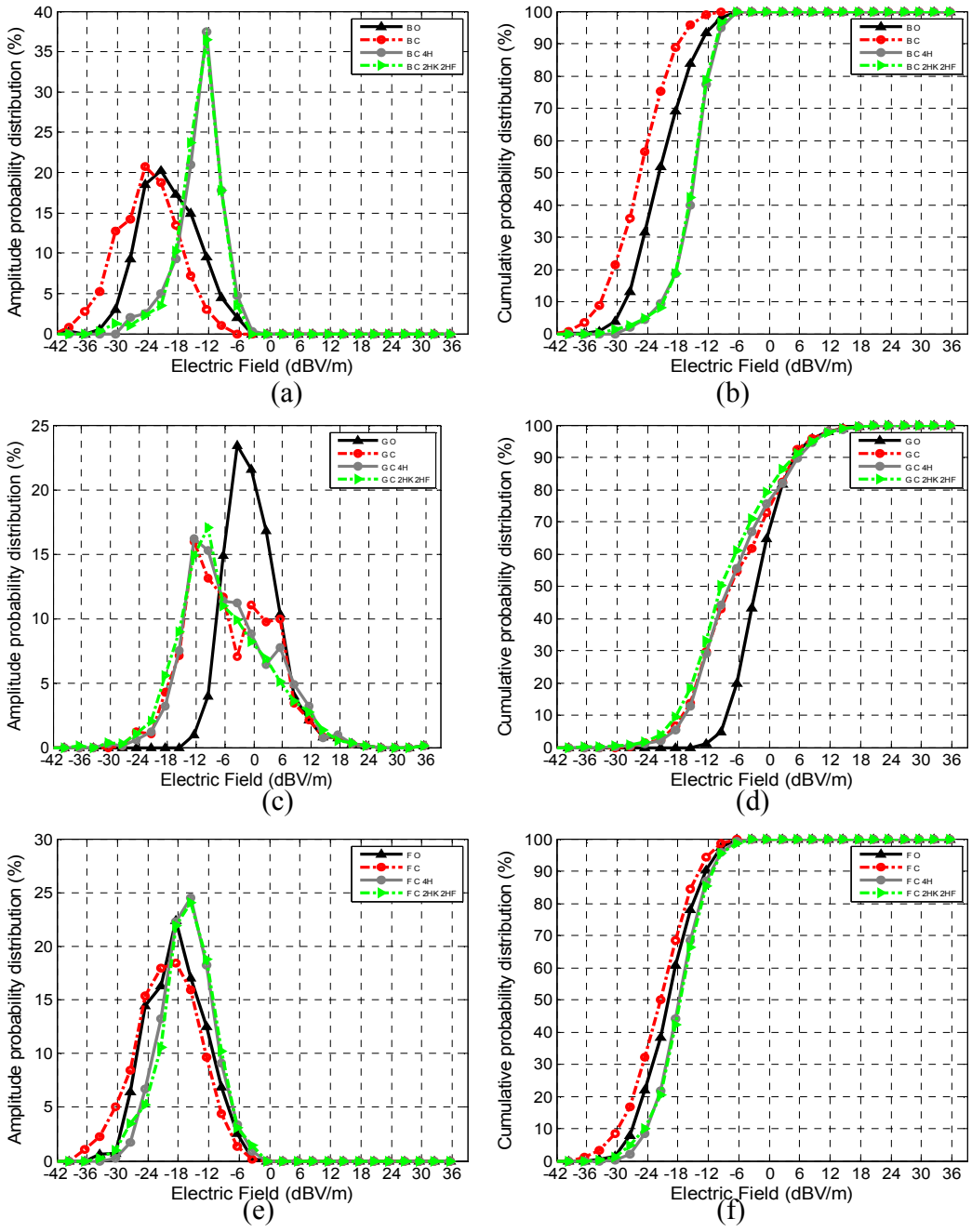

Figure 4.7: Vertical cut analysis at 2.4GHz:

(a) Basement amplitude distribution (b) Basement cumulative distribution (c) Ground Floor amplitude distribution (d) Ground Floor cumulative distribution (e) First Floor amplitude distribution (f) First Floor cumulative distribution.

4.5 Simulation of the E-Field Distributions on Vertical Plane at 868 MHz

The simulation setup and parameters are exactly the same as described in section 3.5. Same twelve scenarios (A to k) that described in the previous section are also investigated in this section.

Same parameters that used in the previous section are used in following simulation scenarios. The samples are selected in a vertical cut plane in all floors and the x-axis is in the same position of the source antenna. 840 samples of the E-field amplitude were obtained from the simulations in each floor (ground floor and first floor), while 400 samples of the E-field amplitude were obtained in the basement due to each floor has two rooms and the basement has one room. The amplitude probability and the cumulative probability distributions are used to analysis the E-field distributions. This section presents the results obtained from the scenarios described in section 4.2. The same three methods (A, B and C) are also used for analysis.

4.5.1 Method A Results

For method A, the E-field amplitude distributions are calculated for the scenarios A, B, J and L at 868 MHz as shown in Figure 4.8. High E-field levels were obtained in the ground floor and some area in the basement and the first floor which are located near to the ground floor ranged between -3 dBV/m to 6 dBV/m for the case of open door and no occupant exist within the Victorian house. The results illustrate that when the door are closed the E-field strength in the front room is reduced by approximately 3 dBV/m. This is due to the low frequency used in the transmitter results in high coverage as shown in Figure 4.8 (b). The E-field distributions in the basement and the first floor have a little variation effect due to the closed door. In case of four occupants are present in the ground floor (two in the kitchen and two in the front room) and the doors are closed, the E-field levels behind the occupants in the kitchen are -6 dBV/m while the E-field levels behind the occupants in the front room are -12 dBV/m. The E-field distribution in the basement and the first

floor are ranged between -12 dBV/m and -27 dBV/m as shown in Figure 4.8 (c). When the occupants are present in the first floor, the E-field distributions behind the occupants are ranged between -12 dBV/m and -21 dBV/m.

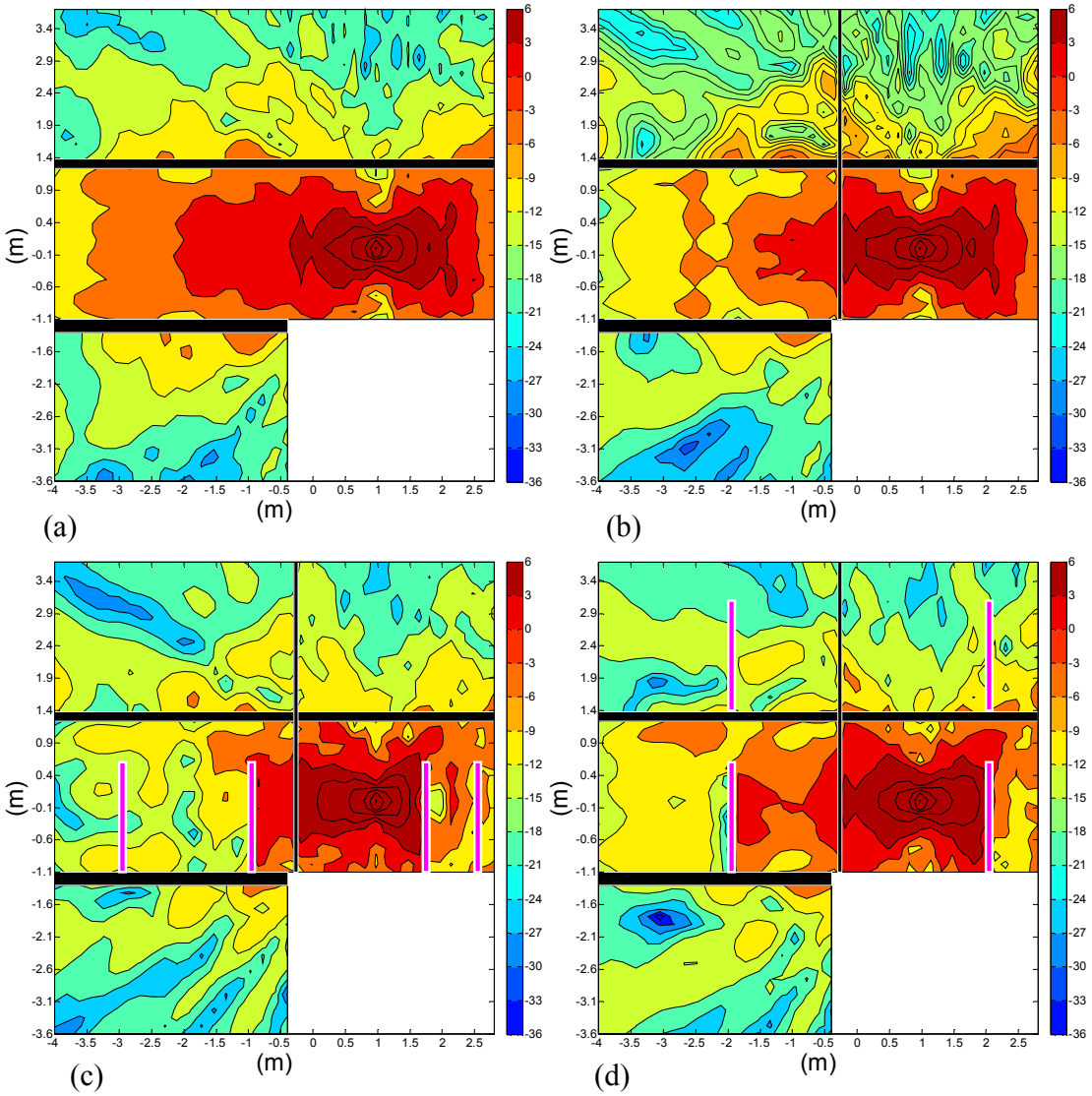

Figure 4.8: Simulated E-field (dBV/m) distributed on vertical cut of Victorian house at 868 MHz:

(a) Scenario A (b) Scenario B (c) Scenario J (d) Scenario L.

4.5.2 Method B Results

For method B, either high or low field E-field distribution levels within the Victorian house are used to obtain the difference between scenarios A (unoccupied, open door) and other scenarios at 868 MHz as shown in Figure 4.9. Scenario (A) is used as a reference for the analysis. The positive values (shown as yellow to red) represent areas with higher E-field distributions when compared to scenario (A). While the negative values (shown as blue and black) represent areas with lower E-field distributions.

Figure 4.9 (a) shows that the E-field distributions in the front room in the ground floor have attenuated ranged between 3 dB and 9 dB when the doors status are changed from open to closed doors. Also the E-field levels in some areas in the basement and the first floor is attenuated by -6 dB due to the doors status changed.

The presence of occupants within Victorian house has a different effect on the E-field distributions. When all four occupants are present in the ground floor (two in the kitchen and two in the front room), the E-field levels behind the occupants in the kitchen and the front room are attenuated ranged between -6 dB and -15 dB. Due to the reflection from the occupants and the walls, the E-field levels in some areas in the bed 1 and the basement are attenuated by 9 dB as shown in Figure 4.9 (b). In case of four occupants are distributed within the house (one in kitchen, one in the front room, one in the bed1 and one in the bed2), the E-field levels behind the occupants are attenuated ranged between -6 dB and -12 dB. The results of all scenarios clearly demonstrate that the presence of the occupants within the house at 868 MHz have a significant effect on the E-field coverage in the Victorian house.

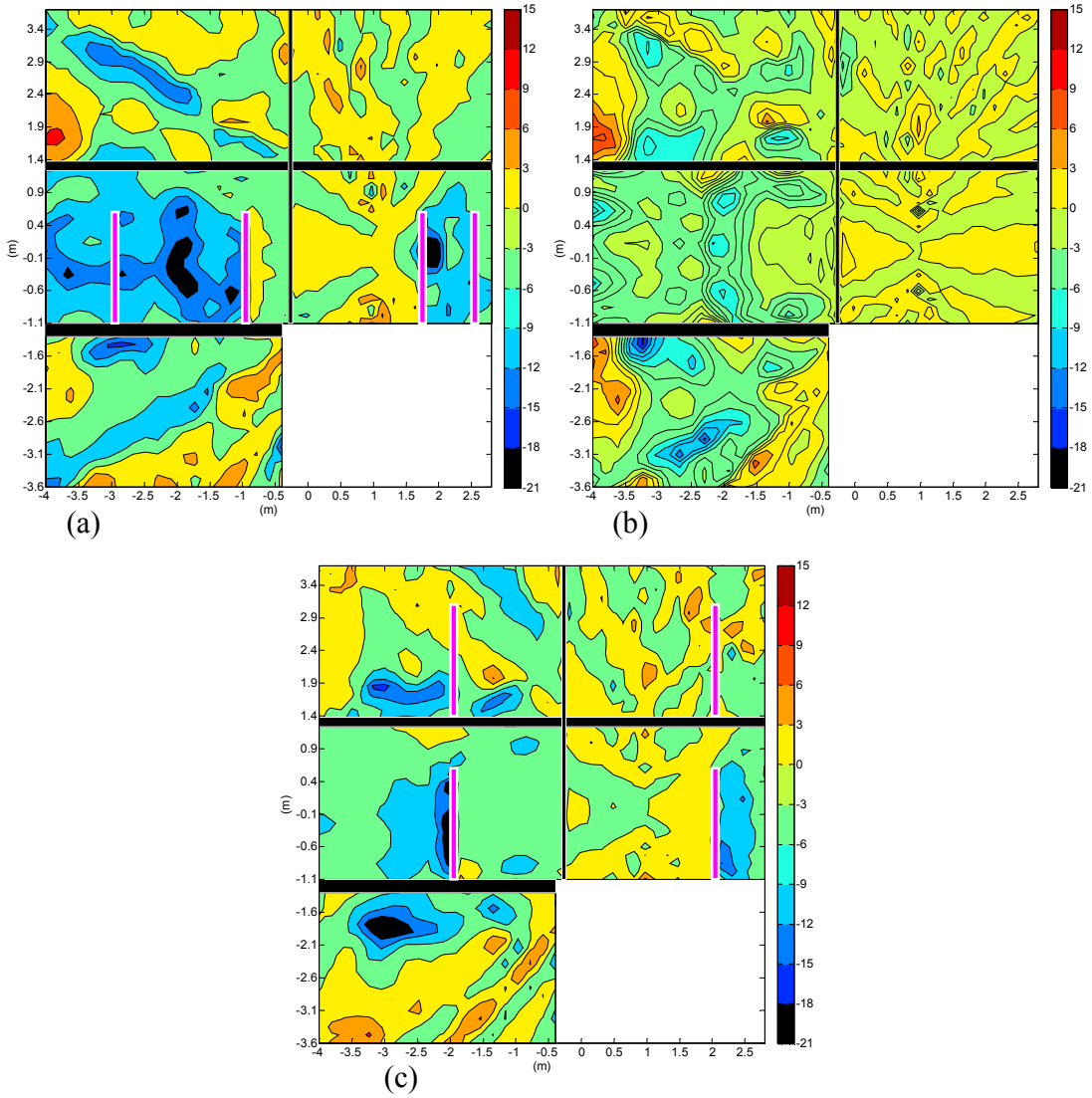

Figure 4.9: Simulated E-field (dB) on vertical cut difference plot between scenarios A (unoccupied, open door) and other scenarios at 868 MHz:
(a) Scenario A & B (b) Scenario A & J (c) Scenario A & L

4.5.3 Method C Results

For method C, the amplitude and cumulative probability distributions are used to provide a comparison between different scenarios of the E-field values in the basement, ground floor and first floor within the Victorian house at 868 MHz as shown in Figure 4.10. It can be seen from the amplitude and the cumulative probability distribution results for the

basement and the first floor that there are a little variations in the E-field distribution values between the four scenarios. It can be seen from the cumulative probability distribution for the basement and the first floor that the average values of the signals for all scenarios in the front room are within 3 dBV/m ranged between -18 dBV/m and -15 dBV/m. Figure 4.10(c) illustrates that the lowest amplitude of the E-field for the ground floor is in case of closed door with two occupants in kitchen and two occupants in the front room scenario with an amplitude probability distribution of 16% at -10 dBV/m. This was due to the presence of four occupants in the ground floor which cause some signals are absorbed and some reflected. The results of the cumulative probability distribution figure show that the average value of the signal in case of the open doors in the ground floor is -2 dBV/m whereas the average value in case of closed doors with two occupants in kitchen and two occupants in the front room scenario in the ground floor is -8 dBV/m. This attenuation is due to the change of the door status from open to closed door and presence of four occupants within the ground floor.

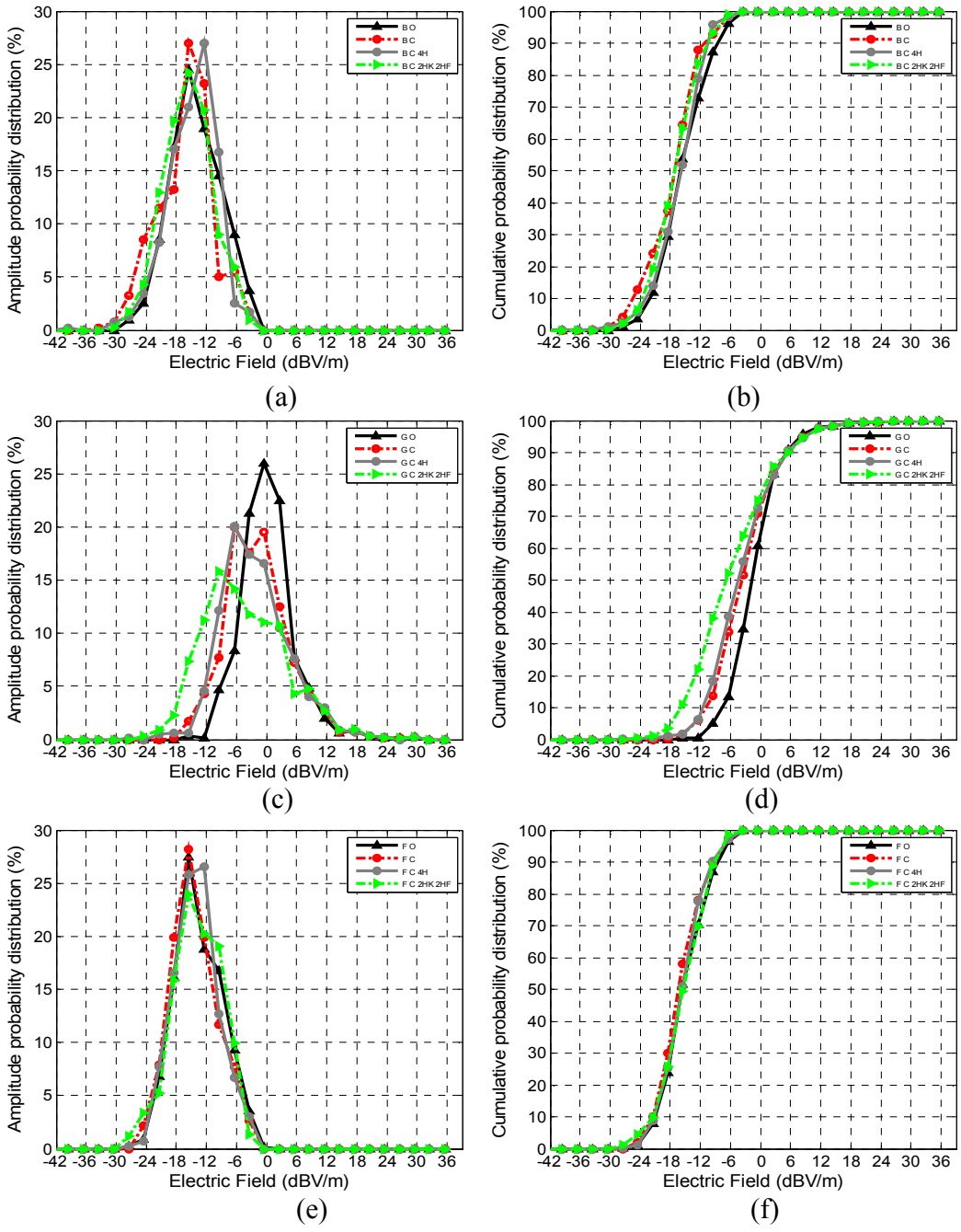

Figure 4.10: Vertical cut analysis at 868 MHz:

(a) Basement amplitude distribution (b) Basement cumulative distribution (c) Ground Floor amplitude distribution (d) Ground Floor cumulative distribution (e) First Floor amplitude distribution (f) First Floor cumulative distribution.

4.6 Simulation of the E-Field Distributions on Vertical Plane at 433 MHz

The E-field is generated using 433 MHz dipole antenna in the following simulations. The parameters that used in these simulations are the same as described in section 3.6. Based on the designed described above, twelve different scenarios are designed named as (A to L).

As described in the previous section, the results focus on the E-field amplitude distributions in a vertical cut plane in all floors of the Victorian house. The amplitude probability and the cumulative probability distributions are used to analysis the E-field distributions. This section presents the results obtained from the scenarios described in section 4.2. The same three methods (A, B and C) are also used for analysis.

4.6.1 Method A Results

For method A, the E-field amplitude distribution in vertical cut within Victorian house in the first floor, ground floor and basement for the scenarios A, B, J and L at 433 MHz were shown in Figure 4.11. In the case of open door and no occupants exist in the Victorian house, a high E-field levels are observed in the ground floor in both the kitchen and the front room ranged between 6 dBV/m to -12 dBV/m. The low E-field distributions are observed in some small areas near to the roof of the first floor and near to the ground of the basement in the front room with value of -24 dBV/m as shown in Figure 4.11 (a). Also it can be seen that the walls between floors have attenuated the propagated signals coming through the walls by 3 dBV/m. The results also show that the closed doors have a little effect on the E-field distributions within the house due to the low frequency used. The low E-field levels are obtained near to the exterior wall in the front room in the ground floor with value of -21 dBV/m. In case of closed doors and two occupants present in the kitchen and two occupants present in the front room, it can be seen that the E-field levels behind the occupants in the kitchen are ranged between -3 dBV/m and -9 dBV/m. While the presence of occupants in the front room, the E-field levels behind the occupants are ranged

between -12 dBV/m and - 21 dBV/m. Figure 4.11 (d) shows that the presence of occupants in the first floor attenuated the E-field coverage behind the occupants in the first floor by 6 dBV/m.

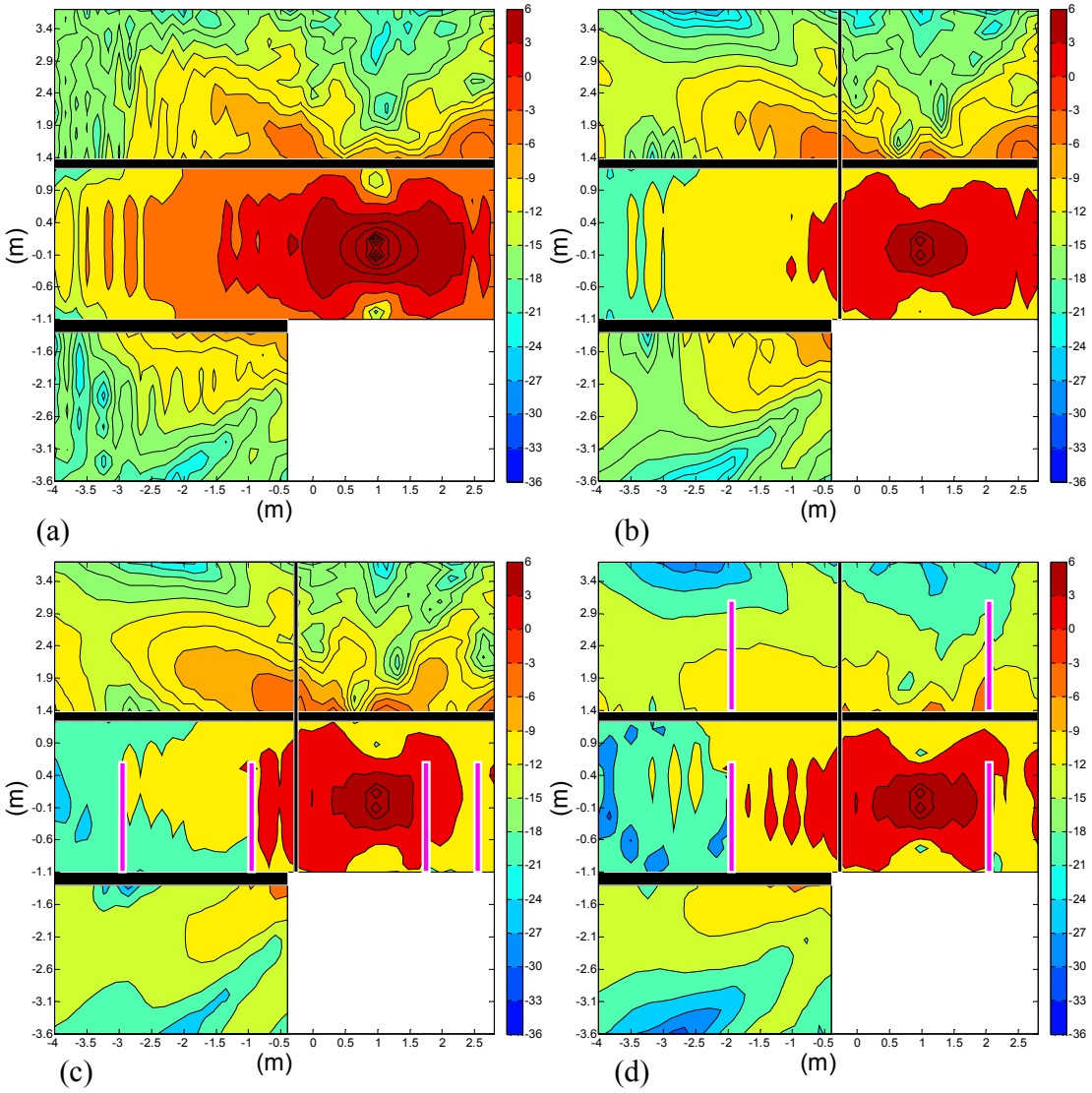

Figure 4.11: Simulated E-field (dBV/m) distributed on vertical cut of Victorian house at 433 MHz:

(a) Scenario A (b) Scenario B (c) Scenario J (d) Scenario L.

4.6.2 Method B Results

For method B, similar investigations to those in the previous section are carried out in this section at 433 MHz. Figure 4.12 illustrates the E-field level differences between scenario A and other scenarios at 433 MHz. It can be seen that the E-field levels in most area in the front room have been attenuated by 6dBV/m due to the closed door between the kitchen and the front room as shown in Figure 4.12 (a). Also the E-field levels in some areas in the basement and in the bed 1 in the first floor have increased by 6 dB due to the doors status changed. When all four occupants are present in the ground floor (two in the kitchen and two in the front room) and the doors are closed, the E-field levels behind the occupants in the kitchen are attenuated ranged between -6 dB and -12 dB. The E-field levels in some spot area in the basement and first floor are improved by 3 dB to 9 dB due to the reflection from the occupants and the walls as shown in Figure 4.12 (b). Due to the presence of two occupants in the front room and the doors are closed, the E-field distributions in most area in the front room is attenuated by -12 dB. In case of four occupants are distributed within the house (one in kitchen, one in the front room, one in the bed1 and one in the bed2), it can be seen that the occupants in the first floor have decreased the E-field distribution by 6 dB. The E-field distributions behind the occupants in the ground floor is attenuated by -9 dB to -18 dB. The E-field distribution in most area in the basement are decreased by 6 dB. The results of all scenarios clearly demonstrate that the presence of the occupants within the house at 433 MHz have a significant effect on the E-field coverage in the Victorian house.

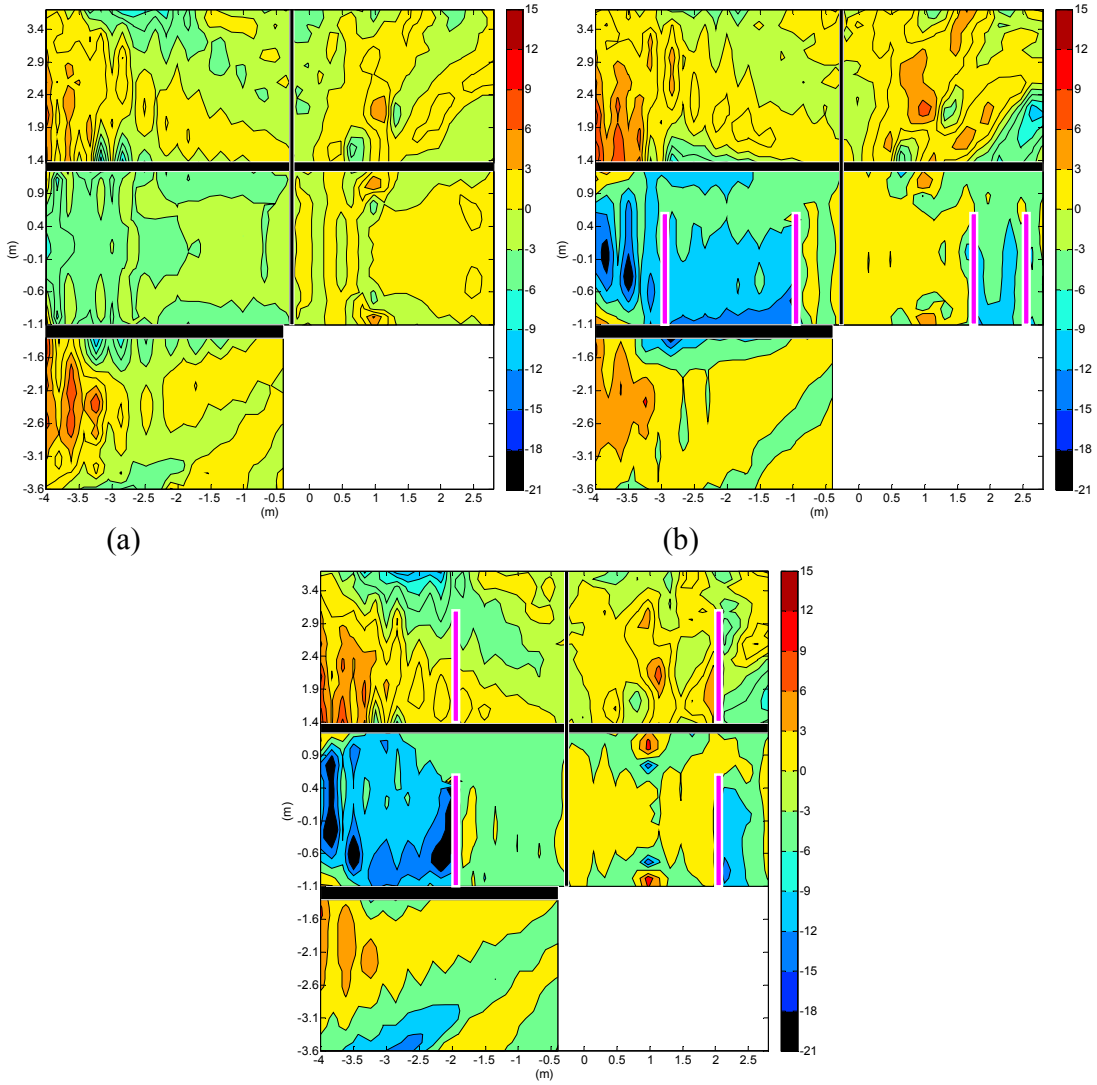

Figure 4.12: Simulated E-field (dB) vertical cut difference plot between scenarios A (unoccupied, open door) and other scenarios at 433 MHz:
(a) Scenario A & B (b) Scenario A & J (c) Scenario A & L.

4.6.3 Method C Results

For method C, the amplitude and cumulative probability distributions are used to analysis the E-field values in the basement, ground floor and first floor within the Victorian house for the four scenarios at 433 MHz as shown in Figure 4.13. The results demonstrate that

the variations in the E-field cumulative probability distributions for the basement and the first floor between the four scenarios are minimal. It can be seen from
Figure 4.13 (a) and Figure 4.13 (e) that the highest amplitude of the E-field in the basement is in case of closed door with two occupants in kitchen and two occupants in the front room scenario with an amplitude probability distribution of 40% at -12 dBV/m. However, the lowest amplitude of the E-field in the ground floor is in case of closed door with two occupants in kitchen and two occupants in the front room scenario with an amplitude probability distribution of 13% at -6 dBV/m. This is due to the presence of four occupants in the ground floor which cause some signals are absorbed and some reflected. Figure 4.13 (d) demonstrates the cumulative probability distributions of the E-field values within the ground floor. It can be seen that there is a variations within the region between 5% to 50% of the E-field cumulative probability distributions in the ground floor which is approximately 8 dBV/m.

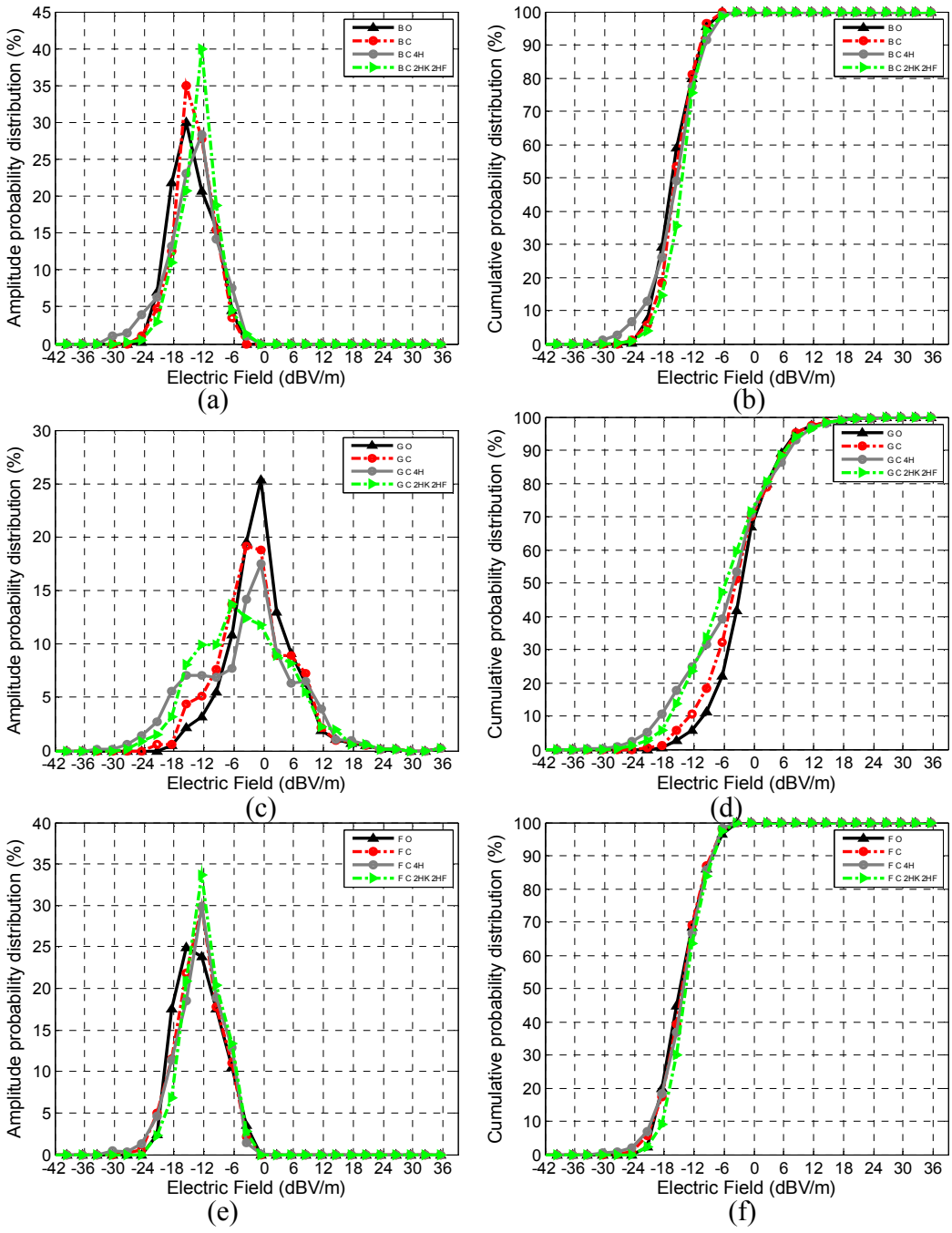

Figure 4.13: Vertical cut analysis at 433 MHz:

(a) Basement amplitude distribution (b) Basement cumulative distribution (c) Ground Floor amplitude distribution (d) Ground Floor cumulative distribution (e) First Floor amplitude distribution (f) First Floor cumulative distribution.

4.7 Summary of Analysis

This section compares the results of the E-field distributions across the frequencies 5.8 GHz, 2.4 GHz, 868 MHz and 433 MHz. The transmitter for all the frequencies placed at the same location which is in the kitchen (1.2 m above the ground, 1.3 m from middle wall and 2.1 m from external wall). At the receiver the same scale is used ranging from -30 dBV/m to 6 dBV/m for all frequencies. Only four scenarios (A, B, J and L) from each frequency are analysed in this section. The effect of the doors status and presence of occupants in the basement, ground floor and first floor within Victorian house on the E-field distributions in the four scenarios is compared between the scenarios and the frequencies.

4.7.1 Analysis of E-field without Occupants

The E-field amplitude results are presented for open door and no occupants scenario within Victorian house for all four frequencies as shown in Figure 4.14. It can be seen from the results that the high E-field coverage in the ground floor for all four frequencies ranged between 6 dBV/m and -12 dBV/m. However, in the first floor and the basement the high E-field coverage at the low frequencies (i.e. 868 MHz and 433 MHz) is higher than at high frequencies (i.e. 5.8 GHz and 2.4 GHz). The walls between floors attenuated the signals coverage at high frequencies more than at the low frequencies. Comparing the coverage signals within the basement across the four frequencies, it can be seen that the highest E-field distributions in the basement is at 433 MHz ranged between -6 dBV/m and -21 dBV/m whereas the lowest E-field distributions in the basement is at 5.8 GHz ranged between -21dBV/m and -33 dBV/m. Also, in the first floor the highest E-field distribution is at 433 MHz whereas the lowest E-field distribution is at 5.8 GHz.

The effect of closing the door on the E-field amplitude coverage at the four frequencies is shown in Figure 4.15. It is observed that the attenuation on the propagated signals due to closing the doors depends on the value of the frequency. The door status (opening or closing) has a significant effect on the E-field distributions within the Victorian house at the high frequencies. It can also be seen that the E-field distributions in the front room in

the ground floor at 5.8 GHz are ranged between -18 dBV/m and -30 dBV/m whereas at 433 MHz were ranged between -9 dBV/m and -18 dBV/m. Comparing the E-field distributions results in the basement for all four frequencies, it is noticed that the high E-field distributions are occurred in most of the area in the basement at low frequencies whereas the low E-field distributions are occurred in the most of area in the basement at high frequencies.

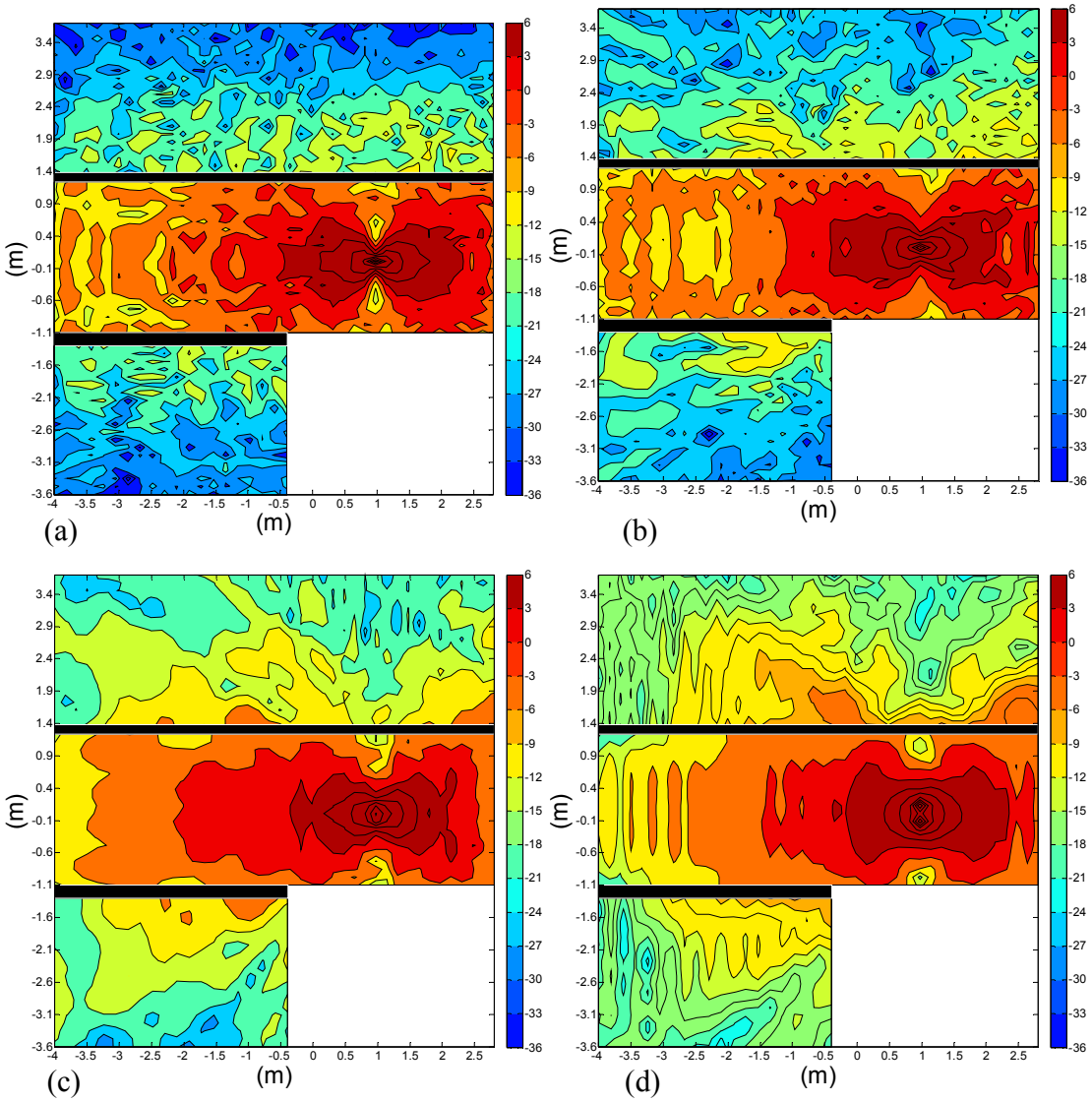

Figure 4.14: Simulated E-field (dBV/m) on vertical cut for open door at different frequencies: (a) 5.8 GHz (b) 2.4 GHz (c) 868 MHz (d) 433MHz.

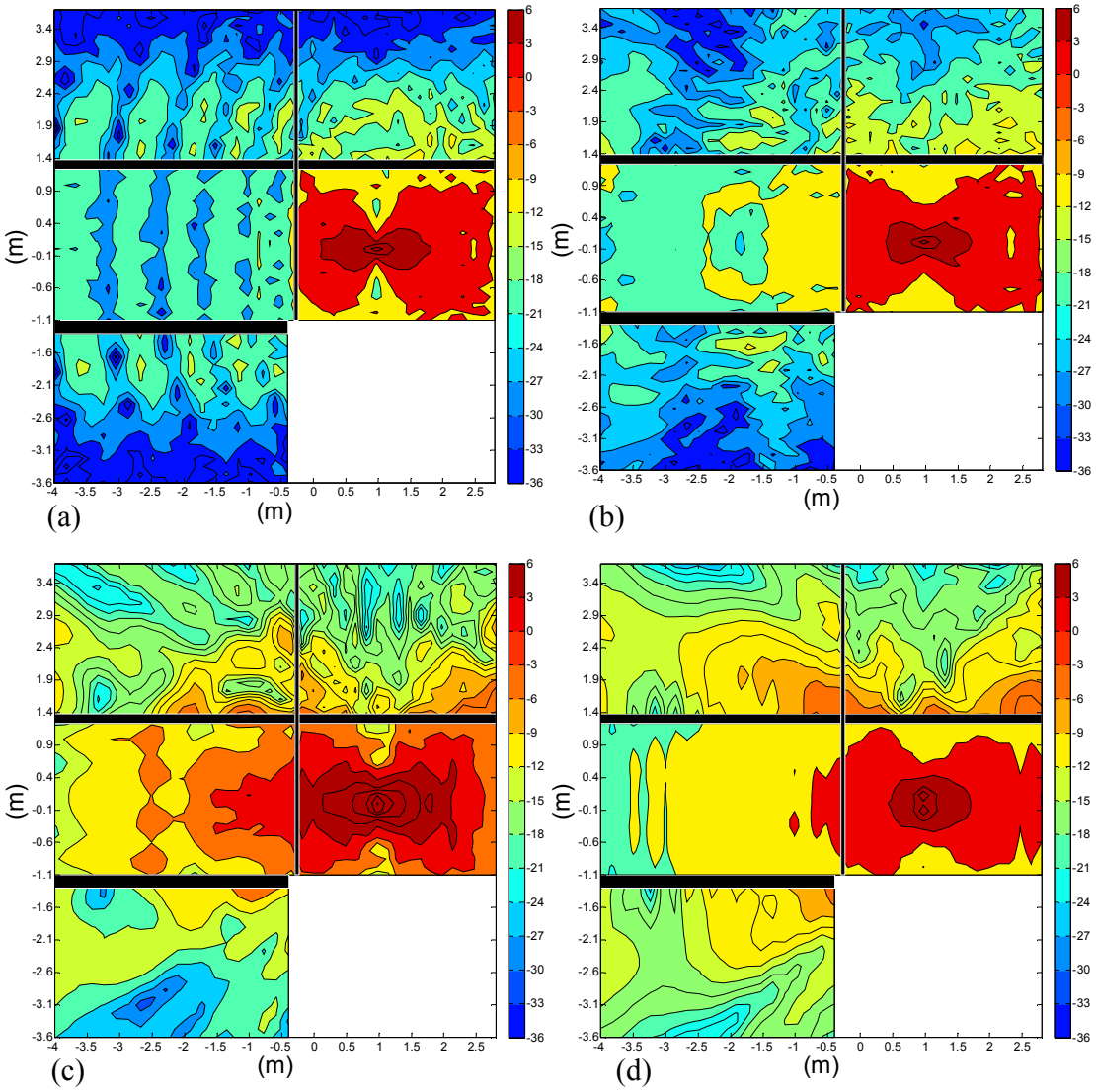

Figure 4.15: Simulated E-field (dBV/m) vertical cut results for closed door at different frequencies:
(a) 5.8 GHz (b) 2.4 GHz (c) 868 MHz (d) 433MHz.

The amplitude and cumulative probability distributions are used to clarify the comparison between the different four investigated frequencies for open door scenario in the basement, ground floor and first floor within the Victorian house. Figure 4.16 (d) illustrates that the E-field distribution in the ground floor for open scenario is similar for all four frequencies. This similarity is due to the presence of the transmitter in the kitchen

and there are no obstructions between the transmitter and the receivers. Comparing the high frequencies (5.8 GHz and 2.4 GHz) and low frequencies (868 MHz and 433 MHz) in the basement and in the first floor for open scenario, the results demonstrate that the cumulative probability distributions for the low frequencies are higher than the high frequencies by 6 dBV/m. Also, it can be seen from cumulative probability distributions that there is a very little variations in the E-field distributions in the basement and the first floor for open scenario at low frequencies. However, the cumulative probability distributions at 5.8 GHz are lower than at 2.4 GHz by 3 dBV/m.

Figure 4.16 (e) shows the lowest E-field amplitude probability distribution values in first floor is at 5.8 GHz and reached 15% at -15 dBV/m.

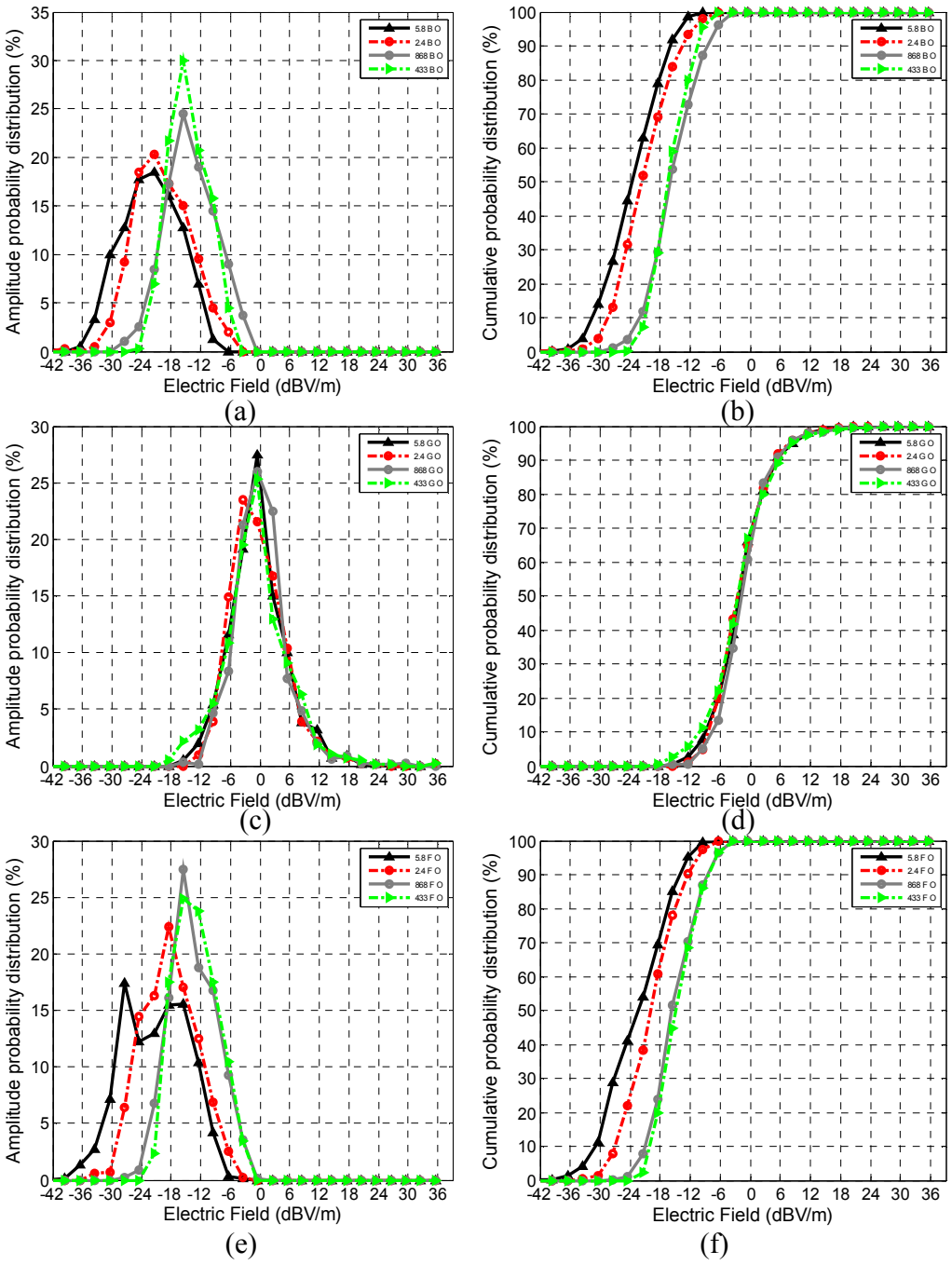

Figure 4.16: Vertical cut analysis at 5.8 GHz, 2.4 GHz, 868 MHz and 433 MHz for open door for configuration A scenarios:

(a) Basement amplitude distribution (b) Basement cumulative distribution (c) Ground Floor amplitude distribution (d) Ground Floor cumulative distribution (e) First Floor amplitude distribution (f) First Floor cumulative distribution.

The E-field amplitude and the E-field cumulative probabilities distributions of closed door scenario are obtained for the four frequencies in the basement, ground floor and first floor within the Victorian house. It can be seen that from Figure 4.17 (d) for the case of closed door scenario in the ground floor there are some noticeable variations in the E-field distribution between the different four frequencies. The results demonstrate that from 0% to 70% of the cumulative probability distributions for the low frequencies are higher than at the high frequencies. The average E-field cumulative probability distributions in ground floor for closed door scenario at low frequencies have similar values which are approximately -3 dBV/m. However, the average E-field cumulative probability distributions values in the ground floor at 5.8 GHz and 2.4 GHz frequencies are -13 dBV/m and -8 dBV/m, respectively. The peak value of the E-field amplitude probability distribution in the first floor at 433 MHz reached 35% at -16 dBV/m while the peak for 5.8 GHz is 15% at -19dBV/m as observed in Figure 4.17 (a). Comparing the average E-field cumulative probability distributions in basement and first floor for closed door scenario for the four frequencies, Figure 4.17 (b) and Figure 4.17 (f) demonstrate that the highest average E-field cumulative probability distributions values is at 433 MHz whereas the lowest average E-field cumulative probability distributions values is at 5.8 GHz. This is because of the high coverage signals of the low frequencies.

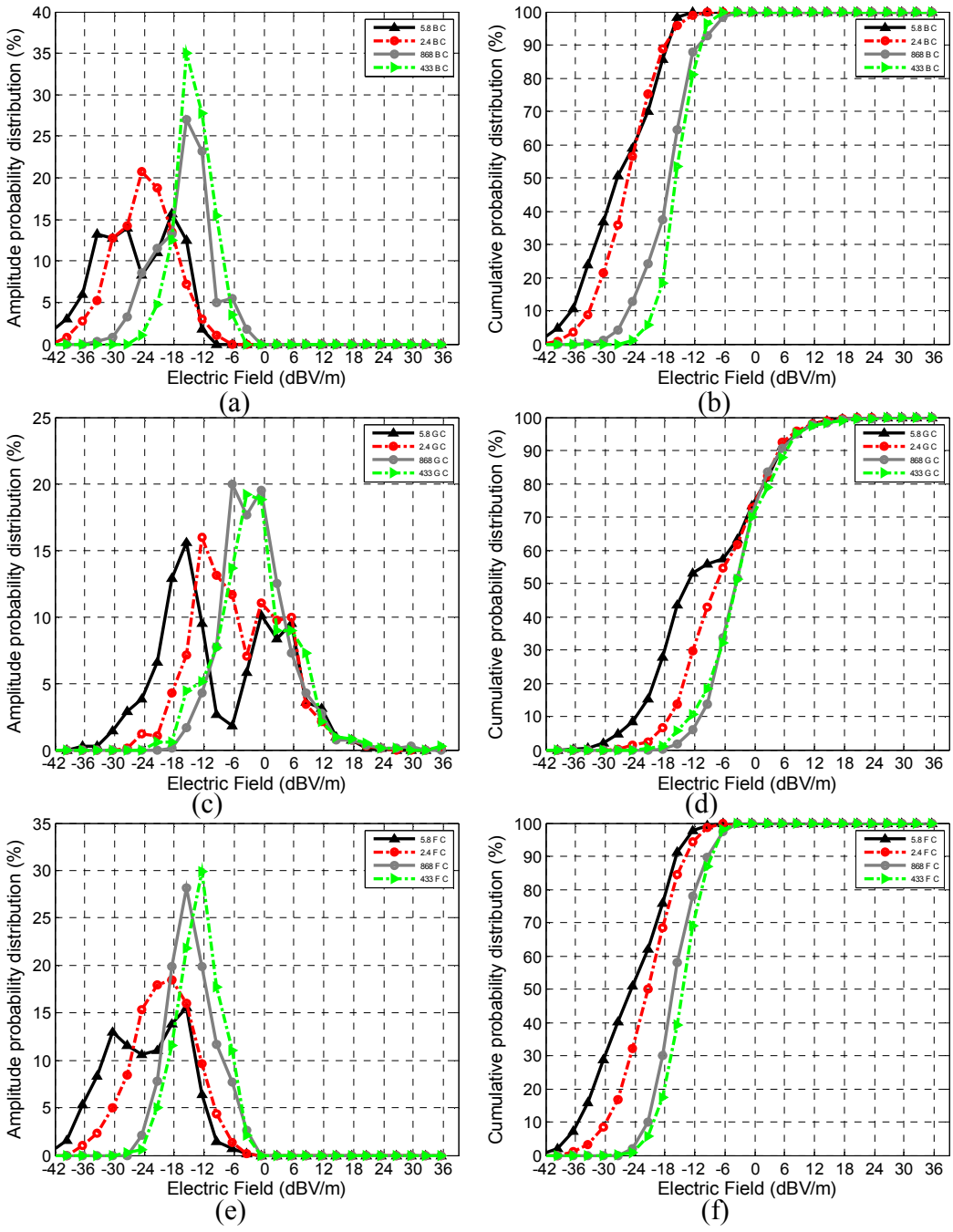

Figure 4.17: Vertical cut analysis at 5.8 GHz, 2.4 GHz, 868 MHz and 433 MHz for closed door for configuration A scenarios:

(a) Basement amplitude distribution (b) Basement cumulative distribution (c) Ground Floor amplitude distribution (d) Ground Floor cumulative distribution (e) First Floor amplitude distribution (f) First Floor cumulative distribution.

The E-field levels within Victorian house are used to obtain the difference between the open door and the closed door scenarios at 5.8 GHz, 2.4 GHz, 868 MHz, 433 MHz as shown in Figure 4.18. The results show that the effect of the doors' status on the E-field distribution is more obvious at high frequencies than at low frequencies. By comparing the E-field distributions in the front room in the ground floor for all four frequencies, it can be seen that the closed doors at high frequencies have attenuated the propagated signals passed through the closed door by nearly 18 dBV/m whereas at low frequencies are attenuated only by 3 dBV/m. At 433 MHz, the difference in E-field coverage between the open and the closed door scenarios in the basement are increased near to the exterior wall by 6 dBV/m. However, at 5.8 GHz the difference in E-field coverage between these scenarios in the basement are attenuated near to the exterior wall by 18 dBV/m. Also, the E-field coverage levels in the first floor at low frequencies are higher than the E-field coverage levels at high frequencies. By comparing the effect of doors on the E-field distribution between the four frequencies, the highest effect is observed at 5.8 GHz. The E-field values in the most of the area in the front room in the ground floor at 5.8 GHz are very low down to -21 dBV/m. This is due to that the propagated signals strength of high frequencies source are less than the propagated signals strength of low frequencies.

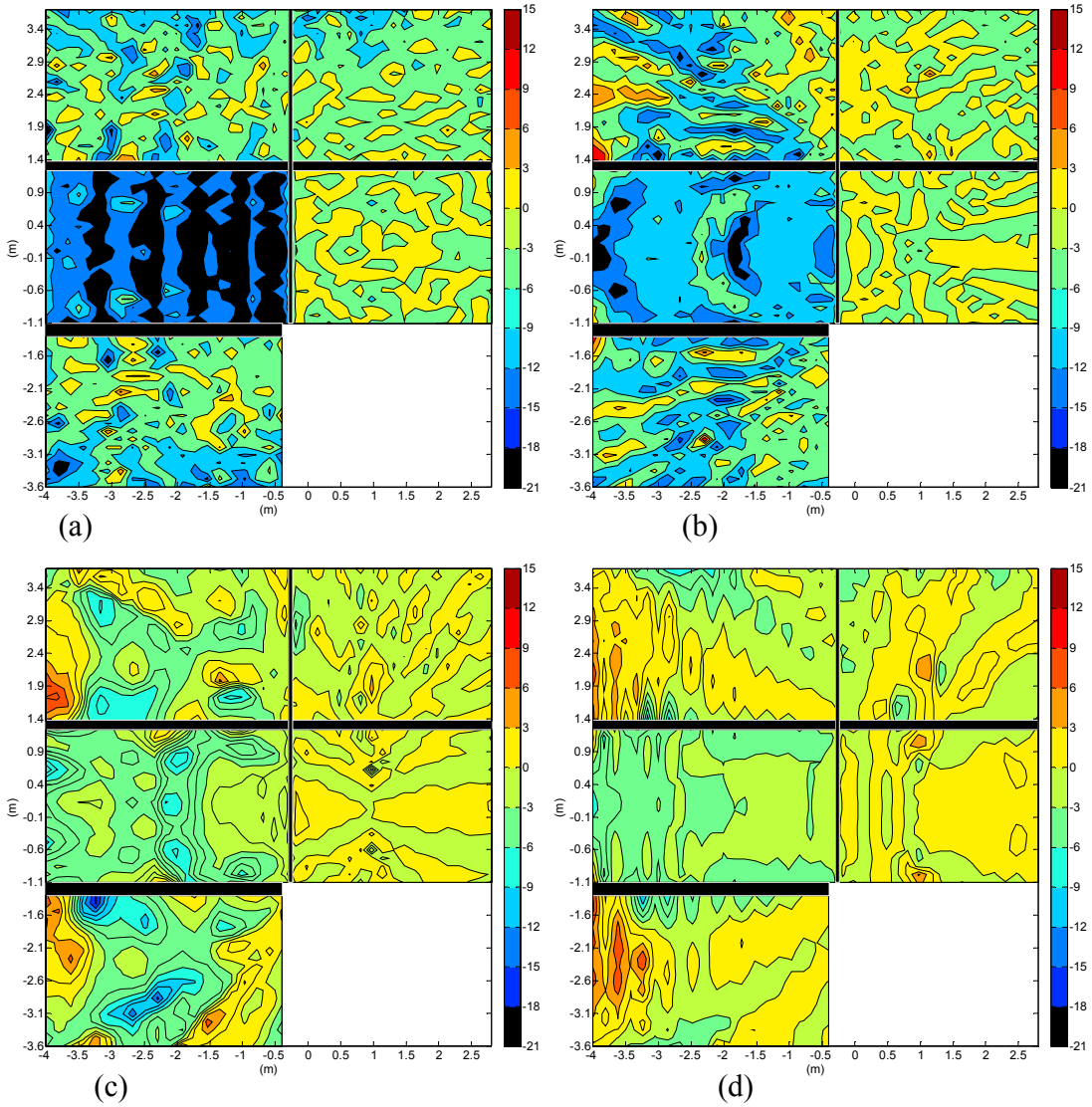

Figure 4.18: Simulated E-field (dBV/m) on vertical cut results for difference between open and closed door scenarios at different frequencies:
(a) 5.8 GHz (b) 2.4 GHz (c) 868 MHz (d) 433MHz.

4.7.2 Analysis of E-field with Occupants

The E-field amplitude distribution within Victorian house in the basement, ground floor and first floor for scenario (L) at all four frequencies are illustrated in Figure 4.19. By comparing the presence of occupants in the kitchen in the ground floor across all the four frequencies, the E-field level values behind occupant at all four frequencies are ranged

between -12 dBV/m and -6 dBV/m. This is due to presence of occupant near to the transmitter. Comparing the effect of the occupant on the E-field coverage in the front room across the four frequencies it has been found that the most significant effect is at the low frequencies. Also, the low E-field distributions within the house have occurred in the basement and the first floor at high frequencies ranged between -21 dBV/m and -33 dBV/m.

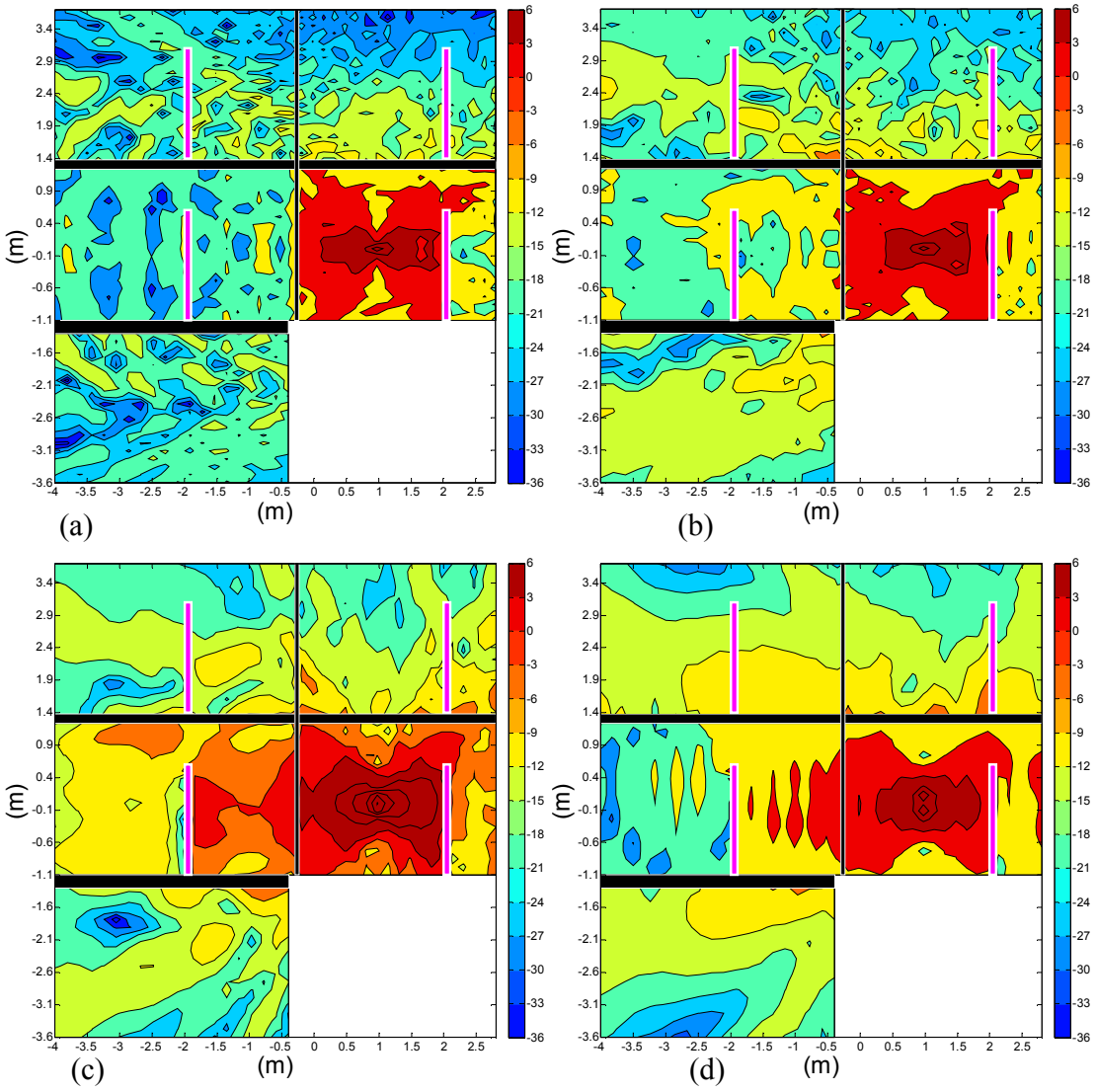

Figure 4.19: Simulated E-field (dBV/m) on vertical cut results for closed door &4human at different frequencies:

(a) 5.8 GHz (b) 2.4 GHz (c) 868 MHz (d) 433MHz.

A comparison between the results of the amplitude and cumulative probability distributions of the E- field values for the scenario (L) for the four frequencies in the basement, ground floor and first floor within the Victorian house is carried out as shown in Figure 4.20. When comparing the E-field values in the ground floor for the all the four frequencies, the results demonstrate that from 0 % to 70 % of the cumulative probability distributions for the low frequencies are higher than for the high frequencies. However, there is no variations of the E-field values from 70 % to 100 % of cumulative probability distribution in the ground floor between the four frequencies which is due to presence of the transmitting source in the kitchen. It can be seen that from Figure 4.20 (c) the peak value of amplitude of the E-field values in the ground floor for the low frequencies are higher than for the high frequencies. The lowest amplitude of the E-field values in the ground floor was at 5.8 GHz with amplitude probability distribution of 16% at -16 dBV/m. The average E-field cumulative probability distributions values in the basement at 2.4 GHz, 868 MHz and 433 MHz are similar with value of approximately -15 dBV/m. However, the average E-field cumulative probability distributions values in the basement at 5.8 GHz are less than the other frequencies by approximately 6 dBV/m. When comparing the E-field values in the first floor for the all the four frequencies in Figure 4.20 (f), the results demonstrate that the cumulative probability distributions for the low frequencies are higher than for the high frequencies. Figure 4.20 (e) shows that the highest amplitude of the E-field values in the first floor is at 433 MHz with amplitude probability distribution of 30 % at -12 dBV/m whereas the lowest amplitude of the E-field values in the first floor is at 5.8 GHz with amplitude probability distribution of 17 % at -15 dBV/m.

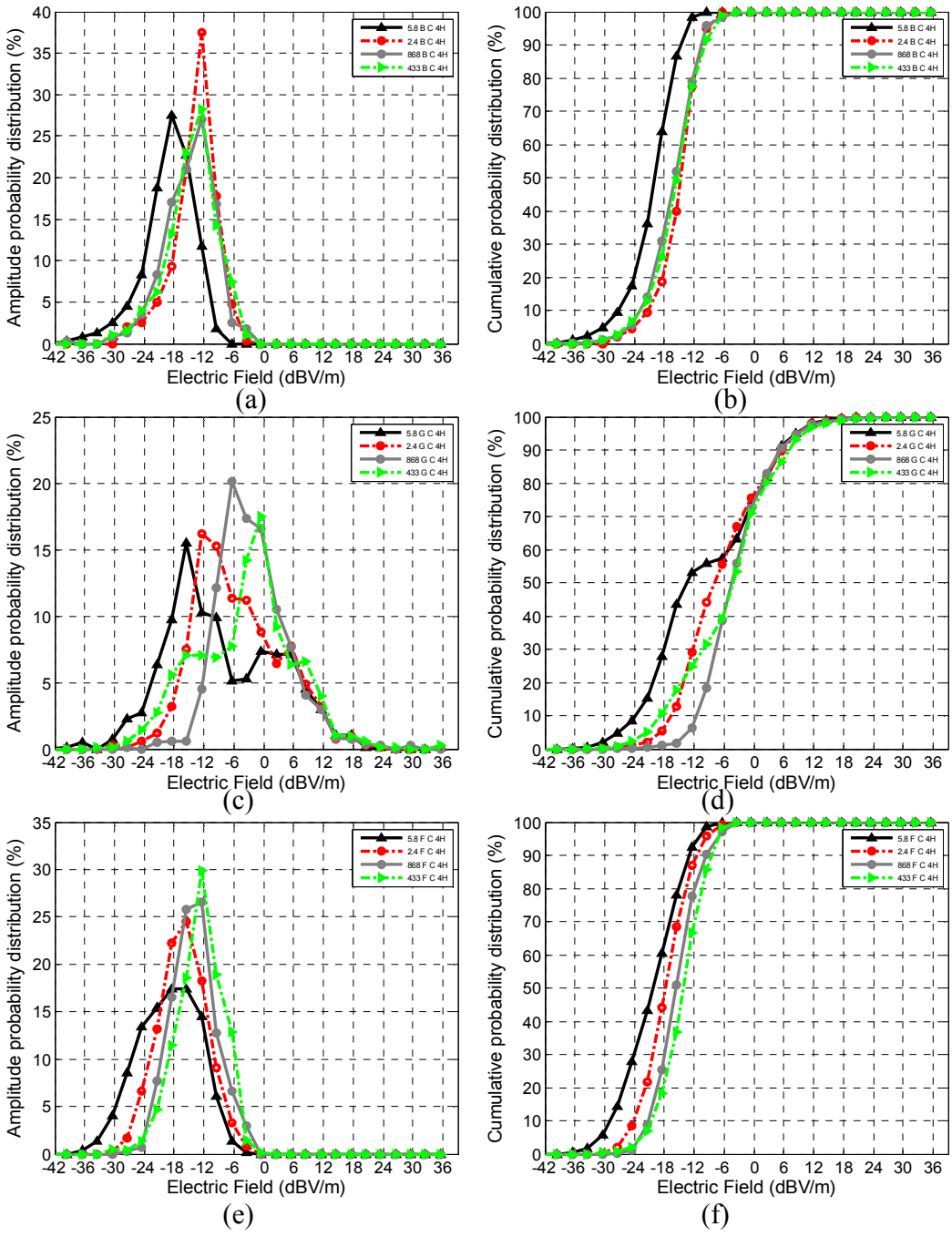

Figure 4.20: Vertical cut analysis at 5.8 GHz, 2.4 GHz, 868 MHz and 433 MHz for closed door with four occupants distributed within the house scenario:

(a) Basement amplitude distribution (b) Basement cumulative distribution (c) Ground Floor amplitude distribution (d) Ground Floor cumulative distribution (e) First Floor amplitude distribution (f) First Floor cumulative distribution.

Figure 4.21 illustrates the simulated results for the E-field difference between the open door scenario and four occupants are distributed within the house (one in kitchen, one in the front room, one in the bed1 and one in the bed2) with the doors are closed scenario at 5.8 GHz, 2.4 GHz, 868 MHz and 433 MHz. It can also be seen that the very low E-field coverage within front room in the ground floor ranged between -12 dBV/m and -21 dBV/m are obtained at high frequencies. By comparing the E-field distributions in the basement at all four frequencies, the results show that the E-field distributions at high frequencies are increased in the most of the area in the basement by 9 dBV/m whereas the low frequencies are attenuated by 6 dBV/m. At 5.8 GHz and 2.4 GHz there is a net increase in the E-field strength at some locations near to the occupants in the bed1 in the first floor between 9 dBV/m and 12 dBV/m. This is due to the constructive and the destructive reflections on the signals caused by the obstacles such as the wall, doors and occupant. However, the E-field levels behind the occupant in bed2 at all four frequencies are attenuated nearly by 6 dBV/m. The nearest occupant from the transmitter in the kitchen has the highest effect on the E-field distributions in the kitchen at 5.8 GHz which attenuated by -18 dBV/m. In general, the effect of the closed doors and occupants on the E-field distributions at high frequencies is higher than at the low frequencies due to the high signal coverage at low frequencies.

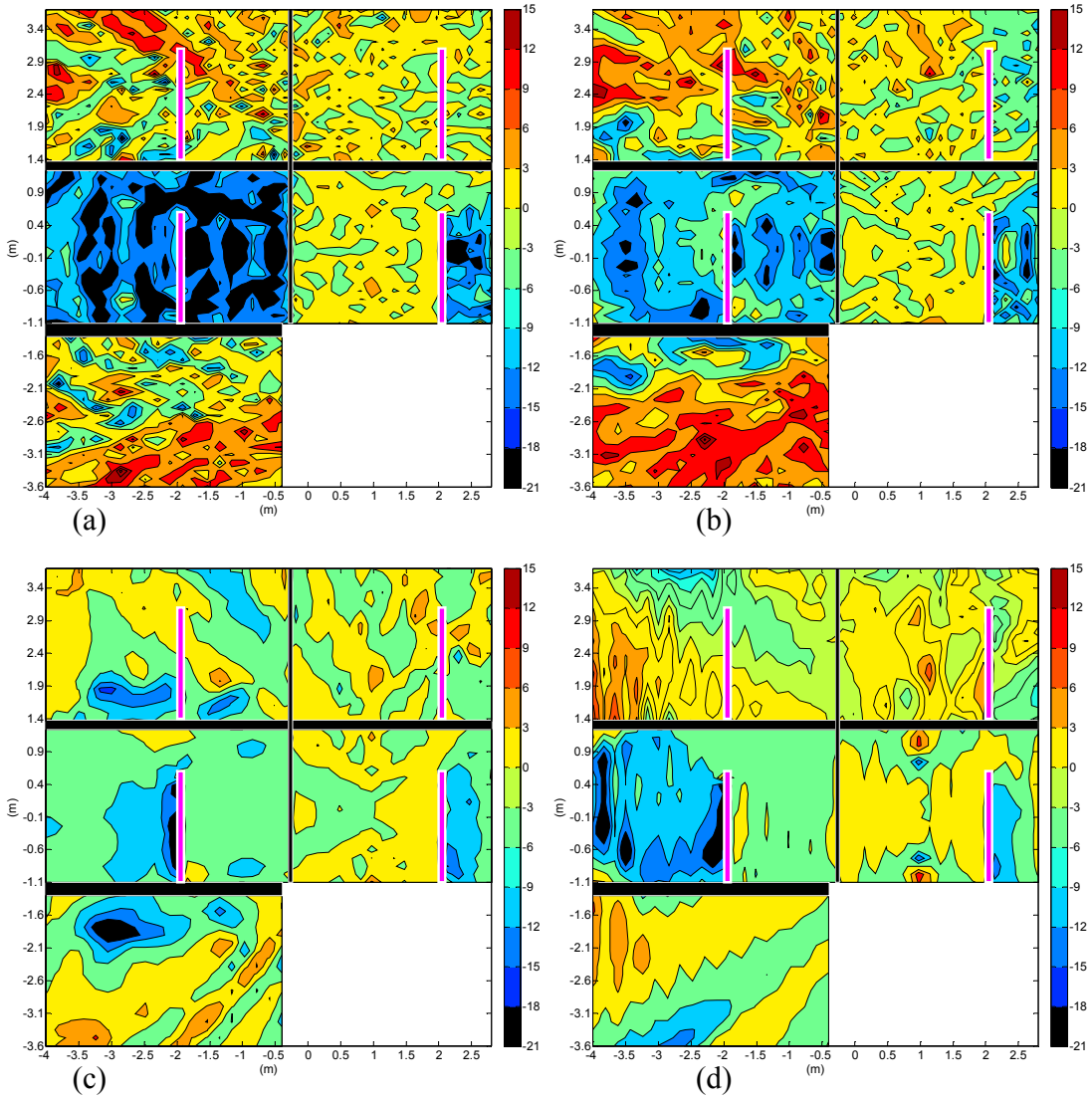

Figure 4.21: Simulated E-field (dBV/m) on vertical cut results for difference between open and closed door with 4 human scenarios at different frequencies:
(a) 5.8 GHz (b) 2.4 GHz (c) 868 MHz (d) 433MHz.

4.7.3 The Average E-field Analysis for All Frequencies

The average E-fields obtained from scenarios A, B, K and L in the basement, ground floor and first floor at 5.8 GHz, 2.4 GHz, 868 MHz and 433 MHz are summarized in Table 4.2. When comparing the average E-field values in the ground floor between the four frequencies, it can be seen that the doors status have a significant effect on the average E-

field values at high frequencies. However, the doors status has a little effect on the average E-field values at low frequencies in the ground floor. The biggest effect of the doors status on the average E-field values is at 5.8 GHz which attenuated by 8 dBV/m. However, the variations in the average E-field values caused by closed door in the ground floor at 868 MHz and 433 MHz are less than 2 dBV/m. It can be seen that the presence of occupants within the house have no effect on the average E-field values in the ground floor at low frequencies. However, the average E-field values in the ground floor at high frequencies are attenuated due to the presence of occupants in the house by 4 dBV/m. The average E-field values in the ground floor at the low frequencies are higher than at the high frequencies.

Comparing the average E-field values in the basement, it can be seen that the impact of the closed doors on the average E-field values in the basement is becoming more apparent at the high frequencies. By comparing scenarios A and B in the high frequencies in the basement, the variations in the average E-field values at high frequencies are approximately 4 dBV/m. When the occupants are existed within the house, the average E-field values in the basement at high frequencies are increased by 5 dBV/m. However, the average E-field values in the basement at low frequencies are unaffected by the presences of human or door status.

It can be observed that the average E-field values in the first floor at high frequencies are attenuated by 3 dBV/m due to changing the doors status from open to closed. When the occupants are presented within the house, the average E-field values in the first floor at high frequencies are increased by 5 dBV/m. By comparing the average E-field values in the first floor at low frequencies for the four scenarios, it can be observed that the variations in the average E-field values caused by closed doors or presences of occupants within the house are less than 2 dBV/m.

Table 4.2: The average electric fields for the four scenarios within basement, ground floor and first floor.

Scenario	Average Electric Field in Basement (dBV/m)				Average Electric Field in Ground floor (dBV/m)				Average Electric Field in First floor (dBV/m)			
	5.8 GHz	2.4 GHz	868 MHz	433 MHz	5.8 GHz	2.4 GHz	868 MHz	433 MHz	5.8 GHz	2.4 GHz	868 MHz	433 MHz
A	-22.2	-19.8	-14.2	-14.6	-0.4	-0.4	0.1	-0.8	-21.3	-18.4	-13.6	-13.0
B	-25.8	-24.1	-16.1	-14.2	-8.6	-5.0	-1.7	-1.8	-23.7	-20.2	-14.4	-12.9
K	-19.0	-13.9	-14.9	-14.5	-8.4	-5.1	-2.2	-3.7	-19.2	-16.3	-14.0	-12.9
L	-21.1	-14.1	-15.7	-13.2	-9.5	-6.4	-4.4	-3.9	-19.1	-16.2	-13.9	-12.1

4.8 Conclusions

In this chapter, an investigation into the changes in the E-field strength within the basement, ground floor and first floor of a Victorian house at 5.8 GHz, 2.4 GHz, 868 MHz and 433 MHz were carried out. Four different Scenarios were compared for opening and closing doors and changing the building's occupancy level. The effects of different obstacles inside the rooms were compared and the one which has the most significant effect on the received E-field strength was highlighted. By comparing the four frequencies in case of open door and no occupants exist in the house, it was seen that the E-field coverage levels in the three floors within Victorian house at the low frequencies are higher than that at the high frequencies. The closing doors have a significant effect on the E-field coverage levels within the house at the high frequencies whereas have less effect on the E-field coverage levels at the low frequencies. The closed doors at high frequencies have attenuated the propagated signals passed through the closed door by nearly 18 dB whereas at low frequencies were attenuated only by 3 dB. Comparing the effect of the occupants on the E-field coverage within the house across the four frequencies, it was found that the human occupants in ground floor have the most significant effect on the E-field level in

the house. However, the presence of occupants in the first floor has less effect on the signal propagation levels than presence of human in the ground floor. By comparing the basement when the occupants were present in the house at all four frequencies, the results showed that the E-field distributions at high frequencies are increased in most area in the basement by 9 dB whereas the low frequencies are attenuated by 6 dB. The nearest occupant from the source transmitter in the kitchen has a biggest effect on the E-field distribution in the kitchen at 5.8 GHz which attenuated by -18dB.

By comparing the average E-field values in case of open door scenario in the ground floor, the results demonstrated that the average E-field values are similar for all four frequencies. However, in the basement and the first floor, the average E-field values at the low frequencies are higher than at the high frequencies. In case of closed doors and the presence of occupants within the house, it was seen that the lowest average E-field values in the basement, ground floor and the first floor for the four frequencies is at 5.8 GHz.

To conclude, the effect of closed doors and occupants on the E-field distributions at high frequencies is higher than at the low frequencies due to a high signal coverage at low frequencies. The simulation results illustrated that the low frequencies provide a better coverage and higher average E-field levels than the high frequencies.

Chapter 5 – Analysis of E-Field Distributions on Horizontal Plane for Configuration B in Single Floor within House

This chapter investigates the distribution of the E-field in configuration B in a horizontal plane. Configuration B is defined as follows, the dipole antenna transmitter is positioned in the corner of the kitchen on the ground floor in a Victorian house for the four frequencies.

5.1 Introduction

Finding the best antenna locations is one of the factors that affect the signal coverage inside the house and for good network planning provides. In this chapter, the opening and closing of doors and the existence of occupants which are the two main factors that affect the E-field strength of a vertically polarized dipole antenna transmitter have been investigated. The dipole antenna transmitter is positioned in the corner of the kitchen near from the middle wall and the external wall. The reasons for this location as most appliances and wireless sensor network located near to the wall in the kitchen. The received fields are plotted for a horizontal plane with respect to transmitter on the ground floor.The E-field distribution operating at the same previous frequencies 5.8 GHz, 2.4 GHz, 868 MHz, 433 MHz within ground floor have been investigated. The scenarios used in the previous chapters have been used in sections 5.2 to 5.5. The simulations of the E-Field distributions at 5.8 GHz, 2.4 GHz, 868 MHz and 433 MHz are presented. A further discussion of previous sections is summarized in section 5.6. Section 5.7 concludes this chapter.

5.1.1 Simulation Scenarios

The experiment setup is the same as described in chapter 3. The same ten different scenarios (A to J) that were used in chapter 3 are used in this chapter except the

transmitting antenna location is moved from the middle of the door in the kitchen to the corner in the kitchen as shown in Figure 5.1 .

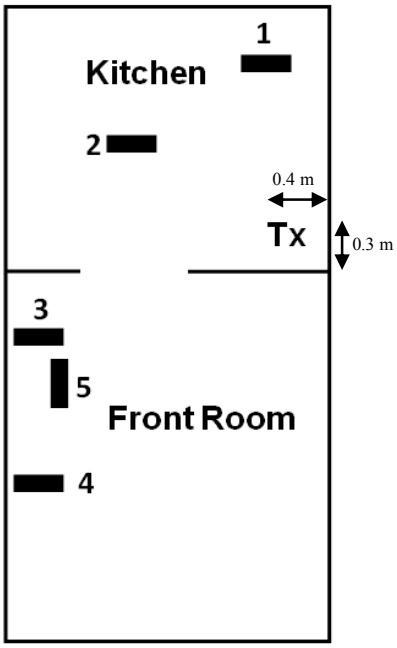

Figure 5.1: Layout of the ground floor of the house showing occupancy locations.

5.2 Simulation of the E-Field Distributions on Horizontal Plane at 5.8 GHz

Simulations were performed using a 5.8 GHz have-wavelength dipole antenna to calculate the E-fields strength. The simulation setup and parameters are exactly the same as described in section 3.3. Analysis was performed for different occupancy scenarios as described in the section 5.1.1.

The results present the E-field amplitude distribution obtained for the ground floor of the Victorian house. Results were sampled in a plane 1.2 m above the ground, at the same height as the source antenna. 840 samples of the E-field amplitude were obtained from the simulations in both the kitchen and front room. The amplitude probability and the cumulative probability distributions of the E-field distribution have been used for analysis purposes. The same three methods (A, B and C) are also used for analysis.

5.2.1 Method A Results

For method A, the E-field distributions results are presented in dBV/m for all ten scenarios from scenario A to scenario J in Figure 5.2 (a) to Figure 5.2 (j). Comparing Figure 5.2 (a) and Figure 5.2 (b) it can be seen that opening or closing the door has a noticeable effect on the E-field distributions within the front room. The results show that when the door is closed the E-field strength is reduced by approximately 9 dBV/m. Also, it can be seen that the presence of one person located in either room has an effect on the field distribution in their local proximity and the effects of shadowing can be clearly seen.

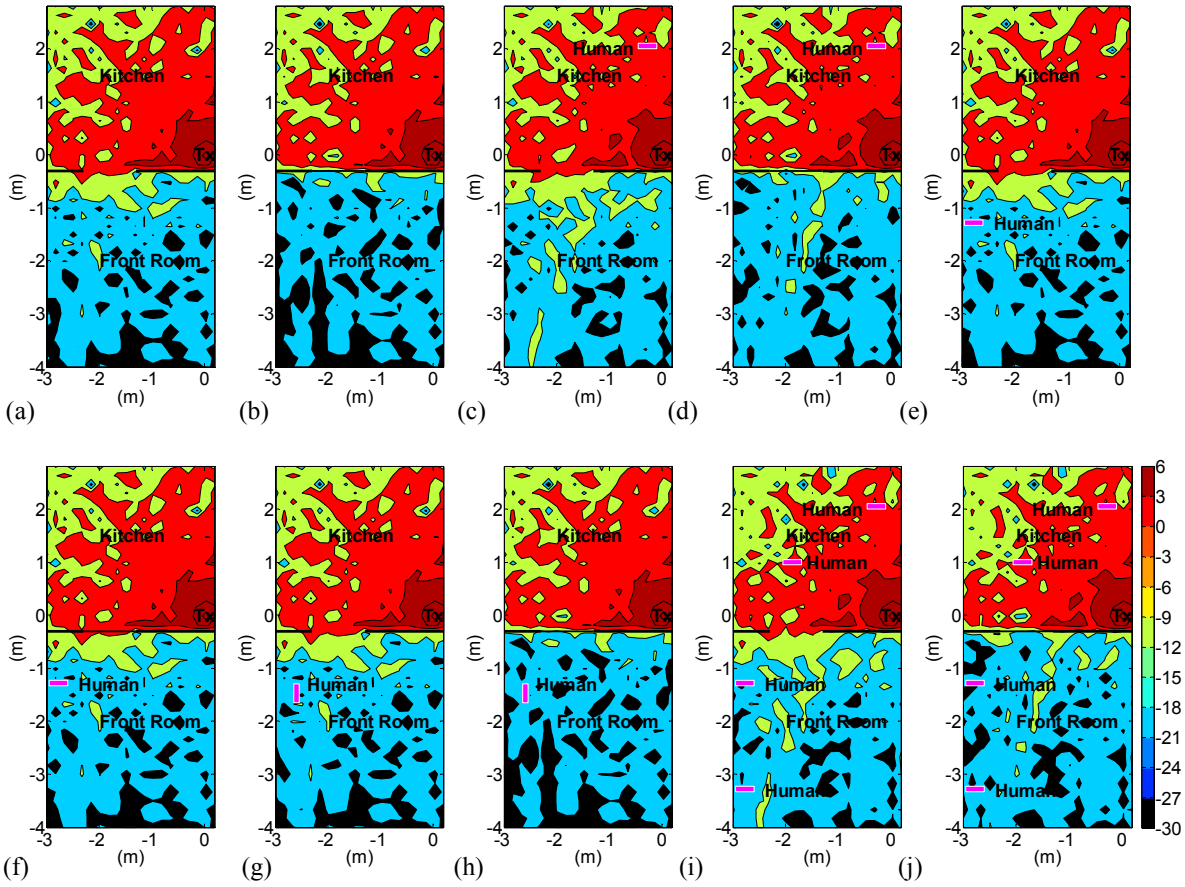

Figure 5.2: Simulated E-field (dBV/m) distributed on the ground floor at 5.8GHz: (a) Scenario A (b) Scenario B (c) Scenario C (d) Scenario D (e) Scenario E (f) Scenario F (g) Scenario G (h) Scenario H (i) Scenario I (j) Scenario J.

5.2.2 Method B Results

For method B, high or low field E-field distribution levels within the Victorian house are used to get difference plots. Simulated results for the difference of the E-field plot between scenarios A (unoccupied, open door) and other scenarios at 5.8 GHz are shown in Figure 5.3, where the E-field strength unit is in dBV/m. Scenario (A) is the reference of analysis and positive values (shown as yellow to red) which represent areas with a higher E-field when compared to scenario (A).

When a human occupant is located at position 1 and/or 2 within the kitchen, the shadowing effect (attenuation) various between 3 dB and 9 dB, as shown in Figure 5.3 (b) to Figure 5.3 (i). Results also show that due to occupants in the kitchen, the E-field strength is increased at some locations within the front room also varying from 3 to 9 dB. The results of all scenarios clearly demonstrate that the doors status (open or closed) have a significant effect on the E-field coverage in the front room. It can be seen that the orientation of the occupant in the front room has a very limited effect on the signal propagation within the front room as shown in Figure 5.3 (d) and Figure 5.3 (f). As the number of occupants increases from 1 to 4, the E-field distributions in some areas in the front room are improved between 3 to 9 dB due to the increase of the reflected signal from them.

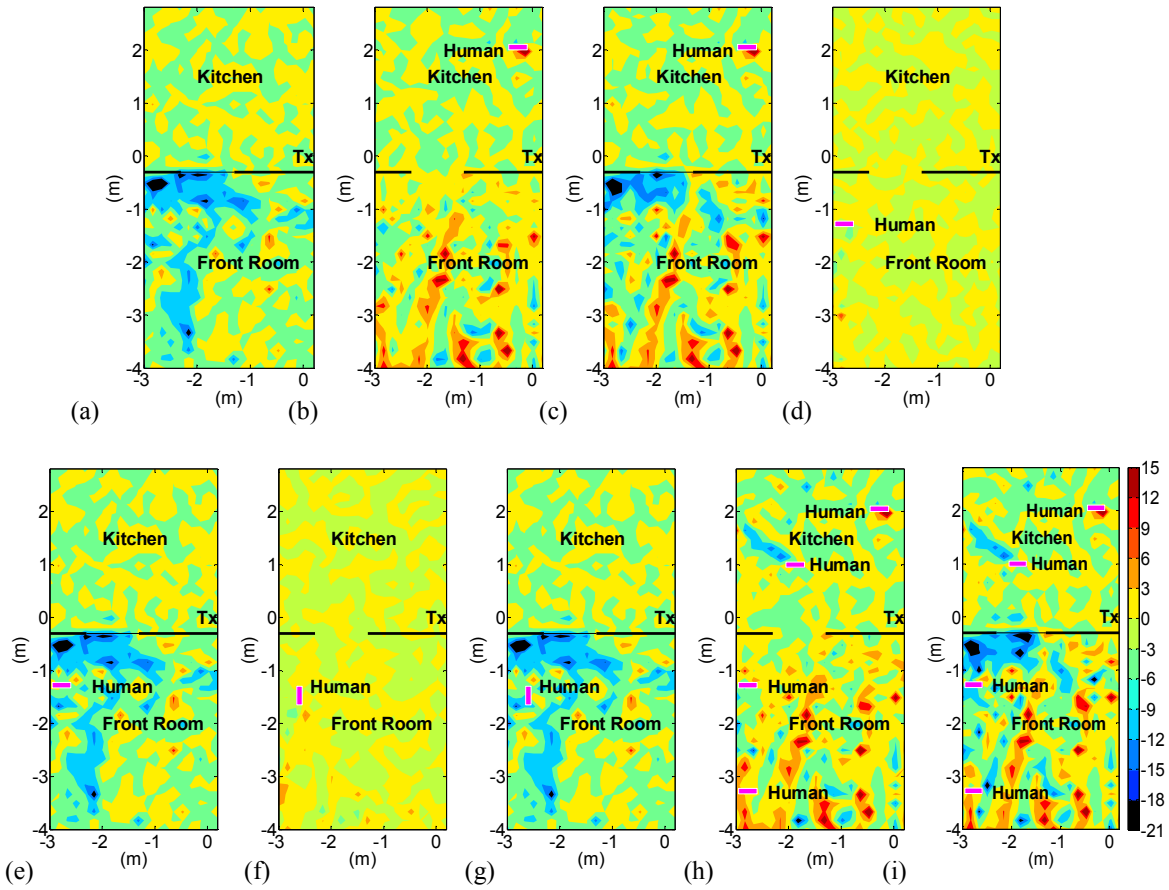

Figure 5.3: Simulated E-field (dB) difference between scenarios at 5.8 GHz: (a) Scenario A & B (b) Scenario A & C (c) Scenario A & D (d) Scenario A & E (e) Scenario A & F (f) Scenario A & G (g) Scenario A & H (h) Scenario A & I (i) Scenario A & J.

5.2.3 Method C Results

For method C, the amplitude and cumulative probability distribution are used to provide simplified comparison between different scenarios of the E-field values within the Victorian house at 5.8GHz. The amplitude and cumulative probability distribution for all scenarios within the kitchen and front room are presented in Figure 5.4 (a) and Figure 5.4 (b), respectively. The x-axis and y-axis represent the distribution of field levels and the probability percentage of the appearance of each field level, respectively. The results

demonstrate that there is no noticeable difference in the E-field distribution in the kitchen for all scenarios, whereas the average E-field distribution increases in the front room when the kitchen is occupied. The closed door has a great effect on the transmitted signal which results in signal degradation. The presence of the human in the kitchen also attenuated the signal levels in the front room. In the case of open door scenarios, it is clear that the presence of the human reduces the average value of the transmitted signal from -15 dBV/m to -18 dBV/m which correspond to 16.6 % compared to when there is no human in the kitchen.

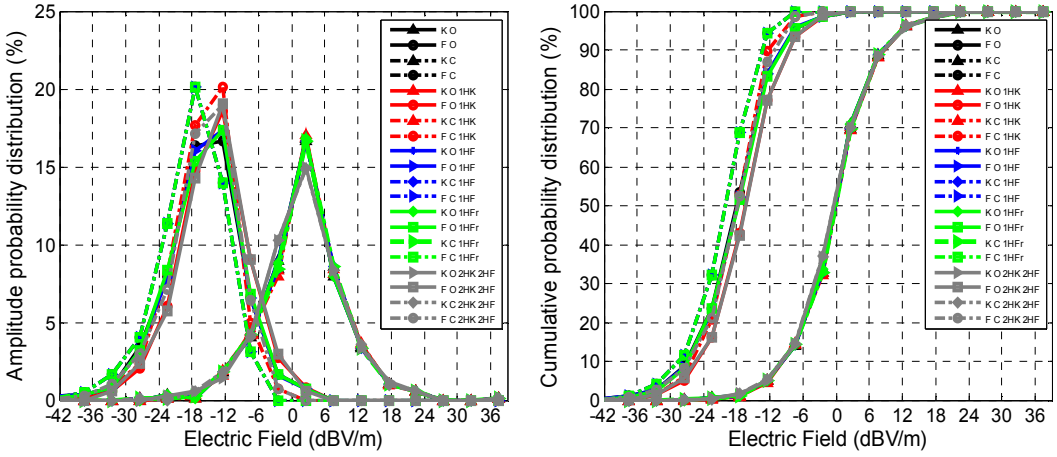

(a) (b)

Figure 5.4: E-field amplitude and cumulative probability distribution at 5.8 GHz for all scenarios from A to J.

5.3 Simulation of the E-Field Distributions on Horizontal Plane at 2.4 GHz

A dipole antenna resonated at 2.4 GHz frequency was used in the simulation to generate the E-field. The simulation setup and parameters are exactly the same as described in the section 3.4 except the transmitting antenna were moved to the corner in the kitchen. Analysis was performed for different occupancy scenarios as described in the section 5.1.1.

Same parameters that used in the previous section are used in following simulation scenarios. Amplitude probability and the cumulative probability distributions of the E-field distribution have been used for analysis purposes. Results obtained from scenario A to scenario J are used in this chapter. The same three methods (A, B and C) are used in this section [84].

5.3.1 Method A Results

For method A, for scenario A to scenario J the E-field distributions results are measured in dBV/m as shown in Figure 5.5 (a) to Figure 5.5 (j). The propagated signals coming through the closed door is attenuated by approximately 6 dBV/m compared to when the door is open as shown in Figure 5.5 (a) and Figure 5.5 (b). In one person scenario in the kitchen, the electric field distribution degraded by 9 dB V/m behind the person. However, the presence of the person in the front room does not have a significant effect on electric field distribution within front room. This is caused by the presence of wall located between the kitchen and front room blocked the transmitter from seeing the human body. Also, it can be seen that when the number of persons are increased to four (two in kitchen and two in the front room) at ground floor, the electric field distribution within the kitchen is decreased behind the human body whereas the field distribution within front room is increased in some locations.

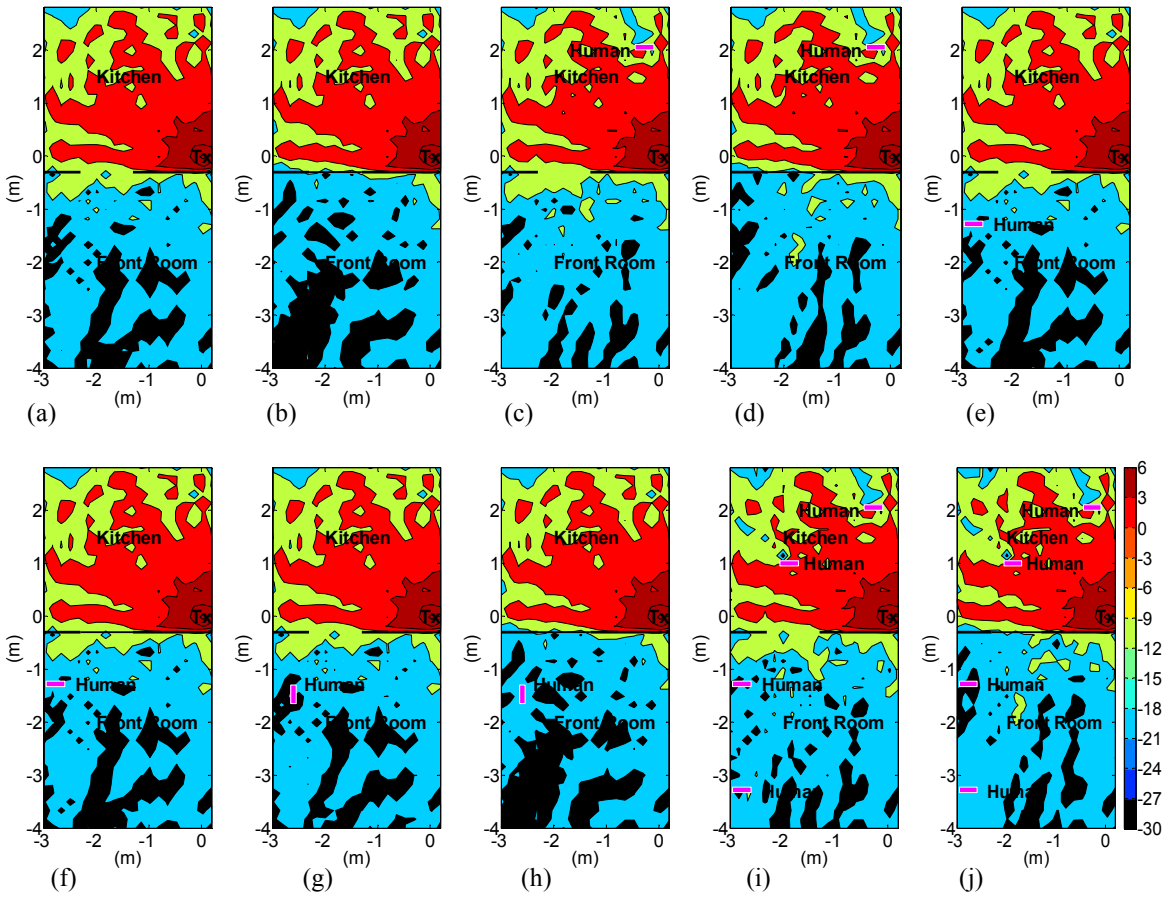

Figure 5.5 : Simulated E-field (dBV/m) distributed on the ground floor at 2.4GHz:
(a) Scenario A (b) Scenario B (c) Scenario C (d) Scenario D (e) Scenario E (f) Scenario F
(g) Scenario G (h) Scenario H (i) Scenario I (j) Scenario J.

5.3.2 Method B Results

For method B, either high or low field E-field distribution levels within the Victorian house are used to obtain the difference between scenarios A (unoccupied, open door) and other scenarios at 2.4 GHz as shown in Figure 5.6. Scenario (A) is used as a reference for the analysis. The positive values (shown as yellow to red) represent areas with higher E-field distributions when compared to scenario (A). While the negative values (shown as blue and black) represent areas with lower E-field distribution.

The shadowing effect (attenuation) due to the occupant in the kitchen at position 1 is about 9 dB as observed in Figure 5.6 (b). It can also be seen that there is a net increase in the E-field strength at some locations within the front room of between 9 and 12 dB due to the occupant in the kitchen.

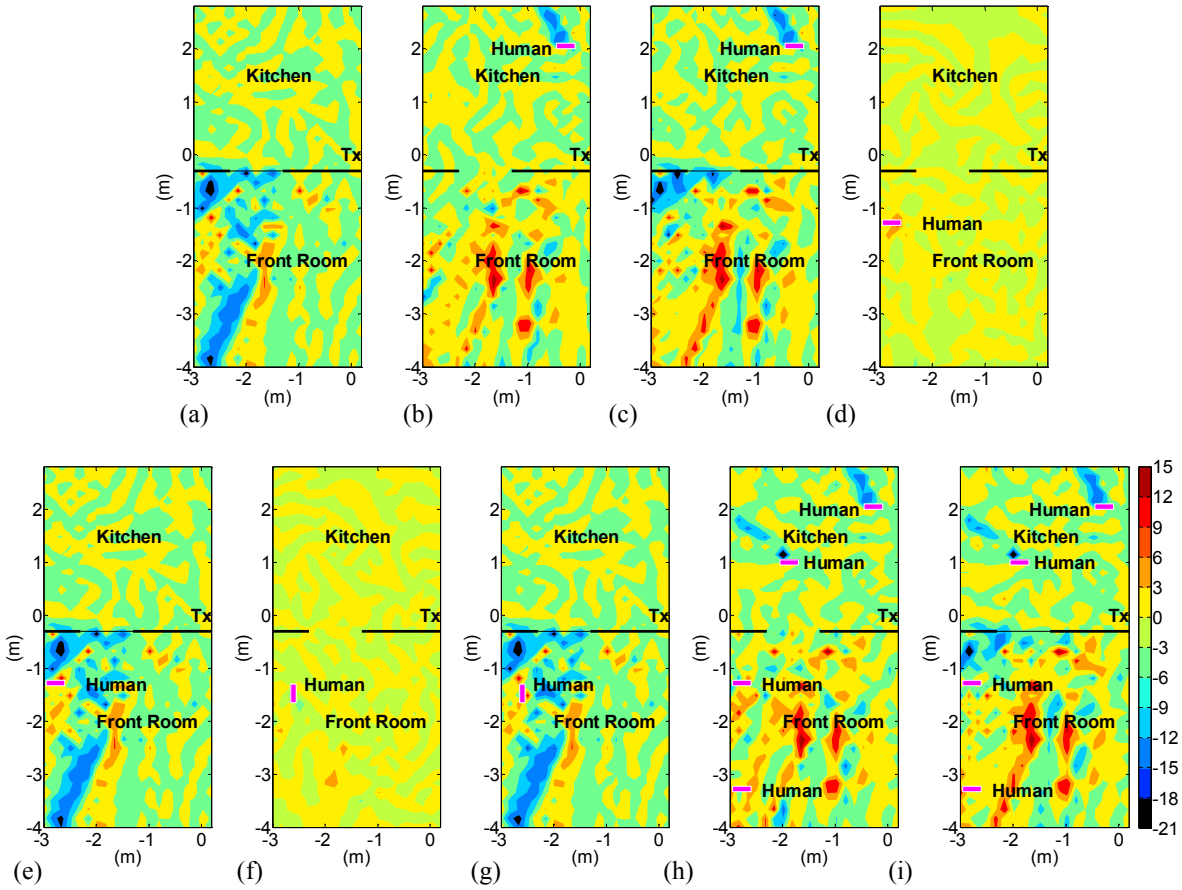

Figure 5.6: Simulated E-field (dB) difference between scenarios at 2.4GHz:

(a) Scenario A & B (b) Scenario A & C (c) Scenario A & D (d) Scenario A & E (e) Scenario A & F (f) Scenario A & G (g) Scenario A & H (h) Scenario A & I (i) Scenario A & J.

5.3.3 Method C Results

For method C, the amplitude and cumulative distribution function are used to provide simplified comparison between different scenarios of the field data within the Victorian house. Figure 5.7 (a) and Figure 5.7 (b) show the results of E-field amplitude distribution

and cumulative probability distributions within the kitchen and front room from scenario A to scenario j, respectively. The x-axis represents the distribution of field levels while y-axis represents the probability percentage of the appearance of each field level. It can be seen that the E-field distribution in the kitchen is similar for all scenarios, whereas in the front room the average E-field distribution increases when the kitchen is occupied. The effects due to transmission losses through the closed door can be clearly seen. The presence of the human in the kitchen also affected the level of the signal in the front room. For the scenario of an open door it is clear that the presence of the human has reduced the average value of the signal from -17 dBV/m to -20 dBV/m, a 3 dBV/m attenuation due to the presence of a human in the kitchen.

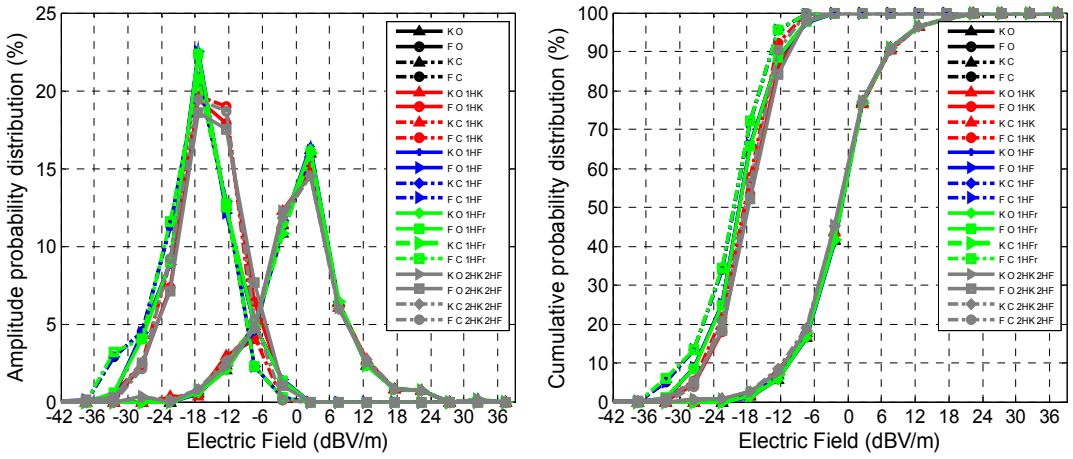

(a) (b)

Figure 5.7: E-field amplitude and cumulative probability distribution at 2.4 GHz for all Scenarios from A to J.

5.4 Simulation of the E-Field Distributions on Horizontal Plane at 868 MHz

Simulations were carried out using 868 MHz dipole antenna to generate the E-fields. The simulation setup and parameters are exactly the same as described in the section 3.5 except the transmitting antenna were moved to the corner in the kitchen. Same ten

scenarios (A to J) that described in the previous section are also investigated in this section.

Same parameters that used in the previous section are used in following simulation scenarios. The amplitude probability and the cumulative probability distributions are used to analysis the E-field distribution. This section presents the results obtained from the scenarios described in section 5.1.1. The same three methods (A, B and C) are also used for analysis.

5.4.1 Method A Results

For method A, the E-field amplitude distribution results are calculated for all ten scenarios from A to J at 868 MHz. Figure 5.8 illustrates the results of E-field amplitude distributions for all ten scenarios at 868 MHz. The propagation of the signal from kitchen to the front room through the closed door is decreased by 3 dBV/m compared to the open door scenario as shown in Figure 5.8 (a) and Figure 5.8 (b). The simulation results show that there is a high E-field near to the door and internal wall in the front room. The human bodies effect on the E-field signals depends on their locations. The presence of human in the kitchen has attenuated the signal from 3 dBV/m to -9 dBV/m as shown in Figure 5.8 (c). However, the human effect in the front room has less impact on the E-field distribution. Figure 5.8 (e) shows the E-field distribution behind the human is degraded by 3 dB V/m whereas when the human is oriented the E-field attenuated by 6 dB V/m.

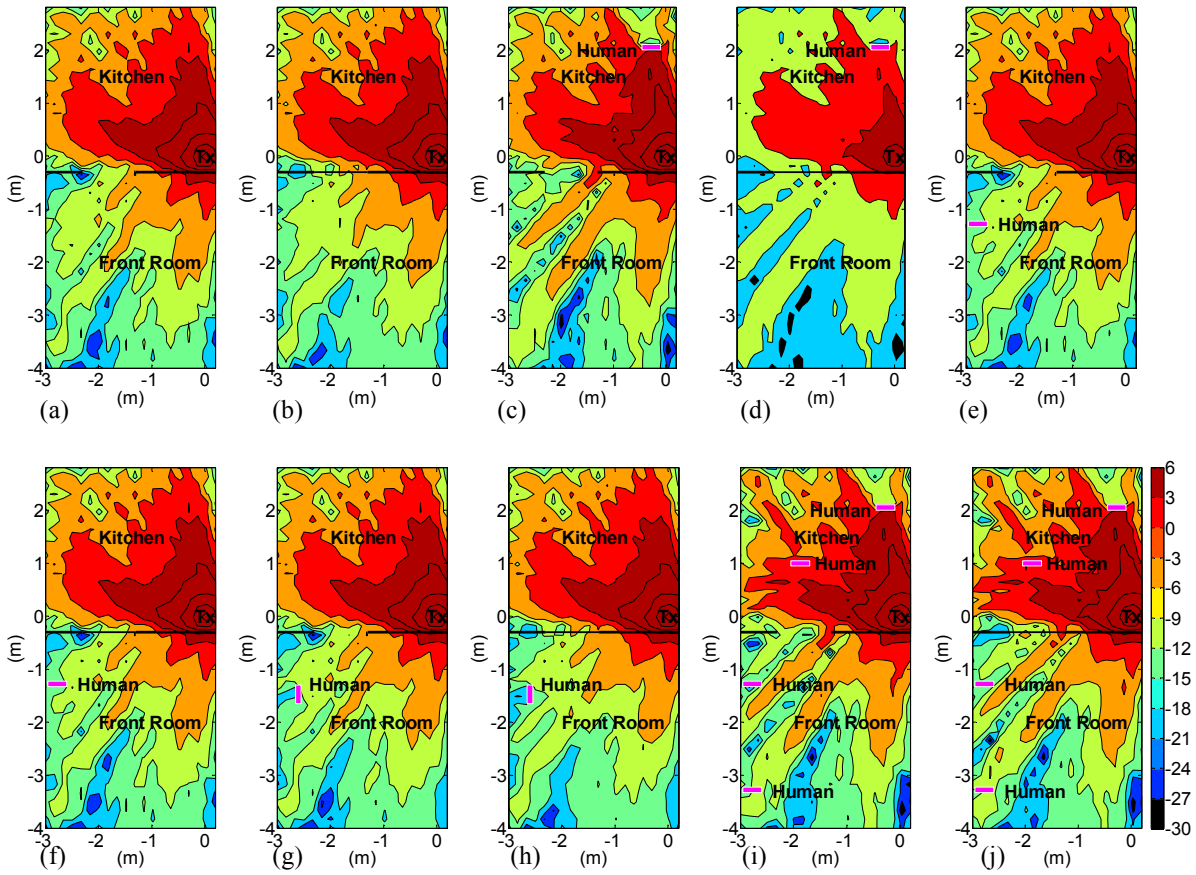

Figure 5.8: Simulated E-field (dBV/m) distributed on the ground floor at 868MHz:
(a) Scenario A (b) Scenario B (c) Scenario C (d) Scenario D (e) Scenario E (f) Scenario F
(g) Scenario G (h) Scenario H (i) Scenario I (j) Scenario J.

5.4.2 Method B Results

For method B, the difference in E-field levels between scenario A and other nine scenarios are calculated at 868 MHz. The aim of these results is to show the field strength level area within the Victorian house. Figure 5.9 shows the results of E-field level difference between the scenario A (which used as a reference) and other nine scenarios at 868 MHz. The figures show that the difference between the two door status is very little. In case of the presence of human in the kitchen, the field level has decreased behind it by 9 dB and in some areas in the kitchen and front room is decreased by 3 dB. The presence of human

in the front room has no effect on the field distribution either in the front room or in the kitchen. When the human is oriented in the front room, the field distributions is attenuated by 6 dB around the human. It can be seen that from Figure 5.9 there is a high field spot close to the door due to the reflection coming from the door and internal wall and is about 6 dB.

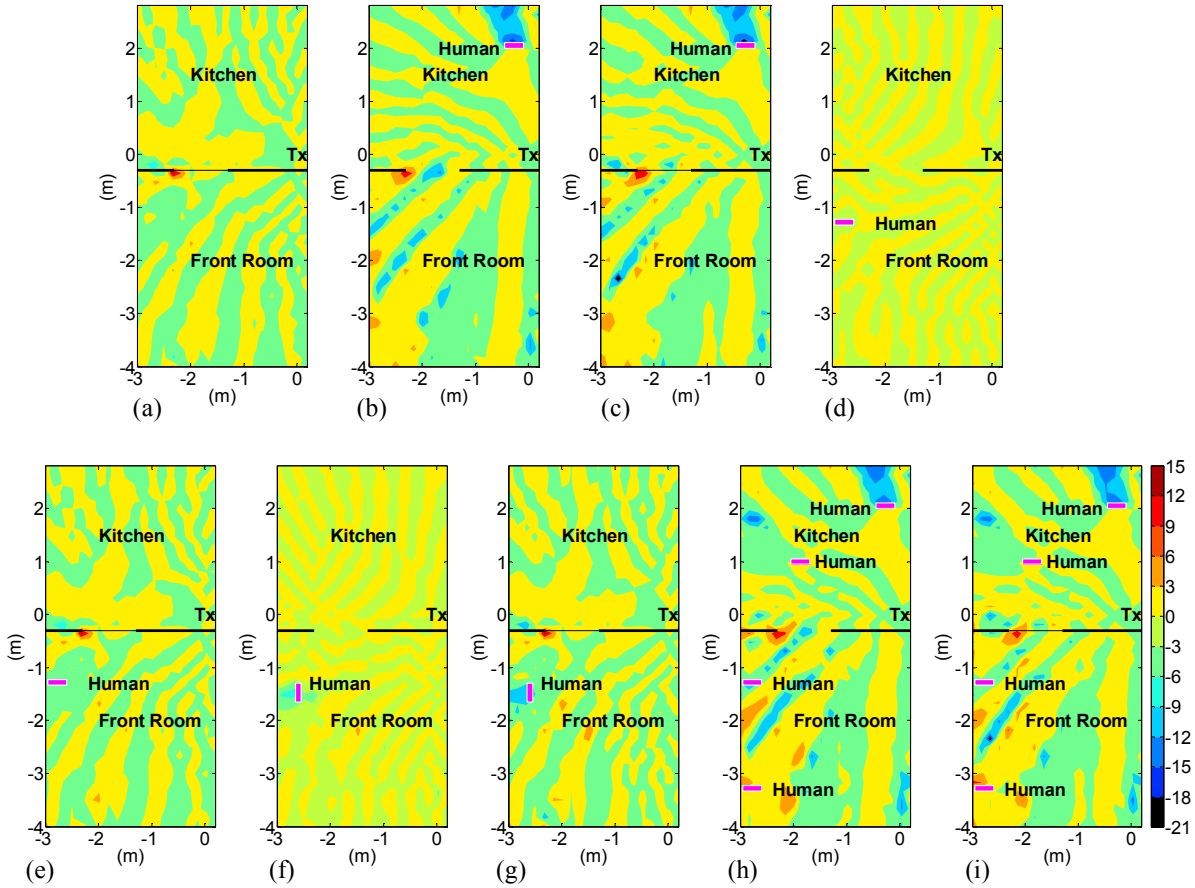

Figure 5.9: Simulated E-field (dB) difference between scenarios at 868MHz: (a) Scenario A & B (b) Scenario A & C (c) Scenario A & D (d) Scenario A & E (e) Scenario A & F (f) Scenario A & G (g) Scenario A & H (h) Scenario A & I (i) Scenario A & J.

5.4.3 Method C Results

For method C, the amplitude and cumulative probability distributions are calculated for the E-field simulated values for all ten scenarios within Victorian house at 868 MHz as shown in Figure 5.10 (a) and Figure 5.10 (b), respectively. The curves on the left side of each figure represent the E-field level for the scenarios in the kitchen while the curves on the right side represent the E-field level for the same scenarios in the front room. It can be seen that from Figure 5.10 (b) the variations in the curves for all scenarios in kitchen and front room are minimal. The average values of the signals in the kitchen are ranged between -13 dBV/m and -11 dBV/m whereas in the front room the average values are -2 dBV/m.

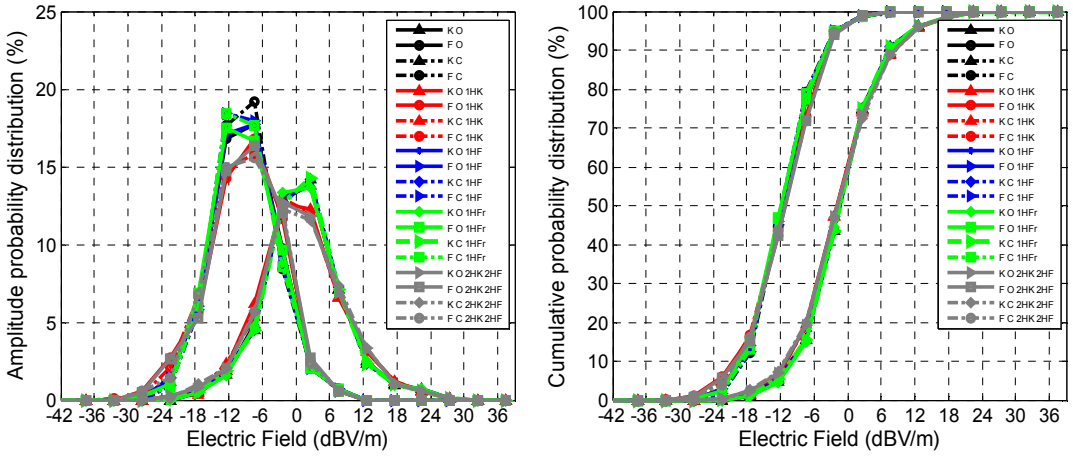

(a) (b)

Figure 5.10: E-field amplitude and cumulative probability distribution at 868 MHz for all scenarios from A to J.

5.5 Simulation of the E-Field Distributions on Horizontal Plane at 433 MHz

The E-field was generated using 433 MHz dipole antenna in the following simulations. The parameters that used in these simulations are the same as described in section 3.6.

Based on the designed described above, ten different scenarios were designed named as (A to J).

As described in the previous section, the results focus on the E-field amplitude distributions for the ground floor of the Victorian house. Again, the E-field is analysed using the amplitude probability and the cumulative probability distributions. This section presents the results obtained from the scenarios described in section 5.1.1.

5.5.1 Method A Results

The E-field amplitude distribution within Victorian house in kitchen and front room for all the described ten scenarios at 433 MHz are shown in Figure 5.11. High E-field levels are obtained in the kitchen and some area in the front room for the case of open door and no occupant exist in the ground floor. The E-field signals are attenuated by 3 dBV/m due to the closed door. When one human is exist in the kitchen, the signal behind the human is attenuated by approximately 5 dBV/m. However, the E-field signal strength in the front left corner area in front room are increased by 6 dBV/m due to multipath effect as shown in Figure 5.11 (c). The human in the front room is far from the source results in the signals propagation has not been affected in the ground floor. However, when the human is oriented in the front room, the coverage signal behind it is attenuated by 4 dBV/m. Figure 5.11 (j) shows that low E-field levels are obtained between 3 dBV/m to 6 dBV/m in some area in kitchen when the number of people is increased to four.

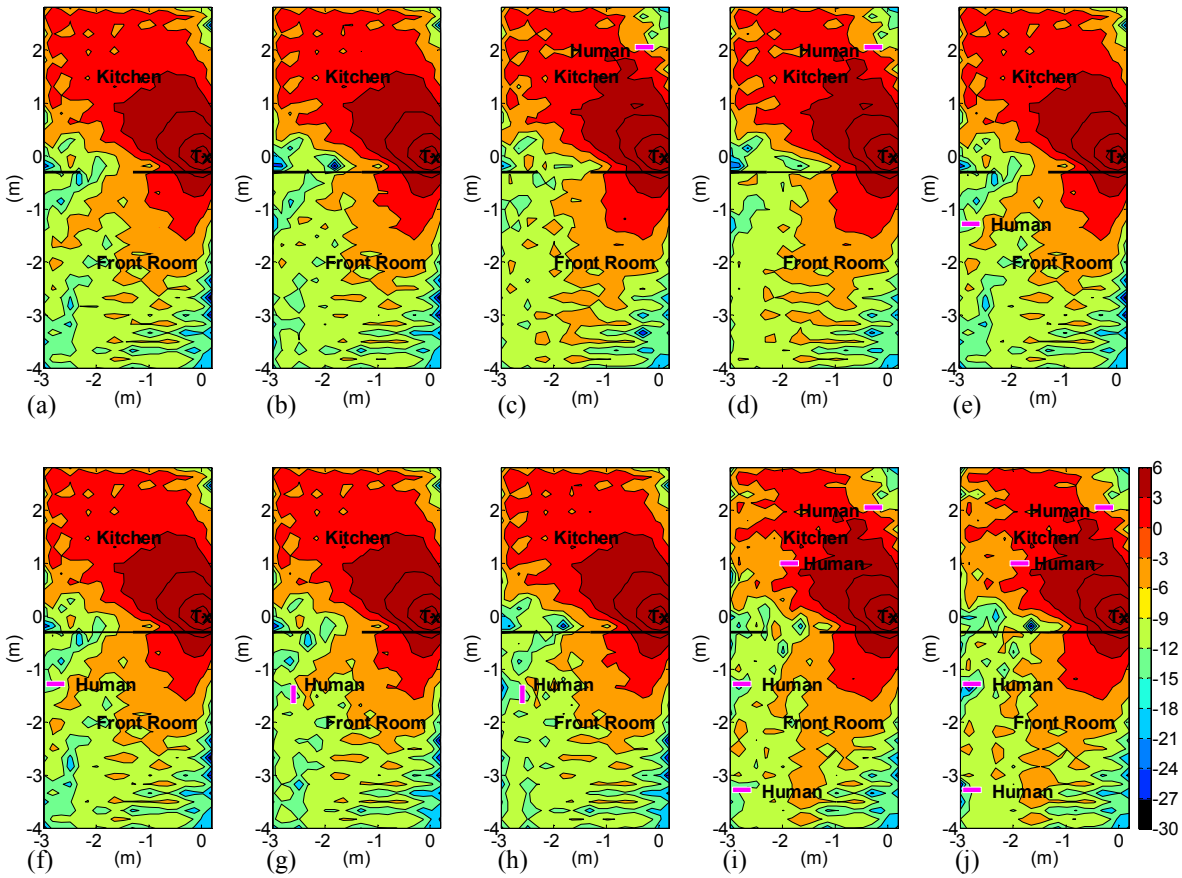

Figure 5.11: Simulated E-field (dBV/m) distributed on the ground floor at 433MHz:
(a) Scenario A (b) Scenario B (c) Scenario C (d) Scenario D (e) Scenario E (f) Scenario F
(g) Scenario G (h) Scenario H (i) Scenario I (j) Scenario J.

5.5.2 Method B Results

Similar investigations to those in the previous section were carried out in this section at 433 MHz. The differences in the E-field distribution are plotted to show the E-field strength variations between the investigated scenarios. Figure 5.12 illustrates the E-field level differences between scenario A and other nine scenarios at 433 MHz. It can be seen that the door between kitchen and front room attenuated the signals by 6 dB. While the presence of the occupants in the kitchen and front room has a different effect on the E-

field distribution in the ground floor. The E-field strength in the kitchen is decreased in range between 6 to 9 dB due to the presence of human in the kitchen as shown in Figure 5.12. As the number of the occupants increased in the kitchen, the E-field distribution in the kitchen is attenuated between 3 dB to 9 dB in the most area of the kitchen. The human in the front room has a negligible effect on the E-field distribution on the front room whereas when the human is orientated in the front room results in the signals attenuated by approximately 5 dB as shown in Figure 5.12 (e) and Figure 5.12 (d), respectively.

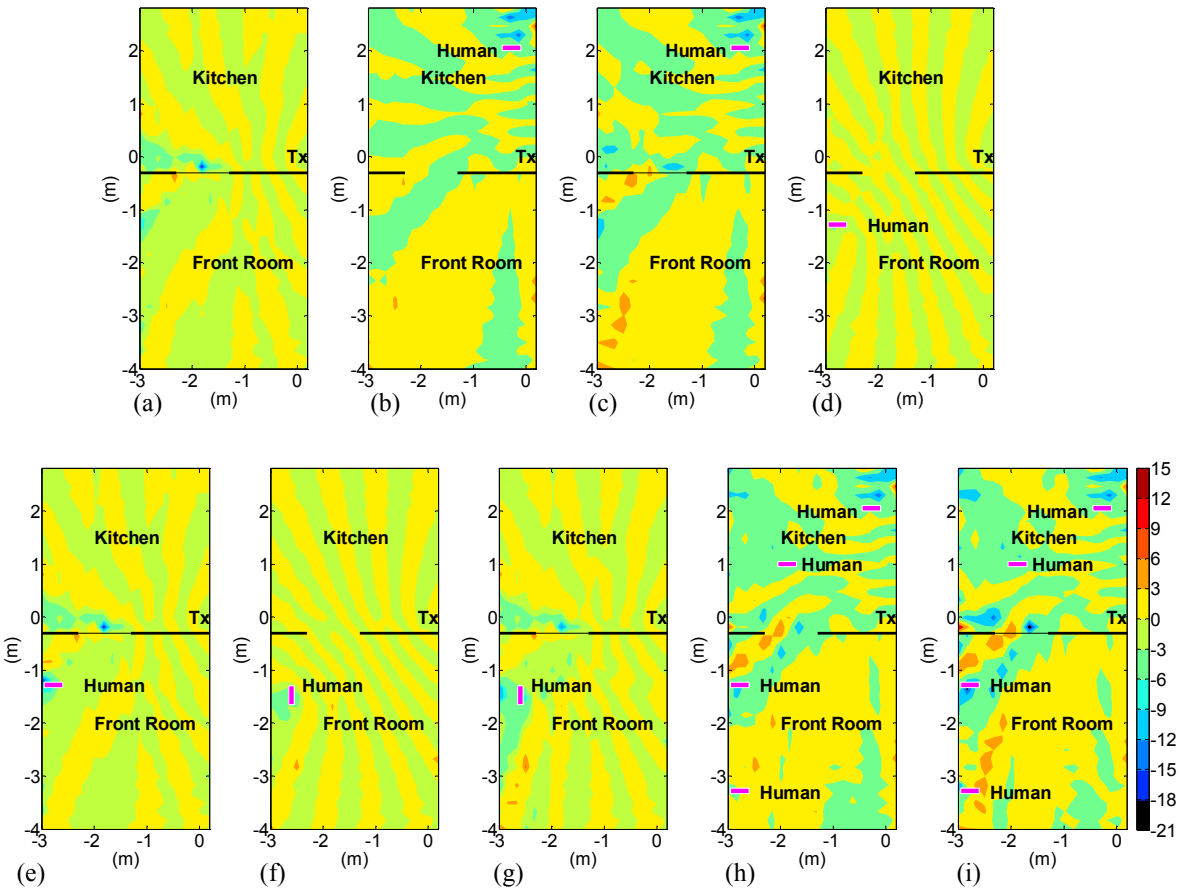

Figure 5.12: Simulated E-field (dB) difference between scenarios at 433MHz:
(a) Scenario A & B (b) Scenario A & C (c) Scenario A & D (d) Scenario A & E (e) Scenario A & F (f) Scenario A & G (g) Scenario A & H (h) Scenario A & I (i) Scenario A & J.

5.5.3 Method C Results

The amplitude and cumulative distributions function are used to analysis the E-field values for the ten scenarios within Victorian house at 433 MHz as shown in

Figure 5.13. The results show that there are very little variations in the E-field distribution values between the scenarios for both the kitchen and the front room.

Figure 5.13 (a) illustrates that the highest amplitude of the E-field in the front room is in case of open door scenario with an amplitude probability distribution of 23 % at -8 dBV/m. The lowest amplitude of the E-field in the kitchen was in case of open door with two occupants in kitchen and two occupants in the front room scenario with an amplitude probability distribution of 14 % at 3 dBV/m. This is due to the presence of four occupants in the ground floor.

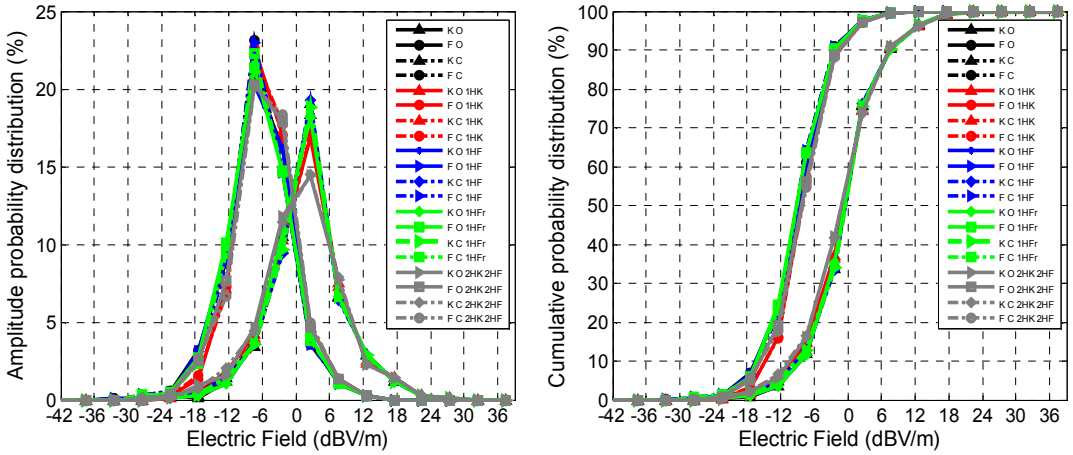

(a) (b)

Figure 5.13: E-field amplitude and cumulative probability distribution at 433 MHz for all Scenarios from A to J.

5.6 Summary of the Analysis

This section compares the results of the E-field amplitude calculations across the frequencies 5.8 GHz, 2.4 GHz, 868 MHz and 433 MHz. The transmitter for all the frequencies placed in the same location in the kitchen as follows: 1.2 m above the ground, 0.3 m from middle wall and 0.4 m from external wall. The scale of the E-field levels that is used at the receiver ranges from -30 dBV/m to 6 dBV/m for all frequencies. The effect of the door status and presence of occupants within ground floor on the E-field distributions across the four frequencies and comparison between them are discussed in the following section.

5.6.1 Analysis of E-field without Occupants

Figure 5.14 illustrates the results of the E-field amplitude for open door and no occupants scenario in the house. Based on these results, the high E-field coverage at the low frequencies (i.e. 868 MHz and 433 MHz) is higher than high frequencies (i.e. 5.8 GHz and 2.4 GHz). The internal wall attenuates the signals coverage at high frequencies more than at the low frequencies. It can also be seen that the E-field levels at high frequencies with the internal wall are -9 dBV/m whereas at low frequencies are only 3 dBV/m. The coverage signals within the front room are decreased by approximately 18 dBV/m at high frequencies with respect to the coverage signals at the low frequencies.

The effect of closing the door on the E-field amplitude coverage at the four frequencies is shown in Figure 5.15. It is observed that closing the door attenuated the propagated signal with various effects at different frequencies. The propagated signals passed through the closed door at high frequencies are attenuated by nearly 9 dBV/m whereas at low frequencies are attenuated only by 3dBV/m.

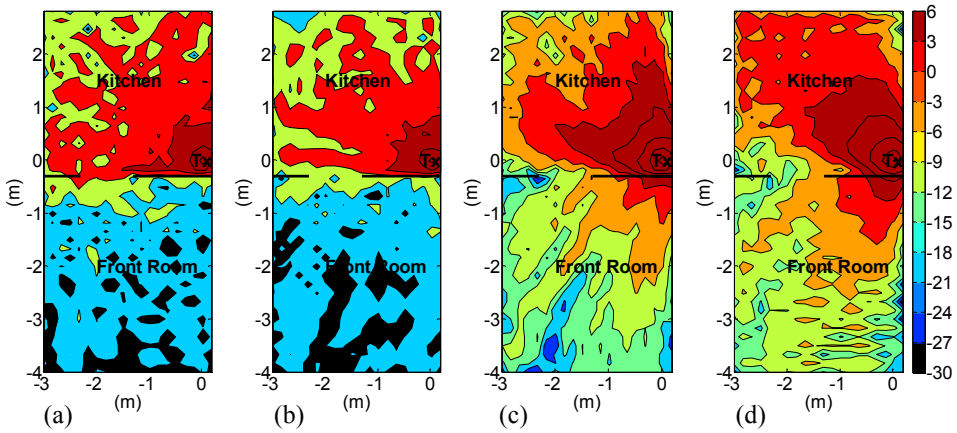

Figure 5.14: Simulated E-field (dBV/m) results for open door at different frequencies: (a) 5.8 GHz (b) 2.4 GHz (c) 868 MHz (d) 433MHz.

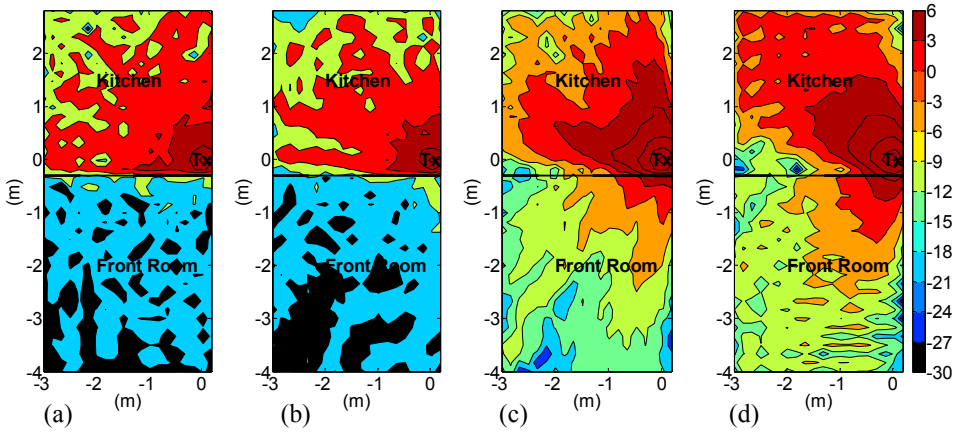

Figure 5.15: Simulated E-field (dBV/m) results for closed door at different frequencies: (a) 5.8 GHz (b) 2.4 GHz (c) 868 MHz (d) 433MHz.

In order to simplify the comparison between the different frequencies, the amplitude and cumulative probability distribution are used to analysis the electric field values for open door scenario within the Victorian house for all frequencies. Figure 5.16 illustrates that there is no noticeable difference in the E-field values in the kitchen for open scenario between all four frequencies. This similarity is due to the presence of the source in the kitchen and there is no obstructions between the transmitted source and received probes. It can be seen that there are variations in the E-field values that located in the front room

for all four frequencies in the case of open door scenario. At 5.8 GHz and 2.4 GHz, the average E-field values in the front room for the open door scenario are -20 dBV/m and -18 dBV/m, respectively as shown in Figure 5.16 (b).

The E-field amplitude and the E-field cumulative probabilities distributions of closed door scenario are obtained for the four frequencies. Figure 5.17 shows the difference in the E-field amplitude probability distribution between the four frequencies in the kitchen is little for the case of closed door scenario. It can be seen that the values of E-field at 5.8 GHz and 2.4 GHz in closed door scenario within front room are identical. However, the E-field distribution at low frequencies are higher than the E-field distribution at high frequencies. The peak value of the E-field amplitude probability distribution at 433 MHz reached 23% at -8 dBV/m while the peak for 868 MHz is 19 % at -8 dBV/m as shown in Figure 5.17 (a). The average E-field cumulative probability distributions in front room at high frequencies have similar values which is approximately -20 dBV/m. However, the average E-field cumulative probability distributions values in front room at low frequencies are -12 dBV/m and -9 dBV/m, respectively.

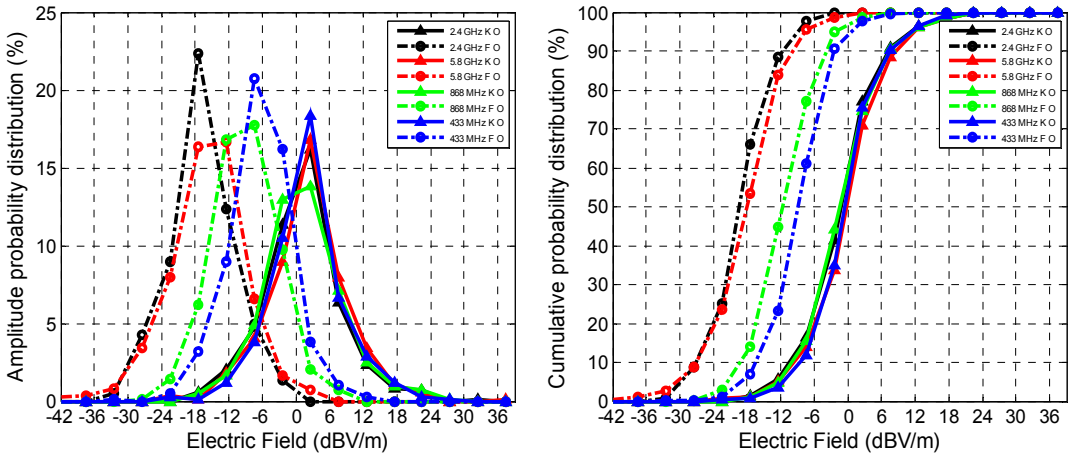

(a) (b)

Figure 5.16 : E-field amplitude and cumulative probability distribution at 5.8 GHz, 2.4 GHz, 868 MHz and 433 MHz for open door scenario.

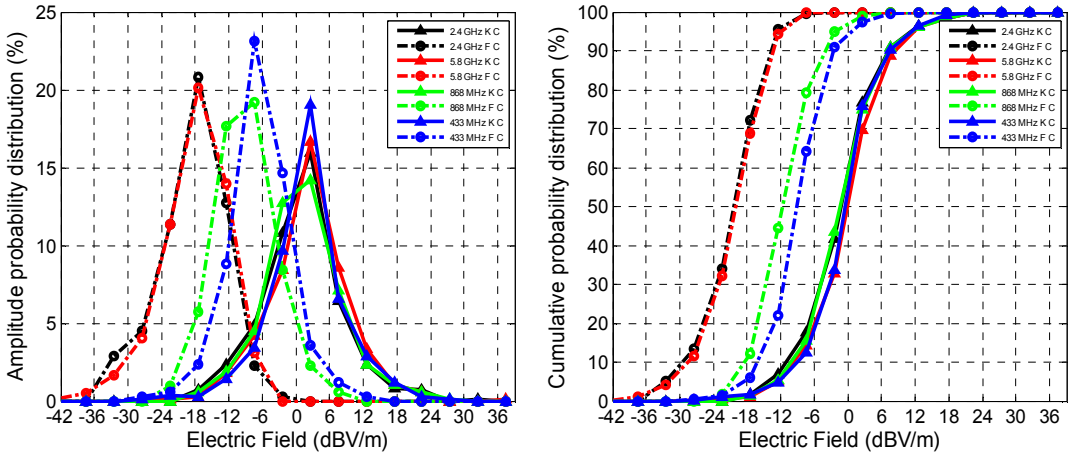

(a) (b)

Figure 5.17: E-field amplitude and cumulative probability distribution at 5.8 GHz, 2.4 GHz, 868 MHz and 433 MHz for closed door scenario.

The E-field levels within Victorian house are used to obtain the differences between the open door and the closed door scenarios at the four difference frequencies as shown in Figure 5.18. It can be observed that the door status can significantly attenuate the E-field coverage at high frequencies. At 868 MHz and 433 MHz, the difference in E-field

coverage between the open and the closed door scenarios in the front room are decreased by 6 dBV/m. However, at 5.8 GHz and 2.4 GHz, the difference in E-field coverage between these scenarios in the front room are attenuated by 18 dBV/m.

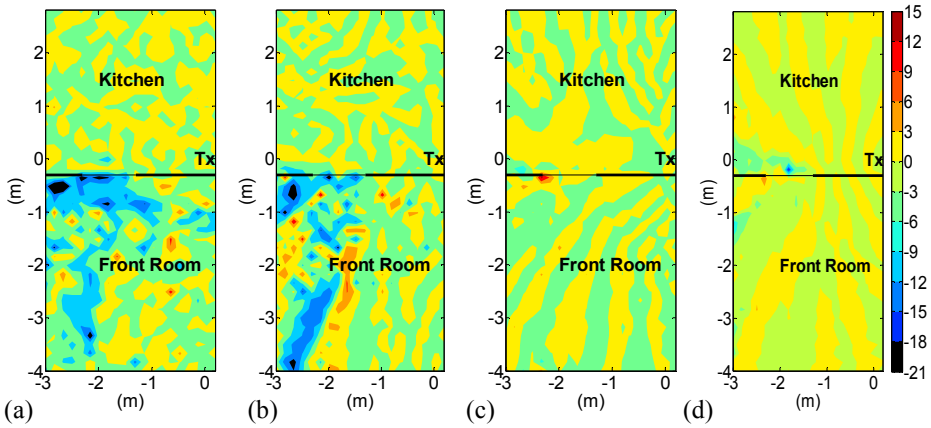

Figure 5.18 : Simulated E-field (dBV/m) difference between open and closed door scenarios at different frequencies:
(a) 5.8 GHz (b) 2.4 GHz (c) 868 MHz (d) 433MHz.

5.6.2 Analysis of E-field with Occupants

Figure 5.19 depicts the E-field amplitude coverage for scenario (I) which includes two occupants in the kitchen and two occupants in the front room with the door is open at all frequencies. Comparing the presence of human in the kitchen across all the frequencies, the E-field level values behind occupant at 5.8 GHz, 2.4 GHz, 868 MHz and 433 MHz were about -12 dBV/m, -3 dBV/m, -9 dBV/m and -3 dBV/m, respectively. Also, when the number of the occupants is increased in the kitchen the signals coverage is significantly attenuated. The effect of occupant on the propagated signals in the front room is less than when the occupant is in the kitchen. This is due the occupant in the front room is far from the source and also there are some obstacles exist between the source and the occupant which weaken the signals coming to the front room. Comparing the effect of the occupant on the E-field coverage in the front room across the four frequencies it has been found

that the most significant effect on the E-field coverage is at 433 MHz with attenuation of -12 dBV/m.

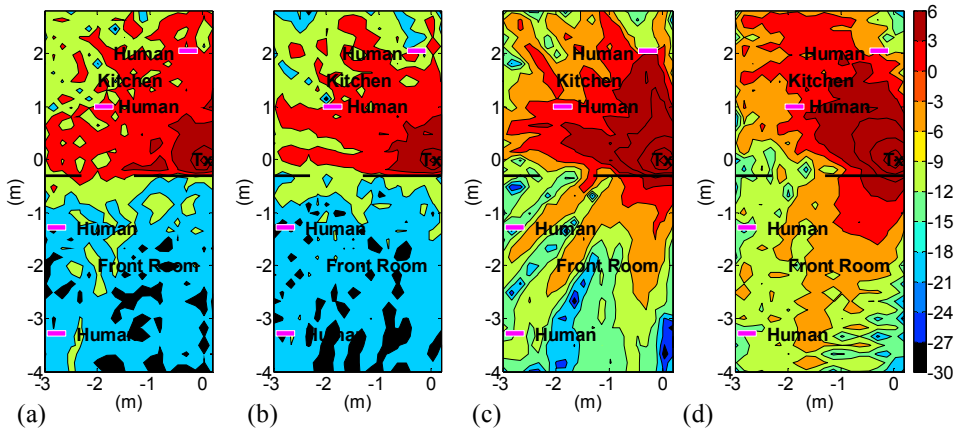

Figure 5.19: Simulated E-field (dBV/m) results for open door &4human at different frequencies: (a) 5.8 GHz. (b) 2.4 GHz. (c) 868 MHz. (d) 433MHz.

Figure 5.20 compares the amplitude and cumulative probability distributions of E- field values for the open door scenario with two occupants exist in the kitchen and another two occupants exist in the front room at all frequencies. When comparing the signal propagation for the all frequencies, significant similarities between the propagated signals in the kitchen is noticed which is due to presence of the transmitted source in the kitchen. In contrast, there are variations in the E-field levels between the four frequencies in the front room. At 433 MHz, the difference in the E-field cumulative probability distribution in the front room is between 0 % and 50 % with value of 33 dBV/m. However, at 2.4 GHz the level difference is about 24 dBV/m. It can be seen that there is a small variation in the E-field cumulative probability distribution in the front room between 5.8 GHz and 2.4 GHz which is approximately 3 dBV/m.

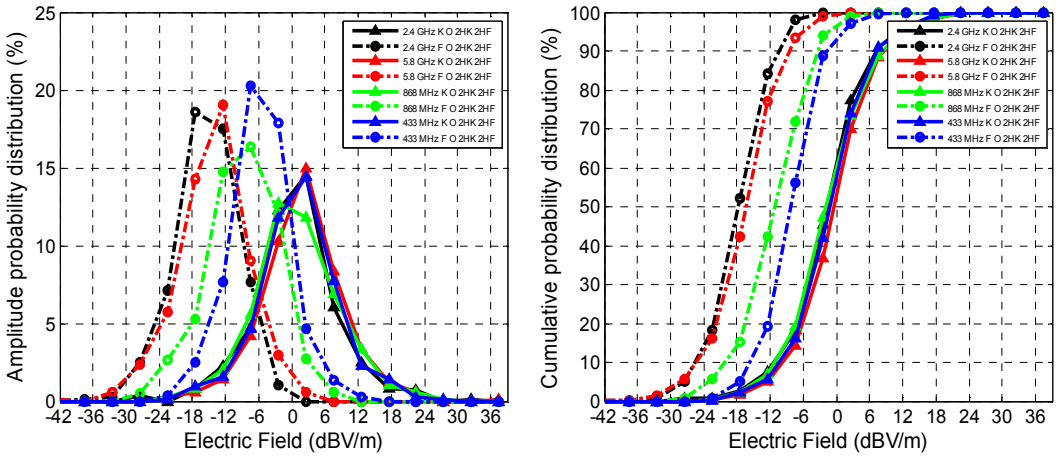

(a) (b)

Figure 5.20: E-field amplitude and cumulative probability distribution at 5.8 GHz, 2.4 GHz, 868 MHz and 433 MHz for open door with two human in kitchen and two human in front room scenario.

The difference in the E-field coverage between the open door scenario and the open door with two occupants in the kitchen and another two occupants in the front room scenario at 5.8 GHz, 2.4 GHz, 868 MHz and 433 MHz are illustrated in Figure 5.21 (a) to Figure 5.21 (d), respectively. The attenuation due to the occupants in the kitchen at the four different frequencies is about 12 dBV/m. It can also be seen that the E-field coverage within kitchen are decreased when the number of the occupants in the kitchen are increased. In the case of the occupants are in the front room at 5.8 GHz and 2.4 GHz there is an increase in the E-field values in some locations in the front room between 9 dBV/m and 12 dBV/m. This is due to the constructive and the destructive reflections on the signals caused by the obstacles such as the wall, doors and human. However, these obstacles have a limited effect on the field coverage levels within the front room at low frequencies as shown in Figure 5.21 (c) and Figure 5.21 (d).

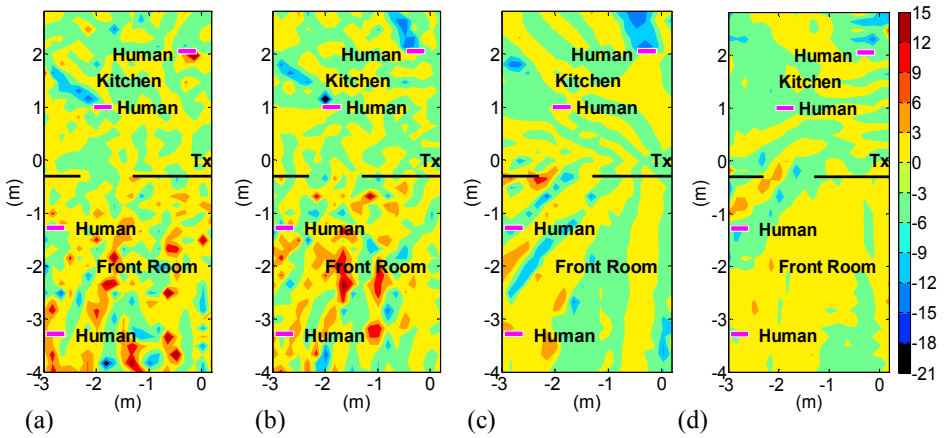

Figure 5.21: Simulated E-field (dBV/m) difference between open door and open door with two human in kitchen and two human in front room scenario at different frequencies: (a) 5.8 GHz. (b) 2.4 GHz. (c) 868 MHz. (d) 433MHz.

5.6.3 The Average E-field Analysis for All Frequencies

The average E-fields obtained for all ten scenarios in the front room and kitchen at 5.8 GHz, 2.4 GHz, 868 MHz and 433 MHz are summarized in Table 5.1. The results show that the average E-field values at 868 MHz and 433 MHz in the front room are unaffected by the presences of human or door status. The impact of the closed doors is becoming more obvious in the 5.8 GHz and 2.4 GHz results. By comparing scenarios A and B in the four different frequencies in the front room, the variations in the average E-field values at 5.8 GHz and 2.4 GHz are approximately 3 dBV/m. However, there are no variations in the average E-field values at 868 MHz and 433 MHz. Also it can be seen that the highest average E-field values in the front room are obtained at the low frequencies. At 5.8 GHz and 2.4 GHz, the effects of door status and occupants on the average E-field values are 4 dBV/m and 3 dBV/m, respectively.

The average E-field values in the kitchen are higher than the average E-field values in the front room. This is due that the transmitter source exist in the kitchen. It can be seen that the average E-field values has reduced when the occupants are placed in the kitchen as shown in scenarios C, d, I and J in Table 5.1. However the occupants in the front room have no effect on the average E-field values in the kitchen. This is due to the reflected

signals from occupants in the front room are weak which their affect is near where their stand. The door status has no effect on the average E-field value within the kitchen for all four frequencies.

Table 5.1: The average electric fields for all scenarios within front room and kitchen.

Scenario	Average Electric Field in Front Room (dBV/m)				Average Electric Field in Kitchen (dBV/m)			
	5.8GHz	2.4 GHz	868 MHz	433 MHz	5.8GHz	2.4 GHz	868 MHz	433 MHz
A	-15.9	-16.9	-9.1	-6.6	2.1	1.1	1.3	1.9
B	-18.2	-18.4	-9.0	-6.6	2.2	1.0	1.3	1.7
C	-14.3	-15.5	-8.9	-5.7	2.2	0.86	0.98	1.6
D	-15.9	-16.2	-8.9	-5.7	2.2	0.78	1.0	1.4
E	-15.8	-16.9	-9.1	-6.6	2.1	1.1	1.3	1.9
F	-18.2	-18.4	-9.0	-6.7	2.2	1.0	1.3	1.7
G	-15.8	-16.8	-9.2	-6.7	2.1	1.1	1.3	1.9
H	-18.2	-18.5	-9.2	-6.7	2.2	1.0	1.3	1.8
I	-14.2	-15.5	-8.9	-5.8	1.96	0.73	0.86	1.2
J	-16.0	-16.0	-8.9	-5.8	1.95	0.67	0.86	1.1

5.7 Conclusions

This chapter presented an investigation into changes in the electric field strength within the ground floor of a Victorian house at 5.8 GHz, 2.4 GHz, 868 MHz and 433 MHz. Different scenarios are considered for changing the building's occupancy level in addition to the status of opening and closing doors. The effects of different obstacles inside the rooms are compared and which has the most significant effect on the received electric field strength is highlight. At 2.4 GHz, results have shown that human occupants in the kitchen can locally change the E-Field by approximately 12 dBV/m whereas human occupants in the kitchen at 5.8 GHz, 868 MHz and 433 MHz can have an effect from 3 dBV/m to 9 dBV/m. The human occupants in front room at 433 MHz have the most significant effect on the electric field level in the front room. However, the presence of

human in the front room has less effect on the signal propagation levels than presence of human in the kitchen.

Results proved that the status of opening or close doors at higher frequencies can locally change the E-Field by approximately 9 dBV/m whereas the doors at lower frequencies have an effect of less than 3 dBV/m. The results showed that the door status or the presence of human within ground floor has no effect on the average of E-field values for all scenarios within the front room at lower frequencies. However, the effects of the door statues and human on the average of the E- field values for all scenarios within front room at higher frequencies are obvious. The simulation results illustrated that the lower frequencies provide a better coverage and higher average E-field levels than the higher frequencies.

In general, there were large variations in the E-field distribution levels in the front room compared to the E-field distribution levels in the kitchen. This is due to the presence of the transmitter source in the kitchen. Finally, the results showed that the human body can cause significant attenuation to the signal due to the shadowing effect.

Chapter 6 – Case Study of Measurements

This chapter evaluates the performance of Zigbee used for smart metering applications within domestic. In order to characterize Zigbee performance, several experiments were carried out at different locations inside the Victorian terraced house at 2.4 GHz [85].

6.1 Methodology

Experiments were carried out in a late-Victorian terraced house that built in around 1890. It's brick construction was brick with a combination of brick and stud for the internal walls. The internal walls of some rooms may still made of lathe/plaster and insulated with rubble. The building has two living floors with a slate and lining roof. In addition to the two floors there is uninhabited basement.

Propagation was measured using two Ember Corp ZigBee modules (ISA3), fitted with an Antenova dielectric SMT antenna and the transmitted power was 2 mW. These devices were used to transmit and receive signals as well as measuring the Link Quality Indication (LQI) and the Received Signal Strength Indication (RSSI). The required power for ISA3 was obtained by a Power Over Ethernet (POE) system and data connectivity to a laptop computer at a reference location. The remote node has its own battery power. Several trials were conducted to measure both RSSI and LQI using InSight software.

6.1.1 Experimental Trials

Three trials were designed to measure the RSSI and LQI inside the Victorian terrace house as shown in Figure 3.3. The trials were conducted at specific point where may the smart meter be installed. The receivers were placed 1.2 m above the floor in each case. The three trials are explained as follows:

- Trial 1 ‘Receiver in the kitchen’: In this trial the transmitter was located on the worktop in the ground floor, this location called 'L0' as indicated in Figure 6.1 (a). The RSSI was measured at some locations where there is a possibility of installing the smart meters such as a doorstep meter reading, the electricity meter in the basement, communicating with to the energy monitor device in the kitchen and may be in other locations. This simulates a system that may be implemented in a standard domestic property.
- Trial 2 ‘Receiver in bedroom’, this trial is aimed to measure the maximum attenuation of the RSSI through special separation. The transmitter was located in the first floor at location L10 as indicated in Figure 6.2 (a). This point is the furthest location from the existing gas and electricity meters at location L3.
- Trial 3 ‘Received power topology’: The transmitter was located in the kitchen and the receiver located in the front room at ground floor. The aim is to cover more locations in the front room that can generate a topographical map of the received power.

Before we start discussing our results, the RSSI and LQI are briefly described in the following sections.

6.1.2 Received Signal Strength Indication (RSSI)

The RSSI is defined as a measurement of the RF power carried in a received radio signal, regardless of its source. The RSSI outputs are expressed in many ways according to the device manufacturers. The range of the power levels in Ember devices are between 0 and -96 dBm. The -96 dBm is the lowest measurable value before communication is disconnected between the two devices. The measured value is based on the highest energy level detected during the received time of a data packet.

6.1.3 Link Quality Indication (LQI)

The LQI is a measure of the link quality between nodes. The values of the LQI are dimensionless ranging from 0–255 where 255 is the highest. The measurement is based on the reliability of the link between two communication nodes. Table 6.1 is summarized the link quality versus the chip error per byte.

Table 6.1: Link Quality Indication (LQI) vs Chip errors per byte.

Chip errors per byte	**LQI**
0	255
1	191
2	127
3	63
4+	0

6.2 Results

This section presents the results of the three trials.

6.2.1 Trial 1 'Receiver in the kitchen'

The locations and the average measured RSSI values superimposed on the floor plans are shown in Figure 6.1. This trial was designed to characterize the signal propagation from the mobile 'sensor' node at many different locations (L1 through L7) with respect to the reference node. The reference was fixed in the kitchen which correspond to L0 on the floor plan. Trial 1 simulated devices in first floor, ground floor and in the basement of the house. Note that the external windows and doors were all kept closed during the trial.

(a) (b)

Figure 6.1: locations of Measurements points and the results on floor plan for trial 1.

Table 6.2 shows the measured values of the RSSI indication and the LQI for each location. The results show that the link quality drops significantly from the maximum value of 255 in the kitchen to 172 at location L1. This is due to the effect of closed door which attenuates the propagated signal coming through the door by 18 dB. The lowest value of RSSI is noticed in the basement and the value is -90 dBm which is close to the Zigbee threshold (-96 dBm). This is due to the reflection, diffraction, scattering and multipath coming from floor, doors and furniture.

Table 6.2: 'Receiver in kitchen' measured data.

Point	Distance (mm)	RSSI (dBm)			LQI
		Min	Avg	Max	
GROUND FLOOR					
L4	3800	-93	-86.5	-81	248.2
L2	5430	-76	-74.8	-74	255
L1	5730	-96	-93	-89	172
BASEMENT					
L3	5860	-94	-90.333	-85	233.7
FIRST FLOOR					
L6	3000	-49	-49	-49	255
L7	4100	-65	-64.5	-64	255
L5	6140	-90	-86.7	-84	255

6.2.2 Trial 2 'Receiver in the bedroom':

This trial was designed to test the signal propagation where the transmitter located in the bedroom and receiver located in the basement and another location outside the front door. Location L3 and LI were used to simulate a device in the basement that take a doorstep meter reading, respectively. In this trail, the reference node was placed in Bedroom 2, and the new reference location is named L10. Figure 6.2 illustrates the average values of the measured RSSI superimposed on the building floor plans.

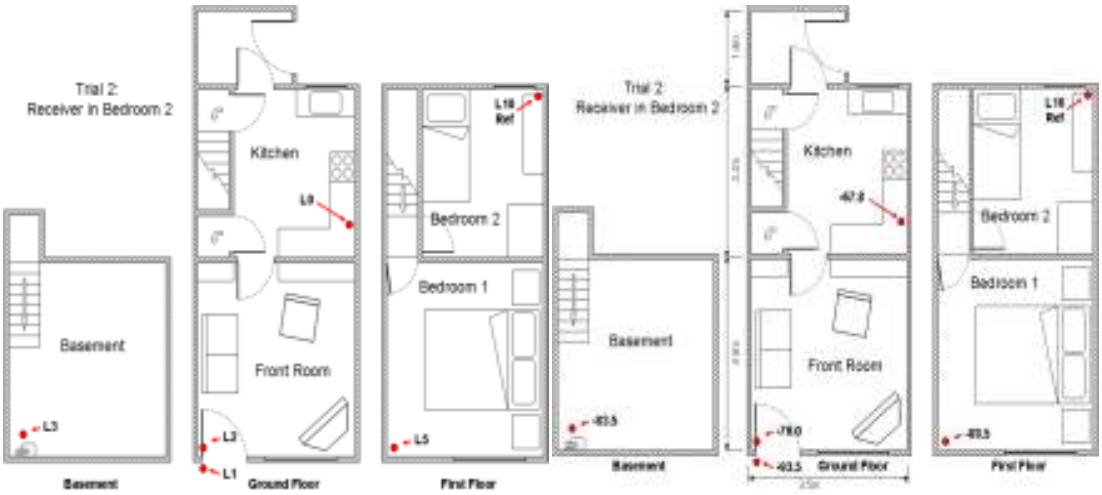

(a) (b)

Figure 6.2: Node locations and the results on floor plan for trial 2.

Table 6.3 depicts the results of RSSI and LQI at each location and the distance between nodes. It is clear from the results that there is a good link quality between all nodes in the building. Although the distance between L10 and L3 is maximum but still there is a good communication link between them. The value of the measured RSSI at L3 was -83.5 dBm. The maximum attenuation is -93.5 dBm at the node located outside the house near to the door which used for the doorstep meter reading.

Table 6.3: Trial 2 'Receiver in the bedroom' measured data.

Point	Distance (mm)	RSSI (dBm)			LQI
		Min	Avg	Max	
FIRST FLOOR					
L5	7630	-92	-88.5	-87	255
GROUND FLOOR					
L0	4580	-68	-67.8	-67	255
L2	8810	-76	-76	-76	255
L1	9260	-94	-93.5	-93	204
BASEMENT					
L3	9820	-85	-83.5	-82	255

6.2.3 Trial 3 'Received power topology':

The third trial measures RSSI contained in the propagation of the signal from the front room to the kitchen on the ground floor. In order to produce a topographical map of the received power, more locations were covered as shown in Figure 6.3. The reference point was moved to the kitchen whereas the sensor node was placed on an expanded polystyrene with a length of 1,2m above the floor and moved around many locations in a horizontal plane. This height was chosen to keep the effects of the kitchen units and wall mounted cupboards as minimum as possible.

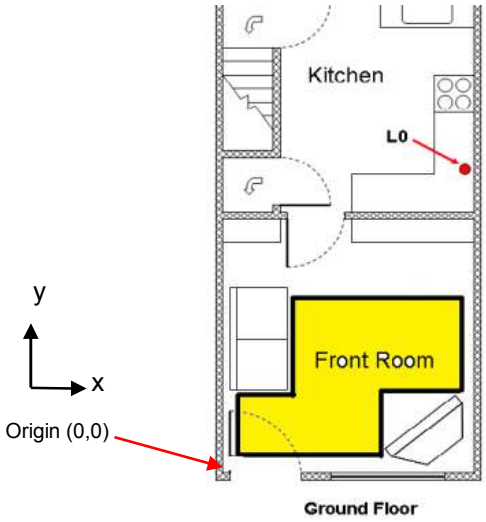

Figure 6.3: Measurement area for trial 3'received power topology'.

Figure 6.4 shows the electromagnetic field strength results of trial 3 in various locations in the front room. The results show clearly the propagation complexity of the electromagnetic field strength within rooms due to attenuation and multipath scattering. There are two areas in front room where the signal could not be measured due to the obstruction by the television and sofa, both of which could not be easily moved. As an expected result, the highest RSSI values were in an area closest to the kitchen and near to the door adjoining the two rooms.

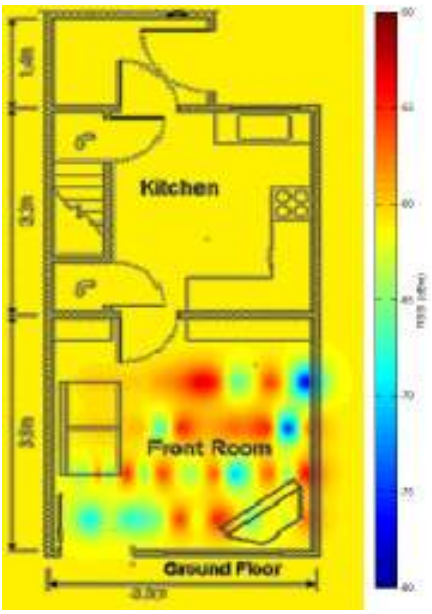

Figure 6.4: Topographical image illustrating measured RSSI from trial 3.

Table 6.4 shows the received power of trial 3 in different locations in the front room. It can be seen from the table that the RSSI near to the origin location have a gradual decreased due to the distance between the transmitter and the receivers.

Table 6.4: Trial 3 – received power topology: average measured RSSI data (-dBm).

		Position from origin x-direction (cm)												
		40	**50**	**60**	**80**	**100**	**120**	**140**	**160**	**180**	**200**	**220**	**240**	**260**	**280**
Position from origin y-direction (cm)	**220**	n/a	n/a	n/a	n/a	n/a	58.5	57.0	53.3	55.0	66.0	62.8	56.0	63.0	77.2
	160	n/a	n/a	n/a	n/a	n/a	66.7	55.0	58.3	58.5	57.0	57.0	56.0	75.3	59.0
	100	63.2	57.5	65.7	55.0	64.8	56.0	63.0	63.2	56.8	70.5	63.5	57.0	64.5	54.0
	40	69.2	66.5	62.8	67.5	66.8	64.0	56.0	62.5	55.0	59.0	65.8	61.0	n/a	n/a

In order to make a comparison between the measurements and simulation, the amplitude and cumulative probability distributions are used. The transmitted power in the simulation

was set to 2 mW. **Error! Reference source not found.** shows the results of the simulated E-field amplitude and its cumulative probability distributions along with the measured received signal strength amplitude and its cumulative probability distributions in the front room at 2.4 GHz. It can be seen that the cumulative probability distribution results show that there is a good agreement between the measured and the simulated results within the region between 0 % and 30 % of the cumulative probability distribution in the front room. The difference between the simulated and measured results in the region between 30 % and 100 % of the cumulative probability distribution is approximately 3 dBV/m in the front room. The amplitude probability distribution results show that there is a noticeable variation between the measurements and the simulation within the region between 15% and 25% in the front room. This is due to the presence of the furniture and clatter in the front room when the measurements was carried out whereas in the simulation the front room was considered to be empty.

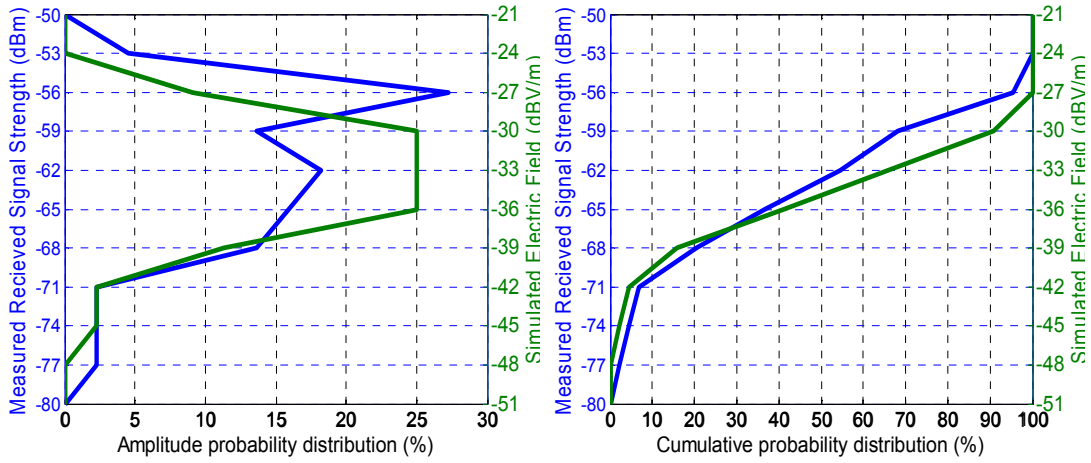

Figure 6.5: Comparisons between simulated E-field (2mW) and measured received signal strength at 2.4 GHz.

6.3 Discussion and Conclusions

This case study characterised the performance of ZigBee devices for smart metering applications within a late Victorian terraced house. Several scenarios are implemented to achieve this goal. The locations used to measure the signals represented the doorstep meter reading, electricity meter and standard domestic appliances. The results showed that the door's status has a significant effect on the received signal strength in the Victorian house. The difference between RSSI at L1 and L2 taking into the account the door status effect was by approximately 18 dB. The maximum attenuation of the RSSI was observed when the transmitter located in the first floor and the receiver located in the basement. In this case the measured RSSI was -90.3 dBm which was closed to the threshold of the communications link between the transmitter and receiver (-96 dBm). Also, the measured RSSI coverage in the front room when the door between kitchen and front room was open showed the highest RSSI values in area near to kitchen. The results demonstrated that the wireless signals can penetrate through several adjacent walls within the same floor, but became very weak at different floors. This indicates that the deployment and positioning of smart meters in domestic properties has to be carefully planned. For installations where Zigbee-based devices are used, other nodes could be utilised to create a mesh network and hence act as repeater.

When the measured results were compared with the simulated results, it can be seen that the differences between the measured results and simulated results were within 3 dB of the cumulative probability distributions. Although there were a noticeable variation between the measured and simulated results in the range between 15 % and 25 % of the amplitude probability distributions, due to the multipath effect which caused by the furniture and clatters in the front room during the measurements. Whereas an empty room was assumed in the simulation of the front room.

Chapter 7 – Conclusion and Future Work

7.1 Conclusion

Wireless technology has grown rapidly and the obvious example for this is the massive use of mobile telephony. Evaluating the performance of wireless systems inside the buildings is very important for propagation planning and design. Since the wireless friendly building is designed to improve the radio frequency performance inside the building, evaluating the wireless system is becoming more important than ever [3]. Furthermore, there are many parameters that influence the propagation of the wave within buildings such as human occupants, doors status, walls, windows, etc. all have a significant impact on received signal strengths and will contribute to fading, multipath and shadowing effects. Characterising the electric field distributions inside the building is the first step toward the deployment of a wireless network. The door status and the human's occupancy are the two main factors that affect the indoor electric field (E-field) propagations. The E-field distribution was investigated at the following frequencies: 433 MHz, 868 MHz, 2.4 GHz and 5.8 GHz. These frequencies are used in indoor wireless communication in the following applications: at 433 MHz, which just above the Trans-European Trunk Radio (TETRA) at 400 MHz used for the emergency services radio communications. At 868 MHz – just below the 900 MHz cellular band used for data telemetry, mobile communication (GSM) at 890-960 MHz; at 2.4 GHz - sensor networks (Zigbee), medical ISM band and Wi-Fi, respectively; at 5.8 GHz – Wi-Fi predominantly. A closed door is one of the main factors that block the propagated signals inside the house. The effect of opening and closing doors investigated at three different cases. In the first case, the receivers are in a horizontal plane with respect to transmitter on the ground floor. The results showed that the door status has a significant effect on the propagated signals at high frequencies and attenuated by 12 dB at high frequencies whereas attenuated only by 3 dB at low frequencies. In the second case, the signal coverage in all floors were investigated as users could be anywhere in the house. Therefore, the received signals were measured in the vertical plane across the three floors in the Victorian house (basement,

ground floor and first floor) and the transmitter antenna was located in the middle of the kitchen at all the four frequencies. In this case, the propagated signals coming to the other room were blocked by closing the door. The results showed that the closed doors at high frequencies have attenuated the propagated signals passed through the closed door by nearly 18 dBV/m whereas at low frequencies were attenuated only by 3 dBV/m. In third case, the dipole antenna transmitter was placed in the corner of the kitchen near from the middle wall and the external wall. The receivers were in a horizontal plane with respect to transmitter on the ground floor. The effect of door status on the signal propagation has the most significant effect at high frequencies. The E-field level was attenuated by 9 dB at high frequencies whereas it was attenuated by only 3 dB at low frequencies due to changing door status. The results confirm that the door status has a great effect on the propagation signals at high frequencies and this effect highly depends on the position of the transmitter and receives whereas at low frequencies the effect of door status remains the same regardless of the position of the revivers and the transmitter.

The human always exist around the house and their bodies may attenuate the E-field signals so for this reason the human effect was also investigated in the three previous cases. The results showed that the effect of humans on the signal propagation depends on the distance between the transmitter and human location and the number of humans inside the house. The presence of human in the kitchen- where the transmitter was located- has more effect on the signal propagation levels than presence of a human in the front room. By comparing the effect of presence of human in kitchen on propagated signals in the different frequencies, it can be seen that signals at 2.4 GHz has been affected the most and was attenuated by 12 dB. The results showed that when the number of humans was increased on the ground floor, the E-field distributions are decreased at all frequencies. The occupants have the biggest effect on the E-field coverage when they became very near the transmitter, for example in the kitchen at 5.8 GHz the signal was attenuated by -18 dB whereas at low frequencies the effect of human is far less than in the case of high frequencies.

Some other parameters that effect the E-field distribution such as the permittivity, the loss tangent and human geometry were investigated. The results showed that the loss tangent

has the biggest effect on the E-field distribution. The results also showed that the thickness of internal wall and the furniture have nearly no effect on the E-field coverage levels. The investigation of human geometry showed that the width of the human has a higher effect than the height and thickness on the E-field distributions.

Our simulations models were validated with an extensive campaign of practical experiments. When the measured results were compared with the simulated results, the differences between the measured and simulated results were within 3 dB of the cumulative probability distributions. The comparison also showed a noticeable variation between the measured and simulated results in the range between 15 % and 25 % of the amplitude probability distributions, due to the multipath effect caused by the furniture and clatters in the front room during the measurements whereas an empty room was assumed in the case of simulations. Finally our results demonstrated that even though different power levels were used in the simulations and in the practical measurements but the effect of the parameters remain the same regardless of the power values.

In summary, our results clearly demonstrate the importance of characterizing the E-Filed distributions inside the building especially at high frequencies before the deployment of any wireless network. Modeling the indoor E-field propagation provide us with clear picture how the E-filed distributed inside the Building and based on this distribution the wireless network can be deployed with high QoS and capacity. Finally, this work provides a foundation for understanding the implications and dominant influencing factors for modelling indoor propagation.

7.2 Recommendations for Future Work

This section outlines some new areas of research for future work based on our finding in this thesis.

- This thesis investigated the E-field distributions at frequencies up to 5.8 GHz. Next logical stage would be to extend the investigation of the E-field

distribution at 60 GHz as the 60 GHz frequency band has been used for indoor short range wireless communication [86] [87].

- Practical measurements for the E-field coverage inside the Victorian house were carried out only at 2.4GHz. It would be very interesting to perform the practical managements at all frequencies investigated and compare it to our simulation results.
- This thesis investigated the E-field in the Victorian house. The next logical step is to investigate E-field distributions in other type of houses and apartments. Also, the area of the house, building's materials, wall thickness, the shape of rooms, the number of floors, etc all these properties affect to the E-field coverage and should by investigated.
- The house in this thesis assumed to be empty house. Therefore, it would be useful to model the house with furniture. Analysing the E-field distributions inside the house with furniture and compared with our study would be very interesting area of study.
- The house in this thesis was not insulated. Therefore it would be very interesting to model the houses that have been insulated using foil backed insulation.

References

[1] J. Wakefield. (2014). *One wi-fi hotspot for every 150 people, says study.* Available: http://www.bbc.co.uk/news/technology-29726632.

[2] A. Raniwala and T.-c. Chiueh, "Coverage and capacity issues in enterprise wireless LAN deployment," *Stony Brook University,* 2004.

[3] A. K. Brown, "The wireless friendly building," in *Antennas and Propagation Conference (LAPC), 2010 Loughborough*, 2010, pp. 62-66.

[4] W. F. Young, C. L. Holloway, G. Koepke, D. Camell, Y. Becquet, and K. A. Remley, "Radio-Wave Propagation Into Large Building Structures—Part 1: CW Signal Attenuation and Variability," *Antennas and Propagation, IEEE Transactions on,* vol. 58, pp. 1279-1289, 2010.

[5] S. S. Haykin, M. Moher, and D. Koilpillai, *Modern wireless communications*: Pearson Education India, 2005.

[6] A. Austin , M. Neve , and G. Rowe "Modelling propagation in multifloor buildings using the FDTD method," *Antennas and Propagation, IEEE Transactions,* vol. *59*, pp. 4239-4246., *2011*.

[7] M. J. Neve, A. C. M. Austin, and G. B. Rowe, "Electromagnetic engineering for communications in the built environment," in *Antennas and Propagation (EUCAP), 2012 6th European Conference on*, 2012, pp. 1-5.

[8] X.-S. Yang, Z.-M. Tian, J.-J. Yuan, Y.-T. Zhang, and W. Shao, "Numerical Study on Indoor Wideband Channel Characteristics with Different Internal Wall " presented at the Radioengineering, 2013.

[9] G. E. Athanasiadou and A. R. Nix, "A novel 3-D indoor ray-tracing propagation model: the path generator and evaluation of narrow-band and wide-band predictions," *Vehicular Technology, IEEE Transactions on,* vol. 49, pp. 1152-1168, 2000.

[10] S. Loredo, L. Valle, and R. P. Torres, "Accuracy analysis of GO/UTD radio-channel modeling in indoor scenarios at 1.8 and 2.5 GHz," *Antennas and Propagation Magazine, IEEE,* vol. 43, pp. 37-51, 2001.

[11] K. S. Butterworth, K. W. Sowerby, and A. G. Williamson, "Base station placement for in-building mobile communication systems to yield high capacity and efficiency," *Communications, IEEE Transactions on,* vol. 48, pp. 658-669, 2000.

[12] K. Hosseini and M. Dehmollaian, "Transmitted fields of a directional antenna in proximity of a wall," *Microwaves, Antennas & Propagation, IET,* vol. 9, pp. 176-184, 2015.

[13] J. H. Tarng, L. Wen-Shun, H. Yeh-Fong, and H. Jiunn-Ming, "A novel and efficient hybrid model of radio multipath-fading channels in indoor environments," *Antennas and Propagation, IEEE Transactions on,* vol. 51, pp. 585-594, 2003.

[14] T. Hult and A. Mohammed, "Assessment of Multipath Propagation for a 2.4 GHz Short-Range Wireless Communication System," in *Vehicular Technology Conference, 2007. VTC2007-Spring. IEEE 65th*, 2007, pp. 544-548.

[15] M. Ayadi and A. Ben Zineb, "Body Shadowing and Furniture Effects for Accuracy Improvement of Indoor Wave Propagation Model," *Wireless Communications, IEEE Transactions on,* vol. PP, pp. 1-1, 2014.

[16] Y. Chang-Fa, W. Boau-Cheng, and K. Chuen-Jyi, "A ray-tracing method for modeling indoor wave propagation and penetration," *Antennas and Propagation, IEEE Transactions on,* vol. 46, pp. 907-919, 1998.

[17] T. K. Sarkar, J. Zhong, K. Kyungjung, A. Medouri, and M. Salazar-Palma, "A survey of various propagation models for mobile communication," *Antennas and Propagation Magazine, IEEE,* vol. 45, pp. 51-82, 2003.

[18] *FEKO Suite 6.2, EM Software & System-S.A. (Pty) Ltd*. Available: http://www.feko.info

[19] H. Huo, W. Shen, Y. Xu, and H. Zhang, "The effect of human activites on 2.4 GHz radio propagation at home environment," in *Broadband Network & Multimedia Technology, 2009. IC-BNMT '09. 2nd IEEE International Conference on*, 2009, pp. 95-99.

[20] L. Nagy, "FDTD and ray optical methods for indoor wave propagation modeling," *Mikrotalasna revija,* vol. 16, pp. 47-53, 2010.

[21] Z. Lai, G. Villemaud, M. Lu, and J. Zhang, "2 Radio propagation modeling," *Heterogeneous Cellular Networks: Theory, Simulation and Deployment,* p. 15, 2013.

[22] K. Yee, "Numerical solution of initial boundary value problems involving maxwell's equations in isotropic media," *IEEE Transactions on Antennas and Propagation,* vol. 14, pp. 302-307, 1966.

[23] K. S. Yee, "Numerical solution of initial boundary value problems involving Maxwell's equations in isotropic media," *IEEE Trans. Antennas Propag,* vol. 14, pp. 302-307, 1966.

[24] A. Taflove and S. C. Hagness, "Computational electrodynamics: the finite-difference time-domain method," *Norwood, 2nd Edition, MA: Artech House, l995,* 1995.

[25] "CST Studio Suite™ 2012, Microwave Studio, CST Getting Started and Tutorials," ed, 2012.

[26] S. D. Gedney, "Introduction to the finite-difference time-domain (FDTD) method for electromagnetics," *Synthesis Lectures on Computational Electromagnetics,* vol. 6, pp. 1-250, 2011.

[27] M. C. Lawton and J. P. McGeehan, "The application of a deterministic ray launching algorithm for the prediction of radio channel characteristics in small-cell environments," *Vehicular Technology, IEEE Transactions on,* vol. 43, pp. 955-969, 1994.

[28] M. Luo, "Indoor radio propagation modeling for system performance prediction," INSA de Lyon, 2013.

[29] Y. Rahmat-Samii, "GTD, UTD, UAT, and STD: A Historical Revisit and Personal Observations," *Antennas and Propagation Magazine, IEEE,* vol. 55, pp. 29-40, 2013.

[30] P. K. Sharma and R. Singh, "Comparative analysis of propagation path loss models with field measured data," *International Journal of Engineering Science and Technology,* vol. 2, pp. 2008-2013, 2010.

[31] J. Baumgarten, C. Kin Lien, A. Hecker, T. Kurner, M. Braun, and P. Zahn, "Performance of prediction models in suburban/rural residential areas at 860, 2300 and 3500 MHz," in *Antennas and Propagation (EUCAP), 2012 6th European Conference on*, 2012, pp. 1412-1416.

[32] *European Cooperation in the Field of Scientific and technical Research, Digital Mobile Radio Towards Future Generation Systems, COST231 Final Report (1999)*. Available: http://www.lx.it.pt/cost231/

[33] A. Mousa, Y. Dama, M. Najjar, and B. Alsayeh, "Optimizing Outdoor Propagation Model based on Measurements for Multiple RF Cell," *International Journal of Computer Applications,* vol. 60, pp. 5-10, 2012.

[34] M. Alim, M. Rahman, M. Hossain, and A. A. Nahid, "Analysis of Large Scale Propagation Models for Mobile Communications in Urban Area," *arXiv preprint arXiv:1002.2187,* 2010.

[35] P. M. Ghosh, M. A. Hossain, A. Z. Abadin, and K. K. Karmakar, "Comparison Among Different Large Scale Path Loss Models for High Sites in Urban, Suburban and Rural Areas," *mh,* vol. 10, p. 1, 2012.

[36] V. Erceg, K. Hari, M. Smith, D. S. Baum, K. Sheikh, C. Tappenden*, et al.*, "Channel models for fixed wireless applications," ed: IEEE, 2001.

[37] V. S. Abhayawardhana, I. J. Wassell, D. Crosby, M. P. Sellars, and M. G. Brown, "Comparison of empirical propagation path loss models for fixed wireless access systems," in *Vehicular Technology Conference, 2005. VTC 2005-Spring. 2005 IEEE 61st*, 2005, pp. 73-77 Vol. 1.

[38] J. Milanovic, S. Rimac-Drlje, and K. Bejuk, "Comparison of propagation models accuracy for WiMAX on 3.5 GHz," in *Electronics, Circuits and Systems, 2007. ICECS 2007. 14th IEEE International Conference on*, 2007, pp. 111-114.

[39] G. Campus and B. B. Bathinda, "The Evolution of Smart Cities," *An International Journal of Engineering Sciences* vol. 3, 2014.

[40] D. Molkdar, "Review on radio propagation into and within buildings," *Microwaves, Antennas and Propagation, IEE Proceedings H,* vol. 138, pp. 61-73, 1991.

[41] A. Turkmani and A. De Toledo, "Radio transmission at 1800 MHz into, and within, multistory buildings," *IEE Proceedings I (Communications, Speech and Vision),* vol. 138, pp. 577-584, 1991.

[42] L. P. Rice, "Radio transmission into buildings at 35 and 150 mc," *Bell System Technical Journal, The,* vol. 38, pp. 197-210, 1959.

[43] J. E. Berg, "Building penetration loss along urban street microcells," in *Personal, Indoor and Mobile Radio Communications, 1996. PIMRC'96., Seventh IEEE International Symposium on*, 1996, pp. 795-797 vol.3.

[44] A. Turkmani, J. Parsons, and D. Lewis, "Measurement of building penetration loss on radio signals at 441, 900 and 1400 MHz," *Journal of the institution of electronic and radio engineers,* vol. 58, pp. S169-S174, 1988.

[45] A. F. de Toledo and A. M. D. Turkmani, "Propagation into and within buildings at 900, 1800 and 2300 MHz," in *Vehicular Technology Conference, 1992, IEEE 42nd*, 1992, pp. 633-636 vol.2.

[46] D. M. Rose and T. Kürner, "Outdoor-to-indoor propagation—Accurate measuring and modelling of indoor environments at 900 and 1800 MHz," in *Antennas and Propagation (EUCAP), 2012 6th European Conference on*, 2012, pp. 1440-1444.

[47] I. Rodriguez, H. C. Nguyen, N. T. K. Jorgensen, T. B. Sorensen, J. Elling, M. B. Gentsch*, et al.*, "Path loss validation for urban micro cell scenarios at 3.5 GHz compared to 1.9 GHz," in *Global Communications Conference (GLOBECOM), 2013 IEEE*, 2013, pp. 3942-3947.

[48] H. Okamoto, K. Kitao, and S. Ichitsubo, "Outdoor-to-indoor propagation loss prediction in 800-MHz to 8-GHz band for an urban area," *Vehicular Technology, IEEE Transactions on,* vol. 58, pp. 1059-1067, 2009.

[49] W. J. Tanis, II and G. J. Pilato, "Building penetration characteristics of 880 MHz and 1922 MHz radio waves," in *Vehicular Technology Conference, 1993., 43rd IEEE*, 1993, pp. 206-209.

[50] J. E. Berg, "Building penetration loss at 1700 MHz along line of sight street microcells," in *Personal, Indoor and Mobile Radio Communications, 1992. Proceedings, PIMRC '92., Third IEEE International Symposium on*, 1992, pp. 86-87.

[51] J.-H. Tarng, Y.-C. Chang, and C. Chih-Ming, "Propagation Mechanisms of UHF radiowave propagation into multistory buildings for microcellular environment," *IEICE transactions on communications,* vol. 81, pp. 1920-1926, 1998.

[52] E. H. Walker, "Penetration of radio signals into buildings in the cellular radio environment," *Bell System Technical Journal, The,* vol. 62, pp. 2719-2734, 1983.

[53] D. C. Cox, R. R. Murray, and A. W. Norris, "Measurements of 800-MHz radio transmission into buildings with metallic walls," *Bell System Technical Journal, The,* vol. 62, pp. 2695-2717, 1983.

[54] R. Gahleitner and E. Bonek, "Radio wave penetration into urban buildings in small cells and microcells," in *Vehicular Technology Conference, 1994 IEEE 44th*, 1994, pp. 887-891.

[55] P. I. Wells, "The attenuation of UHF radio signals by houses," *Vehicular Technology, IEEE Transactions on,* vol. 26, pp. 358-362, 1977.

[56] L. Ferreira, M. Kuipers, C. Rodrigues, and L. M. Correia, "Characterisation of Signal Penetration into Buildings for GSM and UMTS," in *Wireless Communication Systems, 2006. ISWCS '06. 3rd International Symposium on*, 2006, pp. 63-67.

[57] F. Fuschini, M. Barbiroli, G. E. Corazza, V. Degli-Esposti, and G. Falciasecca, "Analysis of Outdoor-to-Indoor Propagation at 169 MHz for Smart Metering Applications," *Antennas and Propagation, IEEE Transactions on,* vol. 63, pp. 1811-1821, 2015.

[58] G. Durgin, T. S. Rappaport, and X. Hao, "Measurements and models for radio path loss and penetration loss in and around homes and trees at 5.85 GHz," *Communications, IEEE Transactions on,* vol. 46, pp. 1484-1496, 1998.

[59] J. H. Tarng, W. R. Chang, and B. J. Hsu, "Three-dimensional modeling of 900-MHz and 2.44-GHz radio propagation in corridors," *Vehicular Technology, IEEE Transactions on,* vol. 46, pp. 519-527, 1997.

[60] M. Salem, M. Ismail, and N. Misran, "An Investigation on the Effects of Wall Parameters on the Indoor Wireless Propagations," in *Research and Development, 2007. SCOReD 2007. 5th Student Conference on*, 2007, pp. 1-5.

[61] P. Ali-Rantala, L. Ukkonen, L. Sydanheimo, M. Keskilammi, and M. Kivikoski, "Different kinds of walls and their effect on the attenuation of radiowaves indoors," in *Antennas and Propagation Society International Symposium, 2003. IEEE*, 2003, pp. 1020-1023 vol.3.

[62] K. A. Remley, G. Koepke, C. L. Holloway, C. A. Grosvenor, D. Camell, J. Ladbury*, et al.*, "Radio-Wave Propagation Into Large Building Structures—Part 2: Characterization of Multipath," *Antennas and Propagation, IEEE Transactions on,* vol. 58, pp. 1290-1301, 2010.

[63] J. T. Zhang and Y. Huang, "Indoor channel characteristics comparisons for the same building with different dielectric parameters," in *Communications, 2002. ICC 2002. IEEE International Conference on*, 2002, pp. 916-920 vol.2.

[64] C. Jinwon, K. Noh-Gyoung, R. Jong-Min, K. Jun-Sung, and K. Seong-Cheol, "Effect of Metal Door on Indoor Radio Channel," in *Personal, Indoor and Mobile Radio Communications, 2007. PIMRC 2007. IEEE 18th International Symposium on*, 2007, pp. 1-5.

[65] D. Porrat and D. C. Cox, "UHF propagation in indoor hallways," *Wireless Communications, IEEE Transactions on,* vol. 3, pp. 1188-1198, 2004.

[66] M. Matsunaga, T. Matsunaga, and M. Nakano, "Modelling and measurement techniques for propagation of indoor wireless communication considering the

building's structure and human bodies," in *Antennas and Propagation Conference (LAPC), 2011 Loughborough*, 2011, pp. 1-4.

[67] J. S. C. Turner, M. F. Ramli, L. M. Kamarudin, A. Zakaria, A. M. Shakaff, D. L. Ndzi*, et al.*, "The study of human movement effect on Signal Strength for indoor WSN deployment," in *Wireless Sensor (ICWISE), 2013 IEEE Conference on*, 2013, pp. 30-35.

[68] S. Zvanovec, P. Pechac, and M. Klepal, " Wireless LAN networks design: site survey or propagation modeling?." presented at the *Radioengineering* 2003.

[69] F. Villanese, W. G. Scanlon, and N. E. Evans, "Statistical characteristics of pedestrian-induced fading for a narrowband 2.45 GHz indoor channel," in *Vehicular Technology Conference, 2000. IEEE-VTS Fall VTC 2000. 52nd*, 2000, pp. 745-750 vol.2.

[70] F. Villanese, N. E. Evans, and W. G. Scanlon, "Pedestrian-induced fading for indoor channels at 2.45, 5.7 and 62 GHz," in *Vehicular Technology Conference, 2000. IEEE-VTS Fall VTC 2000. 52nd*, 2000, pp. 43-48 vol.1.

[71] K. I. Ziri-Castro, W. G. Scanlon, and N. E. Evans, "Characterisation of body-shadowing effects in the indoor environment at 5.2 GHz," in *High Frequency Postgraduate Student Colloquium, 2003*, 2003, pp. 2-5.

[72] H. Tan, J. DasGupta, and K. Ziri-Castro, "Human-body shadowing effects on indoor MIMO-OFDM channels at 5.2 GHz," in *Antennas and Propagation (EuCAP), 2010 Proceedings of the Fourth European Conference on*, 2010, pp. 1-5.

[73] A. Austin, M. J. Neve, and G. B. Rowe, "Modelling inter-floor radio-wave propagation in office buildings," in *Antennas and Propagation Society International Symposium, 2008. AP-S 2008. IEEE*, 2008, pp. 1-4.

[74] M. J. Neve, M. Leung, and J. Cater, "Inter-building propagation modelling for indoor wireless communications system deployment," in *Antennas and Propagation (EuCAP), 2014 8th European Conference on*, 2014, pp. 791-793.

[75] A. J. Motley, "Personal communication radio coverage in buildings at 900 MHz and 1700 MHz," *Electronics Letters,* vol. 24, pp. 763-764, 1988.

[76] A. Austin, M. J. Neve, G. B. Rowe, and R. J. Pirkl, "Modeling the effects of nearby buildings on inter-floor radio-wave propagation," *Antennas and Propagation, IEEE Transactions on,* vol. 57, pp. 2155-2161, 2009.

[77] C. R. Anderson and T. S. Rappaport, "In-building wideband partition loss measurements at 2.5 and 60 GHz," *Wireless Communications, IEEE Transactions on,* vol. 3, pp. 922-928, 2004.

[78] S. Alexander and G. Pugliese, "Cordless communication within buildings: Results of measurements at 900 MHz and 60 GHz," *British Telecom Technology Journal,* vol. 1, pp. 99-105, 1983.

[79] N. Assous, N. Lebedev, R. Daviot, and N. Abouchi, "Wireless Sensors for Instrumented Machines: Propagation Study for Stationary Industrial Environments," in *Computer Aided Modeling and Design of Communication Links and Networks, 2009. CAMAD '09. IEEE 14th International Workshop on*, 2009, pp. 1-5.

[80] J. Gemio, J. Parron, and J. Soler., " Human body effects on implantable antennas for ISM bands applications: Models comparison and propagation losses study.," *Progress In Electromagnetics Research,* vol. 110, pp. 437-452, 2010.

[81] L. Low, Z. Hui, J. M. Rigelsford, R. J. Langley, and A. R. Ruddle, "An Automated System for Measuring Electric Field Distributions Within a Vehicle," *Electromagnetic Compatibility, IEEE Transactions on,* vol. 55, pp. 3-12, 2013.

[82] L. Low, Z. Hui, J. Rigelsford, and R. Langley, "Computed field distributions within a passenger vehicle at 2.4 GHz," in *Antennas & Propagation Conference, 2009. LAPC 2009. Loughborough*, 2009, pp. 221-224.

[83] R. Salvado, C. Loss, R. Gonçalves, and P. Pinho, "Textile Materials for the Design of Wearable Antennas: A Survey," *Sensors (Basel, Switzerland),* vol. 12, pp. 15841-15857, 2012.

[84] Y. H. Alharbi, J. M. Rigelsford, R. J. Langley, and A. O. AlAmoudi, "Analysis of Wireless Propagation Within a Victorian House for Smart Meter Applications " presented at the Antenna and Propagation Conference (LAPC), Loughborough, 2014.

[85] Y. Alharbi, D. Powell, R. J. Langley, and J. M. Rigelsford, "ZigBee wireless quality trials for smart meters," in *Antennas and Propagation Conference (LAPC), 2011 Loughborough*, 2011, pp. 1-4.

[86] S. Collonge, G. Zaharia, and G. El Zein, "Influence of furniture on 60-GHz radio propagation in a residential environment," *Microwave and Optical Technology Letters,* vol. 39, pp. 230-233, 2003.

[87] P. Karadimas, B. Allen, and P. Smith, "Human Body Shadowing Characterization for 60-GHz Indoor Short-Range Wireless Links," *Antennas and Wireless Propagation Letters, IEEE,* vol. 12, pp. 1650-1653, 2013.

Appendix A- Simulation of the E-Field Distributions on Vertical Plane at 5.8 GHz.

This appendix shows the other eight scenarios for method A in section **Error! Reference source not found.**. The scenarios are presented in Table 4.1. The E-field amplitude distribution in vertical cut within the Victorian house in the first floor, ground floor and basement for the scenarios C, D, E, F, G, H, I and K at 5.8 GHz are shown below.

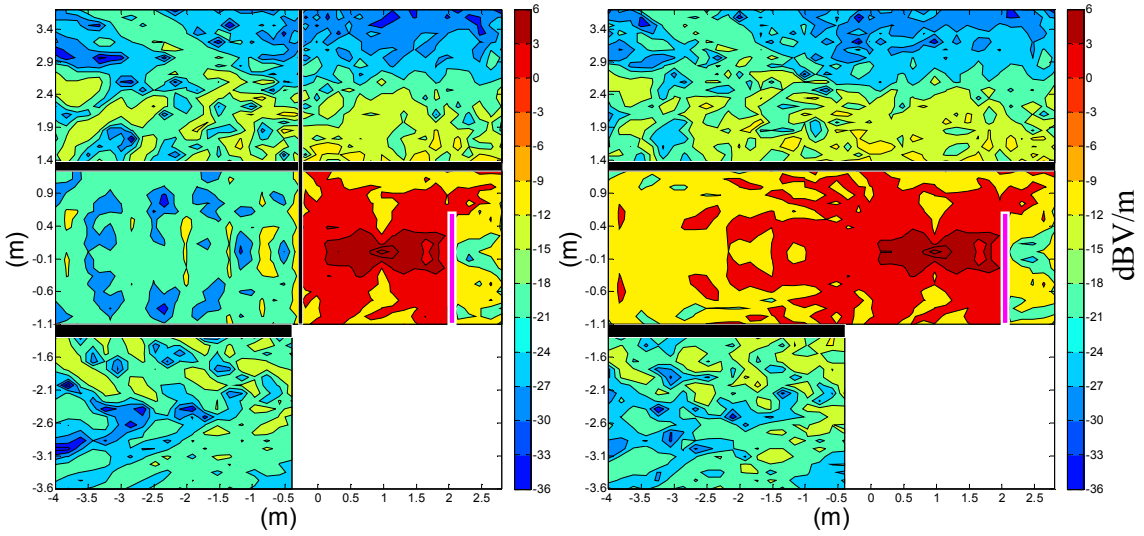

Scenario C

Scenario D

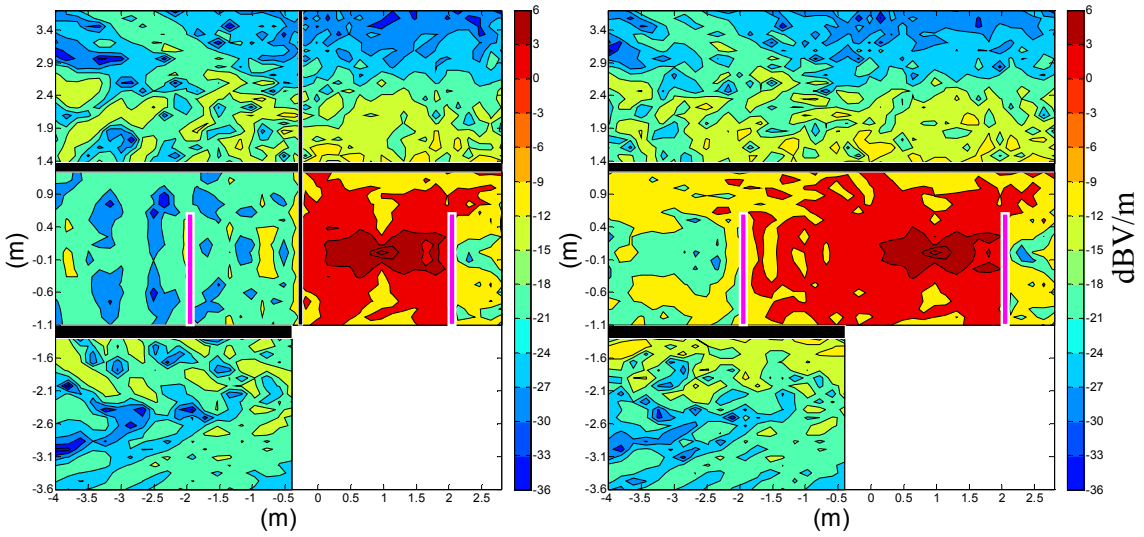

Scenario E

Scenario F

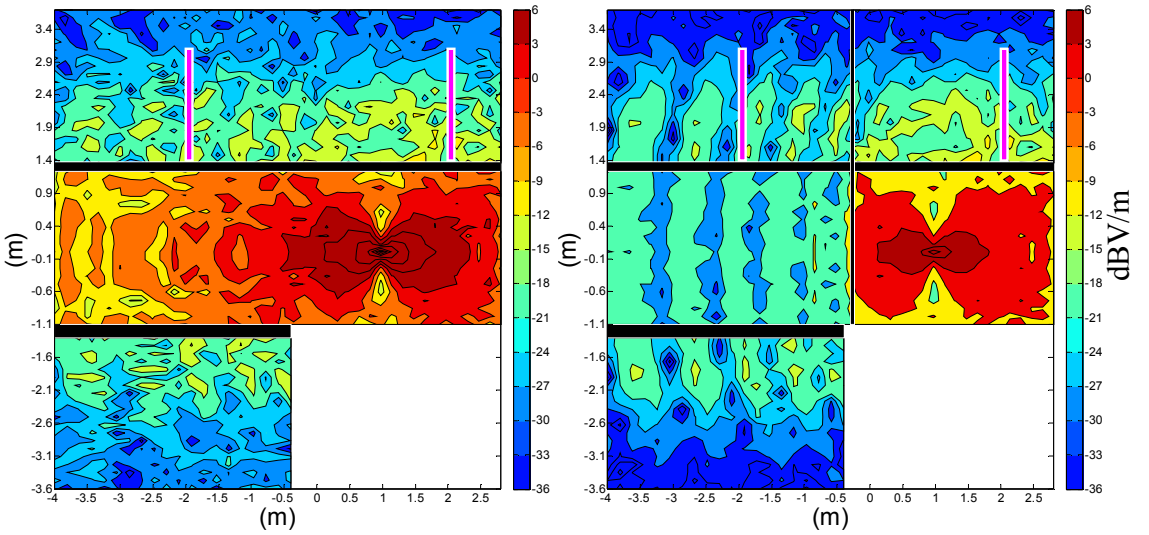

Scenario G

Scenario H

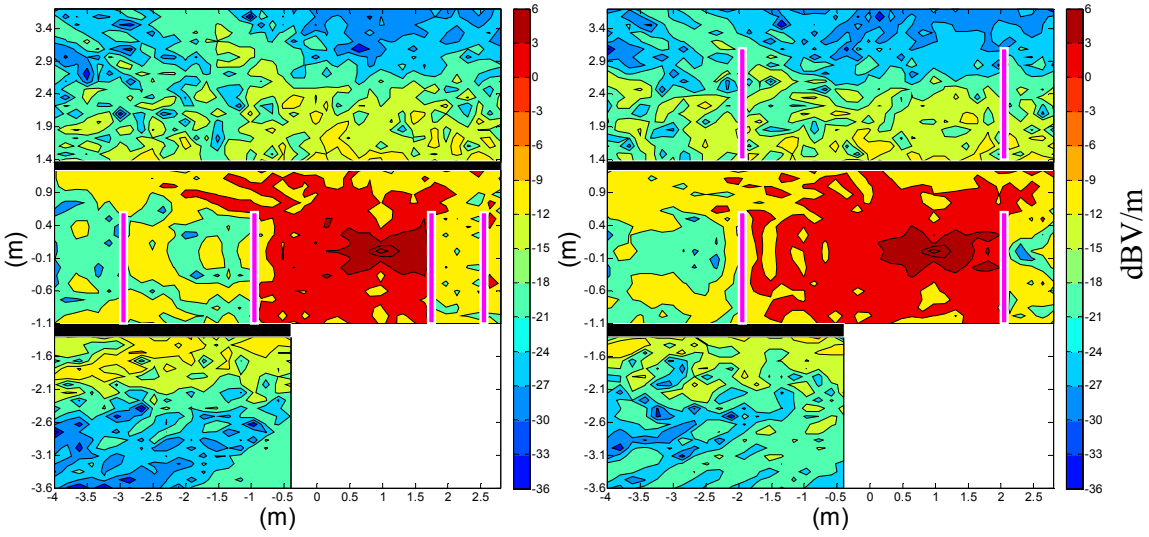

Scenario I

Scenario K

The Difference between Scenario A and Other Scenarios for Vertical Cut at 5.8GHz

These results represent the other eight scenarios for method B in section **Error! Reference source not found.**. The scenarios are presented in Table 4.1. The difference in E-field levels between scenario A and other scenarios are calculated within the Victorian house at 5.8 GHz as shown below.

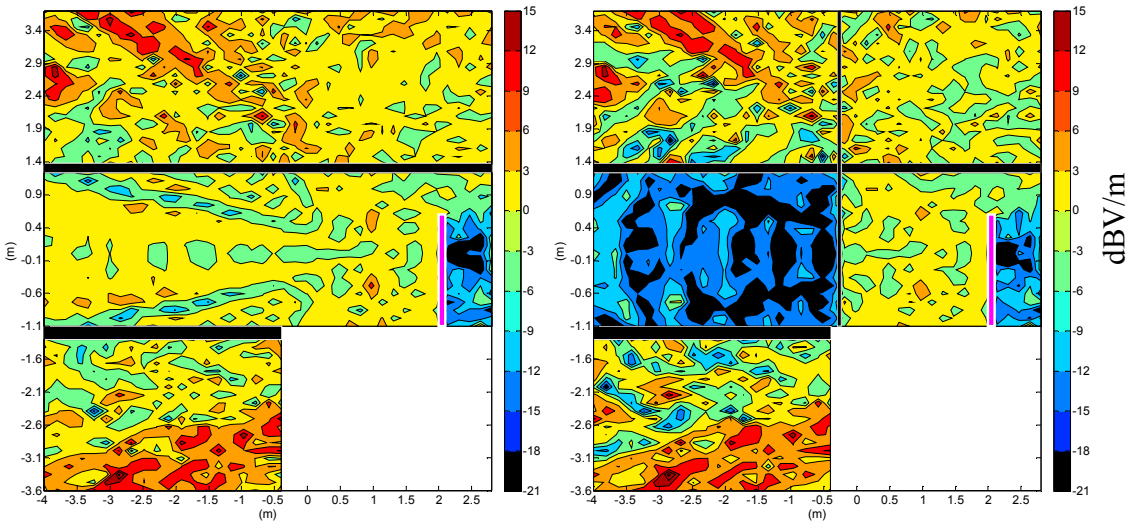

Difference between scenario A & scenario C

Difference between scenario A & scenario D

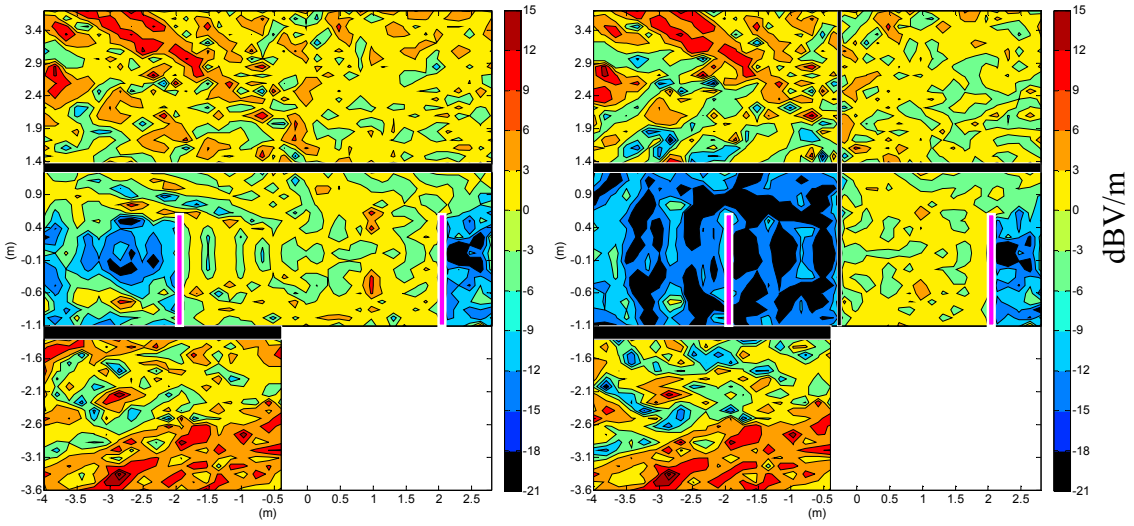

Difference between scenario A & scenario E

Difference between scenario A & scenario F

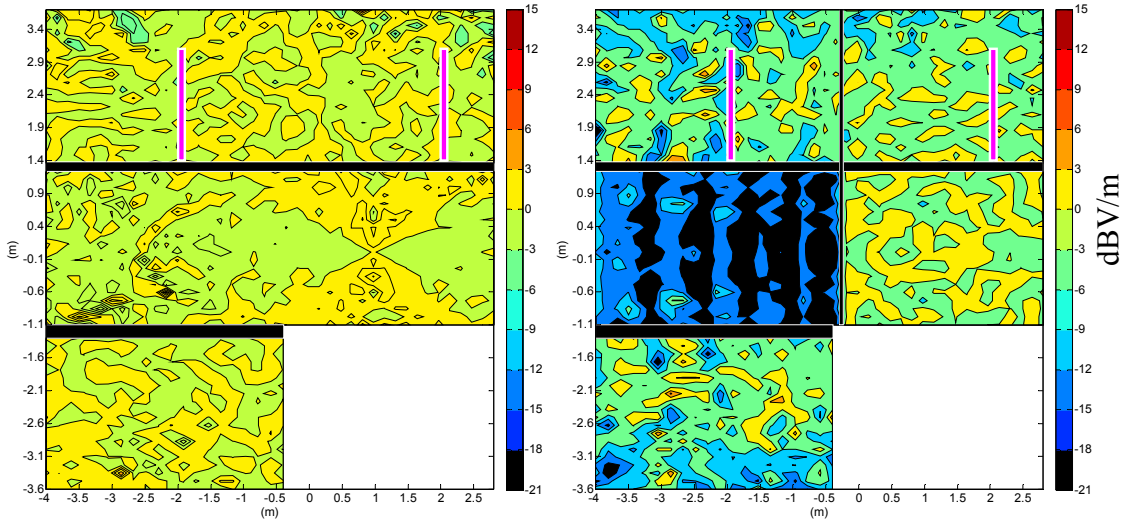

Difference between scenario A & scenario G

Difference between scenario A & scenario H

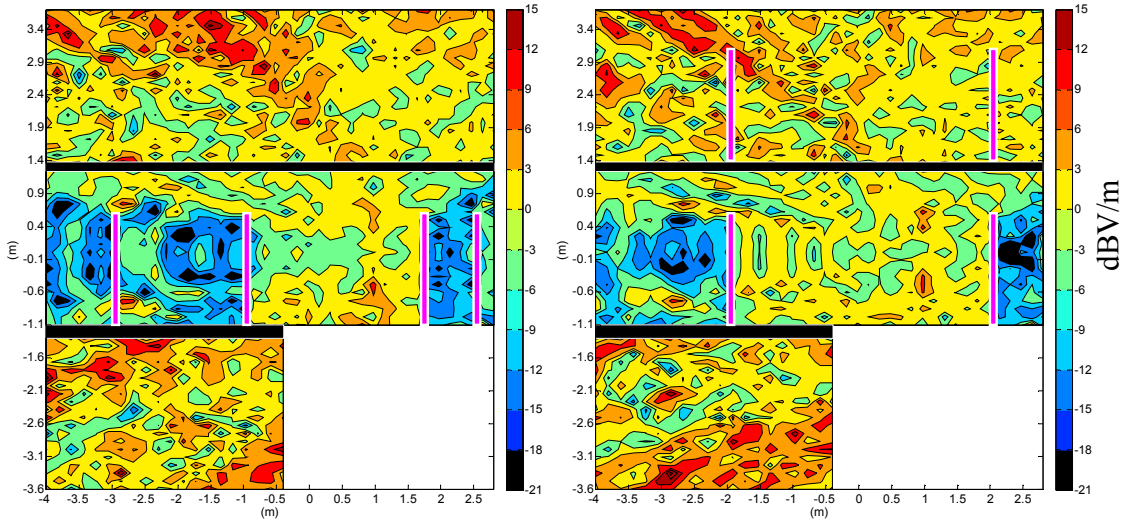

Difference between scenario A & scenario I

Difference between scenario A & scenario K

E-field Amplitude and Cumulative Probability Distribution for Vertical Plane at 5.8GHz

These results illustrate all the twelve scenarios for method C in section **Error! Reference source not found.**. The simulation scenarios are presented in Table 4.1. The amplitude and cumulative probability distributions are used to provide a comparison between different scenarios of the E-field values in the basement, ground floor and first floor within the Victorian house at 5.8 GHz.

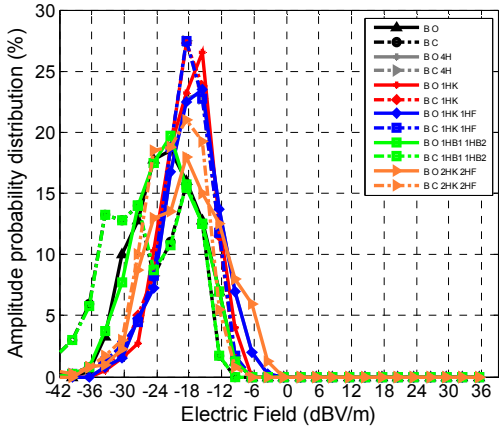

Basement amplitude distribution

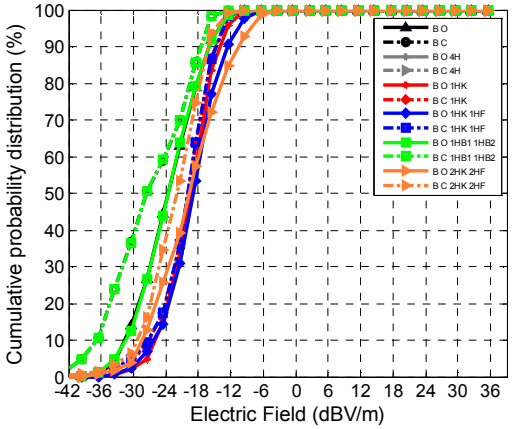

Basement cumulative distribution

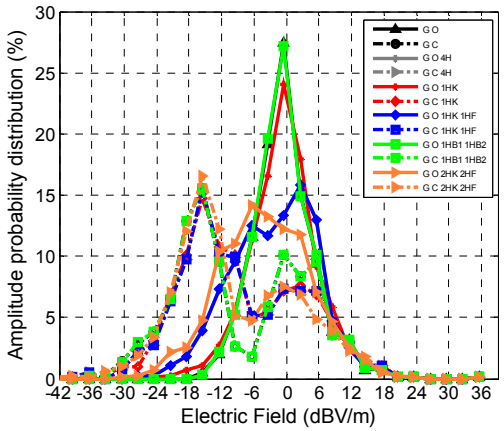

Ground Floor amplitude distribution

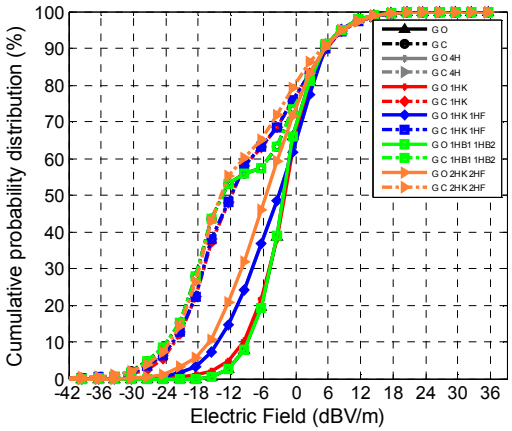

Ground Floor cumulative distribution

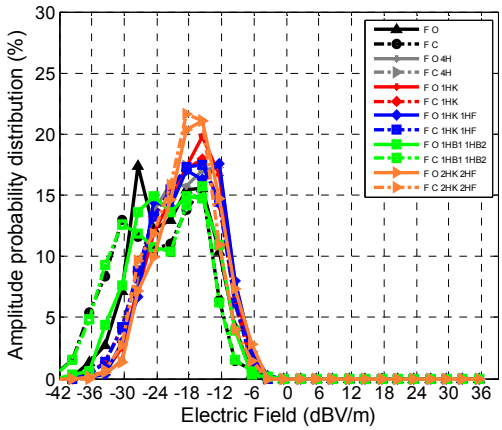

First Floor amplitude distribution

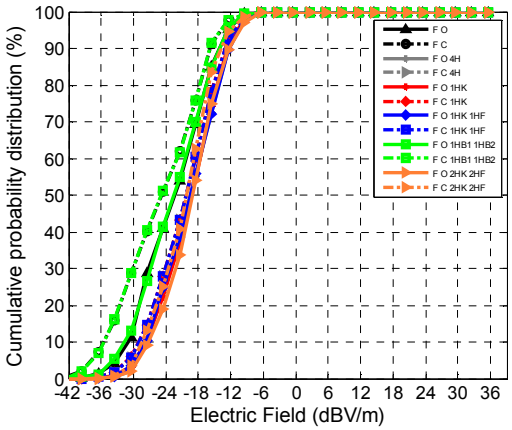

First Floor cumulative distribution

(Key: B = Basement, G = Ground Floor, F=First Floor, O = open door, C = closed door, 2HK = two occupants in the kitchen and 2HF= two occupants in the front room, 1HB1=one occupant in Bedroom 1, 1HB2=one occupant in Bedroom 2).

Appendix B- Simulation of the E-Field Distributions on Vertical Plane at 2.4 GHz.

This appendix illustrates the other eight scenarios for method A in section **Error! Reference source not found.**. The scenarios are presented in Table 4.1. The E-field amplitude distribution in vertical cut within the Victorian house in the first floor, ground floor and basement for the scenarios C, D, E, F, G, H, I and K at 2.4 GHz are shown below.

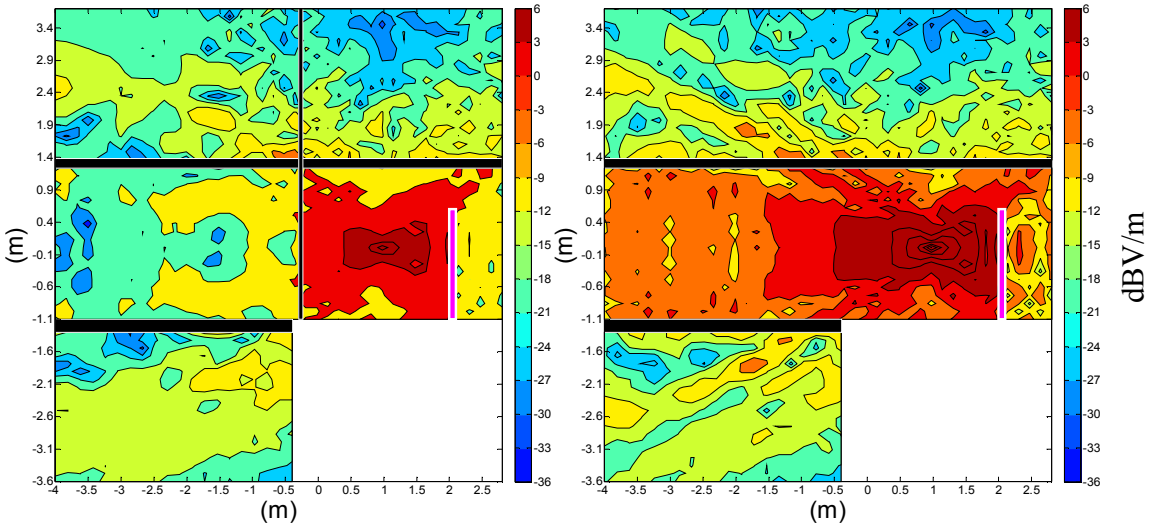

Scenario C

Scenario D

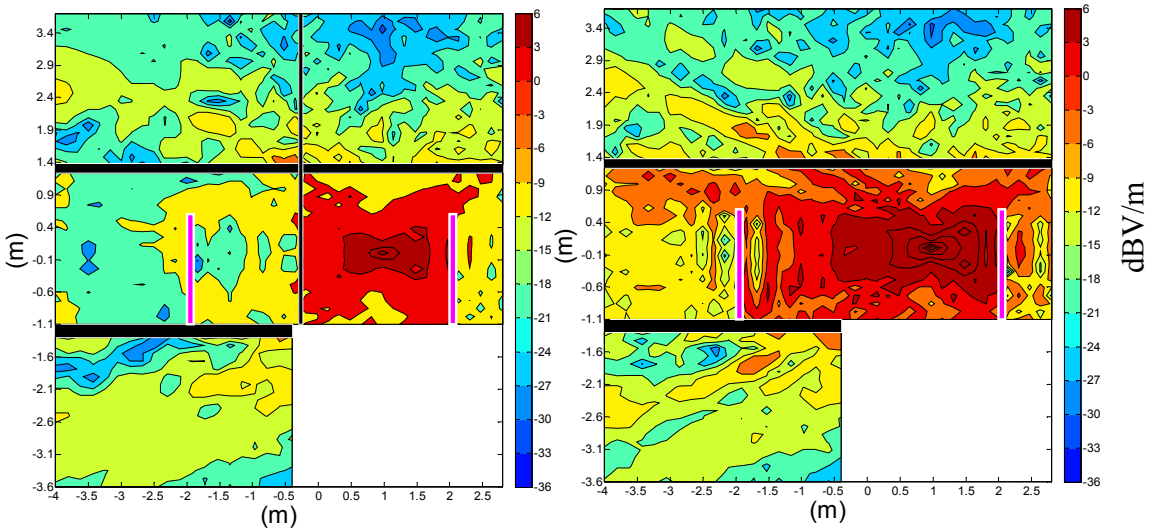

Scenario E

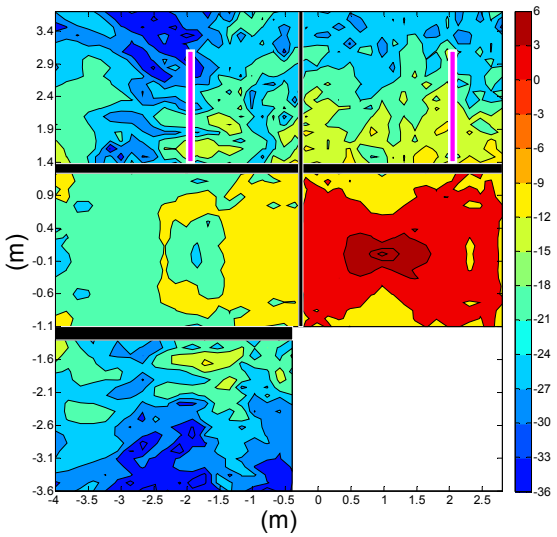

Scenario F

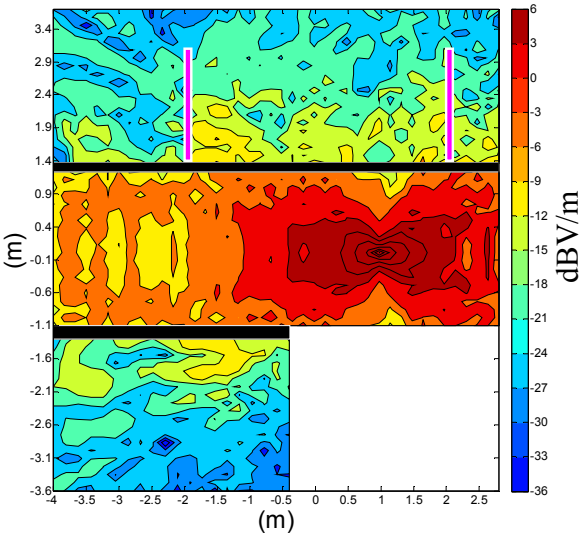

Scenario G

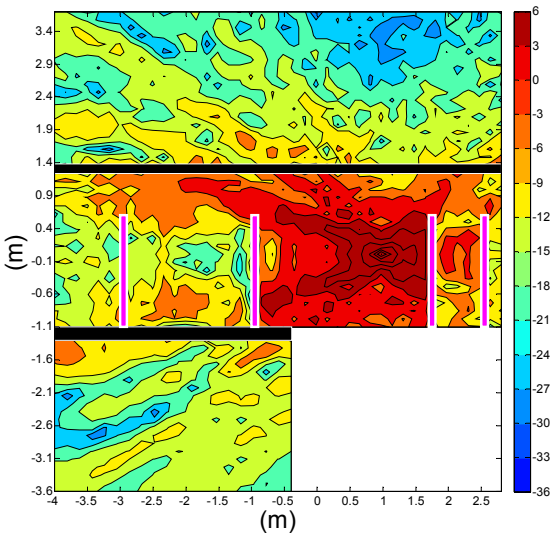

Scenario H

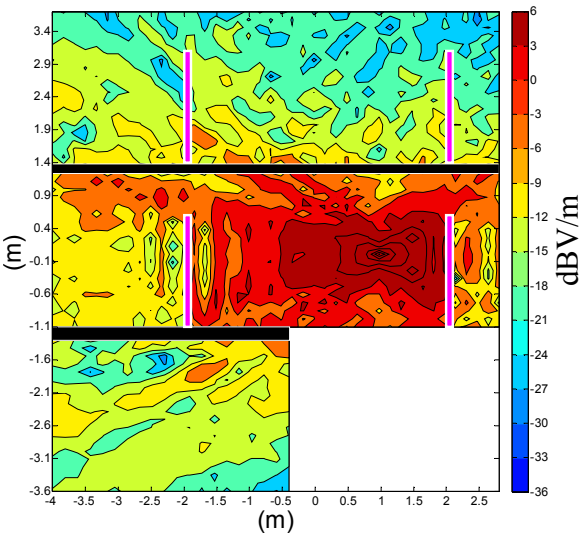

Scenario I

Scenario K

The Difference between Scenario A and Other Scenarios for Vertical Plane at 2.4GHz

These results show the other eight scenarios for method B in section 4.4.2. The scenarios are presented in Table 4.1. The difference in E-field levels between scenario A and other scenarios are calculated within the Victorian house at 2.4 GHz as shown below.

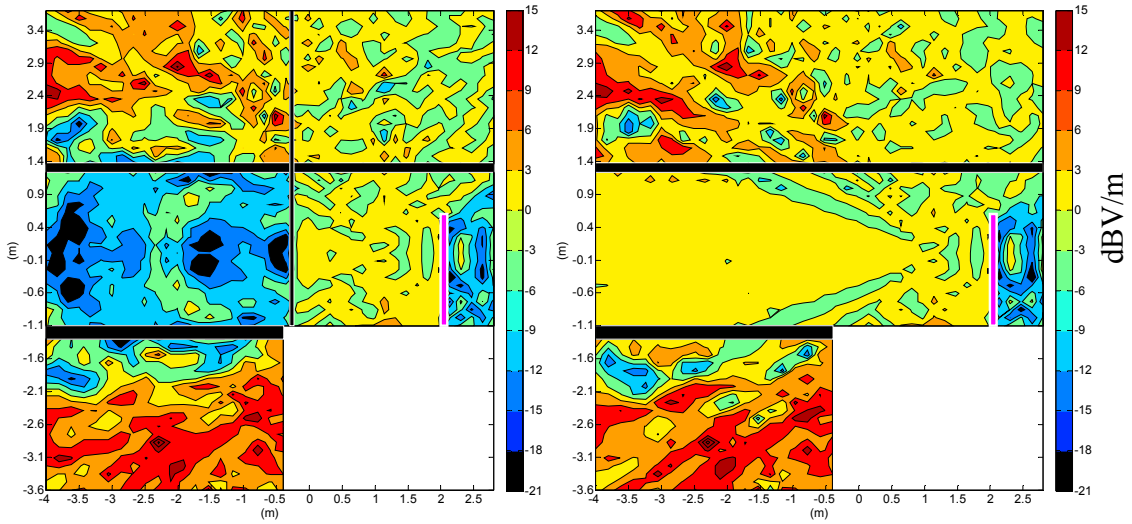

Difference between scenario A & scenario C

Difference between scenario A & scenario D

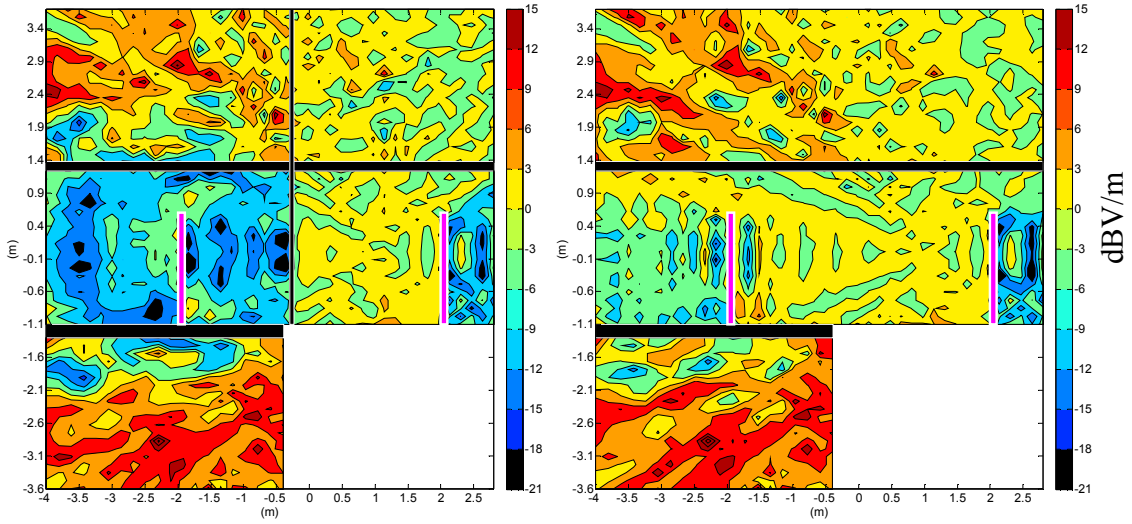

Difference between scenario A & scenario E

Difference between scenario A & scenario F

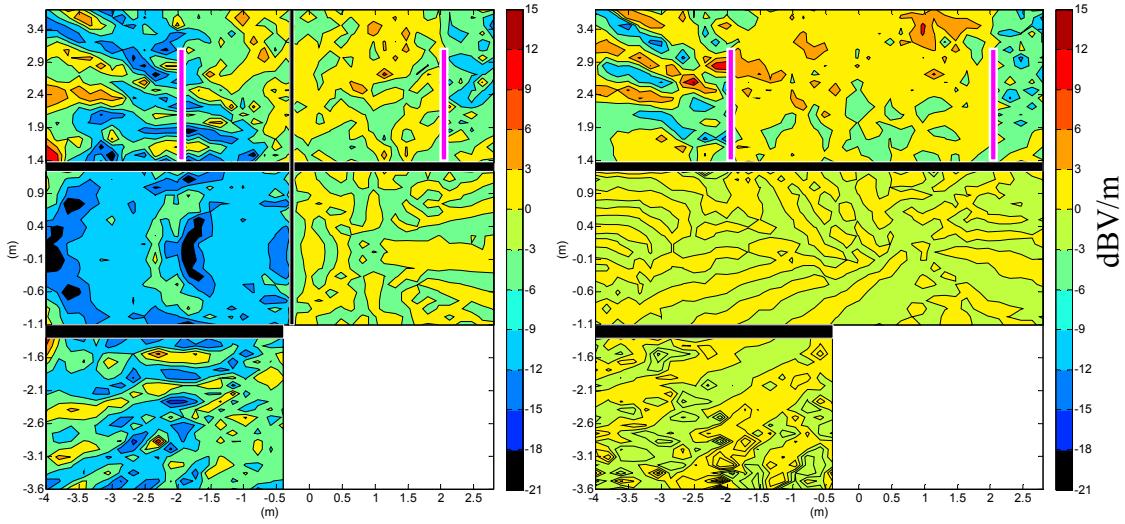

Difference between scenario A & scenario G

Difference between scenario A & scenario H

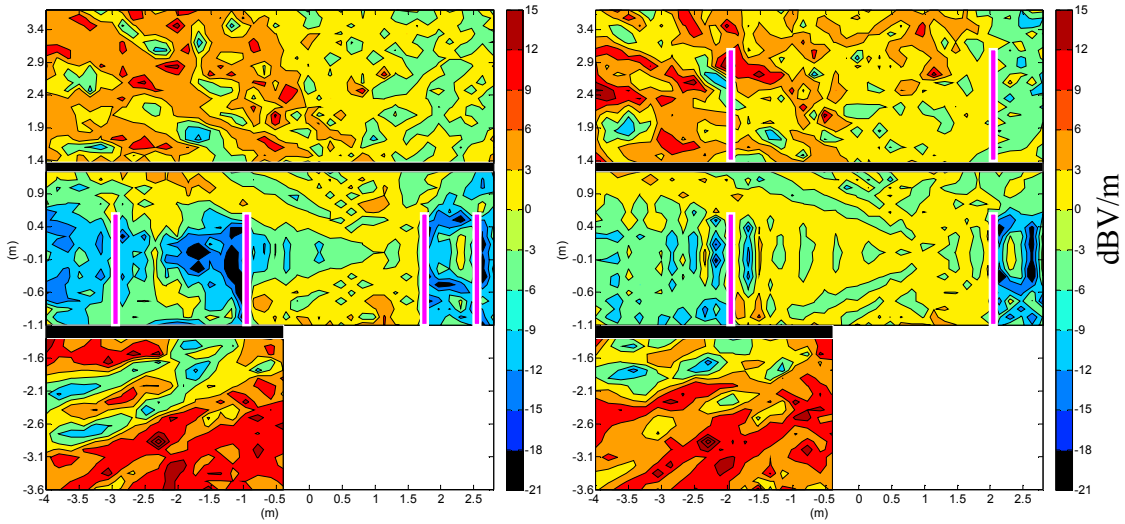

Difference between scenario A & scenario I

Difference between scenario A & scenario K

Appendix B

E-field Amplitude and Cumulative Probability Distribution for Vertical Plane at 2.4 GHz

This results represent all the twelve scenarios for method C in section 4.4.3. The simulation scenarios are presented in Table 4.1. The amplitude and cumulative probability distributions are used to provide a comparison between different scenarios of the E-field values in the basement, ground floor and first floor within the Victorian house at 2.4 GHz.

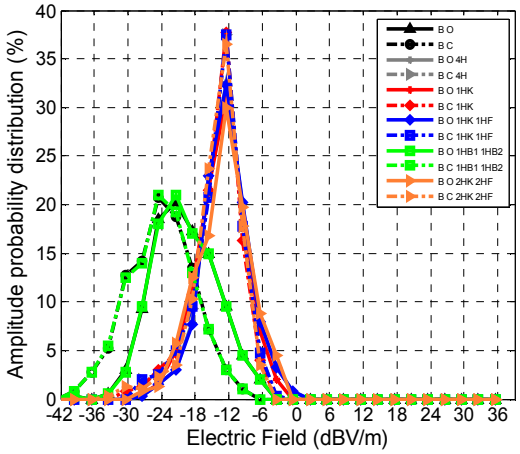

Basement amplitude distribution

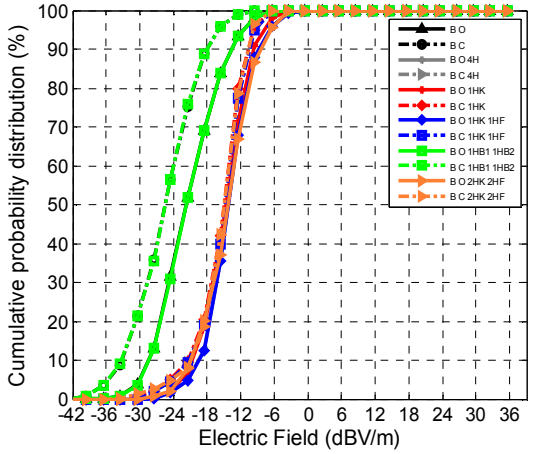

Basement cumulative distribution

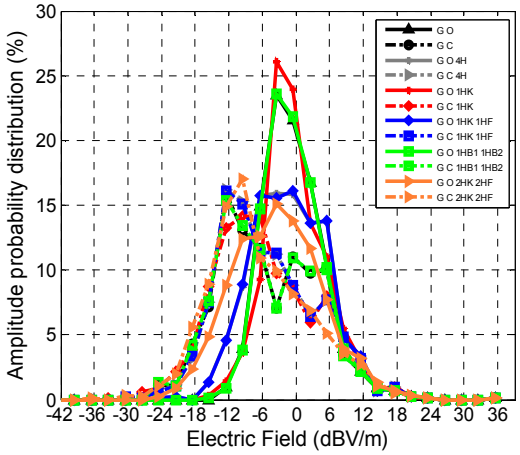

Ground Floor amplitude distribution

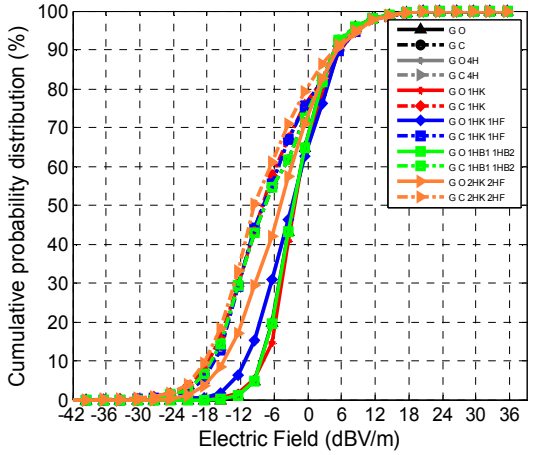

Ground Floor cumulative distribution

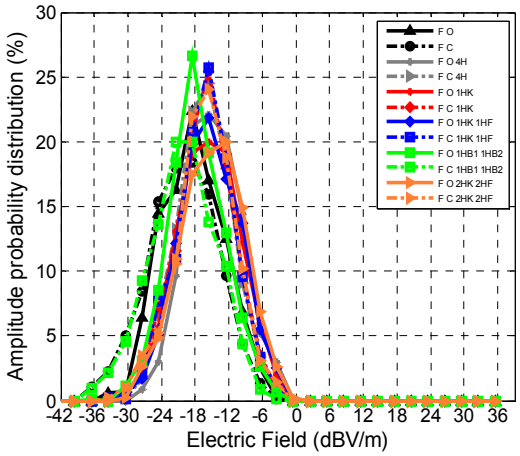

First Floor amplitude distribution

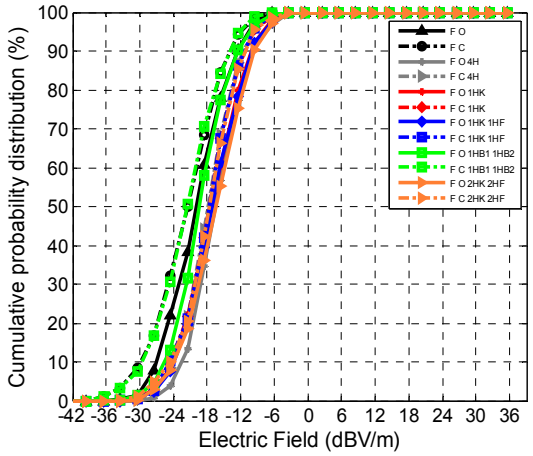

First Floor cumulative distribution

(Key: B = Basement, G = Ground Floor, F=First Floor, O = open door, C = closed door, 2HK = two occupants in the kitchen and 2HF= two occupants in the front room, 1HB1=one occupant in Bedroom 1, 1HB2=one occupant in Bedroom 2).

Appendix C- Simulation of the E-Field Distributions on Vertical Plane at 868 MHz.

This appendix represents the other eight scenarios for method A in section 4.5.1. The scenarios are presented in Table 4.1. The E-field amplitude distribution in vertical cut within the Victorian house in the first floor, ground floor and basement for the scenarios C, D, E, F, G, H, I and K at 868 MHz are shown below.

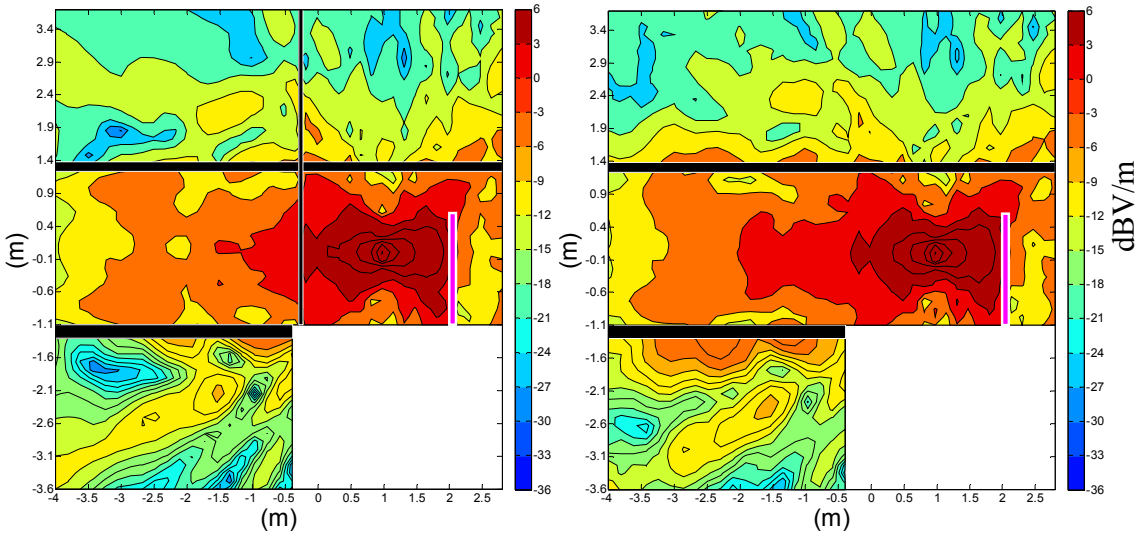

Scenario C

Scenario D

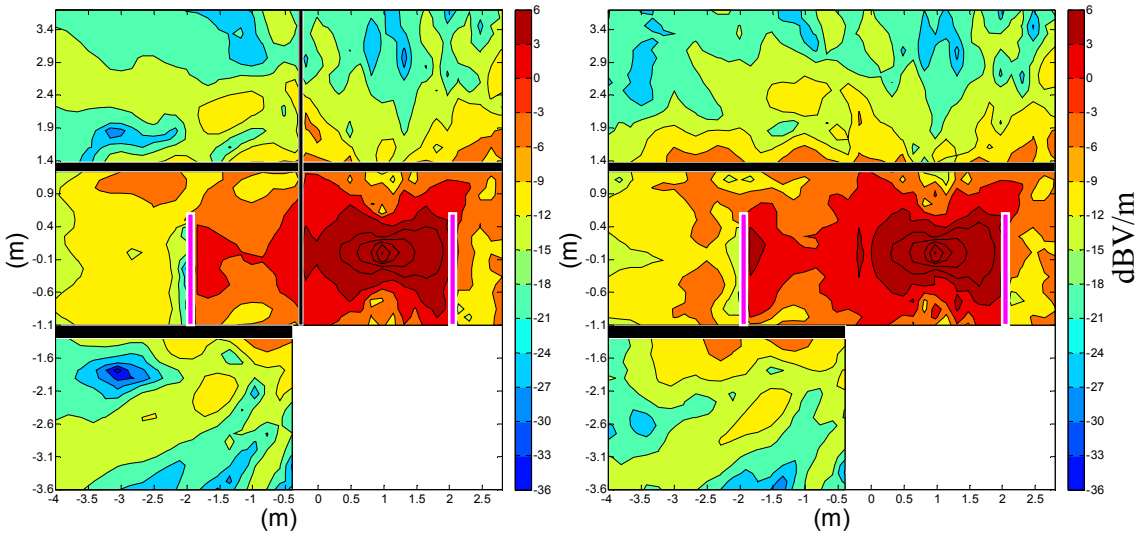

Scenario E

Scenario F

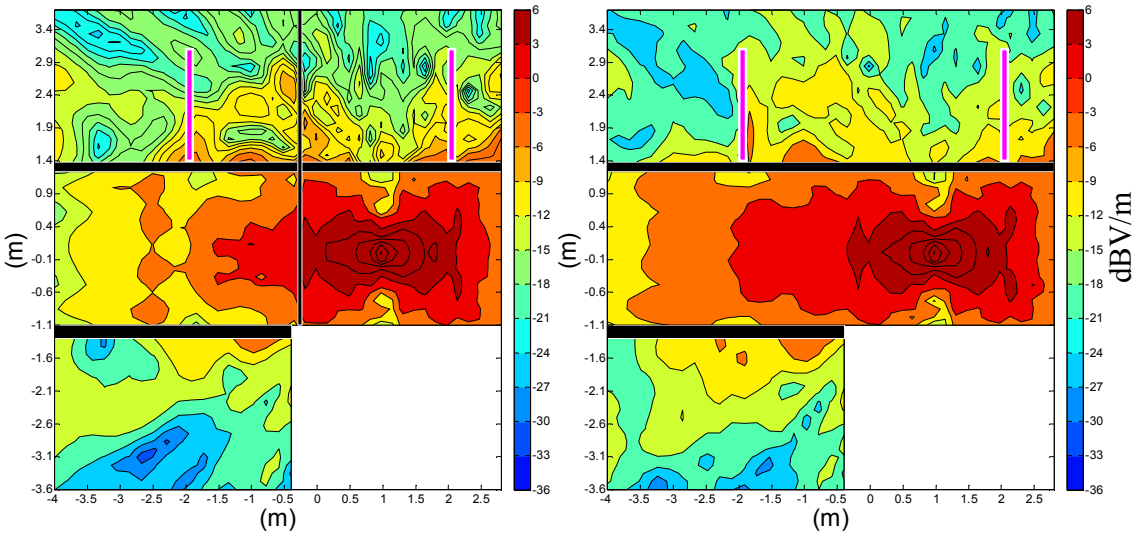

Scenario G

Scenario H

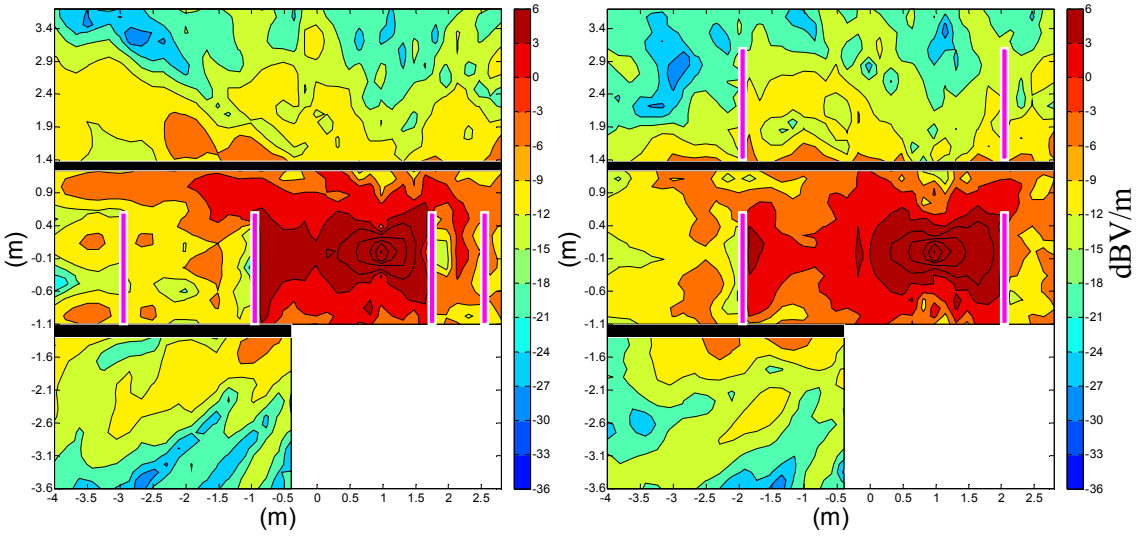

Scenario I

Scenario K

The Difference between Scenario A and Other Scenarios for Vertical Plane at 868 MHz

These results illustrate the other eight scenarios for method B in section 4.5.2. The scenarios are presented in Table 4.1. The difference in E-field levels between scenario A and other scenarios are calculated within the Victorian house at 868 MHz as shown below.

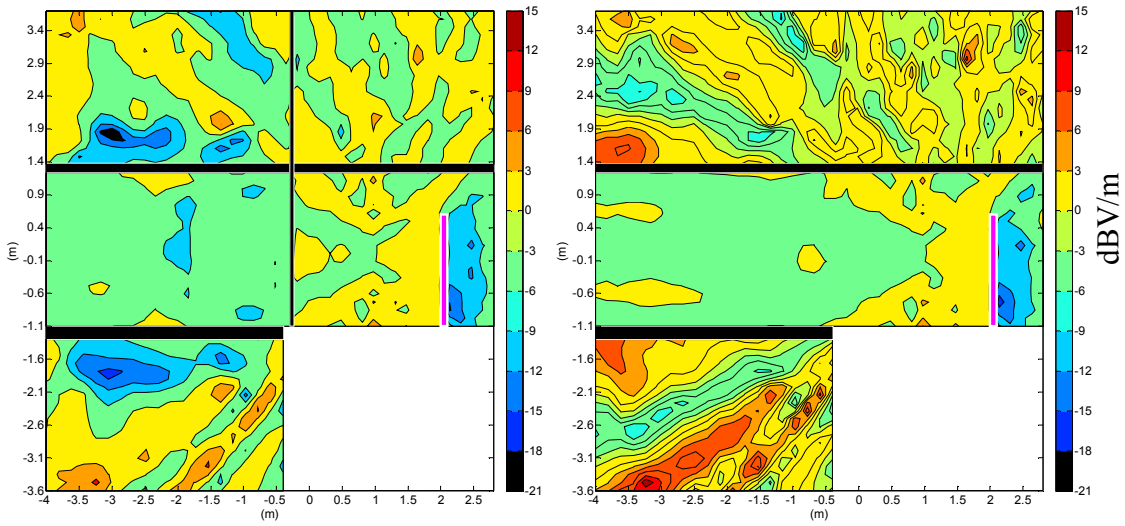

Difference between scenario A & scenario C

Difference between scenario A & scenario D

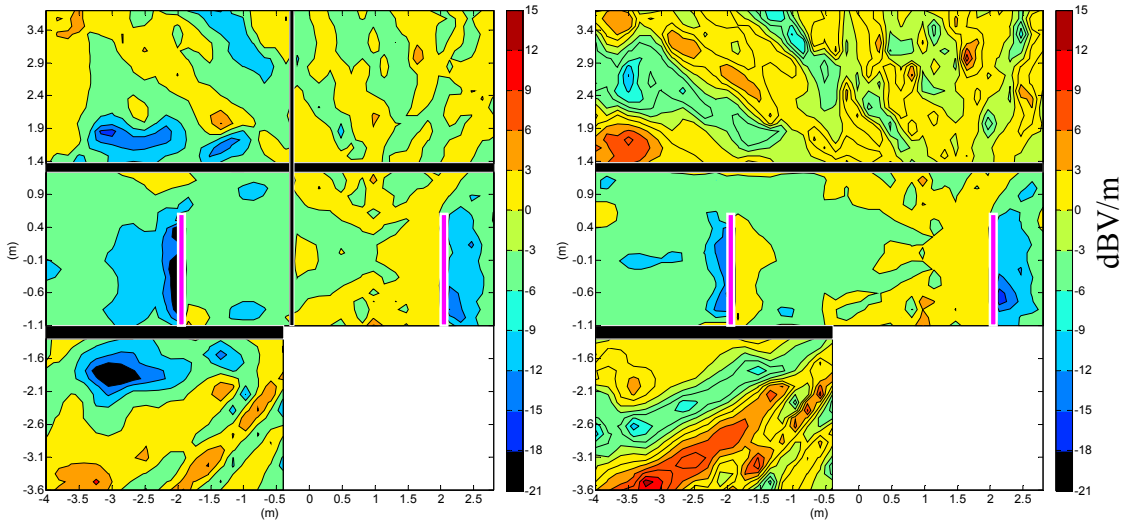

Difference between scenario A & scenario E

Difference between scenario A & scenario F

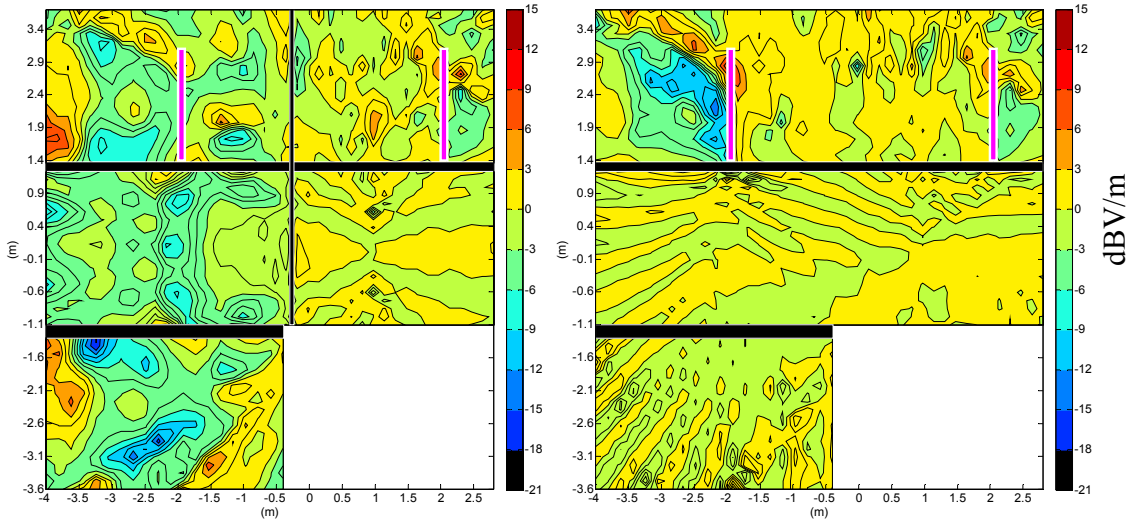

Difference between scenario A & scenario G

Difference between scenario A & scenario H

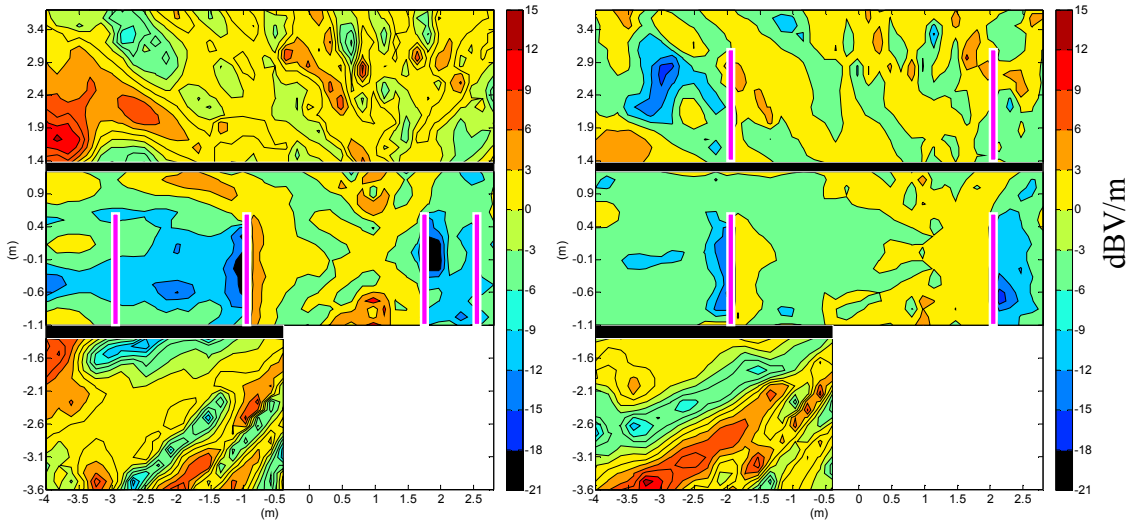

Difference between scenario A & scenario I

Difference between scenario A & scenario K

E-field Amplitude and Cumulative Probability Distribution for Vertical Plane at 868 MHz

These results represent all the twelve scenarios for method C in section 4.5.3. The simulation scenarios are presented in Table 4.1. The amplitude and cumulative probability distributions are used to provide a comparison between different scenarios of the E-field values in the basement, ground floor and first floor within the Victorian house at 868 MHz.

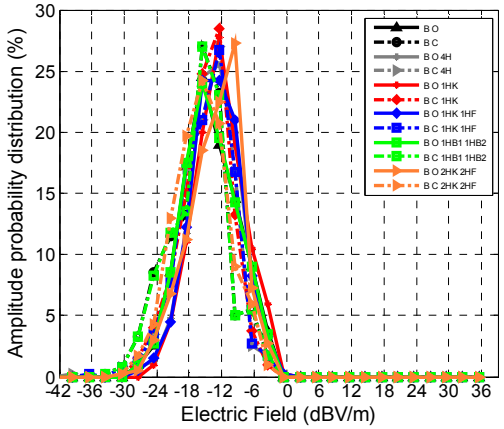

Basement amplitude distribution

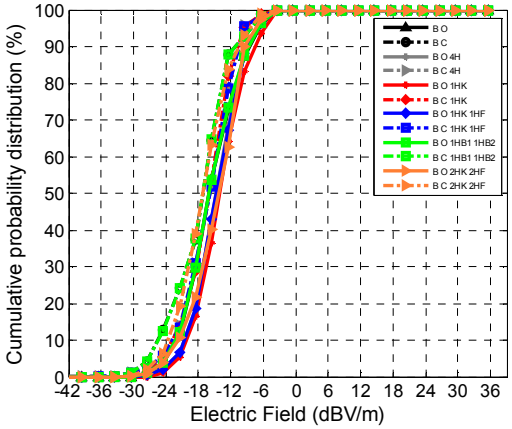

Basement cumulative distribution

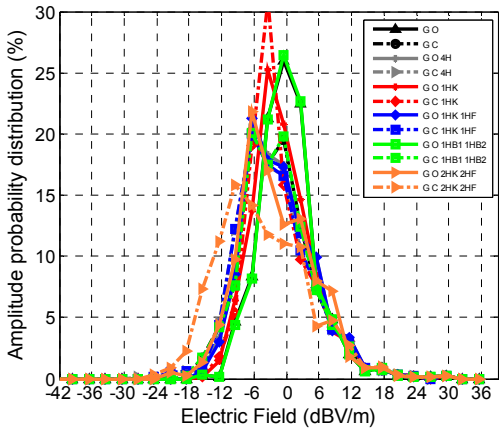

Ground Floor amplitude distribution

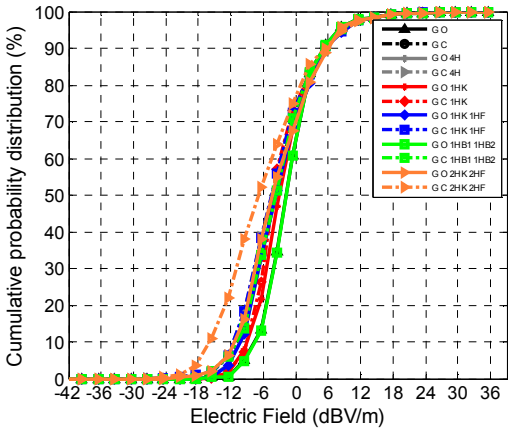

Ground Floor cumulative distribution

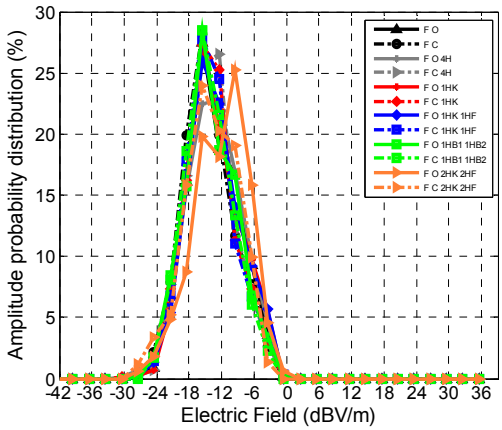

First Floor amplitude distribution

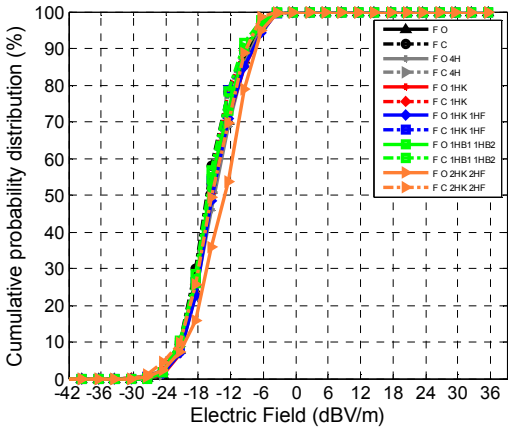

First Floor cumulative distribution

(Key: B = Basement, G = Ground Floor, F=First Floor, O = open door, C = closed door, 2HK = two occupants in the kitchen and 2HF= two occupants in the front room, 1HB1=one occupant in Bedroom 1, 1HB2=one occupant in Bedroom 2).

Appendix D- Simulation of the E-Field Distributions on Vertical Plane at 433 MHz.

This appendix shows the other eight scenarios for method A in section 4.6.1. The scenarios are presented in Table 4.1. The E-field amplitude distribution in vertical cut within the Victorian house in the first floor, ground floor and basement for the scenarios C, D, E, F, G, H, I and K at 433 MHz are shown below.

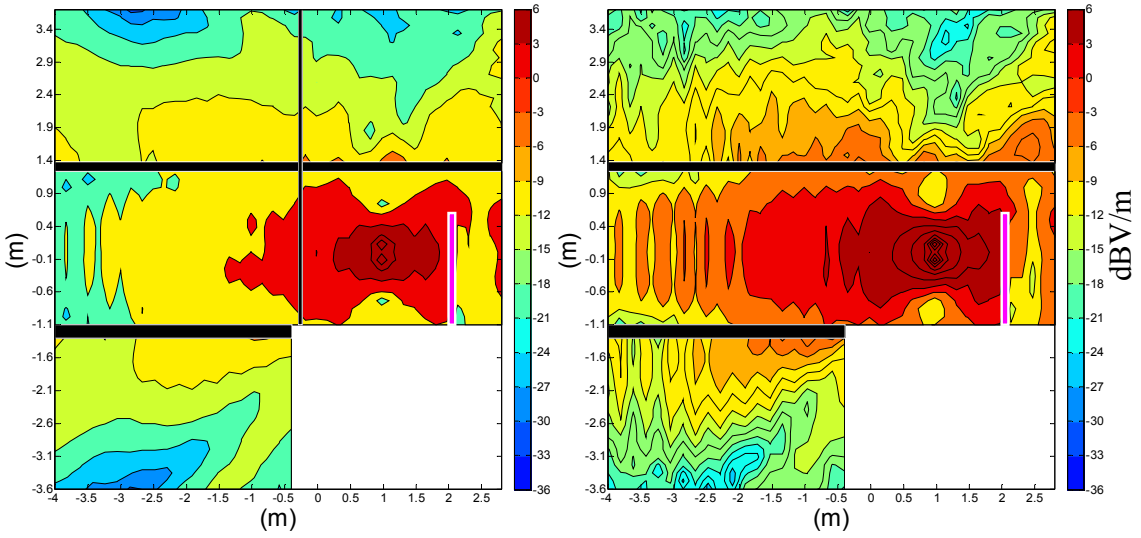

Scenario C

Scenario D

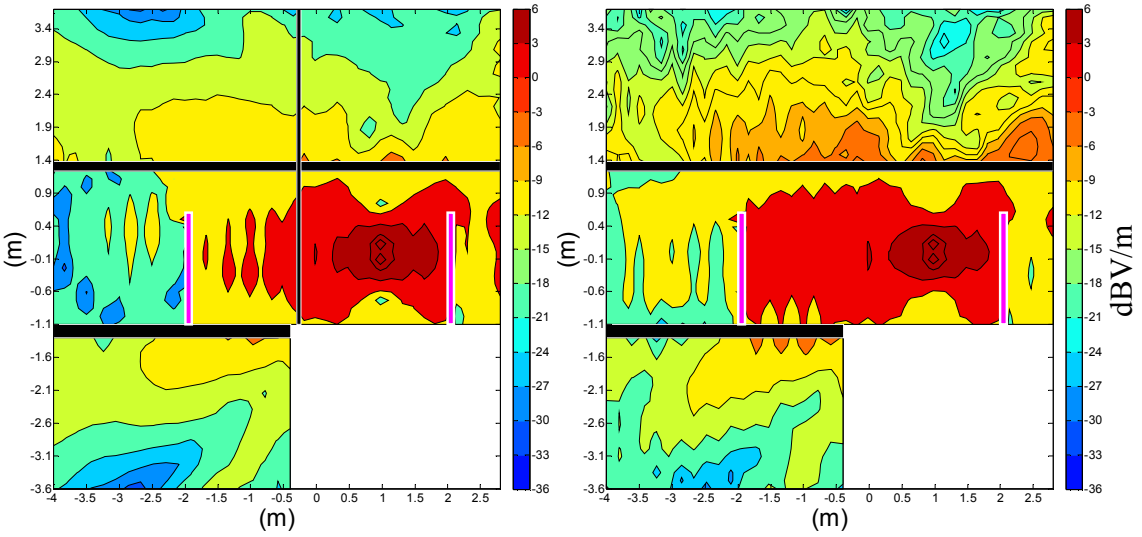

Scenario E

Scenario F

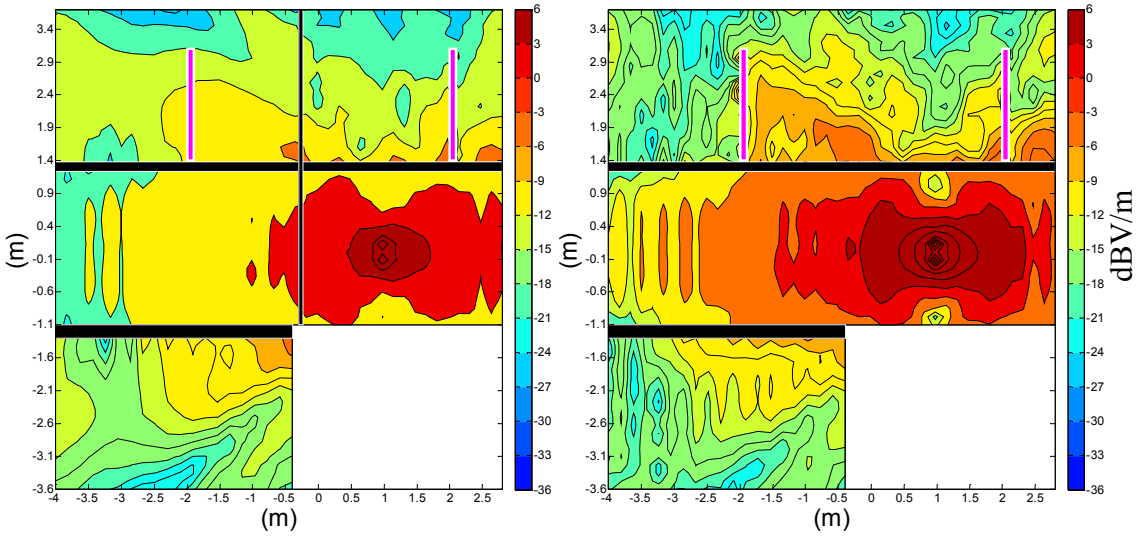

Scenario G

Scenario H

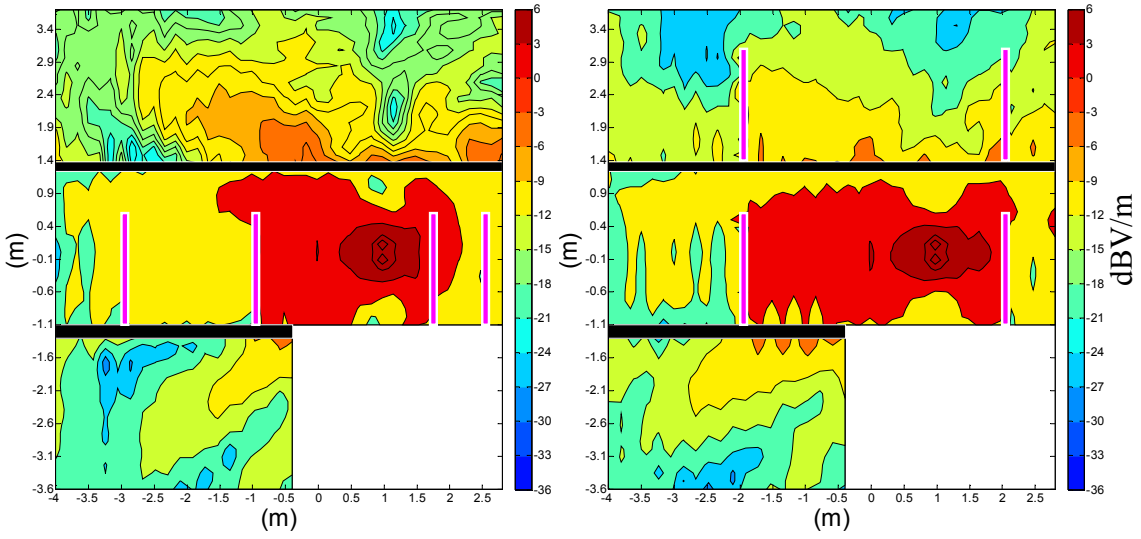

Scenario I

Scenario K

Appendix D

The Difference between Scenario A and Other Scenarios for Vertical Plane at 433 MHz

These results show the other eight scenarios for method B in section 4.6.2. The scenarios are presented in Table 4.1. The difference in E-field levels between scenario A and other scenarios are calculated within the Victorian house at 433 MHz as shown below.

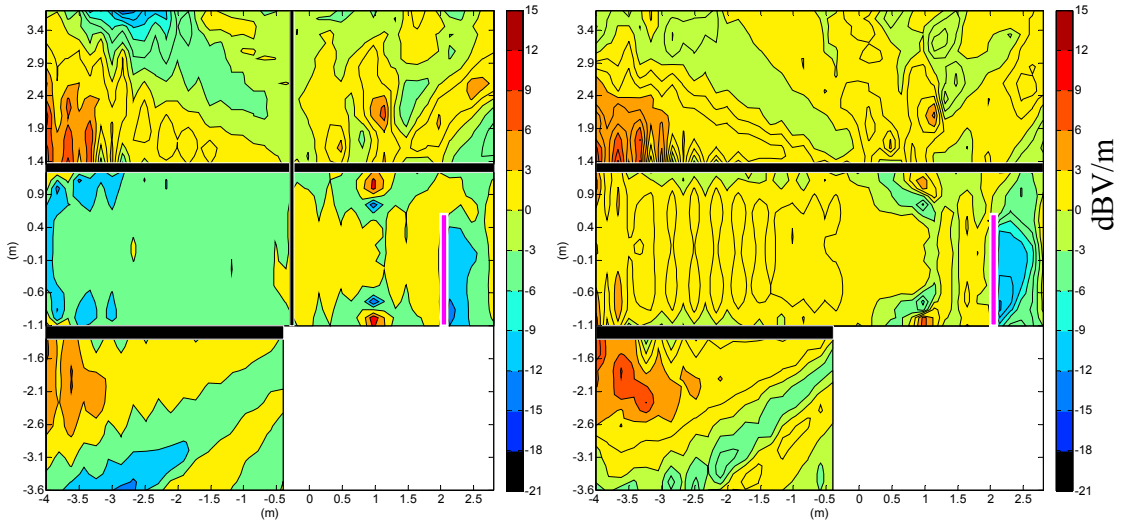

Difference between scenario A & scenario C

Difference between scenario A & scenario

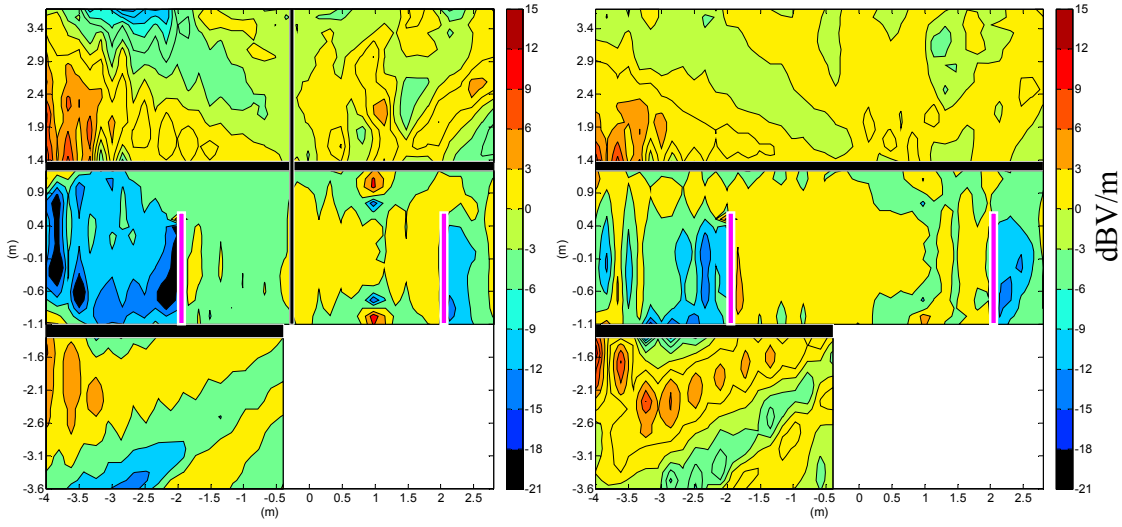

Difference between scenario A & scenario E

Difference between scenario A & scenario F

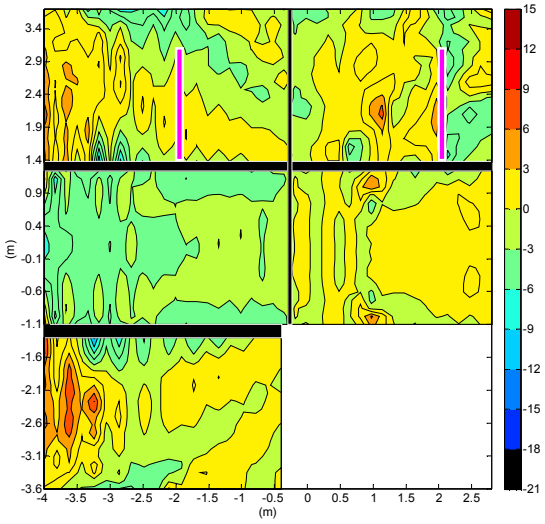

Difference between scenario A & scenario G

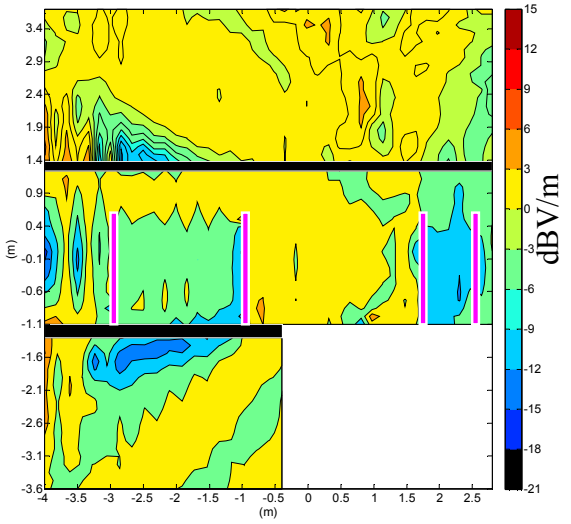

Difference between scenario A & scenario H

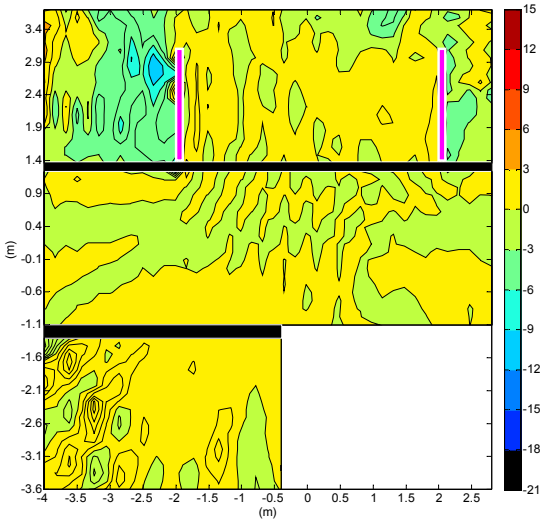

Difference between scenario A & scenario I

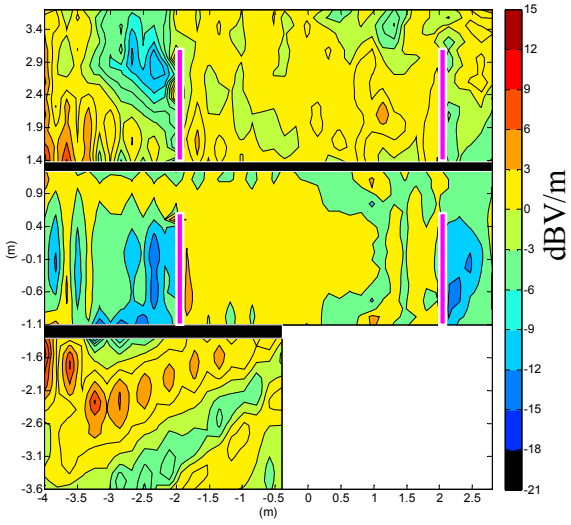

Difference between scenario A & scenario K

E-field Amplitude and Cumulative Probability Distribution for Vertical Plane at 433 MHz

These results represent all the twelve scenarios for method C in section 4.7. The simulation scenarios are presented in Table 4.1. The amplitude and cumulative probability distributions are used to provide a comparison between different scenarios of the E-field values in the basement, ground floor and first floor within the Victorian house at 433 MHz.

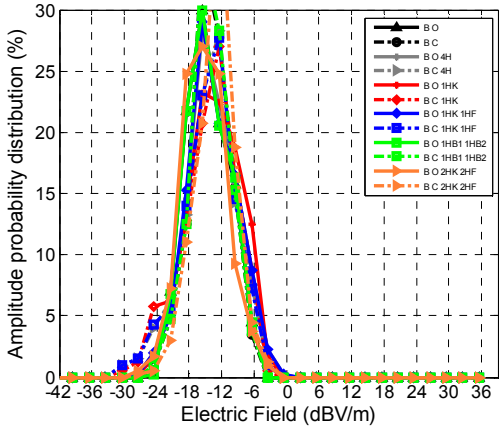

Basement amplitude distribution

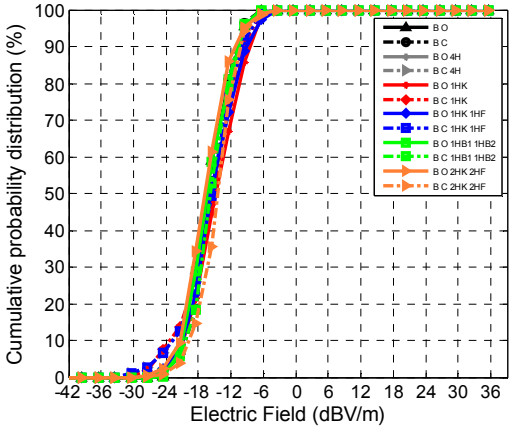

Basement cumulative distribution

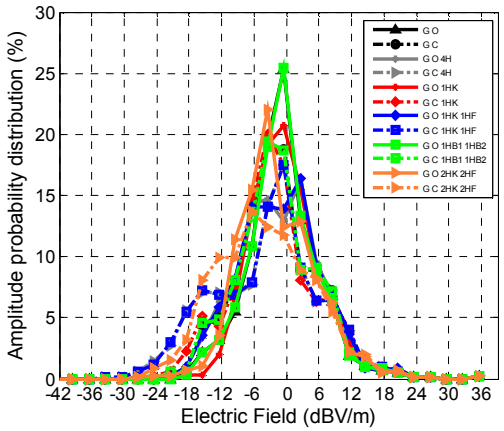

Ground Floor amplitude distribution

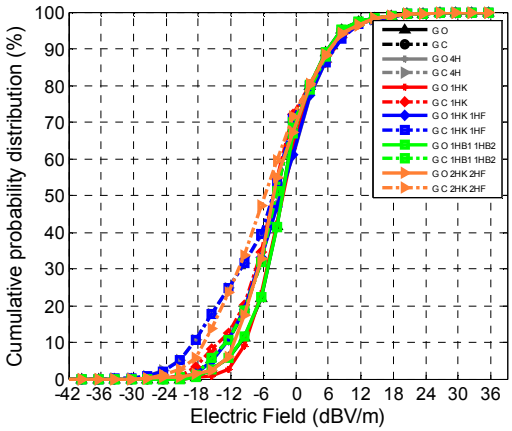

Ground Floor cumulative distribution

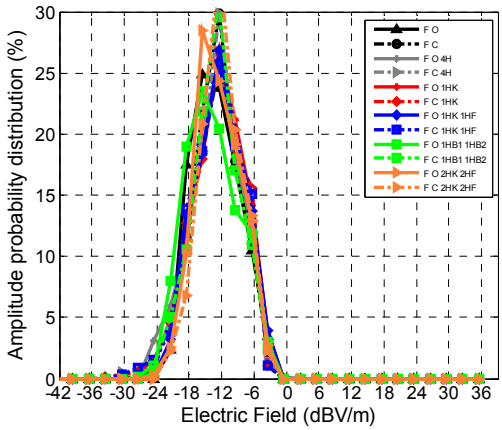

First Floor amplitude distribution

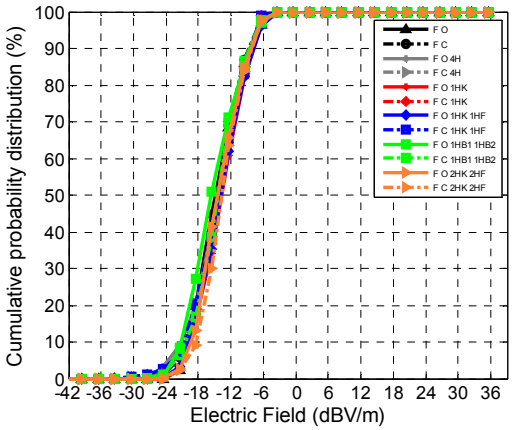

First Floor cumulative distribution

(Key: B = Basement, G = Ground Floor, F=First Floor, O = open door, C = closed door, 2HK = two occupants in the kitchen and 2HF= two occupants in the front room, 1HB1=one occupant in Bedroom 1, 1HB2=one occupant in Bedroom 2).

Appendix E – First Conference Paper

ZigBee Wireless Quality Trials for Smart Meters

Y. Alharbi[1], D. Powell[2], R.J. Langley[3], J.M. Rigelsford[4]

Department of Electronic and Electrical Engineering,
The University of Sheffield, Mappin Street, Sheffield, S1 3JD, UK

[1]yhalharbi1@sheffield.ac.uk
[2]d.powell@sheffield.ac.uk
[3]r.j.langley@Sheffield.ac.uk
[4]j.m.rigelsford@sheffield.ac.uk

***Abstract*— This paper assess the performance abilities of consumer band, wireless, digital network equipment using the ZigBee protocol for smart metering applications. Tests were performed in a typical Victorian terraced house.**

I. INTRODUCTION

In an attempt to combat increasing energy usage, the UK Government is committed to having a "smart meter" in every UK home by approximately 2020. The objective is to make domestic energy consumers aware of their energy usage and behaviours, thereby helping to reduce overall energy usage. Additionally, a national smart electrical grid is proposed to reduce the country-wide energy consumption and to reduce the carbon footprint of the UK.

Recently, wireless technology has growth rapidly and the obvious example for this explosive is the massive use of mobile telephony. The performance of wireless system inside the buildings is becoming very important as the wireless friendly building is designed to improve the radio frequency (RF) performance inside the building [1]. In addition, there are many parameters that influence the propagation of the wave within buildings such as type and structure of building, the construction materials and the incident angle of wave into the wall or windows [3-5]. Frequency Selective Surfaces (FSS), which act as a filter, have been recommended for installation in walls and windows to allow the propagation of desirable RF signals and stop the unwanted signal in buildings [2].

To allow remote, two-way communication between room-based monitors, the smart meter and the energy suppliers, a suitable wireless solution is required. An obvious choice is ZigBee Alliance devices that are designed to operate to this standard. ZigBee is a specification for a suite of high-level, communication protocols which is targeted at RF applications that require a low data rate, long battery life, and secure networking [6]. It is based on the IEEE 802.15.4 standard and is suitable for small, low power digital radios for Wireless Home Area Networks (WHANs), such as wireless light switches with lamps, electrical meters with in-home displays and consumer electronics equipment. ZigBee is also designed to be simpler and less expensive than other Wireless Personal Area Networks (WPANs) such as Bluetooth and WIFI. As a result of the wide range of possible applications for ZigBee, a level of security should be provided for in specific applications [7]. With the increasing usage of sensors and controller devices in buildings, ZigBee-Wireless Mesh Networks (ZigBee-WMNs) are proposed as a cheap and flexible system for controlling automated buildings [8]. Some previous research has investigated the interference between ZigBee and wireless local area networks (WLANs), resulting in a recommendation that in order to maintain satisfactory performance the minimum distance between ZigBee and WiFi should be 8m [9].

This paper assesses the suitability of Zigbee used within domestic properties for smart metering applications. Several experiments were carried out to characterize ZigBee performance at different locations inside the building.

II. METHODOLOGY

Experiments were performed in west Sheffield, South Yorkshire during the winter months of 2010. The building type tested is a late-Victorian terraced house built in approximately 1890. It is a brick construction with a combination of brick and stud internal walls. It is possible that some rooms still have lathe/plaster internal walls insulated with rubble. The building has a slate and lining roof and comprises two inhabited floors, in addition to a brick and stone-walled uninhabited basement. The property has an independent wet heating system with radiators located in each room and the original windows have been replaced with PVC double glazing.

Propagation measurements were performed using two Ember Corp ZigBee modules (ISA3), fitted with an Antenova dielectric SMT antenna. These devices were used to send and receive signals and calculate Link Quality Indication (LQI) and Received Signal Strength Indication. A power over ethernet (POE) system was used to provide power to the ISA3 and data connectivity to a laptop computer at the reference location. The remote node had its own battery power. InSight software adapters were used for programming and data capture, accessed through a TCP/IP. Several trials were conducted measuring both RSSI and LQI.

A. Received Signal Strength Indication (RSSI)

The RSSI is a measurement of the RF power present in a received radio signal, regardless of its source. Device

manufacturers express RSSI outputs in different ways. The Ember devices express the readings in power levels between 0 and -96 dBm, with -96dBm being the lowest measurable result before communication is lost between two nodes. The measurement is based on the highest energy level detected over a specific period of time for the data packet being received. It is worth noting that the energy received may be from any transmitter operating on the same frequency and not necessarily the partner node.

B. Link Quality Indication (LQI)

The reported LQI value is a dimensionless number ranging from 0–255 that represents the link quality of the connectivity between neighbouring nodes as they communicate. The measurement is based on the reliability of a data packet being received when being sent from one node to another. The maximum value represents the best possible link quality, and conversely lower values, i.e. < 200, represent high error rates. For example, an LQI value of 200 represents approximately 80% reliability of receiving a transmitted data packet intact. This can be summarized as shown in Table 1 below. It is possible to achieve over 99% packet success rate with more than 4 chip errors per byte, but once chip errors occur, you are very close to the point of losing connectivity.

TABLE I
LINK QUALITY INDICATION (LQI) VS CHIP ERRORS PER BYTE

Chip errors per byte	LQI
0	255
1	191
2	127
3	63
4+	0

C. Experimental Trials

Three trials were planned for the Victorian terrace house. The trials were designed to extract data simulating communication between a hypothetical, hand-held wireless display device (as proposed by the government for energy monitoring) and a smart meter points at various locations around a typical house. Results would capture the propagation of the signal with respect to the internals walls between the rooms.

- Trial 1 'Receiver in the kitchen', located on the ground floor on the work surface at L0 – a typical location for the display.
- Trial 2 'Receiver in bedroom', located on first floor at L10, which is the furthest location from the existing gas and electricity meters at L3.
- Trial 3 'Received power topology', located on ground floor in the front room.

The ideal location for the fixed reference is in the basement next to the existing gas and electricity meters at L3 but due to power availability and low ambient temperature, this was not possible. Due to reciprocity this will not affect the validity of the data.

III. Results

Figures 1 and 2 show the floor plan of the test site and locations of the measurement points for the first two trials. The three trials are explained in detail as follows.

Fig. 1 Test Site Floor Plan – showing Trial 1 node locations

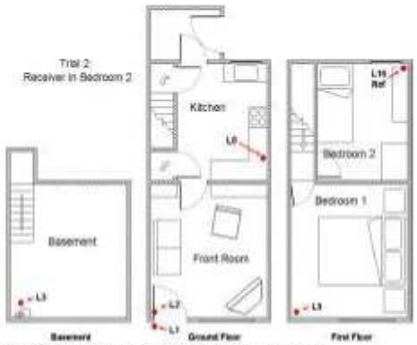

Fig. 2 Test Site Floor Plan – showing Trial 2 node locations

A. Trial 1 'Receiver in the kitchen'

The first trial was designed to test the propagation of the signal from the mobile 'sensor' node at various locations (L1 through L7) with respect to the reference node which was fixed at location L0 in the kitchen. Location L1 was used to simulate a device that would take a doorstep meter reading. Location L3 simulates a node at the electricity meter, in the basement, talking to the energy monitor device in the kitchen. Other locations simulate devices that may be in a standard domestic property. The first trial simulated devices in the basement, ground floor and first floor of the house. Note that the external windows and doors were all closed throughout the trial. Fig. 3 illustrates the average measured RSSI values superimposed on the building floor plans.

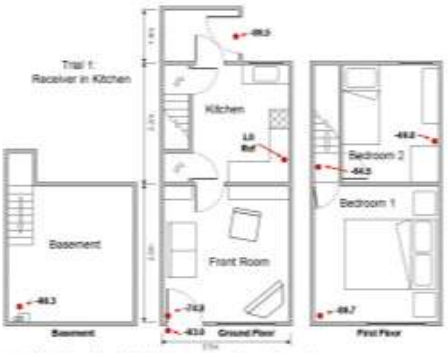

Fig. 3 Trial 1 'Receiver in Kitchen' – Results on floor plan

Table 2 shows the measured values of received signal strength indication and the link quality indication for each location. It can be seen from the table that the link quality drops significantly from the maximum value of 255 in the kitchen to 172 at location L1.

TABLE 2
TRIAL 1 – 'RECEIVER IN KITCHEN' MEASURED DATA

Point	Distance (mm)	RSSI (dBm)			LQI
		Min	Avg	Max	
GROUND FLOOR					
L4	3800	-93	-86.5	-81	248.2
L2	5430	-76	-74.8	-74	255
L1	5730	-96	-93	-89	172
BASEMENT					
L3	5860	-94	-90.333	-85	233.7
FIRST FLOOR					
L6	3000	-49	-49	-49	255
L7	4100	-65	-64.5	-64	255
L5	6140	-90	-86.7	-84	255

B. Trial 2 'Receiver in the bedroom'

The second trial was set up to test the propagation of the signal from the bedroom to the basement and the location outside the front door. The aim was to enable maximum attenuation of the signal via special separation. Location L3 was used to simulate a meter in the basement, with the signal propagating through two wooden floors and one brick wall. Location L1 was used to simulate a device that would take a doorstep meter reading from the setup with the signal propagating through one wooden floor, one internal brick wall and one external brick wall. The reference node was moved to Bedroom 2, and the new reference location is named L10. Fig. 4 illustrates the average measured RSSI values superimposed on the building floor plans.

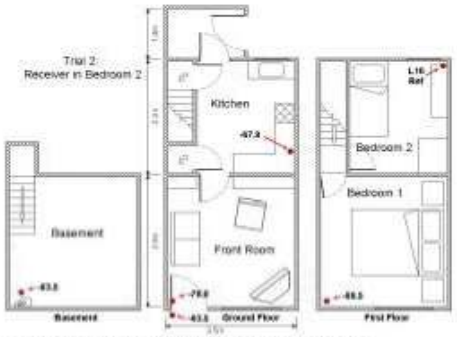

Fig. 4 Trial 2 'Receiver in the Bedroom' – Results on floor plan

Table 3 shows the results of RSSI and LQI at each location and the distance between nodes. There appears to be a good link quality measurement between all nodes in the building now. L10 communicates with maximum link quality between the node in the basement (L3).

TABLE 3
TRIAL 2 - 'RECEIVER IN BEDROOM' MEASURED DATA

Point	Distance (mm)	RSSI (dBm)			LQI
		Min	Avg	Max	
FIRST FLOOR					
L5	7630	-92	-88.5	-87	255
GROUND FLOOR					
L0	4580	-68	-67.8	-67	255
L2	8810	-76	-76	-76	255
L1	9260	-94	-93.5	-93	204
BASEMENT					
L3	9820	-85	-83.5	-82	255

C. Trial 3 'Received power topology'

The third trial investigated the propagation of the signal from the front room to the kitchen on the ground floor of the house. It was decided to cover more locations in the front room to produce a topographical map of the received power, as shown in Fig. 5 below. The reference point was fixed in the kitchen whereas the sensor node was moved to various locations in a horizontal plane 1.2m above the floor on an expanded polystyrene stand. This height was chosen to minimise the effects of the kitchen units and wall mounted cupboards.

Fig. 6 illustrates the results of trial 3 in various locations in the front room. It shows that the complixity of the electromagnatic field strength within rooms due to attenuation and multipath scattering. The two regions shown in black Correspond to areas where data could not be taken due to obstruction by the television and sofa, both of which could not be easily moved. As expected, the highest RSSI values can be seen in an area closest to the kitchen and near to the door adjoining the two rooms.

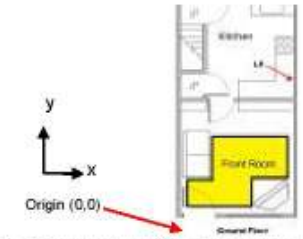

Fig. 5 Measurement area for Trial 3 "Received power topology"

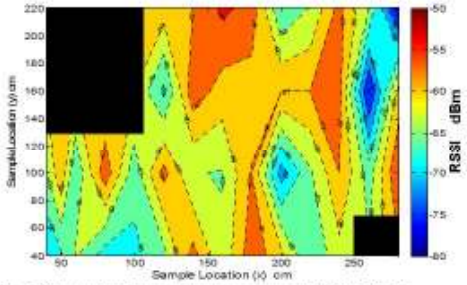

Fig. 6. Topographical image illustrating measured RSSI from Trial 3

IV. Conclusions

This study characterized the performance of ZigBee devices for smart metering applications within a late Victorian terraced house. Results showed that the wireless signals penetrate several adjacent walls within a building and through at least one floor. This indicates that problems of positioning smart meters and their associated displays are unlikely to be encountered in most domestic properties. The results also illustrate that if ZigBee is used within buildings, careful radio and infrastructure planning will be required for blocks of flats, and wireless repeaters or cabled solutions may be required. For installations where Zigbee based devices are used, other nodes could be utilised to create a mesh network and hence act as repeaters.

Methods to simulate wireless propagation in the built environment, including modern and old style housing, is an ongoing topic of research by the authors.

Acknowledgments

The authors would like to acknowledge Ember Corporation for their support in supplying the ZigBee devices. This work was partially funded by an EPSRC Knowledge Transfer Account, project number 009-DHH-010.

References

[1] A. K. Brown, "The wireless friendly building," in *Antennas and Propagation Conference (LAPC), 2010 Loughborough*, 2010, pp. 62-66.

[2] D. C. Kemp, *et al.*, "Enhancing radio coverage inside buildings," in *Antennas and Propagation Society International Symposium, 2005 IEEE*, 2005, pp. 783-786 Vol. 1A.

[3] M. Salem, *et al.*, "An Investigation on the Effects of Wall Parameters on the Indoor Wireless Propagations," in *Research and Development, 2007. SCOReD 2007. 5th Student Conference on*, 2007, pp. 1-5.

[4] W. F. Young, *et al.*, "Radio-Wave Propagation Into Large Building Structures; Part 1: CW Signal Attenuation and Variability," *Antennas and Propagation, IEEE Transactions on*, vol. 58, pp. 1279-1289, 2010.

[5] K. A. Remley, *et al.*, "Radio-Wave Propagation Into Large Building Structures; Part 2: Characterization of Multipath," *Antennas and Propagation, IEEE Transactions on*, vol. 58, pp. 1290-1301, 2010.

[6] A. Z. Alkar, *et al.*, "Web Based ZigBee Enabled Home Automation System," in *Network-Based Information Systems (NBiS), 2010 13th International Conference on*, 2010, pp. 290-296.

[7] L. Hongwei, *et al.*, "Application and Analysis of ZigBee Security Services Specification," in *Networks Security Wireless Communications and Trusted Computing (NSWCTC), 2010 Second International Conference on*, 2010, pp. 494-497.

[8] G. Wenqi, *et al.*, "ZigBee-wireless mesh networks for building automation and control," in *Networking, Sensing and Control (ICNSC), 2010 International Conference on*, 2010, pp. 731-736.

[9] Y. Peizhong, *et al.*, "Developing ZigBee Deployment Guideline Under WiFi Interference for Smart Grid Applications," *Smart Grid, IEEE Transactions on*, vol. 2, pp. 110-120, 2011.

TABLE 4
TRIAL 3 – RECEIVED POWER TOPOLOGY: AVERAGE MEASURED RSSI DATA (dBm)

Position from origin y-direction (cm)	Position from origin x-direction (cm) 40	50	60	80	100	120	140	160	180	200	220	240	260	280
220	n/a	n/a	n/a	n/a	n/a	58.5	57.0	53.3	55.0	66.0	62.8	56.0	63.0	77.2
160	n/a	n/a	n/a	n/a	n/a	66.7	55.0	58.3	58.5	57.0	57.0	56.0	75.3	59.0
100	63.2	57.5	65.7	55.0	64.8	56.0	63.0	63.2	56.8	70.5	63.5	57.0	64.5	54.0
40	69.2	66.5	62.8	67.5	66.8	64.0	56.0	62.5	55.0	59.0	65.8	61.0	n/a	n/a

Appendix F – Second Conference Paper

Analysis of Wireless Propagation Within a Victorian House for Smart Meter Applications

Yasir H. Alharbi[#1], Jonathan M. Rigelsford [#2], Richard J. Langley[#3] and Ahmed O. AlAmoudi [#4]
[#] Department of Electronics and Electrical Engineering,
University of Sheffield
Mappin Street, Sheffield, S1 3JD, United Kingdom
[#1] yhalharbi1@sheffield.ac.uk, [#2] j.m.rigelsford@sheffield.ac.uk, [#3] r.j.langley@sheffield.ac.uk, and [#4] alamoudi@kacst.edu.sa

***Abstract*— Smart meters utilizing wireless technology could help to improve building energy efficiency. Wireless smart meters have to be carefully deployed in the building to ensure reliable communication and optimize signal strength. This simulation study considers how changing the configuration within a Victorian terraced house affects the electric field strength. Ten scenarios are presented to investigate the effect of doors and human occupancy on RF signal propagation.**

Keywords—Smart meter, propagation, RF, wireless.

I. Introduction

The European Community has committed to save energy among most of European Union (EU) nations [1]. Currently, power consumers in the UK are given the estimated reading of electricity, gas and water every three months. In most cases they are not fully aware of the total power consumption and may consume more than they expect. The UK government aims to let most customers get a real indication of their consumption by 2020. To achieve this a smart meter will be installed in every home, with the aim of raising consumer awareness of energy consumption and thereby reducing overall domestic energy consumption [2].

Smart wireless meters are used to record and display the energy consumption of a household for the purpose of optimal power management. They offer consumers the potential for lower energy bills by making them more aware of their energy usage and can benefit energy suppliers by providing higher resolution data on customer demand. Smart wireless meters therefore have to effectively communicate with each other. A variety of commercial standards are available for wireless sensor networks (WSN) communication, such as Bluetooth, 6lowpan, Wireless HART, Z-wave and ZigBee. The latter has proven to be an appropriate solution for the smart meters [3].

Improving the performance of wireless systems is becoming a very important element especially inside buildings. For a wireless friendly building, improving the signal coverage is one of the main issues studied in the literature [4]. There are many parameters that can affect the radio frequency (RF) signal's propagation inside the buildings. Among them are the structure of building, the type of materials and the incident angle of wave into the wall, windows or any other obstacles [5].

Researchers have investigated the effects of various building dielectric parameters and structures of internal wall on the performance of wideband channels [6, 7]. The results have shown that the path loss increases if one of the permittivity, loss tangent or thickness of the wall is increased. A door state (open or closed) and presence of people on indoor environment have a big impact on propagation of the signal. In [8] the author has studied the affect of the doors when they are open or closed on the propagation for the cases of line of sight (LOS) and non line of sight (NLOS) using finite element method (FEM) simulations at 2.4GHz. It was clear that the door status has a more significant effect on the signal strength in the LOS scenario, whereas the door status has a small effect on the signal propagation in the NLOS scenario.

The effect of human body on wireless signals in an indoor environment has been investigated. It has been reported that the strength of the electric field distribution through a wall obstacle is higher than when it passes through people [9]. Also, the influence of human movement on wireless sensor networks in indoor radio propagation has been studied in [10 -12] and it was concluded that the electric field is significantly affected by the number of people and their mobility in the rooms. The signal level is decreased in case of slow speed movement but the trend at slow and medium speeds have the same effect as the number of people is increased.

In this paper, the electric field (E-field) strength of a dipole antenna transmitter operating at 2.4 GHz in different locations within a Victorian terraced house has been investigated. Simulations were performed using the electromagnetic simulation tool FEKO [13]. Several scenarios were investigated to address the critical factors in the positioning of smart meters. E-field distributions of the ground floor, comprising a kitchen and front room have been analyzed for different occupancy scenarios.

II. Simulation of Victorian House using Feko.

A. Experiment setup and House specifications.

The simulation was implemented in a typical Victorian terrace house of three levels as shown in Fig. 1. The simulated house includes a basement, ground floor and first floor. Its geometry has been described in [14], along with preliminary experimental results. The first floor has two bedrooms and the ground floor includes the front room and kitchen. The kitchen is 3.5 m wide and x 3.2 m long, while the front room is 3.5 m wide and 3.8 m long. The materials and dimension of house construction are listed in Table I.

Fig. 1. Victorian terrace house used in this work.

TABLE I. MATERIALS AND DIMENSION OF HOUSE CONSTRUCTION.

No	Objects	Material	Dimensions
1	External wall	Brick	20 cm
2	Internal wall	Brick	10 cm
3	Floor	Wood	10 cm
4	Ceiling	Wood	10 cm
6	Door	Wood	5 cm

Simulations were performed using a 2.4GHz dipole antenna to generate the E-fields and was positioned in the kitchen 1.2 m above the ground, 0.3 m from middle wall and 0.4 m from external wall. This represents a typical location for a smart meter display located on a kitchen work surface. The properties of materials used in simulating the house are shown in Table II.

TABLE II. MATERIAL DIELECTRIC PROPERTIES AT 2.4GHz.

Materials	Permittivity (ε)	Loss tangent (tan δ)
Brick	3.8	0.55
Wood	2.1	0.23
Plasterboard	2.41	0.09
Plastic	2.2	0.005
Glass	6.39	0.129

The FEKO simulation suite was used to optimize the locations of the transmitters and receivers within the house to get maximum received field where the simulation parameters are carefully configured. The numerical analysis technique used in the simulation was Geometrical Optics (GO). GO is suitable for solving a large model and inhomogeneous structures [13]. The maximum angular resolutions used in the GO calculations were θ=0.15 ° and ϕ= 0.08°. The maximum number of ray interaction used is 2. Thin Dielectric Sheet (TDS) is used to model the walls and rooms of the building. In such cases, the walls are modelled with one surface and the real thickness defined in a layered structure.

Analysis was performed for different occupancy scenarios as described in the following section. The dielectric properties of the human body at 2.4 GHz have been have been chosen as described in [15], where the whole body relative permittivity was ε_r=52.7 and conductivity σ=1.95 S/m. The length of the dipole antenna is 57.46 mm. The wire segment radius of the dipole antenna is 2 mm and the global mesh sizes have been selected as standard.

B. *Scenarios of simulation.*

Ten different scenarios were designed (A to J) to investigate the statistical significance of human occupancy and the effects of opening doors and the presence of humans on the electric field distribution in the rooms. These scenarios are defined in Table II. Fig. 2 illustrates the layout of the ground floor of the house and shows the relative locations of the occupants, the door and the transmitting antenna.

TABLE III. SCENARIOS USED FOR STATISTICAL ANALYSIS.

	Occupied	Door Open	Locations	Rotation
A	No	Yes	-	-
B	No	No	-	-
C	Yes (x1)	Yes	1	-
D	Yes (x1)	No	1	-
E	Yes (x1)	Yes	3	-
F	Yes (x1)	No	3	-
G	Yes (x1)	Yes	5	90°
H	Yes (x1)	No	5	90°
I	Yes (x4)	Yes	1,2,3 and 4	-
J	Yes (x4)	No	1,2,3 and 4	-

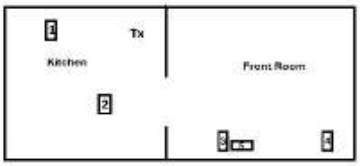

Fig. 2. Layout of the ground floor of the house showing occupancy locations.

III. RESULTS AND DISCUSSIONS

E-field amplitude distributions were calculated for the ground floor of the Victorian house. Results were sampled in a plane at the same height as the source antenna (1.2 m above the ground). 840 samples of the E-field amplitude in both the kitchen and front room have been used. Amplitude probability and the cumulative probability distributions of the E-field distributions have been used for analysis purposes as described in [16] and [17]. Results obtained from scenarios A, B, C and D are used in this short paper.

A. E-field Distribution Difference Calculations

E-field distribution difference plots are used to give a general overview of the spot regions of high or low field levels within the Victorian house. E-field distribution difference plots for a given frequency ΔE(f), have been generated using Equation 1.

$$\Delta E(f) = E(f)_n - E(f)_{Ref} \quad (1)$$

whereby $E(f)_{Ref}$ is the E-field distribution of the reference scenario (typically A), and $E(f)_n$ is the E-field distribution of the scenario of interest. These results can be used to visualize and quantify differences in E-field strength between the ten scenarios described in Section II.

Fig. 3 shows simulated results for the E-field difference plot between scenarios A (unoccupied, open door) and C (occupied at location 1 in the kitchen, open door) at 2.4GHz. The E-field strength is shown in dBV/m and positive values (shown as yellow to red) represent areas with a higher E-field when compared to the reference scenario (A). The negative values (shown as green and blues) represents a weaker E-field when compared to the reference scenario (i.e. the values obtained from the reference scenario are higher than those for scenario C). The shadowing effect (attenuation) due to the occupant in the kitchen at position 1 was about 9 dBV/m as observed in Fig. 3. It can also be seen that there is a net increase in the E-field strength at some locations within the front room of between 9 and 12 dBV/m due to the occupant in the kitchen.

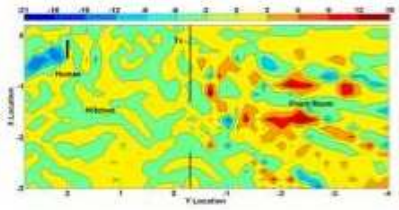

Fig. 3. Simulated E-field difference plot between scenarios A (unoccupied, open door) and C (occupied at location 1 in the kitchen, open door) at 2.4GHz.

B. E-Field Amplitude Distribution

The amplitude distribution function is used to provide simplified comparisons between different scenarios of the field data within the Victorian house. Figure 4 shows the E-field amplitude distribution within the kitchen and front room for scenarios A, B, C and D. The x-axis represents the distribution of field levels while y-axis represents the probability percentage of the appearance of each field level. It can be seen that the E-field distribution in the kitchen is similar for all four scenarios, whereas in the front room the average E-field distribution increases when the kitchen is occupied.

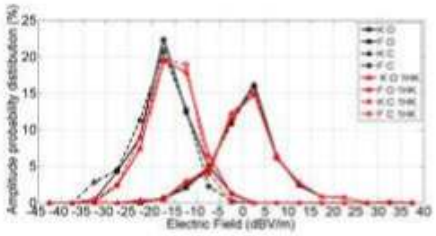

Fig. 4. E-field amplitude probability distribution for scenarios A, B, C & D (key: K = kitchen, F = front room, O = open door, C = closed door, 1HK = 1 one occupant in the kitchen).

C. Cumulative Probability Distribution

The cumulative probability distribution for scenarios A, B, C and D are presented in Fig. 5. The effects due to transmission losses through the closed door can be clearly seen. The presence of the human in the kitchen also affected the level of the signal in the front room. For the scenario of an open door it was clear that the presence of the human has reduced the average value of the signal from -17 dBV/m to -20 dBV/m, a 3dBV/m attenuation due to the presence of a human in the kitchen.

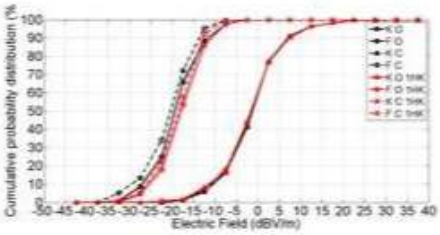

Fig. 5. E-Field cumulative probability distribution of scenarios A, B, C & D.

IV. CONCLUSION

This paper presents an investigation into changes in the electric field strength within the ground floor of a Victorian house at 2.4GHz. Scenarios are compared for opening and closing doors and changing the building's occupancy level. This work builds on the authors' previously published experimental results where good correlation between measurements and predictions has been shown [14]. Results have shown that a human occupant can locally change the E-Field by approximately 9dBV/m. The doors have an effect of less than 3dBV/m. In general, there was a large variation in E-field distribution levels in the front room when compared to the kitchen. This is due to the presence of the transmitter source in the kitchen. The front room is affected more by the constructive and destructive reflections and diffractions of the RF signals. Areas of high or low E-field strength are dependent on the propagation path as a measure of multiple wavelengths. Finally

and unsurprisingly, it is shown that the human body can cause attenuation of the signal resulting in a shadowing effect, for a short distance near to the human body.

Further studies will investigate other commonly used frequencies such as 5.8GHz, 868MHz and 433 MHz.

REFERENCES

[1] L. Zakiya. *Reasons to Save Energy*. Available: http://www.ehow.com/print/about_5571663_reasons-save-energy.html

[2] (2012). *SMART METERS*. Available: http://www.decc.gov.uk/en/content/cms/tackling/smart_meters/smart_meters.aspx

[3] L. Hongwei, J. Zhongning, and X. Xiaofeng, "Application and Analysis of ZigBee Security Services Specification," in *Networks Security Wireless Communications and Trusted Computing (NSWCTC), 2010 Second International Conference on*, 2010, pp. 494-497.

[4] A. K. Brown, "The wireless friendly building," in *Antennas and Propagation Conference (LAPC), 2010 Loughborough*, 2010, pp. 62-66.

[5] W. F. Young, C. L. Holloway, G. Koepke, D. Camell, Y. Becquet, and K. A. Remley, "Radio-Wave Propagation Into Large Building Structures—Part 1: CW Signal Attenuation and Variability," *Antennas and Propagation, IEEE Transactions on*, vol. 58, pp. 1279-1289, 2010.

[6] X.-S. YANG, Z.-M. TIAN, J.-J. YUAN, Y.-T. ZHANG, and W. SHAO, "Numerical Study on Indoor Wideband Channel Characteristics with Different Internal Wall " presented at the Radioengineering, 2013.

[7] J. T. Zhang and Y. Huang, "Indoor channel characteristics comparisons for the same building with different dielectric parameters," in *Communications, 2002. ICC 2002. IEEE International Conference on*, 2002, pp. 916-920 vol.2.

[8] T. Hult and A. Mohammed, "Assessment of Multipath Propagation for a 2.4 GHz Short-Range Wireless Communication System," in *Vehicular Technology Conference, 2007. VTC2007-Spring. IEEE 65th*, 2007, pp. 544-548.

[9] M. Matsunaga, T. Matsunaga, and M. Nakano, "Modelling and measurement techniques for propagation of indoor wireless communication considering the building's structure and human bodies," in *Antennas and Propagation Conference (LAPC), 2011 Loughborough*, 2011, pp. 1-4.

[10] J. S. C. Turner, M. F. Ramli, L. M. Kamarudin, A. Zakaria, A. M. Shakaff, D. L. Ndzi, *et al.*, "The study of human movement effect on Signal Strength for indoor WSN deployment," in *Wireless Sensor (ICWISE), 2013 IEEE Conference on*, 2013, pp. 30-35.

[11] H. Huo, W. Shen, Y. Xu, and H. Zhang, "The effect of human activites on 2.4 GHz radio propagation at home environment," in *Broadband Network & Multimedia Technology, 2009. IC-BNMT '09. 2nd IEEE International Conference on*, 2009, pp. 95-99.

[12] S. Zvanovec, P. Pechac, and M. Klepal, " Wireless LAN networks design: site survey or propagation modeling?." presented at the *Radioengineering* 2003.

[13] *FEKO Suite 6.2, EM Software & System-S.A. (Pty) Ltd*. Available: http://www.feko.info

[14] Y. Alharbi, D. Powell, R. J. Langley, and J. M. Rigelsford, "ZigBee wireless quality trials for smart meters," in *Antennas and Propagation Conference (LAPC), 2011 Loughborough*, 2011, pp. 1-4.

[15] J. Gemio, J. Parron, and J. Soler., "Human body effects on implantable antennas for ISM bands applications: Models comparison and propagation losses study.," *Progress In Electromagnetics Research*, vol. 110, pp. 437-452, 2010.

[16] L. Low, Z. Hui, J. M. Rigelsford, R. J. Langley, and A. R. Ruddle, "An Automated System for Measuring Electric Field Distributions Within a Vehicle," *Electromagnetic Compatibility, IEEE Transactions on*, vol. 55, pp. 3-12, 2013.

[17] L. Low, Z. Hui, J. Rigelsford, and R. Langley, "Computed field distributions within a passenger vehicle at 2.4 GHz," in *Antennas & Propagation Conference, 2009. LAPC 2009. Loughborough*, 2009, pp. 221-224.